UNIVERSIDADE ESTADUAL PAULISTA

INSTITUTO DE GEOCIÊNCIAS E CIÊNCIAS EXATAS (IGCE)

CAMPUS DE RIO CLARO

Programa de Pós-Graduação em Geologia Regional

Área de Geologia Regional

ESFENÓFITAS DO MONUMENTO NATURAL DAS ÁRVORES FOSSILIZADAS DO TOCANTINS, BACIA DO PARNAÍBA (PERMIANO, BRASIL)

RODRIGO NEREGATO

Orientadora: Profa. Dra. Rosemarie Rohn Davies

Tese de Doutorado elaborada junto ao Programa de Pós-Graduação em Geociências - Área de concentração em Geologia Regional para obtenção do Título de Doutor em Geologia Regional.

Rio Claro - SP

Outubro de 2012

561 Neregato, Rodrigo
N444e Esfenófitas do monumento natural das árvores fossilizadas do Tocantins, Bacia do Parnaíba (Permiano, Brasil) / Rodrigo Neregato. - Rio Claro : [s.n.], 2012
187 f. : il., figs., tabs.

Tese (doutorado) - Universidade Estadual Paulista, Instituto de Geociências e Ciências Exatas
Orientador: Rosemarie Rohn Davies

1. Paleobotânica 2. Esfenófitas permianas. 3. Formação motuca. 4. Floresta petrificada. I. Título.

Ficha Catalográfica elaborada pela STATI - Biblioteca da UNESP
Campus de Rio Claro/SP

COMISSÃO EXAMINADORA

Profa. Dra. Rosemarie Rohn Davies
IGCE/Unesp/Rio Claro (SP)

Prof. Dr. Joel Carneiro de Castro
IGCE/Unesp/Rio Claro (SP)

Prof. Dr. Roberto Iannuzzi
Universidade Federal do Rio Grande do Sul/Porto Alegre (RS)

Profa. Dra. Fresia Soledad Ricardi-Branco
IG/Unicamp/Campinas (SP)

Prof. Dr. Jefferson Prado
Instituto de Botânica/Divisão de Fitotaxonomia/São Paulo (SP)

We must become the changes we want to see in the world.

Mahatma Ghandi

Sonhem o mundo,
Não essa pálida visão da realidade.

Neil Gaiman in “Sandman: a história de mil gatos”

Para minha família,
pelo incondicional apoio ao longo de todos esses anos de universidade e
pela compreensão da minha ausência muitas vezes necessária.
Para Tucum também,
companheiro inquebrantável em todos os momentos.

AGRADECIMENTOS

À minha orientadora, por me apresentar à Paleobotânica e aceitar me orientar em um tema tão árido. Parte do que sou certamente se deve a ela;

Gostaria de externar meus profundos agradecimentos à banca examinadora, cujos comentários foram importantíssimos para melhorar substancialmente este trabalho: Prof. Dr. Joel Carneiro de Castro, Prof. Dr. Roberto Iannuzzi, Profa. Dra. Fresia Soledad Ricardi-Branco e ao Prof. Dr. Jefferson Prado;

À Sra. Suzana Rohn por todo o tempo dispendido em traduzir os indecifráveis artigos em alemão;

Ao querido amigo Roberto Iannuzzi por tudo que fez por mim durante estes anos de doutorado: campos, paleobotânica, conversas, conselhos, risadas… É sempre muito bom tê-lo presente;

Gostaria imensamente de agradecer as amigas Tati e Fran pelo apoio e carinho em todos os muitos momentos difíceis desta tese;

Ao Prof. Dr. Norberto Morales, coordenador do Programa de Pós-Graduação em Geologia Regional, pela inspiração que é;

À nossa secretária Rosângela Vacello. É sempre muito bom ter um anjo da guarda nos protegendo;

Ao técnico do Laboratório de Laminação, Júnior, por todas as dicas e ajuda durante o polimento dos fósseis estudados;

Ao amigo Gouveia por toda a ajuda com o inglês da tese. Grande amigo;

Aos amigos Ronny Röβler, Ramona Schwab, Mathias Merbitz, Ralph Kretzschmar, e em especial a Zhou ‘’Jumper’’ Feng, Thorid Zierold e Melaine Kutloch, do Museu für Naturkunde, Chemnitz, por tornarem tão agradáveis meus dias na Alemanha;

Ao Sr. João, da empresa Jet Service Jateamento, que gentilmente nos emprestou seu jato de areia para limparmos os fósseis;

À Profa. Fresia Ricardi-Branco, do Instituto de Geociências, Unicamp, que gentilmente nos emprestou seu equipamento fotográfico, e ao Rafa, por ter nos acolhido tão comodamente em sua casa;

Ao paleobotânico Robert Noll, de Tiefenthal, Alemanha, que muitíssimo contribuiu na descrição dos fósseis estudados aqui. E pelo ótimo vinho também;

Um agradecimento mais que especial a Mab, Nakao e em especial ao tio Ivo, meus companheiros de república nestes últimos anos. Foi um convívio imensamente bom;

Ao Conselho Nacional de Desenvolvimento Científico e Tecnológico pela concessão da bolsa de estudo (Processo número 141365/2008-0).

RESUMO

Pela primeira vez são descritos, em detalhe, caules de esfenófitas permianos da Bacia do Parnaíba, atribuídos ao gênero *Arthropitys*, anteriormente conhecidos nas Províncias Florísticas Euramericana e Cataísica. Apresentam-se permineralizados por sílica, com preservação celular, em depósitos fluviais que provavelmente foram controlados por estações secas e úmidas bem definidas. Diversos exemplares possuem ramos conectados ou tocos de ramos. Com base em suas características anatômicas e morfológicas, estão sendo propostas cinco novas espécies: *Arthropitys isoramis* e *Arthropitys tabebuiensis* apresentam cavidades medulares grandes, enquanto *Arthropitys buritiranensis* possui cavidade de dimensões médias; estas espécies possivelmente habitaram as margens dos rios; *Arthropitys tocantinensis* e *Arthropitys barthelli* apresentam cavidades das medulas muito pequenas com corpo secundário bastante maciço, interpretando-se que tenham ocupado áreas mais afastadas das drenagens, com substratos mais firmes. Um exemplar de *Arthropitys isoramis*, com 2.35 m de comprimento e 12 cm de diâmetro máximo, é o primeiro, em âmbito mundial, a preservar a raiz. Ao contrário das reconstruções clássicas do gênero, nas quais a raiz seria similar ao da esfenófita moderna *Equisetum*, o sistema radicular está disposto verticalmente e de modo contínuo em relação ao caule, formado por três eixos verticais e outros mais oblíquos. *Arthropitys tabebuiensis* assemelha-se significativamente a *Arthropitys bistriata* do Asseliano-Sakmariano de Chemnitz, Alemanha, o que corrobora outras evidências paleobotânicas desta idade para a Formação Motuca e sugere algum intercâmbio florístico entre a região da Bacia do Parnaíba e a Província Euramericana.

Palavras-chave: *Arthropitys*, esfenófitas, Bacia do Parnaíba, Formação Motuca, Permiano.

ABSTRACT

Permian sphenophyte stems from the Parnaíba Basin are described in detail for the first time and classified into *Arthopitys* genera, previously known in the Euramerican and Cathaysian Floristic Province. They are silica-permineralized with cell preservation and were found in fluvial deposits, which originated under probable marked dry and wet seasons. Several specimens have connected branches or branch-stumps. Based on their anatomical and morphological characteristics, five new species are proposed: *Arthropitys isoramis* and *Arthropitys tabebuiensis* have large pith cavities whereas *Arthropitys buritiranaensis* show a little smaller pith; these species possibly lived at the river side sites. *Arthropitys tocantinensis* and *Arthropitys barthelli* have relatively small pith cavitys and massive secondary bodies, suggesting that they occupied distal areas, where the soil was more aggregate. One of the specimens of *Arthropitys isoramis* has 2.35 m long and 12 cm wide and present exceptional preservation, and is the first in global ambit to preserve an attached root. Differently from the traditional reconstructions based on the modern *Equisetum*, the studied specimen presents a vertical root which is continuous with respect to the stem, formed by three vertical axes and smaller more oblique axes. *Arthropitys tabebuiensis* is relatively similar to *Arthropitys bistriata* from the Asselian-Sakmarian interval in Chemnitz, Germany. This fact corroborates other paleobotanical evidence of this age to Motuca Formation suggesting that there were some floristic relationships with the Euramerican Province during the Permian.

Key words: *Arthropitys*, sphenophytes, Parnaíba Basin, Motuca Formation, Permian.

ÍNDICE

ÍNDICE DE FIGURAS/FIGURES

ÍNDICE DE TABELAS/TABLES

ÍNDICE DE ESTAMPAS/PLATES

I: Aspectos gerais

1. Introdução

Este trabalho objetiva descrever as esfenófitas encontradas na área do Monumento Natural das Árvores Fossilizadas do Tocantins (MNAFTO), localizada entre as cidades de Araguaína e Filadélfia, norte do estado de Tocantins, em estratos permianos da Bacia do Parnaíba. Os fósseis analisados constituem-se de caules e ramos preservados tridimensionalmente, através do processo de permineralização por sílica, pertencentes ao órgão-gênero *Arthropitys* Goeppert, 1864-5, e foram encontrados nas fazendas Andradina, Buritirana e Peba.

A área de estudo, conhecida internacionalmente como sítio fossilífero há mais de 150 anos, foi categorizada pelo governador do Estado de Tocantins, em 2000, como Unidade de Conservação de Proteção Integral segundo o SNUC (Brasil – Ministério do Meio Ambiente, 2000), visando coibir o progressivo depauperamento dos fósseis da região. Os fósseis mais abundantes encontrados na área pertencem aos gêneros *Tietea* e *Psaronius* (samambaias); secundariamente, são encontradas gimnospermas e esfenófitas.

O presente trabalho possui três capítulos, dos quais o segundo e o terceiro já se encontram redigidos na língua inglesa, idioma da pretendida publicação e também visando possibilitar a discussão de aspectos taxonômicos e paleoambientais com o Dr. Ronny Röβler, Diretor do Museu de Ciências Naturais de Chemnitz, Alemanha, e Robert Noll, paleobotânico associado, que colaboraram no estudo dos fósseis e disponibilizaram exemplares depositados na referida instituição.

O Capítulo I, de caráter introdutório, aborda aspectos da geologia da área, da paleofitogeografia, paleoclimatologia, os processos de fossilização, entre outros, para entender o contexto paleoambiental dos fósseis em análise.

O Capítulo II traz uma revisão das espécies de *Arthropitys* Goeppert, 1864-5. Esta etapa mostrou-se essencial à compreensão do gênero e acabou sendo posteriormente incorporado à tese como capítulo que será submetido à publicação como um catâlogo crítico do gênero.

O Capítulo III descreve espécies inéditas do gênero *Arthropitys*, a saber: *A. isoramis*, *A. tabebuiensis*, *A. tocantinensis*, *A. barthelii* e *A. buritiranensis*, de maiores afinidades anatômicas e morfológicas com as espécies da América do

Norte e Europa. Foram intepretadas como pertencentes aos estratos mais basais da Formação Motuca, viventes em um ambiente fluvial de rios entrelaçados em condições climáticas possivelmente semi-áridas. Através de comparações com as espécies euroamericanas, foram associadas ao intervalo Asseliano-Sakmariano (~295 Ma), Eopermiano.

2. A Terra e as floras no Neopaleozóico

Levando-se em consideração que os vegetais fósseis do MNAFTO representam uma flora que existiu em paleolatitude relativamente baixa do Gondwana, com registro exclusivo na Bacia do Parnaíba, cabem considerações prévias sobre os aspectos paleogeográficos, paleoclimáticos e paleofitogeográficos do final do Paleozóico.

2.1. Paleogeografia e paleoclimas

Inúmeras reconstruções paleogeográficas do globo terrestre para o final do Paleozóico retratam o extenso continente Pangea, resultado da convergência gradual de diversas placas tectônicas (Scotese & Mckerrow, 1990; Barrow & Fawcett. 1995; Crowell, 1995; Parrish, 1995; Scotese & Langford, 1995; Rees et al., 1999; Golonka & Ford, 2000; Gibbs et al., 2002; Roscher & Schneider, 2006; Schneider et al., 2006; Poulsen et al., 2007; Blakey, 2008). Sua configuração aproximou-se a um “C” estendido de pólo a pólo, com a região central localizada próxima ao Equador (Figuras I.1 a I.3). Era banhado pelo Mar de Tétis a leste e pelo Oceano Pantalassa a oeste. Regiões que hoje pertencem principalmente à China, Malásia, Indochina e Irã constituíram grandes ilhas no Mar de Tétis e não pertenceram à Pangea.

Uma das últimas fases na formação deste supercontinente, durante o Carbonífero e o Permiano, foi a colisão do Gondwana com a placa do Hemisfério Norte (Laurrússia), correspondendo à Orogenia Herciniana (Variscana), com o soerguimento de uma imensa cordilheira em terrenos hoje pertencentes ao norte da África, sul da Europa e sul da América do Norte. Roscher & Schneider (2006) sugeriram que o movimento rotatório no sentido horário da placa do Gondwana causou colisões diácronas com a Laurrússia e, portanto, soerguimentos de montanhas consecutivos, sem formar um cinturão “transpangeana” contínuo, nem muito elevado. Nesta hipótese, os autores interpretaram que no início do

Permiano ainda persistia um braço de mar do Oceano Pantalassa no oeste da Pangea, entre terrenos hoje pertencentes à América do Sul e América do Norte (Oceano “Rheic”). No sudoeste do Gondwana também ocorreu uma orogenia, formando as Sierras Australes da Argentina, Montanhas do Cabo no Sul da África e as Montanhas Transantárticas. Neste contexto, a Bacia do Parnaíba encontrava-se em situação cratônica, distante das áreas tectonicamente ativas.

Muitos trabalhos que tratam da paleogeografia também abordam interpretações paleoclimáticas (Rowley et al., 1985; Scotese & Mckerrow, 1990; Barrow & Fawcett. 1995; Crowell, 1995; Parrish, 1995; Scotese & Langford, 1995; Rees et al., 1999; Golonka & Ford, 2000; Gibbs et al., 2002; Roscher & Schneider, 2006; Schneider et al., 2006; Poulsen et al., 2007; Blakey, 2008). Um fato bastante relevante do paleoclima no final do Paleozóico refere-se à glaciação permo-carbonífera nas altas latitudes do Gondwana. As interpretações dos autores variam ligeiramente quanto ao intervalo de tempo total abrangido pela glaciação, o número e a duração dos intervalos interglaciais, a extensão das geleiras, assim como os efeitos da glaciação sobre o clima e a circulação oceânica em outras regiões da Pangea. Outras discussões referem-se à influência das cordilheiras, como aquelas da Orogenia Herciniana, sobre a circulação atmosférica e a pluviosidade em distintas regiões do Hemisfério Norte.

Admite-se, em geral, que a glaciação terminou um pouco após o início do Permiano (Asseliano-Sakmariano), ao menos nas bacias da América do Sul e da África (talvez um pouco mais tarde na Antártica e na Austrália). No Carbonífero, iniciou-se paralelamente à glaciação, uma longa fase de aridização nas regiões subtropicais pontuada por algumas fases ligeiramente mais úmidas (nas fases interglaciais). O nível relativo do mar apresentou claras variações de acordo com a expansão ou a retração das geleiras no Gondwana, fundamental na geração de imensos depósitos de carvão em sítios de sedimentação costeiros. Após a glaciação, num longo intervalo de tempo que abrangeu também boa parte do Mesozóico, as faixas de aridez se ampliaram. Iniciou-se um regime climático de monções nas proximidades do Mar de Tetis, ou seja, ventos sopravam do mar para o continente no verão e do continente para o mar no inverno. Assim, áreas anteriormente quentes e úmidas passaram a apresentar forte sazonalidade, com verões chuvosos e invernos bastante secos (Parrish, 1995). Outro fator que certamente influenciou o clima durante o Permiano, especialmente no final do

período, foi um intenso vulcanismo no oeste da Sibéria e no oeste da América do Sul, com a provável liberação de grandes volumes de gás carbônico para a atmosfera (Rees et al., 1999; Golonka & Ford, 2000).

Segundo Roscher & Schneider (2006), o embaiamento do Oceano Pantalassa no oeste da Pangea (Oceano “Rheic”), antes do seu fechamento, teria contribuído para a manutenção de condições ainda relativamente úmidas nas baixas latitudes durante boa parte do Carbonífero e início do Permiano. O rigor da aridez somente teria aumentado com o fechamento deste braço de mar e com as mudanças de circulação oceânica após a glaciação. Estes autores também ressaltaram a importância do sistema de monções nas baixas latitudes e a forte sazonalidade (verões e invernos secos, primaveras e outonos úmidos). Neste sentido, o controle climático das cordilheiras da Orogenia Herciniana pode ter sido menor do que anteriormente estimado.

Modelos paleoclimáticos globais para o Permiano permitem visualizar as possíveis condições climáticas que dominavam na Bacia do Parnaíba, embora os dados usados ainda sejam escassos ou incertos, além de negligenciarem características locais da bacia. Crowley et al. (1989) através de modelos para o Kazaniano (hoje aproximadamente Mesopermiano), estimaram que na latitude de 30^{o}S, onde possivelmente estava situada a margem meridional da Bacia do Parnaíba durante o Permiano, a temperatura anual média ficava entre 20 e 40^{o}C.

Gibbs et al. (2002) traçaram para o Sakmariano (Eopermiano) e o Wordiano (Mesopermiano) a precipitação diária e a direção resultante dos ventos (Figura I.1) e a temperatura da superfiície (Figura I.2) para os meses dezembro-janeiro-fevereiro (DJF) e junho-julho-agosto (JJA), mostrando, respectivamente, precipitação entre 0 e 4 mm/dia, ou seja, precipitação de clima desértico ou temperado úmido, e temperatura na superfície entre 15 e 20^{o}C para a área ocupada pela bacia.

Rees et al. (1999) modelaram para o Sakmariano e o Wordiano os possíveis biomas terrestres com base na concentração de CO_2 atmosférico (Figura I.3), estando a bacia entre um bioma desértico ou temperado úmido.

No entanto, pela exuberância da flora permiana da bacia, o clima se aproximou muito mais ao temperado úmido e menos ao desértico.

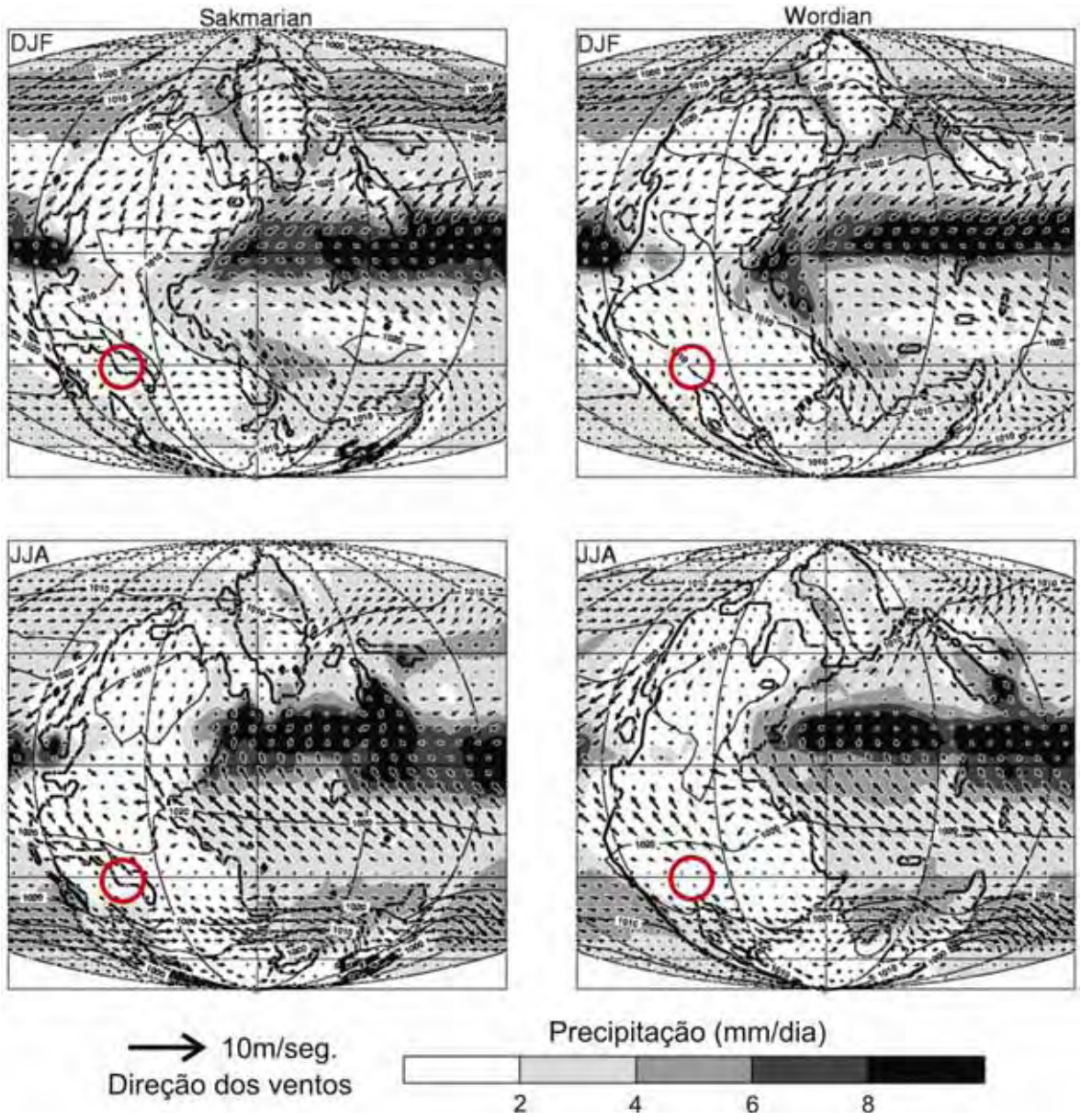

Figura I.1. Proposta de Gibbs et al. (2002) para a precipitação diária e para as direções resultantes dos ventos para o Sakmariano (Eopermiano) e Wordiano (Mesopermiano). O círculo vermelho indica a posição aproximada da bacia para o período.

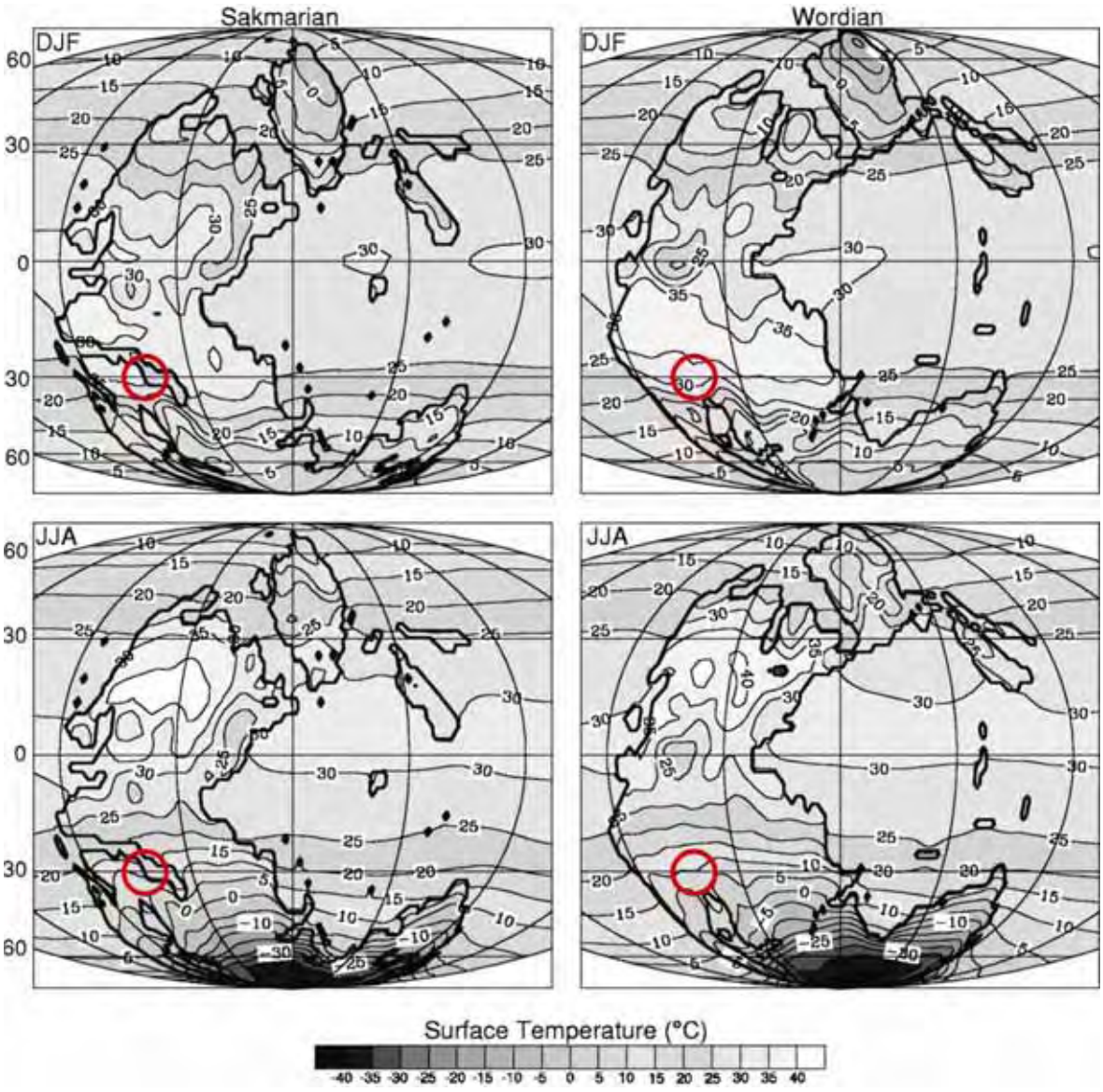

Figura I.2. Proposta de Gibbs et al. (2002) para a temperatura média sazonal da superfície terrestre para o Sakmariano (Eopermiano) e Wordiano (Mesopermiano). O círculo vermelho indica a posição aproximada da bacia para o período.

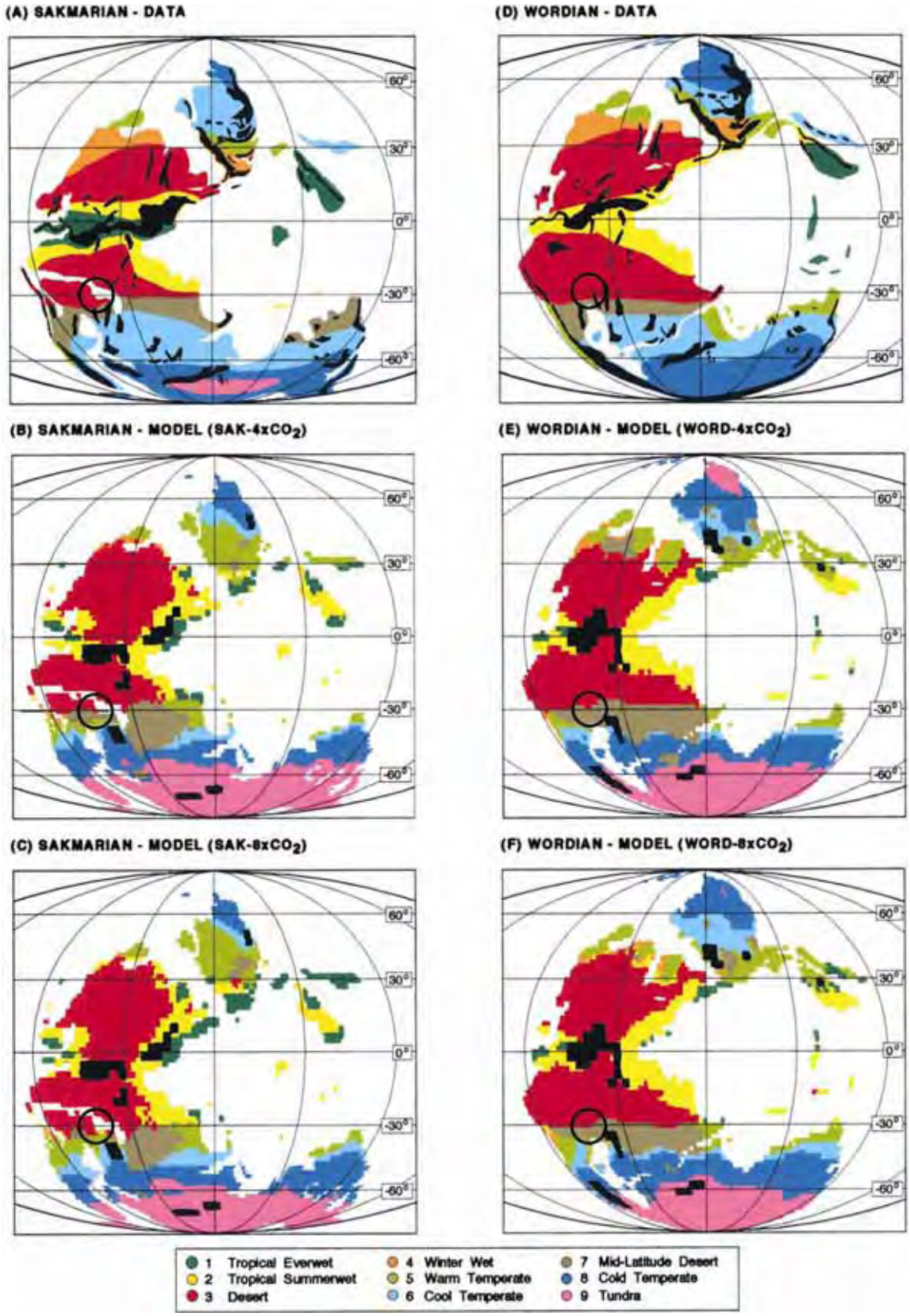

Figura I.3. Proposta de Rees et al. (2002) para os biomas do Sakmariano (Eopermiano) e Wordiano (Mesopermiano). **B** e **E** mostra os biomas modelados a partir de quatro vezes a concentração atual de CO_2; **C** e **F** a partir de oito vezes a concentração atual de CO_2, tendo como base as paleofloras encontradas nos biomas dos respectivos períodos. O círculo preto indica a posição aproximada da bacia para o período.

2.2. As províncias florísticas no Neopaleozóico

De maneira geral, as biotas continentais se modificaram no contexto das mudanças climáticas e geográficas ocorridas ao longo do tempo, principalmente a flora (DiMichele & Aronson, 1992). Tradicionalmente, as reconstruções das floras carboníferas do Hemisfério Norte mostram extensos ambientes flúvio-deltáicos com turfeiras dominadas por grandes licófitas e florestas úmidas em áreas adjacentes melhor drenadas (Falcon-Lang, 2003; Falcon-Lang & DiMichele, 2010). Contudo, este modelo pode ter sido restrito às regiões costeiras, pois as áreas mais interiores possivelmente foram mais secas, dominadas por cordaites (Falcon-Lang, 2003). Igualmente, o modelo de florestas úmidas representaria bem os intervalos interglaciais, enquanto que os intervalos glaciais pacerem ter sido mais secos, com sazonalidade mais marcada, quando predominavam cordaites, coníferas e pteridospermas (Falcon-Lang & DiMichele, 2010). Nas fases glaciais, elementos das florestas úmidas provavelmente sobreviviam em pequenos refúgios e, após cada fase glacial, retornavam às áreas das bacias sedimentares, porém gradualmente empobrecidos (Falcon-Lang & DiMichele, 2010). As licófitas de grande porte foram os vegetais que mais declinaram nas fases glaciais, enquanto aumentava a proporção relativa de samambaias arborescentes (Pfefferkorn & Leary, 1977). Estas últimas foram aparentemente menos afetadas pelas mudanças climáticas porque seus esporos podiam ser dispersos pelo vento e não só pela água (Falcon-Lang & DiMichele, 2010).

Portanto, a convergência de fatores como a glaciação no Gondwana, o início da aridização nas latitudes mais baixas e o aparecimento de possíveis barreiras geográficas (as grandes cordilheiras da Orogenia Herciniana), reduziram o potencial de dispersão de muitas espécies vegetais, especialmente daquelas de grande porte. Estas foram sendo substituídas por espécies menores e mais endêmicas. Assim, estabeleceram-se quatro principais províncias florísticas a partir do final do Carbonífero (Meyen, 1987; Wnuk, 1996) (Figura I.4):

- Província Angárica: ocupou áreas onde hoje se encontra a Sibéria, a Groenlândia, Spitzbergen, o norte dos países bálticos, a Mongólia e o leste dos Urais;
- Província Euramericana: ocupou áreas onde hoje se encontra a América do Norte, o norte da África, o leste da Europa e a Ásia;

- Província Cataísica: ocupou áreas onde hoje se encontra a China, o Japão, a Coréia, o Vietnã, o Laos, a Tailândia e a Indonésia;
- Província Gondwânica: ocupou áreas onde hoje se encontra o sul da América do Sul, o sul da África, Madagascar, Antártica, Austrália, Nova Zelândia, Nova Guiné e a Índia.

Ao longo do Permiano, tendo em vista o aumento da aridez, cada província dividiu-se em mais subprovíncias (Figura I.4).

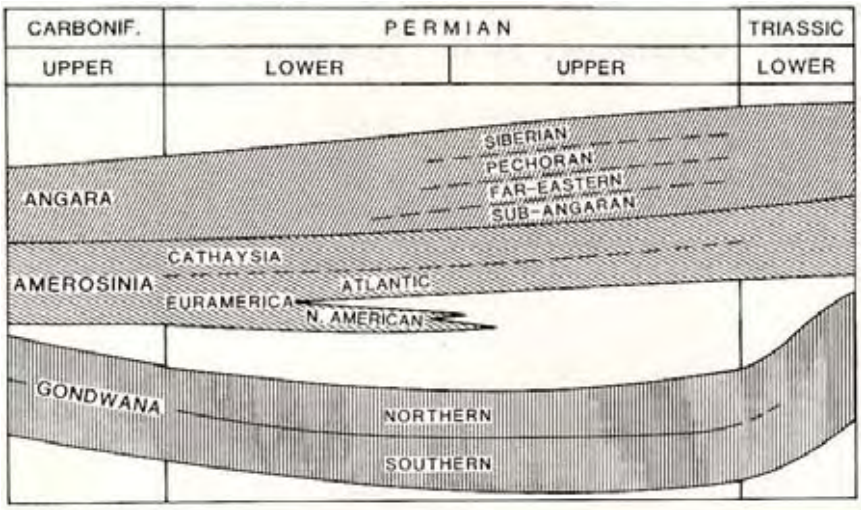

Figura I.4. Províncias florísticas para o Neocarbonífero, Permiano e Eotriássico (Meyen, 1987).

Na América do Sul, especialmente na Argentina, o registro fossilífero sugere relativo endemismo florístico desde o início do Carbonífero (Iannuzzi & Pfefferkorn, 2002). A partir deste momento, a flora esteve fortemente influenciada pela glaciação. A Bacia do Paraná tem tafofloras em depósitos interglaciais a partir do Neocarbonífero até o início do Permiano, apresentando glossopterídeas e assim evidenciando a instalação da "Flora de *Glossopteris*", a qual caracterizou todo o Permiano das latitudes altas a médias do Gondwana. Ao longo do Permiano, diversos elementos desta flora continuaram endêmicos, porém determinadas esfenófitas (e.g., *Phyllotheca, Sphenophyllum*) e samambaias (*Astherotheca*) lembram fortemente espécies da Euramérica e podem ter migrado desta região à Bacia do Paraná durante e após a glaciação (Rohn & Rösler, 1987). Os caules de samambaias *Tietea singularis* e *Psaronius,* do intervalo Eo a Mesopermiano na Bacia do Paraná, são os elementos compartilhados com a Bacia do Parnaíba.

No norte da África (Argélia e Marrocos), embora em continnte gondwânico, ocorrem vegetais fósseis neocarboníferos e eopermianos com claras afinidades à Flora Euramericana (Lejal-Nicol, 1985; El Wartiti et al., 1990). Da mesma forma, na Venezuela encontram-se vegetais eopermianos semelhantes aos do Oeste da América do Norte e não aos típicos do Gondwana (Ricardi et al., 1997; Ricardi-Branco et al., 2005; Ricardi-Branco, 2008), com diversas esfenófitas preservadas como moldes, porém predominam as espécies que sugerem relativa escassez de água, clima semi-árido ou fortemente sazonal, que representariam uma flora do Gondwana em região equatorial (Ricardi et al., 1997; Ricardi-Branco et al., 2005; Ricardi-Branco, 2008). A Figura I.5 ilustra a distribuição destas províncias paleoflorísticas acima e as zonas climáticas para o Eopermianao.

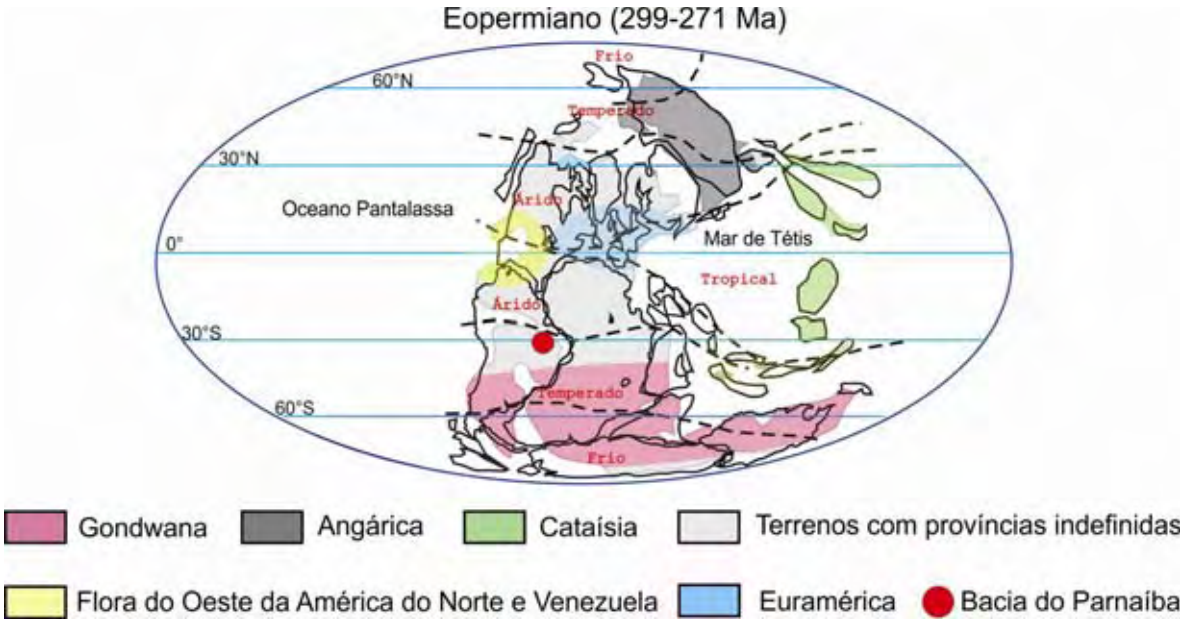

Figura I.5. Mapa do globo terrestre durante o Eopermiano mostrando a distribuição das províncias paleoflorísticas, as zonas climáticas e a localização da Bacia do Parnaíba. Mapa baseado em Scotese (2009). Províncias paleoflorísticas segundo Chaloner & Lacey (1973), Chaloner & Meyen (1973), Meyen (1987), Cleal & Thomas (1991), Ricardi-Branco et al. (2005) e Ricardi-Branco (2008).

Durante o Permiano, as províncias Euramericana e Gondwânica experimentaram variações na diversidade e na composição florística (Figura I.6). Na primeira, a diversidade decresceu do Eo para o Mesopermiano, permanecendo baixa no Neopermiano, enquanto na segunda ocorreram duas fases com aumento e queda de diversidade, atingindo valores máximos em

meados do Eopermiano e próximo à passagem do Meso ao Neopermiano; os valores mínimos estariam no início do Mesopermiano.

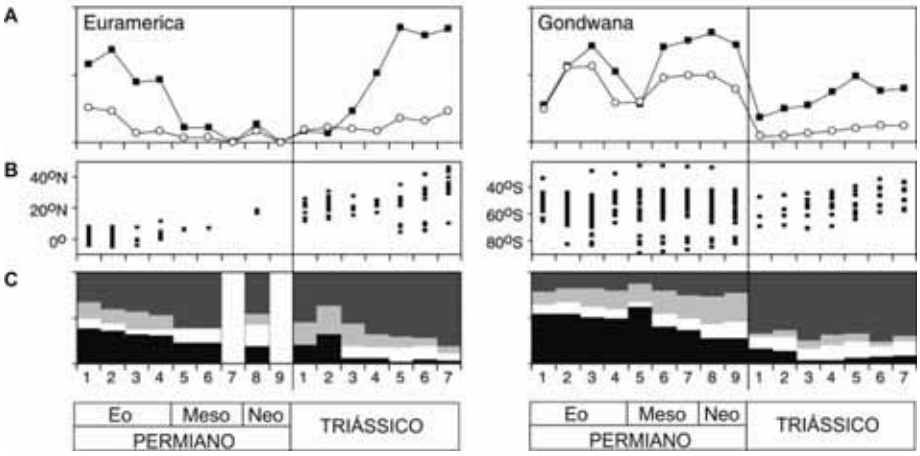

Figura I.6. **A**: distribuição temporal da riqueza genérica para a flora; **B**: distribuição latitudinal da riqueza genérica; **C**: porcentagem composicional dos grandes grupos vegetais durante o Permiano e Triássico: preto: *Cordaites*, *Gigantopteris*, *Glossopteris*, licófitas e pteridospermas; cinza escuro: cicadófitas, samambaias, ginkgófitas, peltaspermas e pinales; cinza claro: esfenófitas; branco: período sem registro (Rees, 2002).

3. A Bacia do Parnaíba

A Bacia do Parnaíba apresenta rochas sedimentares (e algumas vulcânicas) depositadas sobre a Plataforma Sul-Americana, ocupando a porção centro-norte do supercontinente Gondwana (Figura I.7), com aproximadamente 600.000 km^2 na porção Norte-Nordeste do território brasileiro, nos estados do Pará, Tocantins, Piauí, Maranhão, Ceará e Bahia (Góes & Feijó, 1994) e também com depósitos no noroeste da África (Milani & Thomas-Filho, 2000).

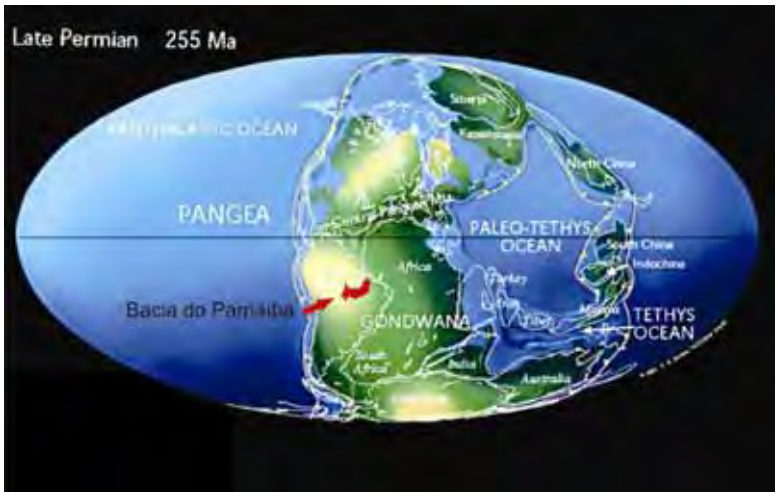

Figura I.7. Localização aproximada da Bacia do Parnaíba no Gondwana durante o Neopermiano (mapa paleogeográfico segundo Scotese, 2009).

O pacote sedimentar da Bacia do Parnaíba subdivide-se em cinco supersequências (Góes & Feijó, 1994; Vaz et al., 2007): Siluriana (~440-395 Ma), representada pelo Grupo Serra Grande; Mesodevoniana-Eocarbonífera (~400-330 Ma), Grupo Canindé; Neocarbonífera-Eotriássica (~310-220 Ma), Grupo Balsas; Jurássica (~165-155 Ma), Formação Pastos Bons, e Cretácea (~120-85 Ma), formações Grajaú, Codó e Itapecuru. Assim, os depósitos têm idade entre o Eo-Siluriano e o Meso-Cretáceo.

As três primeiras supersequências correspondem a ciclos transgressivo-regressivos originados pelas flutuações dos níveis dos mares epicontinentais e pelas orogenias de caráter global, enquanto as duas últimas são depósitos predominantemente continentais (Vaz et al., 2007).

Outra interpretação geral sobre a bacia foi feita por Silva et al. (2003): pelo fato dos grupos possuírem histórias tectonossedimentares muito distintas, pertenceriam a bacias distintas dentro da Província Parnaíba, sendo assim designadas como bacias do Parnaíba (Siluriano-Triássico), Alpercatas (Jurássico-Cretáceo), Grajaú (Cretáceo) e do Espigão-Mestre (Cretáceo). Essas bacias são delimitadas por discordâncias que também são os elementos delimitadores das supersequências de Góes & Feijó (1994).

3.1. Estratigrafia da Bacia do Parnaíba no Permiano

Durante o intervalo Neocarbonífero-Eotriássico (~310-220 Ma), depositou-se na bacia o Grupo Balsas, que compreende, ascendentemente, as formações Piauí, Pedra de Fogo, Motuca e Sambaíba (Figura I.8). As formações Pedra de Fogo e Motuca, de interesse direto para este trabalho, serão discutidas abaixo e afloram desde o nordeste do Maranhão até o norte do Tocantins, passando pelo oeste do Piauí, sudeste e sul do Maranhão (Figura I.10).

3.1.1. Formação Pedra de Fogo

A Formação Pedra de Fogo foi definida por Plummer (1948 apud Lima & Leite, 1978) para classificar as camadas ricas em sílex e *Psaronius* que afloram no vale do Rio Pedra de Fogo entre Pastos Bons e Nova Iorque (MA). A unidade aflora quase continuamente na porção centro-sul da bacia (Coimbra, 1983), alcançando 600 km de extensão na direção leste-oeste e 80 km de largura (Faria Jr. & Trukenbrodt, 1980).

Segundo Aguiar (1971), a formação apresenta sedimentação cíclica, em que cada ciclo é constituído, da base para o topo, por arenito, arenito fino ou siltito, calcário oolítico ou concrecionário e na parte superior folhelhos esverdeados fossilíferos e lentes de calcário.

Segundo Faria Jr. & Trukenbrodt (1980), a unidade ocorre em superfície na região centro-sul da bacia com espessura média de 100 m, apresentando variações laterais de acordo com a área analisada e pode ser dividida em:

Membro Sílex Basal, em contato concordante com a Formação Piauí, tem natureza clástico-química e aproximadamente 20 metros de espessura. É composto por um pacote de siltitos a folhelhos cinza, marrons e arroxeados intercalados por camadas dolomíticas e com algumas concreções de sílex escuro (Faria Jr. & Trukenbrodt, 1980);

Membro Médio, de natureza predominantemente clástica fina e inicia-se com os arenitos ou siltitos às vezes carbonáticos (Faria Jr. & Trukenbrodt, 1980);

Membro Trisidela, novamente de natureza clástico-química, ocorre na região central e oeste da bacia e representa um pacote de 40 metros constituído por camadas dolomíticas cinza, intercalados com siltitos, folhelhos carbonáticos cinza esverdeados a verdes com concreções e níveis de sílex (Faria Jr. & Trukenbrodt, 1980).

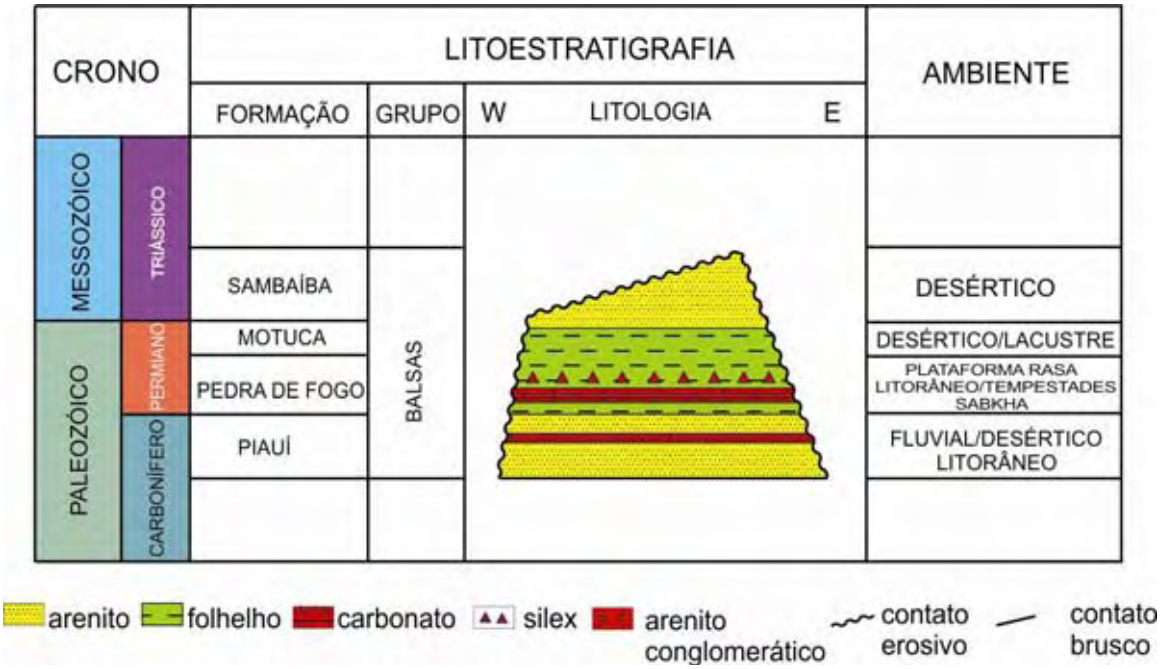

Figura I.8. Coluna estratigráfica da Bacia do Parnaíba durante o Pennsylvaniano-Eotriássico, segundo Góes & Feijó (1994).

Pinto & Sad (1986), realizaram importante trabalho na borda sudoeste da bacia e subdividiram a formação nos membros Inferior, Médio e Superior, coincidindo bastante bem com o trabalho de Faria Jr. & Trukenbrodt (1980).

A fauna encontrada apresenta escamas de paleoniscídeos, dentes de crossopterígeos e xenacantus, espinhos de nadadeiras de ctenacantus (Silva-Santos, 1946, 1990), o anfíbio *Prionosuchus plummeri* (Price, 1948) e fragmentos de peixes paleonisciformes, ctenacantiformes, xenacantiformes, holocéfalos e dipnóicos (Cox & Hutchinson, 1991). Faria Jr. & Trukenbrodt (1980) destacaram a ocorrência de estromatólitos. Até o momento, nenhum autor registrou caules de samambaias preservadas in situ em camadas sedimentares, apenas roladas.

Em relação às idades, não existem dados conclusivos. Price (1948) com base no anfíbio *Prionosuchus* e Cruz et al. (1972 apud Lima & Leite (1978) com base em esporomorfos atribuíram idade eopermiana à Formação Pedra de Fogo. Lima & Leite (1978), também com base em esporomorfos atribuíram idade Eo-Mesopermiana à formação. No entanto, o Permiano ainda não era dividido em Eo, Meso e Neo, dificultando qualquer correlação mais acurada. Dino et al. (2002), atribuíram idade neopermiana para o Membro Trisidela. No entanto, os autores sugerem forte correlação com a Formação Flowerpot, Oklahoma, EUA, a qual apresenta idade artinskiana-kunguriana, portanto eopermiana (Lucas, 2004). Assim, os trabalhos acima não são conclusivos sobre as idades.

3.1.2. Formação Motuca

A Formação Motuca foi definida por Plummer (1948 apud Lima & Leite, 1978) para denominar os folhelhos avermelhados com lentes de calcário e anidrita que ocorrem acima da Formação Pedra de Fogo nos arredores da Fazenda Motuca, entre São Domingos e Benedito Lima (MA). A unidade tem aproximadamente 300 metros de espessura e é constituída por siltito castanho avermelhado, arenito branco fino a médio e subordinadamente folhelhos, anidrita branca e raros calcários (Góes & Feijó 1994; Vaz et al. 2007).

Lima Filho (1991) considerou que a Formação Motuca é similar à Formação Pedra de Fogo, ocorrendo concentrações de evaporitos na porção basal, mas diferindo pela presença de corpos arenosos de grande espessura. Segundo Coimbra (1983), a formação é constituída por siliciclastos nas classes

silte e areia muito fina de má seleção, com maior proporção de arenitos na porção superior.

Em relação ao ambiente deposicional, Lima & Leite (1978) consideraram a formação de origem continental, flúvio-eólica, com algumas incursões marinhas, principalmente na porção média, e possíveis ambientes lagunares pela ocorrência de calcáreo e gipsita. A Figura I.9 ilustra uma estratificação cruzada de provável canal fluvial. Faria Jr. (1984 apud Góes & Feijó, 1994), analisando a região de Araguaína-Filadélfia interpretou que a formação representaria um ambiente do tipo *sabkha* continental. Góes & Feijó (1994) sugeriram ambiente desértico com lagos associados e eventuais influências marinhas. Segundo Dias-Brito & Castro (2005) ‘’... há um grande domínio de sistemas continentais na Formação Motuca (fluvial, deltáico e lacustre), contrapondo-se aos sistemas marinhos da Formação Pedra de Fogo’’.

Em relação ao clima, Lima & Leite (1978) consideraram-no árido pela predominância de sedimentos vermelhos, ferruginosos, e pela presença de evaporitos.

Em relação às idades, Mesner & Wooldridge (1964 in Lima & Leite, 1978) registraram a presença do gastrópode *Pleurotomaria* sp. e de peixes dos gêneros *Paleoniscus* e *Elonichtys*, atribuindo à formação idade neopermiana. Góes & Feijó (1994) também a posicionaram no Neopermiano (Kazaniano-Tatariano).

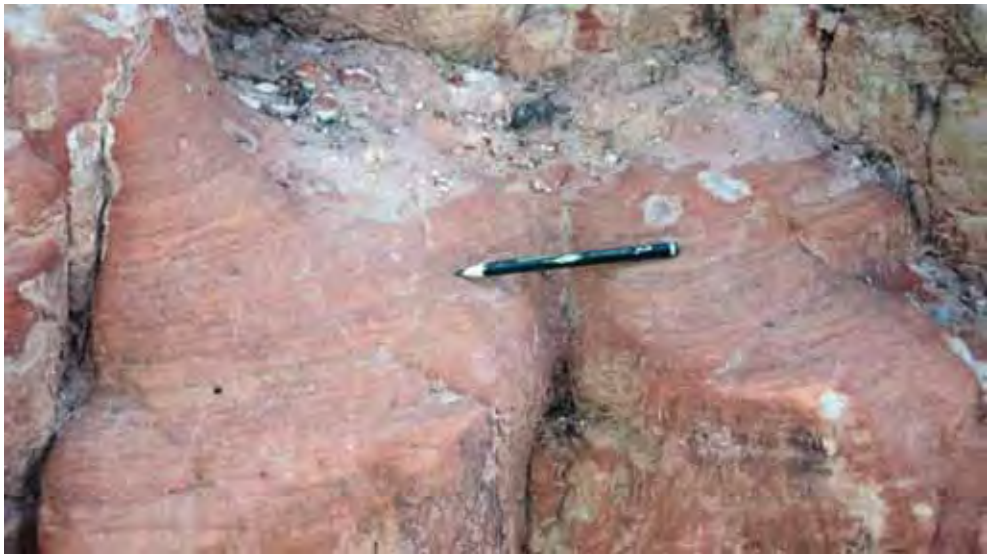

Figura I.9. Arenito fino avermelhado da Formação Motuca com estratificações cruzadas acanaladas, de provável canal fluvial. Afloramento localizado na Rua Getúlio Vargas, na cidade de Pastos Bons (MA).

3.1.3. Posicionamento estratigráfico dos caules fósseis

Uma questão muito importante para este trabalho é o posicionamento estratigráfico dos fósseis encontrados. Os vegetais fósseis frequentemente ocorrem rolados sobre o solo, misturados com os blocos de sílex, o que dificulta o reconhecimento de sua posição estratigráfica original. Além disso, as formações Pedra de Fogo e Motuca ainda não mereceram estudos detalhados em todas as áreas da bacia.

Segundo Barbosa & Gomes (1957) e Aguiar (1971) as formações Pedra de Fogo e Motuca são caracterizadas por uma sedimentação cíclica, uma repetição periódica de arenito, sedimentos finos como siltitos e folhelhos, arenito fino e sobreposição de pacotes carbonáticos.

Barbosa & Gomes (1957) relataram que não foram encontradas madeiras silicificadas em pacotes carbonáticos e enfatizaram ‘‘...que um dos autores (F.A. Gomes) durante cerca de seis anos de trabalhos estratigráficos no Maranhão, somente encontrou *Psaronius in situ* em folhelhos do topo da coluna paleozoica...’’ (p.24) e que os outros achados “...referem-se a fragmentos transportados em diversos ciclos de erosão posteriores à sua deposição original’’ (p.24-25). É importante ressaltar que o topo desta coluna paleozoica se refere à Formação Pedra de Fogo, pois na época do trabalho a Formação Motuca era interpretada como triássica.

Faria Jr. & Trukenbrodt (1980) identificaram a ocorrência de madeiras silicificadas/*Psaronius* em camadas de siltitos e arenitos finos avermelhados com manchas brancas, pertencentes aos estratos mais superiores do Membro Trisidela e “muito embora tenham os carbonatos da Formação Pedra de Fogo uma extensa distribuição na bacia, as biotas, normalmente associadas a esses tipos de rochas, estão praticamente ausentes ou ocorrem localmente em determinadas áreas’’ (p.746).

Segundo Pinto & Sad (1986), que estudaram a estratigrafia na região entre Araguaína e Filadélfia (TO), a penúltima camada do terceiro ciclo dentro da Formação Pedra de Fogo (Membro Trisidela) é constituída por arenitos finos e siltitos carbonáticos e, a última camada, por siltitos creme não carbonáticos (Figura I.11). O início do quarto ciclo dentro do Grupo Balsas, já interpretado como Formação Motuca, inicia-se com arenito fino a médio, avermelhado e esbranquiçado, com estratificação cruzada, onde foram encontradas madeiras

silicificadas (Figura I.11). Portanto, estes autores consideraram que os fósseis na região estudada devem pertencer à Formação Motuca. Esta interpretação foi aceita por Dias-Brito & Castro (2005) e Dias-Brito et al. (2007), os últimos autores a realizaram estudos estratigráficos na região.

3.2. A área do Monumento Natural das Árvores Fósseis do Tocantins (MNAFTO)

O MNAFTO possui área de aproximadamente 32.000 ha e ocupa a região sudoeste da bacia (Dias-Brito et al., 2007), com duas principais superfícies de aplainamento: uma inferior, na cota entre 200 e 250 m, preservada pelos leitos de sílex da Formação Pedra de Fogo ou pela silicificação do arenito basal da Formação Motuca, e outra superior, na cota 500 m preservada pelos arenitos eólicos da Formação Sambaíba (Pinto & Sad, 1986). As rochas aflorantes no MNAFTO pertencem às formações Pedra de Fogo, Motuca e Sambaíba (Dias-Brito & Castro, 2005) com predomínio de afloramentos da Formação Motuca (Dias-Brito et al., 2007). As esfenófitas estudadas aqui foram encontradas nas fazendas Andradina, Buritirana e Peba (Figura I.10), cujos perfis estratigráficos e imagens do local são mostrados, respectivamente, nas figuras I.12 e I.13.

A Fazenda Peba ocupa a região oeste do monumento e apresenta grandes quantidades de *Psaronius*, poucos troncos de gimnospermas e raras esfenófitas (Capretz, 2010). Os caules ocorrem segmentados transversalmente, alguns com comprimentos superiores a 10 metros e diâmetro alcançando 1,2 metros. Alguns fósseis possuem um envoltório silicificado de arenito, indicativo de sua ‘’imersão’’ em arenitos fluviais e agora encontrados sob a superfície pelos episódios de erosão das rochas que os portavam (Dias-Brito & Castro, 2005).

A Fazenda Andradina ocupa a região central do monumento próximo ao Distrito de Bielândia e apresenta grandes quantidades de caules de samambaias e em menor quantidade troncos de gimnospermas e caules de esfenófitas (Capretz, 2010).

A Fazenda Buritirana ocupa a região leste do monumento e apresenta grandes quantidades de caules de samambaias arborescentes, em menor quantidade troncos de gimnospermas e caules de esfenófitas, além de folhas e pecíolos de samambaias (Dias-Brito & Castro, 2005; Capretz, 2010).

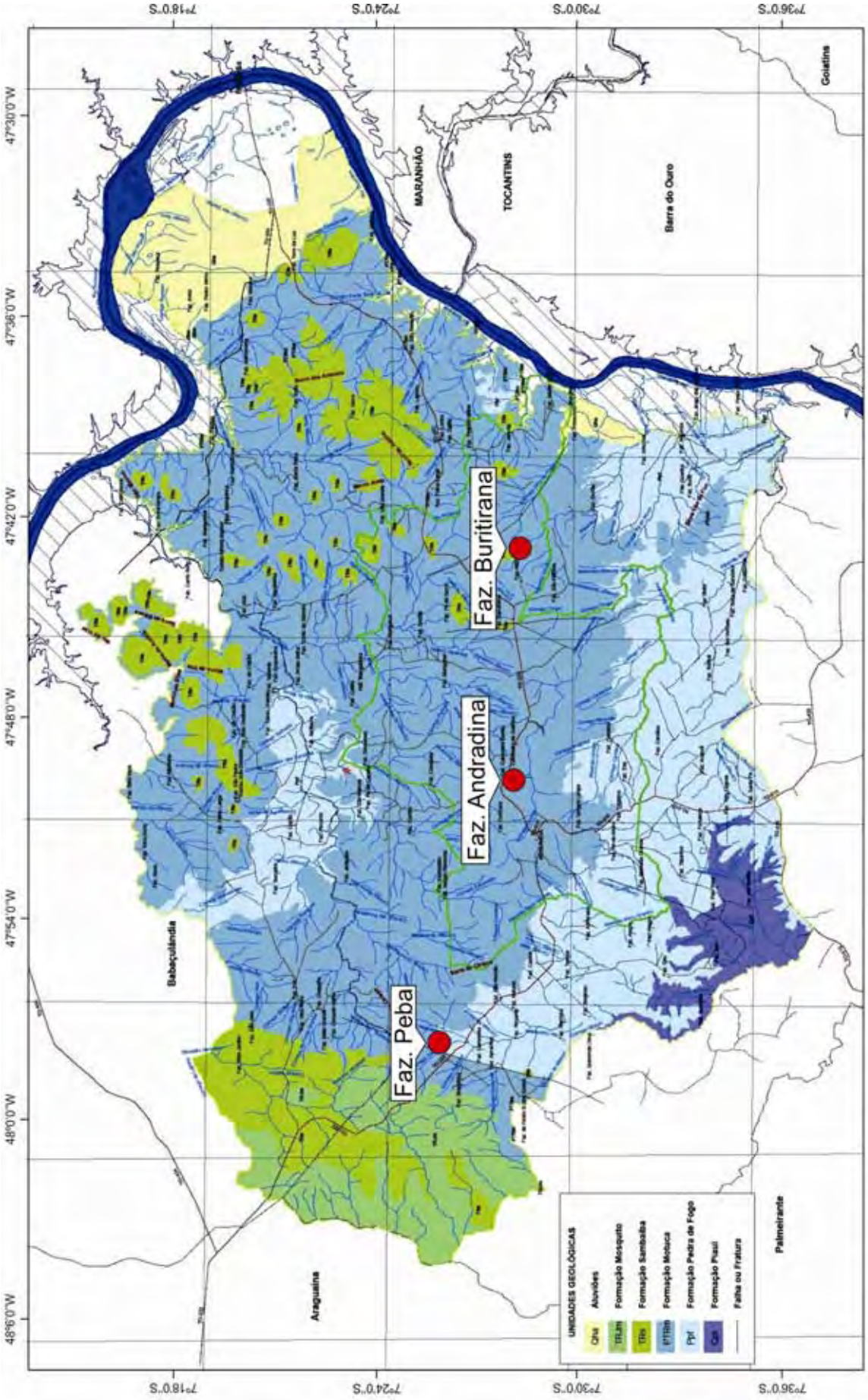

Fig. I.10: Mapa geológico da Bacia do Parnaíba com a localização das fazendas onde os fósseis foram encontrados.

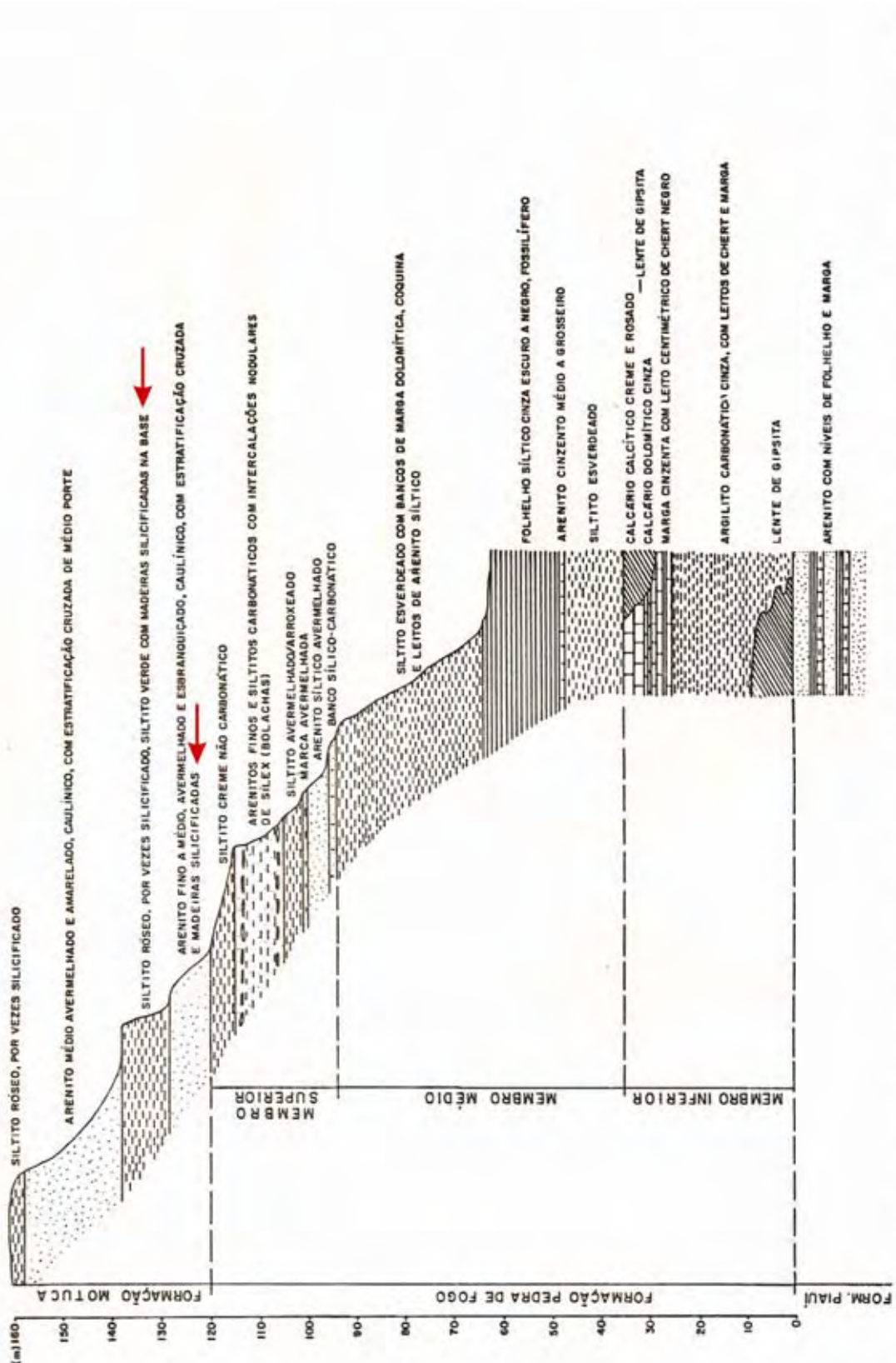

Fig. I.11. Perfil estratigráfico elaborado por Pinto e Sad (1986) para a borda sudoeste da Bacia do Parnaíba, na região de Araguaína-Filadélfia (TO), com as setas indicando os pacotes em que foram encontrados as madeiras silicificadas.

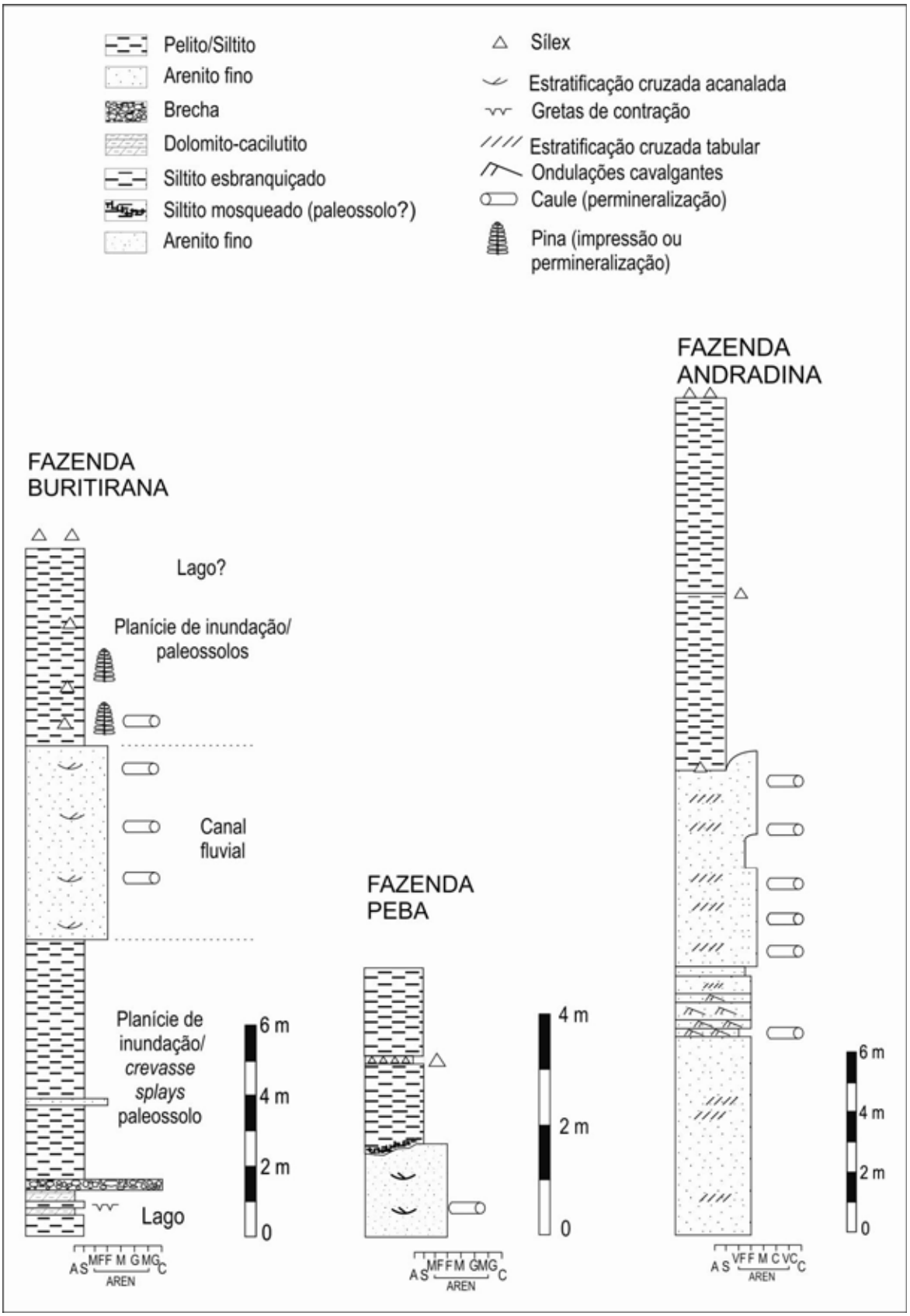

Figura I.12. Perfis estratigráficos das fazendas Andradina, Buritirana e Peba com o posicionamento dos fósseis (Dias-Brito et al., 2007).

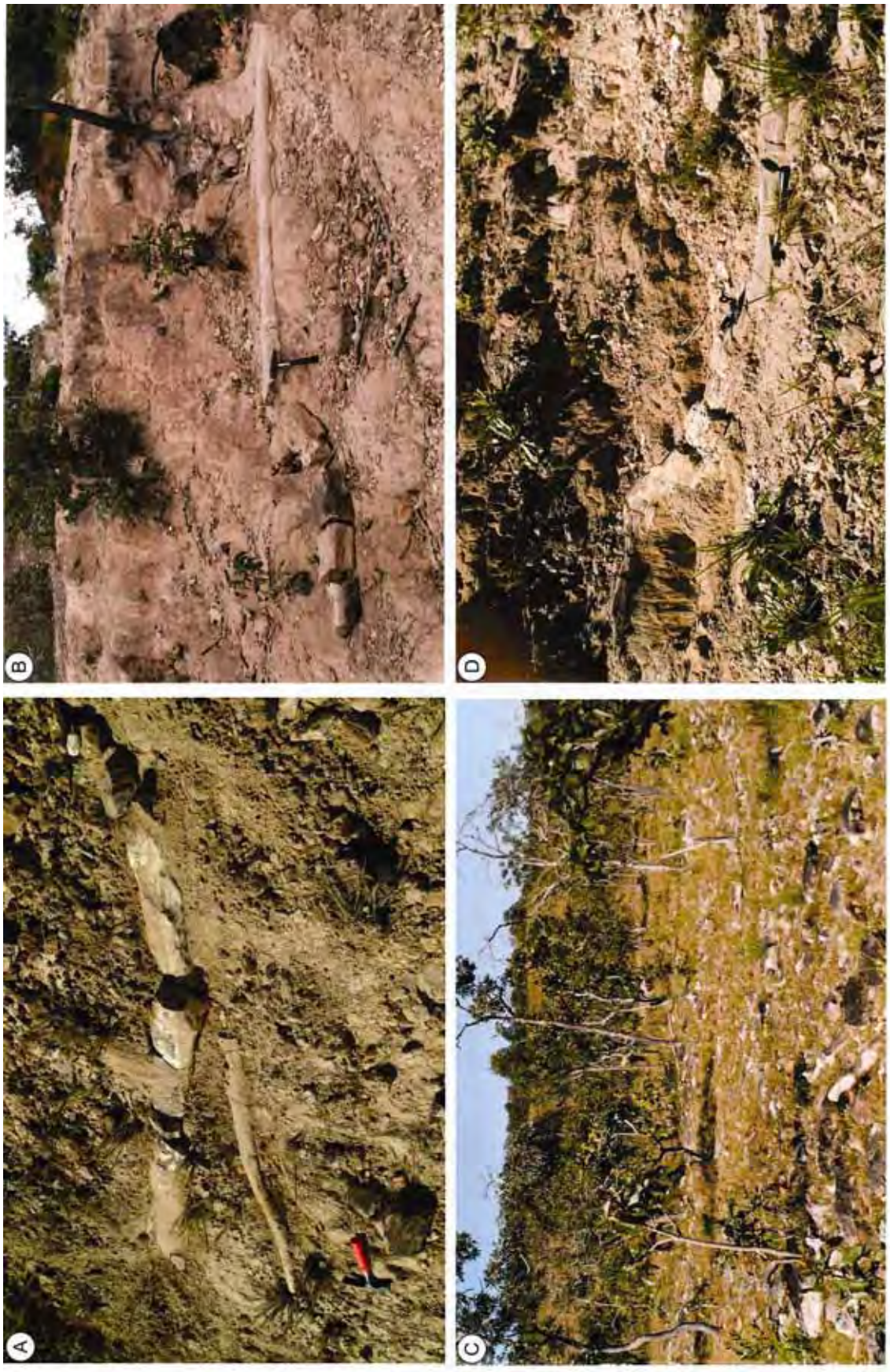

Fig. I.13. Fotos dos fósseis espalhados pelo chão nas fazendas Andradina (A-C) e Buritirana (D): um verdadeiro paraíso para os paleobotânicos.

3.3. Vegetais fósseis encontradas na Bacia do Parnaíba e no MNAFTO e suas implicações paleofitogeográficas e cronoestratigráficas

A Bacia do Parnaíba durante o intervalo Neocarbonífero-Permiano posicionava-se geograficamente entre duas grandes províncias florísticas, a Euramericana e a Gondwânica. Nas palavras de Mussa & Coimbra (1987):

‘‘... que repercussões teriam as componentes das associações permianas da Bacia do Parnaíba sobre as gondwânicas, ou, vice-versa?’’

Além disso, quais seriam as influências da flora euramericana sobre a flora da bacia? Assim, a Tabela I.1 abaixo traz uma revisão sobre os fósseis vegetais encontrados na Bacia do Parnaíba durante o Permiano como subsídio para posterior discussão paleofitogeográfica da área.

Espécie	Classificação Taxonômica	Hábito de vida	Localidades das espécies na Bacia do Parnaíba e os autores que as descreveram	Idade atribuída pelos autores	Outras ocorrências do gênero
Psaronius brasiliensis	**Samambaia** Ordem Marattiales Família Psaroniaceae	arborescente	entre Oieras e São Gonçalo do Amarante e entre Araguaína e Filadélfia (TO) - Brongniart (1872)		Bacia do Paraná, Alemanha, França, EUA, China
Psaronius arrojadoi			Chapada do Jaboti (MA) - Pelourde (1914); Herbst (1985); Monumento Natural das Árvores Fossilizadas do Tocantins (MNAFTO) - Tavares (2011)	Eopermiano - Herbst (1985)	
Psaronius sinuosus			Araguaína (TO) - Herbst (1999); Rößler & Noll (2002)	Eopermiano - Herbst (1999)	
Tietea singularis	**Samambaia** Ordem Marattiales Família Psaroniaceae	arborescente	região de Araguaína (TO) - Herbst (1986); Rößler & Noll (2002); MNAFTO - Tavares (2011)	Permiano - Herbst (1986)	Bacia do Paraná
Tietea derbyi			Carolina (MA) - Herbst (1992)	Permiano	
Fernia costata	**Samambaia** Ordem Marattiales	provavelmente arborescente	Fazenda Buritirana - MNAFTO - Tavares (2011)	Eopermiano-Mesopermiano	endêmico
Tocantinorachis buritiranaensis	**Samambaia** Ordem Marattiales	herbáceo, arbustivo ou arborescente	Fazenda Buritirana - MNAFTO - Tavares (2011)	Eopermiano	endêmico
Pecopteris sp. 1	**Pteridófila** Incetae sedis		Fazenda Buritirana - MNAFTO - Tavares (2011)	Eopermiano-Mesopermiano	cosmopolita
Pecopteris sp. 2	**Pteridófila** Incetae sedis		Fazenda Buritirana - MNAFTO - Tavares (2011)	Eopermiano-Mesopermiano	

Grammatopteris freitasii	**Samambaia** Ordem Filicales Família *Incertae sedis*	arborescente	entre Araguaína e Filadélfia (TO) - Rößler & Galtier (2002a)	Permiano	Alemanha e França
Dernbachia brasiliensis	**Samambaia** Ordem Filicales? Família *Incertae sedis*	arborescente	entre Araguaína e Filadélfia (TO) - Rößler & Galtier (2002b)	Permiano	endêmico
Botryopteris nollii	**Samambaia** Ordem Filicales Família Botryopteridaceae	epífita	entre Araguaína e Filadélfia (TO) - Rößler & Galtier (2003)	Permiano	Alemanha, França, Bélgica, EUA, China
Araguainorachis simplissima	**Samambaia? Pteridosperma?**	herbáceo, arbustivo ou arborescente	rodovia Carolina-Riachão, trevo para Araguaína - Mussa & Coimbra (1987)	Eo a Mesopermiano	endêmico
Arthropitys cacundensis	**Esfenófita** Ordem Calamitales Família Calamitaceae	arborescente	entre Araguaína (TO) e Carolina (MA), a oeste de Bielândia - Coimbra & Mussa (1984)	Mesocarbonífero a Eopermiano	França, Alemanha, Inglaterra, EUA e China
Arthropitys isoramis			MNAFTO - este trabalho	Eopermiano	
Arthropitys tabebuiensis			MNAFTO - este trabalho	Eopermiano	
Arthropitys tocantinensis			MNAFTO - este trabalho	Eopermiano	
Arthropitys barthelii			MNAFTO - este trabalho	Eopermiano	
Arthropitys buritiranensis			MNAFTO - este trabalho	Eopermiano	
Sphenophyllum sp.	**Esfenófita** Ordem Sphenophyllales Família Sphenophyllaceae	herbáceo	entre Araguaína e Filadélfia (TO) - Rößler & Noll (2002)	Permiano	cosmopolita
Amyelon bieloi	**Gimnosperma** Clas. Coniferopsida Ordem Cordaitales	arbustivo ou arbóreo	entre Araguaína (TO) e Carolina (MA), a oeste de Bielândia - Coimbra & Mussa (1984)	Mesocarbonífero a Eopermiano	Inglaterra, EUA, Escócia, China, França
Carolinapitys maranhensis	**Gimnosperma** Ordem Cordaitales?	arbustivo ou arbóreo	entre Araguaína (TO) e Carolina (MA), a oeste de Bielândia - Coimbra & Mussa (1984)	Mesocarbonífero a Eopermiano	endêmico
Cyclomedulloxylon parnaibense	**Gimnosperma** Ordem Pteridospermales?	arbustivo ou arbóreo	rodovia Carolina-Riachão, na altura do trevo para Araguaína (TO) - Mussa & Coimbra (1987)	Eo a Mesopermiano	endêmico
Cycadoxylon brasiliense	**Gimnosperma** Ordem Pteridospermales (Cycadoxyleae)	arbustivo ou arbóreo	rodovia Carolina-Riachão, na altura do trevo para Araguaína (TO) - Mussa & Coimbra (1987)	Início do Mesopermiano	França e Inglaterra
Teresinoxylon euzebioi	**Gimnosperma Ordem** Pteridospermales (Cycadoxyleae)	arbustivo ou arbóreo	Teresina (PI) – Caldas et al. (1989)	Início do Mesopermiano	endêmico
Parnaiboxylon sp.	**Gimnosperma**	arbóreo	MNAFTO - Kurzawe et al. (2013a)	Permiano	endêmico

Parnaiboxylon rohnae	**Gimnosperma**	arbóreo	MNAFTO - Kurzawe et al. (2013a)	Permiano	endêmico
Scleroabietoxylon chordas	**Gimnosperma**	arbóreo	MNAFTO - Kurzawe et al. (2013a)	Permiano	endêmico
Ductoabietoxylon solis	**Gimnosperma**	arbóreo	MNAFTO - Kurzawe et al. (2013a)	Permiano	endêmico
Taeniopitys tocantinensis	**Gimnosperma**	arbóreo	MNAFTO - Kurzawe et al. (2013b)	Permiano	Antártica
Taeniopitys sp.	**Gimnosperma**	arbóreo	MNAFTO - Kurzawe et al. (2013b)	Permiano	
Kaokoxylon punctatum	**Gimnosperma**	arbóreo	MNAFTO - Kurzawe et al. (2013b)	Permiano	Índia, Austrália, África do Sul, Argentina, Antártica
Damudoxylon buritiranaensis	**Gimnosperma**	arbóreo	MNAFTO – Kurzawe et al. (2013b)	Permiano	Índia, Austrália e África do Sul
Damudoxylon humile	**Gimnosperma**	arbóreo	MNAFTO - Kurzawe et al. (2013b)	Permiano	
Damudoxylon rosslerii	**Gimnosperma**	arbóreo	MNAFTO - Kurzawe et al. (2013b)	Permiano	

Tabela I.1: vegetais fósseis encontrados na Bacia do Parnaíba durante o Permiano com classificação taxonômica, hábito de vida, localidade em que foram encontradas, autores que as descreveram e registro em outras localidades.

Pela tabela acima, nota-se a presença de 35 espécies distribuídas em três grandes grupos vegetais: samambaias, gimnospermas e esfenófitas. Dentro desses grupos, as samambaias estão representadas por 13 espécies distribuídas em 9 gêneros, as gimnospermas por 15 espécies em 11 gêneros e as esfenófitas por sete espécies em dois gêneros.

Entre as samambais, quatro gêneros são endêmicos (*Fernia*, *Tocantinorachis*, *Dernbachia* e *Araguainorachis*), representando 44,5% dentro do grupo; entre as gimnospermas, *Carolinapitys*, *Cyclomedulloxylon*, *Teresinoxylon*, *Parnaiboxylon*, *Ductoabietoxylon* e *Scleroabietoxylon* são endêmicos, representando 54,5% dentro do grupo [o gênero *Dadoxylon* não foi considerado por ter sido invalidado por Bamford & Philippe (2001) e Kurzawe & Merlotti (2009)]; os dois gêneros de esfenófita, *Arthropitys* e *Sphenophyllum*, são cosmopolitas. Em relação ao endemismo total, 45,5% dos gêneros são endêmicos, o que justificaria, segundo o conceito de Wnuk (1996), classificar a área como uma Região Florística distinta no contexto florístico do Neopaleozóico.

3.4. O processo de fossilização dos vegetais na Bacia do Parnaíba

Os caules petrificados aqui estudados se formaram através do processo descrito por Schopf (1975) como permineralização celular: soluções saturadas em determinados íons, comumente carbonatos ou silicatos, penetram nos espaços intercelulares e no lúmen da célula após o evento de deposição do vegetal. Paulatinamente, por processos intempéricos e microbiológicos, as células e os tecidos vão sendo decompostos, mas antes da decomposição completa das paredes das células, ocorre a precipitação de substâncias a partir dos íons em solução, preservando a estrutura tridimensional do corpo vegetal.

O tipo mais comum de permineralização é o relacionado à precipitação de sílica. Na grande maioria dos casos, o processo inicia-se com o soterramento do vegetal por cinzas vulcânicas, onde a sílica é muito abundante (Spicer, 1991; Scott & Collinson, 2003; Mustoe, 2003; Matysová et al., 2010). No entanto, o processo também pode ocorrer em depósitos sem cinzas vulcânicas, como em bancos de areia de rios (Mussa & Coimbra, 1984; Weibel, 1996; Mustoe, 2003; Matysová et al., 2010; entre outros). Após a primeira etapa da fossilização, podem decorrer milhares de anos até a total silicificação do vegetal.

Em ambientes pouco ricos em sílica, os silicatos podem tornar-se disponíveis a partir da alteração intempérica de feldspatos, minerais de argila e outros minerais, originando ácido silícico (H_4SiO_4). Sua concentração em águas continentais depende de vários fatores, como o pH da água. Altas concentrações são alcançadas em condições muito alcalinas (pH>10), como em poros de solos ou depósitos sedimentares rasos sujeitos a longas estações secas. Quando as soluções impregnam os espaços dos vegetais, o ácido silícico pode encontrar moléculas do vegetal com radicais hidroxila (-OH), ocorrendo ligações por pontes de hidrogênio. Com a eliminação gradual da água por evaporação, ocorre a polimerização da sílica em diversas etapas até originar opala, calcedônia ou quartzo microcristalino. Adicionalmente, com a degradação orgânica do tecido vegetal, gera-se, entre outros, o gás carbônico (CO_2), o qual forma ácido carbônico (H_2CO_3) e, assim, abaixa localmente o pH do meio e reduz a solubilidade da sílica. Nestas condições, o ácido silícico que impregnou o vegetal sofre precipitação como sílica coloidal ($SiO_2.nH_2O$), posteriormente passando para opala, calcedônia ou quartzo microcristalino

Spicer (1991) e Scott & Collinson (2003) dividiram o processo de fossilização de vegetais em duas etapas. Na primeira, equivalendo à permineralização propriamente dita, as substâncias precipitadas ocupam os lúmens das células e as paredes celulares permanecem praticamente intactas; posteriormente, as paredes celulares também podem sofrer impregnação pelas substâncias, o que corresponde à etapa denominada como petrificação. Por outro lado, Drum (1968) e Leo & Barghoorn (1976), através de experimentos de laboratório, notaram a deposição da sílica primeiramente na superfície interna da parede celular, a qual apresenta maior resistência à degradação, produzindo réplicas dos espaços celulares. Assim, embora os dois termos - permineralização e petrificação - não sejam exatamente sinônimos, são aqui usados com o mesmo sentido.

Scurfield & Segnit (1984) sintetizaram o processo em cinco etapas principais: i) entrada da sílica em solução ou na forma coloidal no tecido vegetal; ii) preenchimento dos poros das paredes celulares; iii) decomposição das paredes celulares concomitantemente com a formação de um molde da estrutura tridimensional do tecido vegetal; iv) deposição da sílica em espaços vazios da parede silicificada, simultaneamente ou não com o preenchimento do lúmen; v) petrificação completa com perda de água e possível transformação da sílica de uma forma a outra através da substituição ou recristalização. Alguns trabalhos, embora numa escala de tempo infinitamente menor que a escala geológica, demonstraram experimentalmente a viabilidade do processo acima (Drum, 1968; Leo & Barghoorn; 1976).

Na Bacia do Parnaíba, a paisagem era composta por um sistema fluvial com bancos de areia nos canais e nas margens, onde se fixavam os vegetais. Não há evidências de vulcanismo na bacia durante o Permiano (Matysová et al., 2010). O processo da permineralização era facultado muito provavelmente pela sazonalidade climática: nas estações úmidas, alteração de minerais silicáticos; nas estações secas, quando águas intersticiais se tornavam muito alcalinas (pH>10), transporte e concentração do ácido silícico e precipitação da sílica nos vegetais (pH<10). O processo de permineralização dos caules de esfenófitas deve ter ocorrido muito rapidamente após a deposição dos vegetais, considerando-se a manutenção da forma cilíndrica original de muitos exemplares. É provável que em tais caules o processo de fossilização se iniciou enquanto se encontravam em

posições muito rasas de sepultamento, sem pressão significativa de sedimentos sobrepostos. Alguns caules de esfenófitas sofreram maior compactação, inclusive tendo ocorrido colapso da cavidade da medula. Ainda assim, seu corpo secundário não sofreu significativas deformações e as células mantiveram suas formas originais. Portanto, os caules mais achatados também devem ter experimentado um processo de permineralização bastante rápido.

4. O estado da arte da Classe Sphenopsida

A Classe Sphenopsida (do grego *spheno*, cunha + *phyton*, planta) constitui-se de plantas com hábitos herbáceos, arbustivos, arbóreos e até mesmo trepadores. Como grande característica diagnóstica possui a parte aérea articulada, composta por entrenós delimitados por uma linha nodal; internamente, um diafragma separa um nó do outro na linha nodal. Os entrenós são marcados por estrias e sulcos que se dispõem longitudinalmente e marcam interna e externamente a posição do sistema vascular. São plantas radialmente simétricas. Os representantes modernos apresentam rizomas subterrâneos de onde partem raízes adventícias.

Os caules apresentam ramificação monopodial. Nesses surgem verticilos de pequenas folhas que em alguns gêneros se fundem na base formando uma bainha. As folhas são classificadas como megafilos (Antunes & Pinto, 2006; Tomescu, 2008). Os ramos surgem nos nós e, em geral, sua presença é inferida através das cicatrizes no caule, que podem ser circular, subcircular ou elipsoidal (Taylor & Taylor, 1993). O cilindro vascular é do tipo protostélico a sifonostélico, com maturação tanto endarca quanto exarca (Taylor et al., 2009).

As estruturas reprodutivas estão arranjadas em estróbilos que ficam localizados no ápice da planta. Ao menos no gênero *Equisetum*, os anterozóides necessitam da água pra alcançar a oosfera (Raven et al., 2001), como ilustra a Figura I.14.

Traverse (2007) atribui às esfenófitas esporos do tipo *Calamospora*, embora Balme (1995) descreva uma série de outros grupos em que esse tipo espeorofítico pode ser encontrado. Os esporos de *Equisetum* apresentam um elatério, enrolados ao redor do esporo quando em condições úmidas e desenrolados quando em condições secas (Foster & Gifford, 1974).

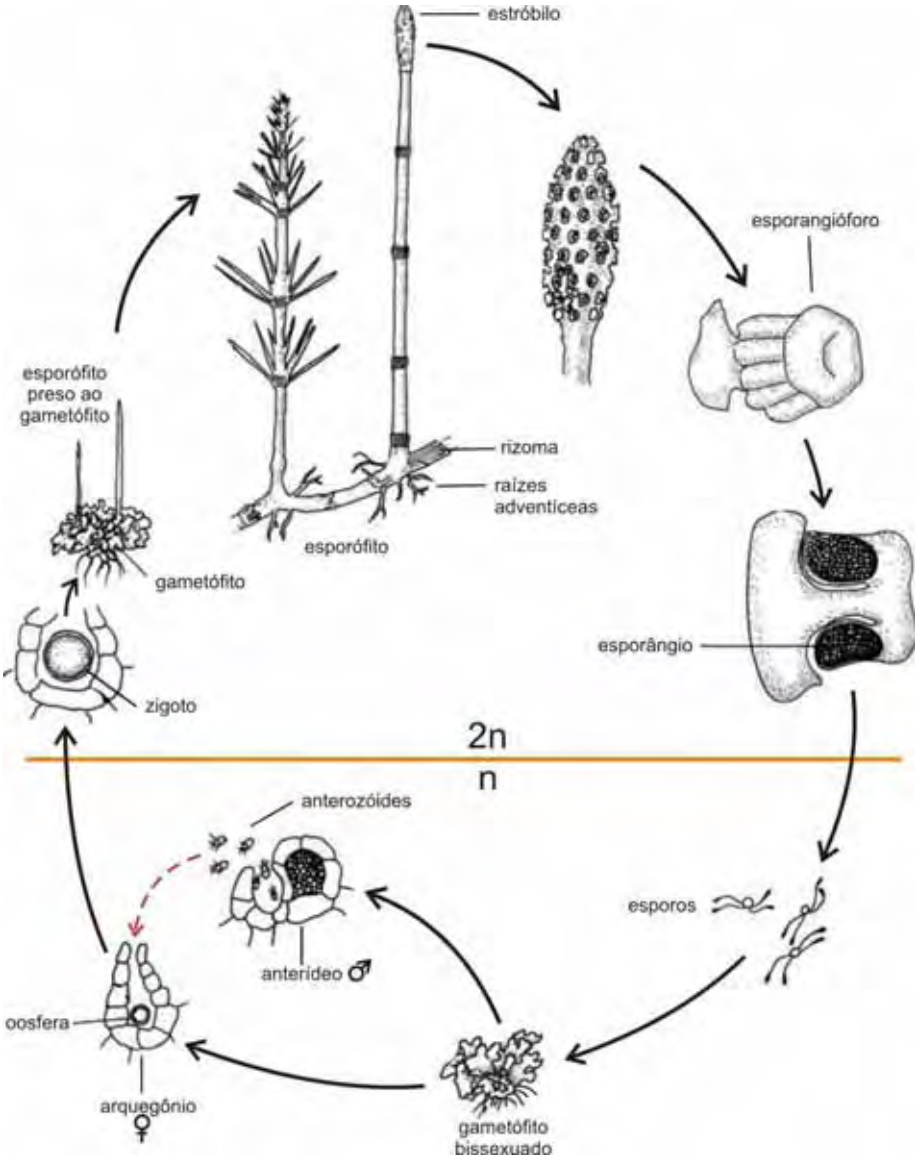

Figura I.14. Ciclo de vida de *Equisetum*. Nesse gênero, o anterozóide necessita da água para alcançar a oosfera (modificado de Taylor & Taylor, 1993).

Anatomicamente, as esfenófitas apresentam uma grande medula central e a maioria das espécies possui apenas crescimento primário. Os gêneros *Archaeocalamites*, *Arthropitys*, *Arthroxylon*, *Calamitae* e *Sphenophyllum* possuem crescimento secundário. As espécies que apresentam apenas desenvolvimento primário possuem canais carinais, responsáveis pela condução de água, e canais valeculares, que representam reservatórios de oxigênio; espécies com crescimento secundário apenas canais carinais (Figura I.15).

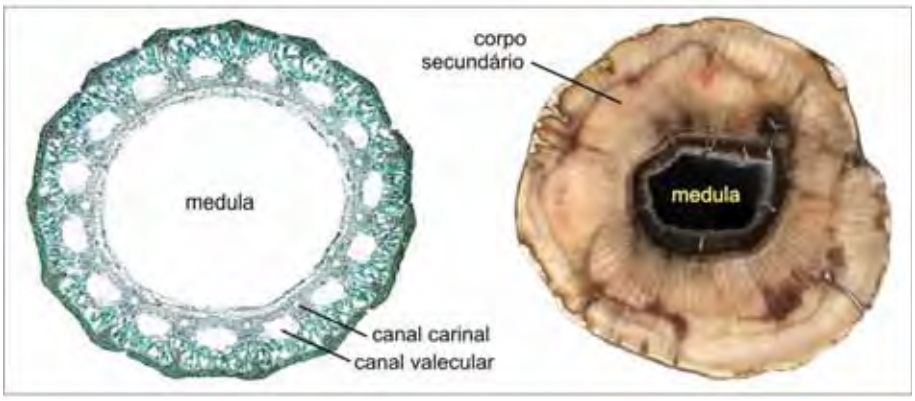

Figura I.15. Cortes transversais mostrando a diferença entre espécies que apresentam apenas desenvolvimento primário, como em *Equisetum* sp. (esquerda) e espécies que apresentam desenvolvimento secundário, como em *Arthropitys* sp. Imagem da esquerda: www.digicoll.library.wisc.edu/WebZ/initialize?ses.

Segundo Skog & Banks (1973), a Ordem Sphenophyllales e as espécies do gênero *Archaeocalamites* derivaram das trimerófitas via *Ibykales* durante o Neodevoniano-Mississippiano (Figura I.16). Stewart & Rothwell (1993) também se detiveram sobre o tema e propuseram um quadro um pouco mais completo para as relações de parentesco dentro do grupo (Figura I.17).

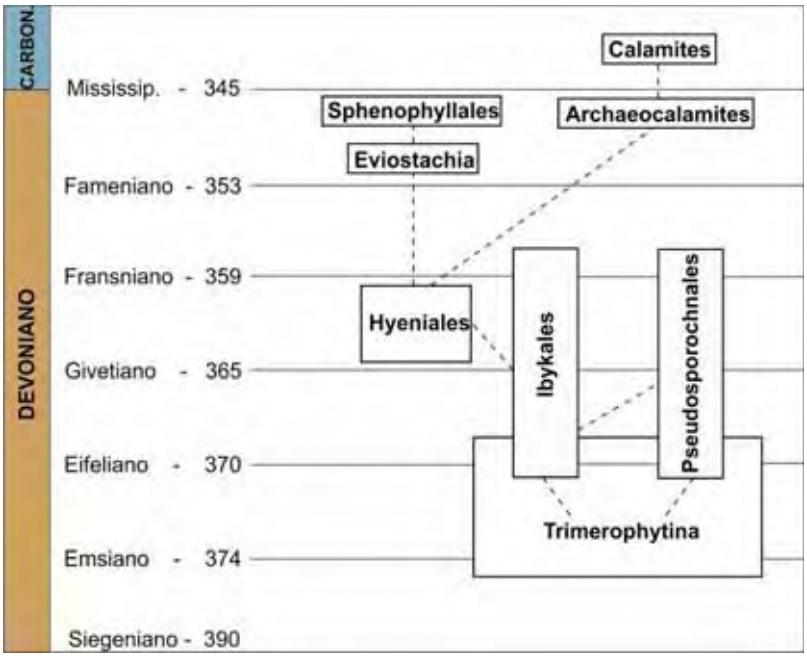

Figura I.16. Relações de parentesco entre as Trimerophytina, Ibykales e as Hyeniales segundo Skog & Banks (1973).

Ibyka amphikoma figura como o ancestral das esfenófitas, representada por impressões/compressões encontradas em sedimentos mesodevonianos no Estado de Nova Iorque. A espécie possui ramificação monopodial, ramos

dispostos de modo helicoidal cobertos por pêlos, folhas tridimensionais, sistema vascular protostélico tri-lobado e esporângios elípticos (Skog & Banks, 1973).

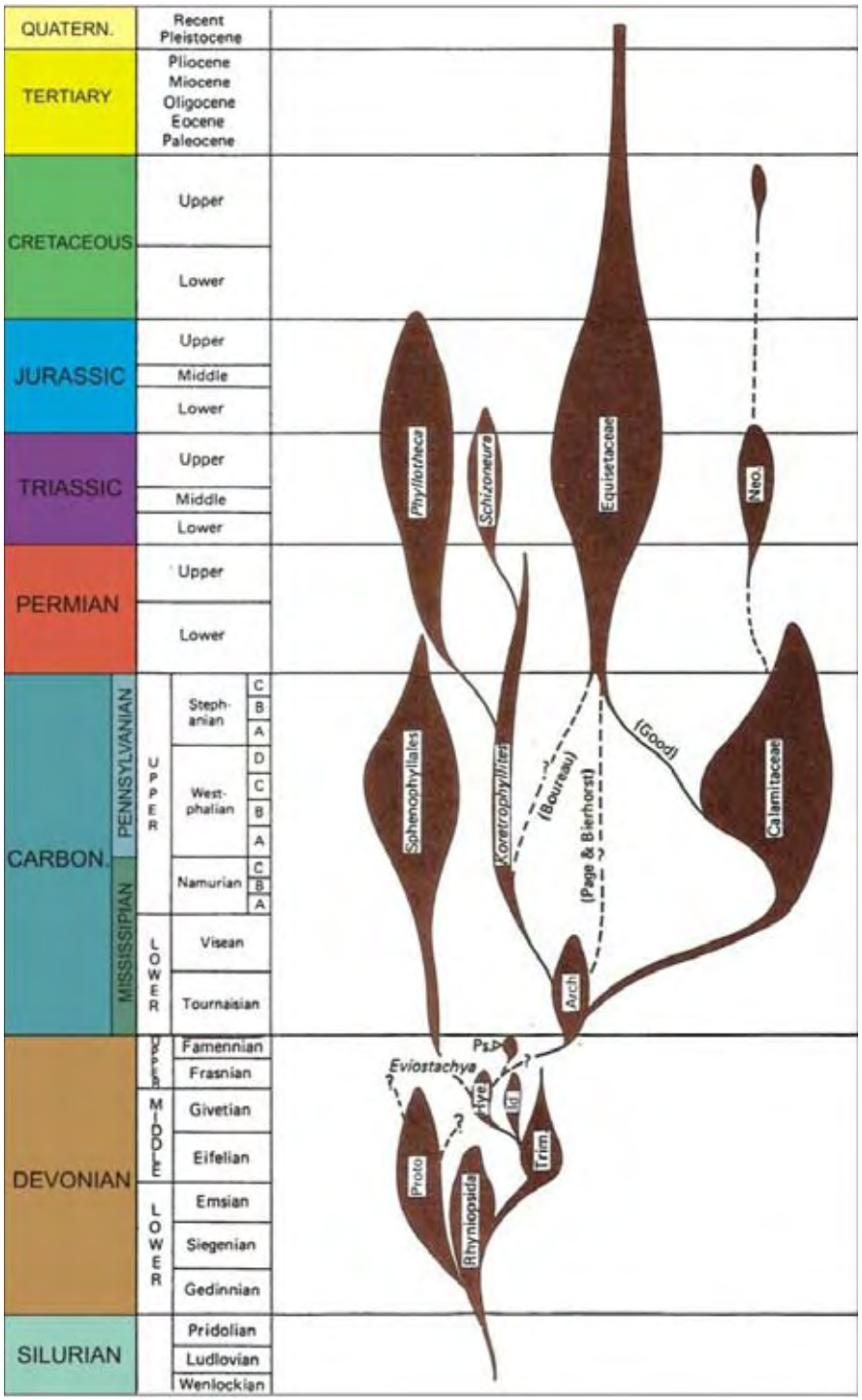

Figura I.17. Proposta de Stewart & Rothwell (1993) para as relações de parentesco dentro do grupo das esfenófitas ao longo do tempo geológico. Arc: Archaeocalamites; Hye: Hyeniales; Id: Iridopteridales; Neo: Neocalamitaceae; Proto: Protolepidodendrales; Ps: Pseudoborniales.

Há um consenso entre os autores que durante o Carbonífero e o Eo-Permiano, as esfenófitas herbáceas e arbóreas foram muito abundantes e co-

existiram com as licófitas, sendo consideradas como o segundo grupo em importância na constituição das florestas deste período, alcançando grande diversificação e distribuição mundial (Foster & Gifford, 1974; Rößler & Noll, 2010). Hoje, resta apenas o gênero *Equisetum*, composto por 25 espécies (Stewart & Rothwell, 1993).

As ordens da Classe Sphenopsida

As ordens da Classe Sphenopsida são separadas de acordo com seus esporangióforos (Meyen, 1987).

- Delevoryas (1962) dividiu a classe em cinco ordens: Hyeniales (†), Pseudoborniales (†), Sphenophyllales (†), Calamitales (†) e Equisetales;

- Boureau (1964) dividiu a classe em quatro ordens: Hyeniales (†), Pseudoborniales (†), Sphenophyllales (†) e Equisetales;

- Ogura (1972) dividiu a classe em seis ordens: Protoarticulales (†), Sphenophyllales (†), Cheirostrobales (†), Pseudoborniales (†), Calamariales (†) e Equisetales;

- Meyen (1987) dividiu a classe em três ordens: Sphenophyllales (†), Equisetales e Calamitales (†);

- Taylor & Taylor (1993) e Taylor et al. (2009) dividiram a classe nas Ordens Pseudoborniales (†), Sphenophyllales (†) e Equisetales;

- Frey (2009) dividiu a classe nas Ordens Pseudoborniales (†), Sphenophyllales (†), Calamitales (†) e Equisetales.

Meyen (1987) considerou que a Ordem Pseudoborniales foi pobremente descrita, não a considerando como tal. Outra divergência diz respeito às ordens Equisetales e Calamitales. Historicamente, Equisetales incluía esfenófitas herbáceas sem crescimento secundário, enquanto Calamitales incluía indivíduos arborescentes com crescimento secundário (Taylor et al., 2009). Frey (2009) considerou Calamitales para as esfenófitas com crescimento secundário e Equisetales para aquelas sem crescimento secundário, sendo essa última proposta utilizada neste trabalho (Figura I.18). Abaixo, segue-se uma breve descrição das ordens e suas principais famílias segundo Boureau (1964) e Taylor et al. (2009).

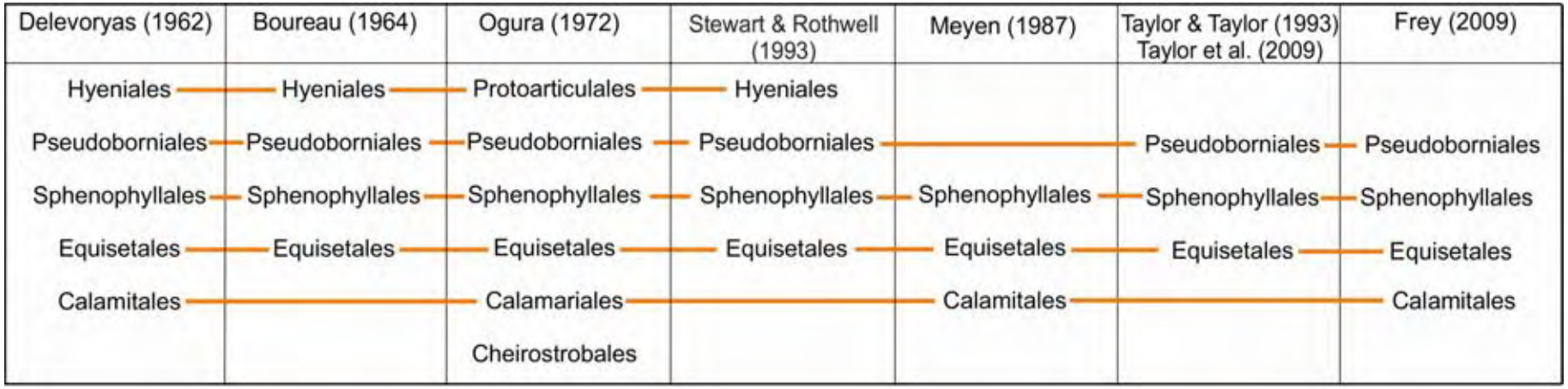

Figura I.18. Classificação da Ordem Sphenopsida por diferentes autores. A linha vermelha indica correspondência das ordens entre os autores.

1) Ordem Pseudoborniales (†): ordem monoespecífica. *Pseudobornia ursina* (Figura I.19), de idade neodevoniana, encontrada na Ilha Bear, sul de Spitsbergen, apresenta caules monopodiais com diâmetro basal de até 60 cm, 15 a 20 metros de altura e preservadas como impressão. Os nós são distintos com espaçamentos de até 80 cm. Os ramos podem chegar a três metros de comprimento, diâmetro de até 10 cm e estão dispostos em verticilo. As folhas são dicotomizadas, podem chegar a 6 cm de comprimento e 1 cm de largura. As venações não são conhecidas. Os estróbilos apresentam comprimento de até 30 cm e dispostos na porção terminal dos ramos. Cada unidade fértil é formada de brácteas em verticilo e esporangióforos divididos em dois segmentos; os esporângios inserem-se nestes e encerram os esporos em sua porção abaxial.

Figura I.19. *Pseudobornia ursina*. Ilustração da esquerda: Frey (2009). Ilustração da direita: Taylor et al. (2009).

2) Ordem Sphenophyllales (†) (Figura I.20): são encontradas do Devoniano ao Triássico, com seu apogeu no Carbonífero e muito abundantes como compressões e impressões. São plantas pequenas, eretas, de crescimento monopodial e que podiam alcançar até 1 metro de altura. Existem autores que consideram a ordem como arbustiva enquanto outros como trepadeiras. O gênero

Sphenophyllum (Figuras I.21 e I.22), que engloba caules e folhas, é bastante característico desta ordem. O caule não apresenta medula, possui um estelo triarco e um cilindro de xilema secundário formado por traqueídes e raios de xilema. As folhas são estreitas na base, alargam-se em direção ao ápice, a venação se divide dicotomicamente por toda a lâmina foliar e a margem distal é bastante denteada.

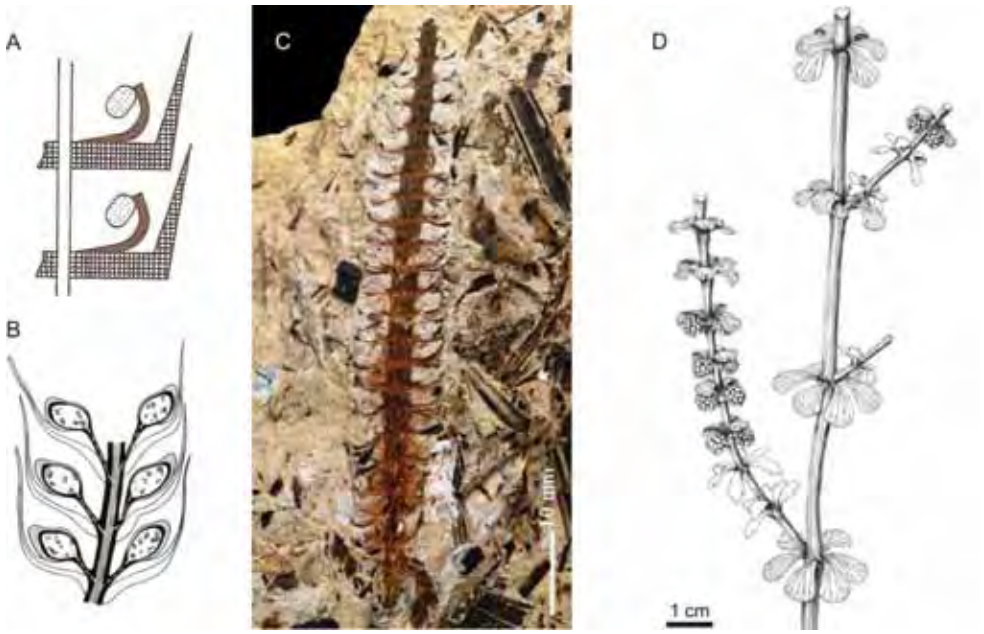

Figura I.20. A: Estróbilo esquemático da Ordem Sphenophyllales: em preto o esporangióforo, em hachurado as brácteas e pontilhado os esporângios (Meyen, 1987); **B**: Corte longitudinal de *Sphenostrobus thompsonii* (Boureau, 1964). **C**: Impressão de *Bowmanites* sp. **D**: Ilustração de *Lilpopia raciborskii* (Kerp, 1984a).
C: http://www.nrm.se/images/18.494d73201246d535da780006242/S139411-p04+Bowmanites+sp..jpg., em 06/08/2012.

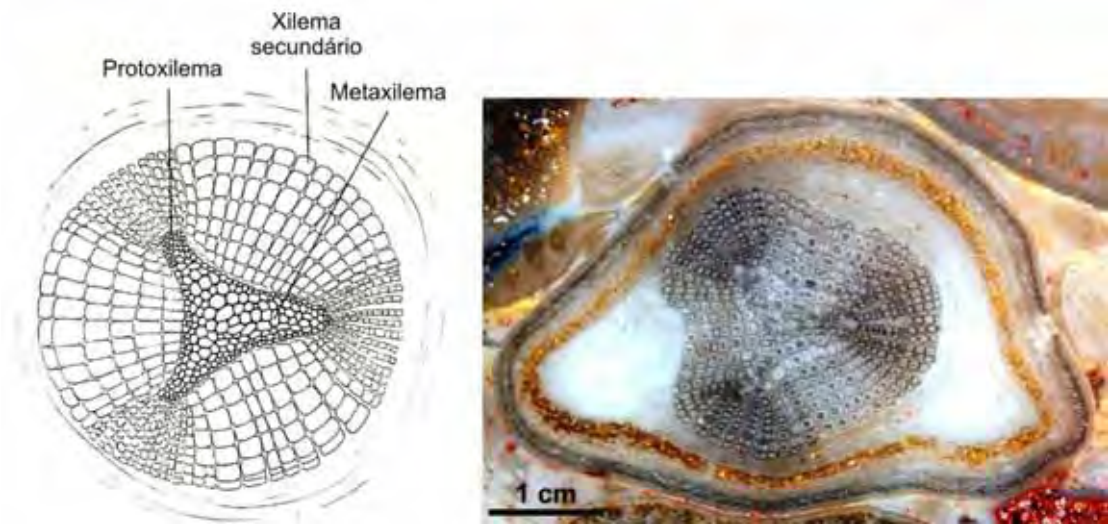

Figura I.21. Ilustração da esquerda: caule de *Sphenophyllum* sp. (Foster & Gifford, 1974). Imagem da direita: corte transversal de um caule de *Sphenophyllum* sp.

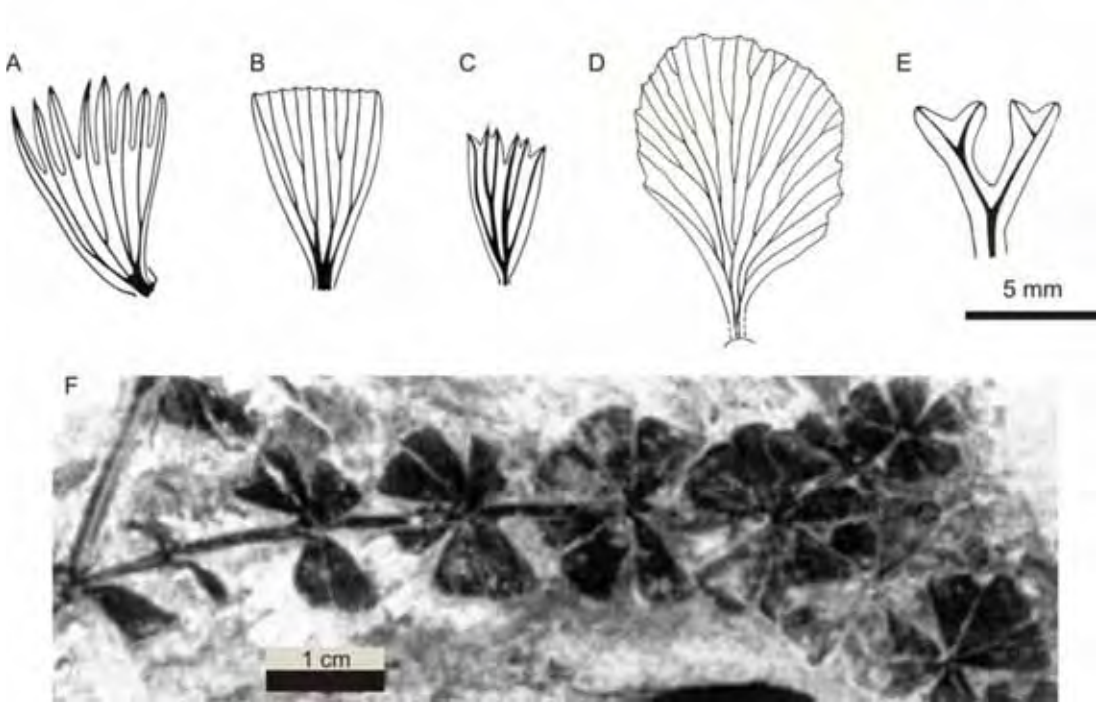

Figura I.22. Tipos foliares de *Sphenophyllum* sp. **A**: Folha de *Sphenophyllum cornutum.* **B**: Folha de *Sphenophyllum emarginatum.* **C**: Folha de *Sphenophyllum angustifolium*. **D**: Folha de *Sphenophyllum obovatum.* **E***:* Folha de *Sphenophyllum arkansanum.* **F**: Impressão de *Sphenophyllum emarginatum.* Figuras A-E: Abbott (1958). Figura F: *Sphenophyllum emarginatum* (Batemburg, 1977).

Os gêneros *Sphenophyllostachys, Sphenostrobus, Eviostachya, Volkmannia, Peltastrobus, Cheirostrobus, Bowmanites e Sentinostrobus* são constituídos de estróbilos, cuja diferenciação se dá pelo formato do estelo do eixo, número de esporangióforos por bráctea, conexão dos esporângios nos esporangióforos, número de apêndices por nó e pela morfologia dos esporos (Good, 1975; Riggs & Rothwell, 1985). *Gondwanophyton* e *Lilpopia* representam caules férteis.

3) Ordem Calamitales (Figura I.23): essa ordem compreende 12 órgãos-gênero de família *incertae sedis* relativos a moldes medulares, folhas com estrutura celular preservada, folhas preservadas como impressões, raízes com estrutura celular preservada e raízes preservadas como impressões **(Grupo I)**, e mais 6 famílias bem caracterizadas **(Grupo II)**, detalhadas abaixo.

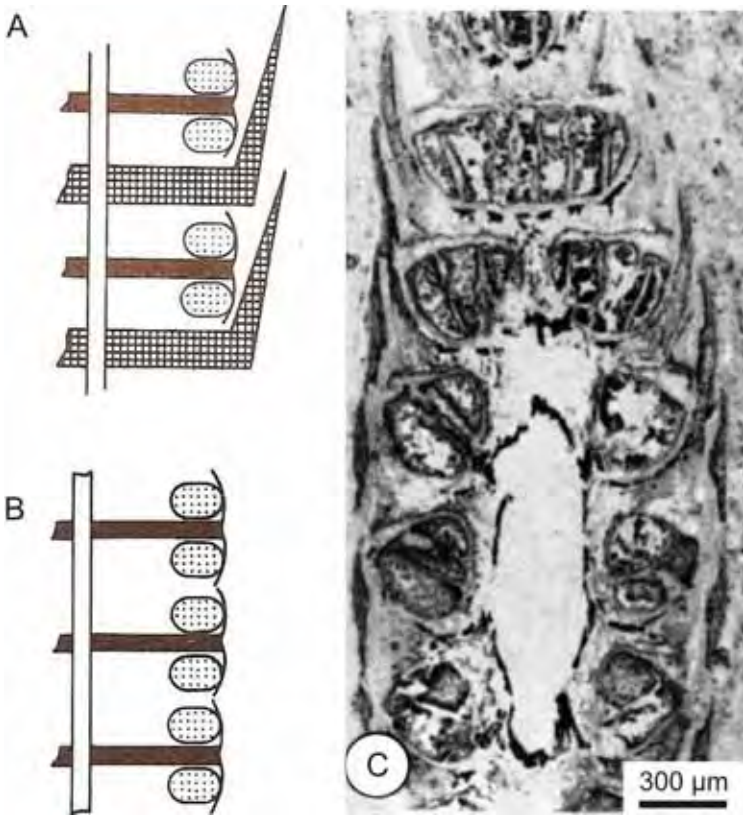

Figura I.23. A e B: Estróbilos esquemáticos da Ordem Calamitales: em preto o esporangióforo, em hachurado as brácteas e pontilhado os esporângios (Meyen, 1987); **C**: Impressão de *Palaeostachya* sp. (Good & Taylor, 1974).

Grupo I

I.1. Gênero *Paracalamites* Zalessky, 1927 (Figura I.24)

Constituído de moldes medulares. Como característica comum, todos os espécimes deste gênero possuem estrias e sulcos que não se desviam na passagem de um nó a outro. Como são caules de difícil classificação, muitas vezes é preciso conhecer a natureza das folhas e/ou dos ramos férteis. Caules com folhas muito dicotomizadas pertencem à Família Archaeocalamitaceae; com associações às folhas de *Annularia* e portando cones de *Angarotheca* são colocados na Família Apocalamitaceae; com folhas fixas com uma ou duas dicotomias podem pertencer à Família Authophyllitaceae. Associações com órgãos foliares permitem colocar exemplares de *Paracalamites* em famílias como Phyllotecaceae, Schizoneuraceae ou Sorocaulaceae.

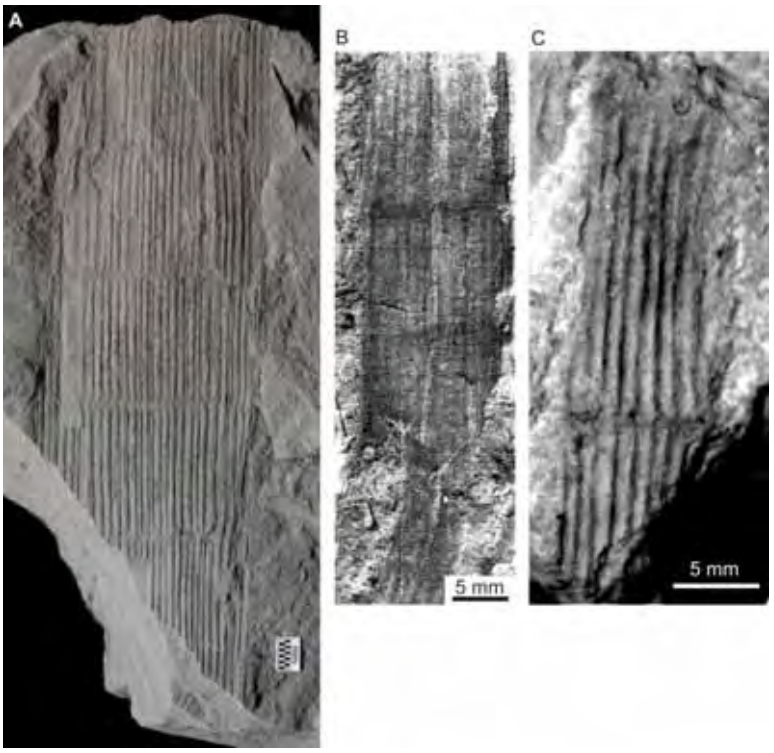

Figura I.24. **A**: Impressão de *Paracalamites australis*. **B**: Impressão de *P. levis* (Zampirolli & Bernardes-de-Oliveira, 2000). **C**: Impressão de *P. australis* (Mune & Bernardes-de-Oliveira, 2007). **A**:www.nrm.se/en/menu/researchandcollections/departments/palaeobotany/collections/databases/paustralia/paustraliaewington/paustraliaewingtontaxa.16123.html em 01/02/2012.

I.2. Gênero *Annularia* Sternberg, 1823 (Figura I.25)

Órgãos foliares conhecidos como impressões. As folhas são lanceoladas ou espatuladas, possuem base pouco embainhada, de modo que os verticilos formam um invólucro curto e longo ao redor do ramo. Apresentam veia única de largura entre 1/7 a ½ da largura total da folha.

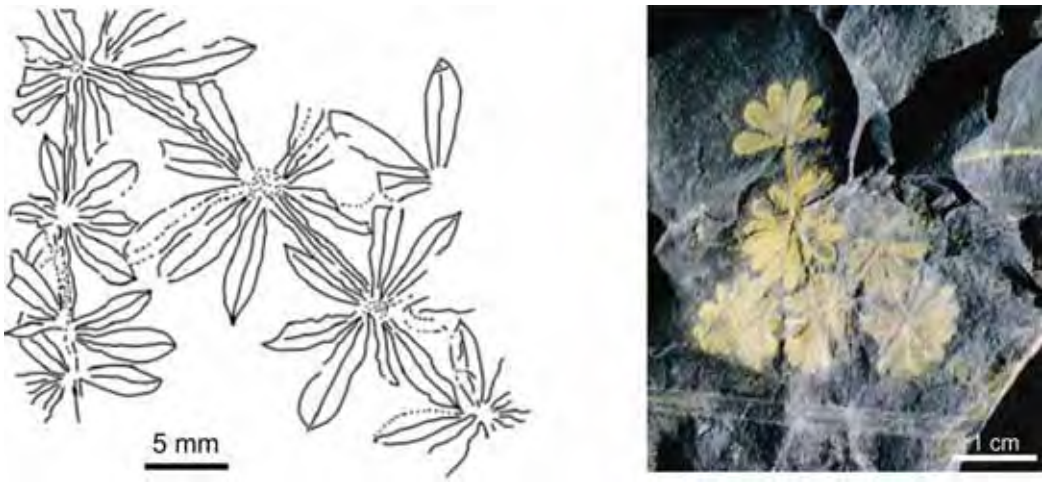

Figura I.25. Ilustração da esquerda: *Annularia* sp. (Banerjee et al., 2009). Imagem da direita: *Annularia* sp. http://www.xs4all.nl/~steurh/engcalam/eannulsp.html, em 02/01/2011.

I.3. Gênero *Asterophyllites* Brongniart, 1822 (Figura I.26)

Órgãos foliares preservados como impressões. Folhas com formato aciculado, ápice acuminado, apresentam bainha invaginante e apenas uma veia de largura igual a ¼ ou ½ da largura total da folha. As folhas dispõem-se em dois verticilos nos nós, formando com o ramo principal um ângulo de aproximadamente 60^{o} geralmente tocando o nó acima.

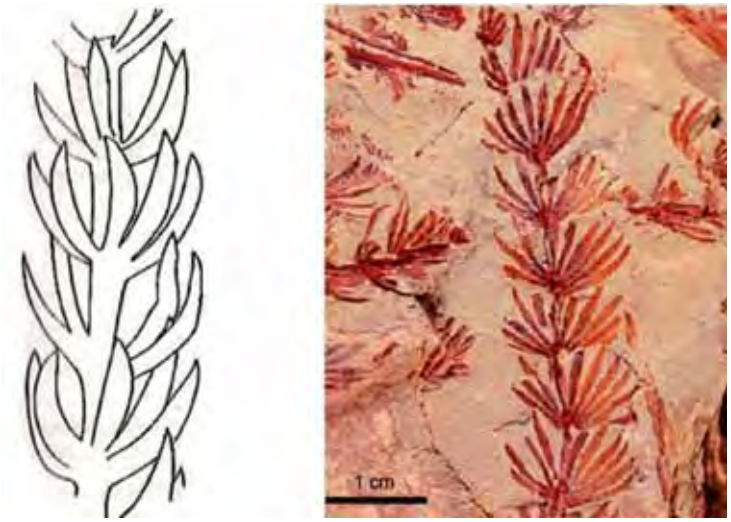

Figura I.26. Ilustração da esquerda: *Asterophyllites* sp. (Boureau, 1964). Imagem da direita: *Asterophyllites* sp. (Taylor et al., 2009).

I.4. Gênero *Lobatanullaria* Kawasaki, 1927 (Figura I.27)

Órgãos foliares preservados como impressões. Folhas uninervadas, espatuladas, oblanceoladas e lineares, dispostas em verticilos em um plano quase paralelo ao eixo, com um formato de “avental”.

Figura I.27. Ilustração da esquerda: *Lobatannularia* sp. (Boureau, 1964). Imagem da direita: *Lobatannularia* sp. (Taylor et al., 2009).

I.5. Gênero *Annulariopsis* Zeiller, 1903 (Figura I.28)

Órgãos foliares preservados como impressões. Folhas lanceoladas ou espatuladas, livres até a base, com cada verticilo em um plano praticamente perpendicular ao caule.

Figura I.28. A: impressão de *Annulariopsis inopinata* (Boureau, 1964). **B**: Impressão de *Annulariopsis* sp. (www.nrm.se/.../schweitzertaxaab.9411.html em 16/02/2011).

I.6. Gênero *Dicalamophyllum* Sterzel, 1880 (Figura I.29)

Órgãos foliares com estrutura celular preservada. Folhas bifurcadas, retilíneas ou pouco encurvada, pontuadas ou aciculadas. Um dos lados convexo ou arredondado e outro mais retilíneo, apresentando dois sulcos bem marcados contendo linhas de estômatos. Em um dos lados pode haver apenas um sulco longitudinal mediano pouco marcado. Folha percorrida por apenas um feixe vascular mediano, com xilema pouco desenvolvido.

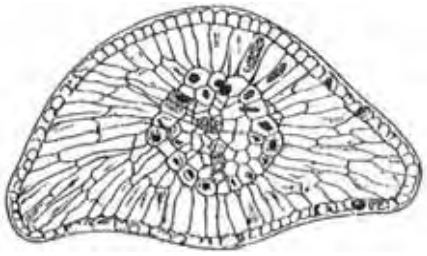

Figura I.29. Corte transversal de *Dicalamophyllum* sp. (Boureau, 1964).

I.7. Gênero *Myriophylloides* Hick & Cash, 1881 (Figura I.30)

Raízes com estrutura celular preservada. Apresenta em corte transversal

estrutura sifonotélica tetrarca ou poliarca, com reduzido parênquima medular. O protoxilema é mesarco ou endarco.

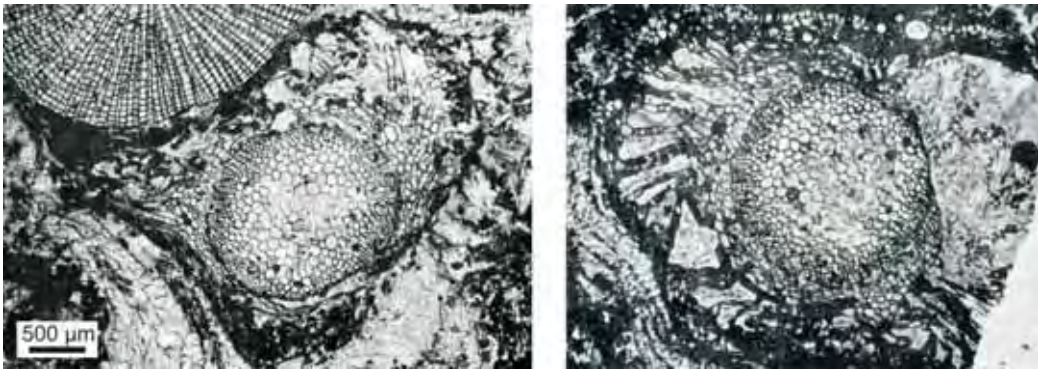

Figura I.30. Cortes transversais de *Miryophylloides williamsonii* (Leistikow, 1962).

I.8. Gênero *Astromyelon* Williamson, 1878 (Figura I.31)

Raízes com estrutura celular preservada. Em corte transversal, o gênero possui grande quantidade de células parenquimáticas medulares e elementos secundários contínuos em volta desta. O protoxilema é mesarco.

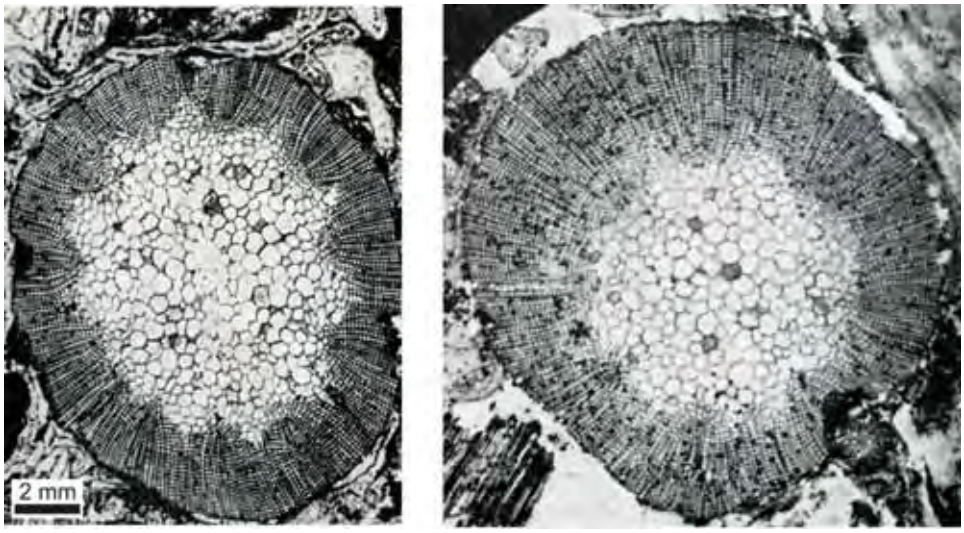

Figura I.31. Cortes transversais de *Astromyelon williamsonii* (Leistikow, 1962).

I.9. Gênero *Asthenomyelon* Leistikow, 1962 (Figura I.32)

Raízes com estrutura celular preservada. Apresenta em corte transversal reduzida quantidade de células parenquimáticas na medula e grandes lacunas radiais. O protoxilema é mesarco.

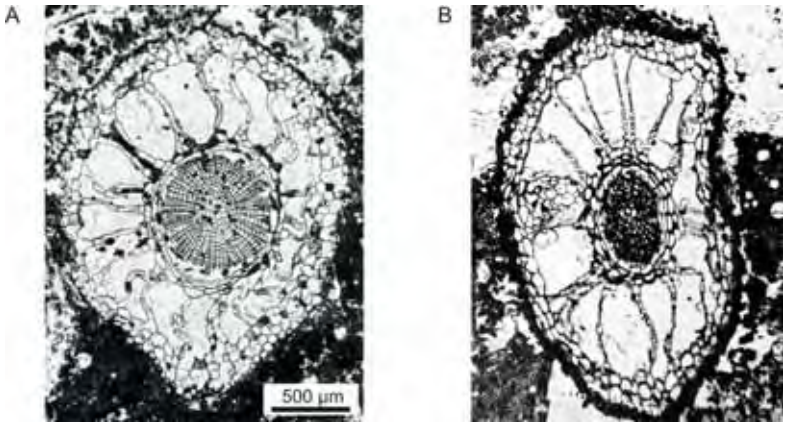

Figura I.32. A e **B**: Cortes transversais, respectivamente, de *Asthenomyelon adversale e Asthenomyelon tenuitrabeculatum* (Leistikow, 1962).

I.10. Gênero *Zimmermannioxylon* Leistikow, 1962 (Figura I.33)

Raízes com estrutura celular preservada, actinostética poliarca, com reduzida zona medular e ausência de xilema secundário. *Zimmermannioxylon* apresenta protoxilema mesarco.

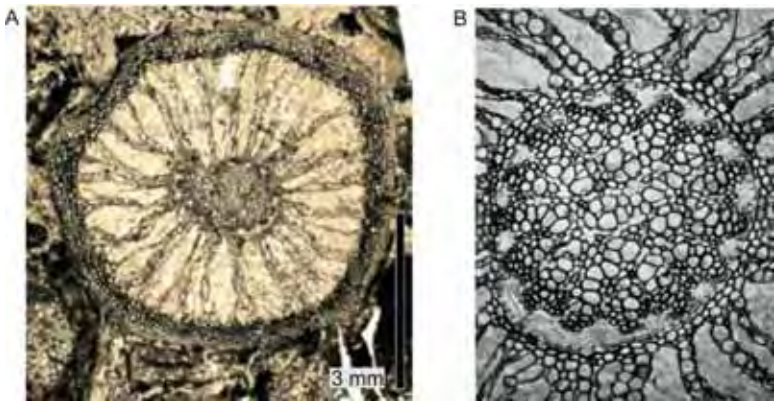

Figura I.33. A e **B**: Cortes transversais de *Zimmermannioxylon multangulare.* **A**: Taylor et al. (2009). **B**: Leistikow (1962).

I.11. Gênero *Myriophyllites* Artes, 1925 (Figura I.34)

Raízes preservadas como impressão/compressão, com raízes adventíceas não articuladas portando pêlos radiculares dispostos aleatoriamente por toda a estrutura.

I.12. Gênero *Pinnularia* Lindley & Hutton, 1832

Raízes preservadas como impressão/compressão, com raízes adventíceas não articuladas com pêlos radiculares dispostos em duas fileiras opostas.

Figura I.34. Impressão de *Myriophyllites* sp. (Taylor et al. 2009).

Grupo II

II.1. Família Archaeocalamitaceae Stur, 1875 (Figura I.35)

Essa família compreende esfenófitas primitivas com estruturas vegetativas e cones de frutificação. A família está baseada no gênero *Archaeocalamites* Stur, 1875, preservado como moldes externos, moldes medulares e permineralizações. A grande característica do gênero é que as estrias longitudinais não se desviam na passagem de um nó a outro, apresentando por isso terminações retangulares bastante diferentes do gênero *Calamites*. Quando preservados como permineralizações, o caule apresenta o corpo secundário com uma lacuna subterminal e os raios fasciculares e interfasciculares não muito separados uns dos outros como em *Arthropitys*. Outros gêneros desta família: *Pothocites* (estróbilos), *Pothocitopsis* (estróbilos), *Protocalamostachys* (estróbilos) e *Protocalamites* (caule).

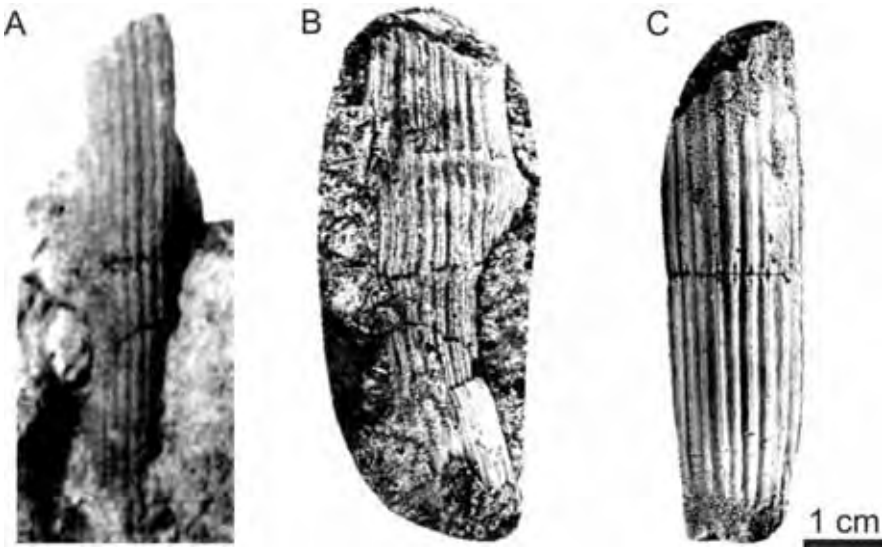

Figura I.35. Impressões de *Archaeocalamites radiatus*. **A**: Lacey & Eggert (1964). **B** e **C**: Orlova (2007).

II.2. Família Autophyllitaceae Radczenko, 1960 (Figura I.36)

Família constituída por cinco gêneros dos quais três representam caule preservados como impressões. Os caules são finos, longos, com nós bastante aparentes e folhas em verticilo muitas vezes bifurcadas. As estrias se desviam pouco na passagem de um nó a outro. Os gêneros *Sphenasterophyllites*, *Autophyllites, Asterocalamopsis* e *Suvundukia* representam caules enquanto *Dichophyllites* folhas.

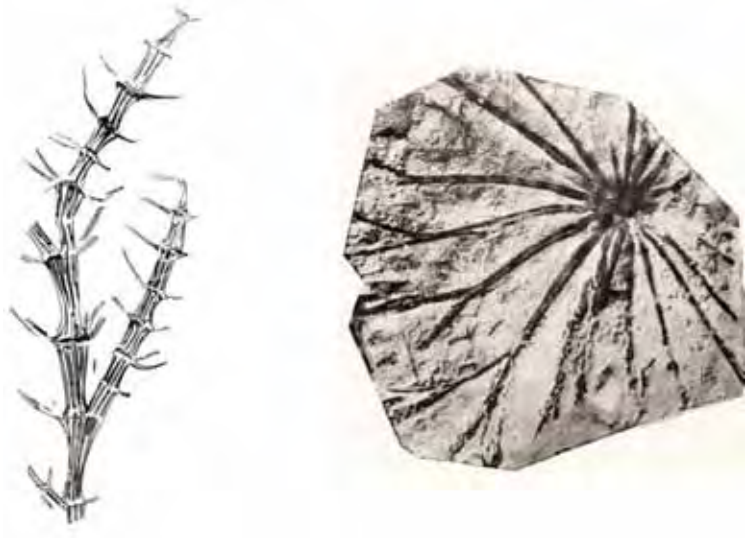

Figura I.36. Ilustração da esquerda: reconstituição de um ramo de *Suvundukia aciculata*. Imagem da direita: impressão de folhas bifurcadas de *Dichophyllites karagandensis* (Boureau, 1964).

II.3. Família Apocalamitaceae Radczenko, 1957 (Figura I.37)

Compreende esfenófitas do Paleozóico Superior que associa caules do tipo *Calamites*, com estrias e sulcos que se deviam na passagem de um nó a outro, folhas associadas de *Annularia, Annulina* ou *Lobatannularia* e estróbilos do gênero *Angarotheca.* O gênero *Neocalamites*, representado por moldes medulares, impressões de caules, ramos com folhas e estróbilos, e caracterizado por apresentar caules longos e irregularmente ramificado. Os sulcos e estrias são pouco pronunciados. As folhas inserem-se nos nós, são muito compridas, lineares, aciculares, unica nervação e livres na base como em *Annularia*. Além dos gêneros acima, *Neocalamostachys* representa estróbilos.

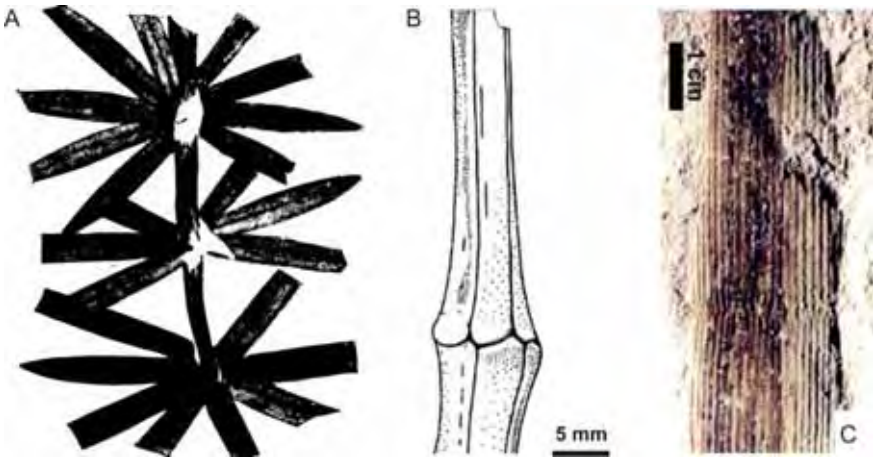

Figura I.37. A: Ilustração de um ramo com folhas de *Neocalamites* (Berry, 1912). **B**: Ilustração de *Neocalamites tubulatus*. **C**: Impressão de *Neocalamites tubulatus*. **B** e **C**: Naugolnykh (2009).

II.4. Família Calamitaceae Suckow, 1784

Composta de esfenófitas com hábito arbustivo e arborescente e indivíduos atingindo alturas de até 10 metros e diâmetro do caule de até 12 centímetros. É a família com a maior diversidade conhecida. As impressões de caules são as estruturas mais conhecidas dessa família, enquanto estruturas com preservação celular são relativamente raras.

II.4.1. Caules conhecidos como impressões e moldes medulares

O gênero *Calamites* Suckow, 1784 (Figura I.38) representa moldes medulares caules de superfície praticamente lisa com estrias e sulcos muito finos que se desviam na passagem de um nó para outro. As cicatrizes dos ramos são grandes, circulares, semicirculares, ovais ou quadradas, mais ou menos afastadas. Os ramos laterais são pequenos na inserção e aumentam rapidamente de tamanho, assim como sua complexidade interna. As ramificações são verticiladas ou dispostas irregularmente pelo caule. As cicatrizes foliares são pequenas, elípticas ou circulares e dispostas de modo verticilado. As folhas são uninervadas, delgadas, aciculares ou lanceoladas com uma base dilatada que às vezes forma uma bainha. Recentemente, DiMichele e Falcon-Lang (2012) propuseram que a grande maioria dos moldes medulares correspondem a moldes externos.

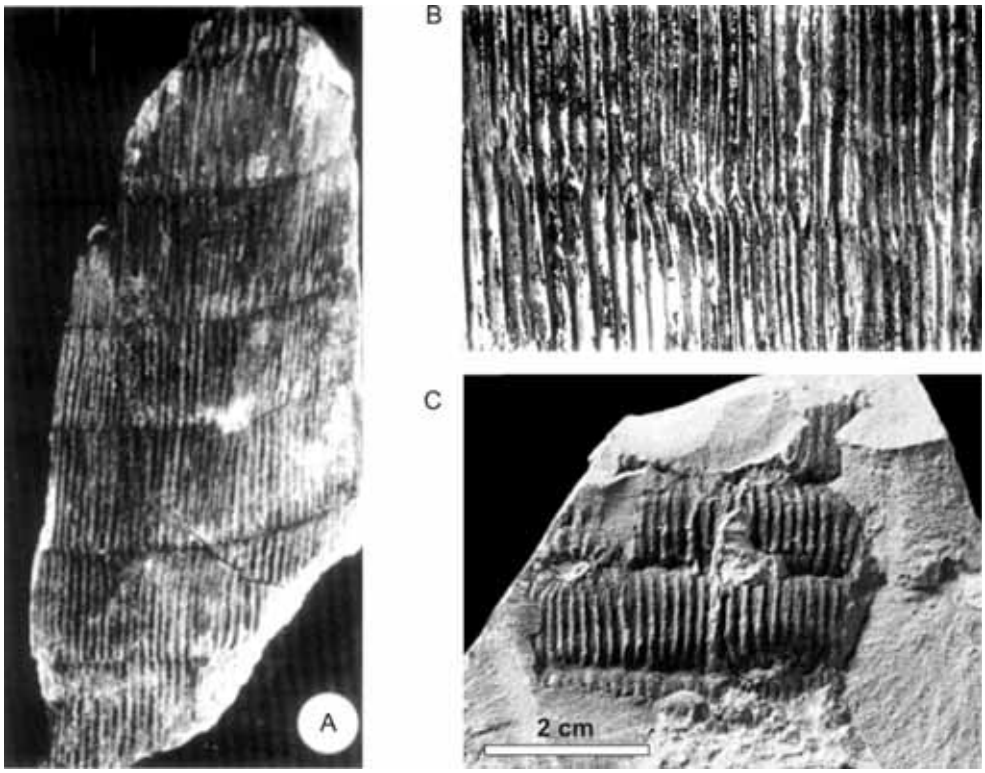

Figura I.38. A e **B**: Moldes medulares de *Calamites gigas* (Kerp, 1984b). **C**: Molde medular de *Calamites crucinatus* (Charbonier et al., 2008).

II.4.2. Caules conhecidos como permineralizações (Figuras I.39 e I.40)

A diferenciação entre os três gêneros de caules permineralizados se faz através de cortes transversais e tangenciais (Andrews, 1952).

Arthropitys e *Arthroxylon* apresentam em corte transversal corpo secundário muito semelhante, formado por feixes fasciculares (traqueídes e células parenquimáticas) e feixes interfasciculares (células parenquimáticas). Neste corte, *Calamitae* diferencia-se dos dois gêneros anteriores por apresentar os feixes fasciculares ladeados por traqueídes de menor tamanho, apresentando a sequência: traqueídes grandes- traqueídes pequenos- feixes interfasciculares- traqueídes grandes- traqueídes pequenos.

*Arthropity*s e *Arthroxylon* se diferenciam pelo corte tangential: *Arthropity*s apresenta feixes interfasciculares com suas células parenquimáticas de formato quadrado ou ligeiramente retangular enquanto em *Arthroxylon* estas são extremamente alongadas.

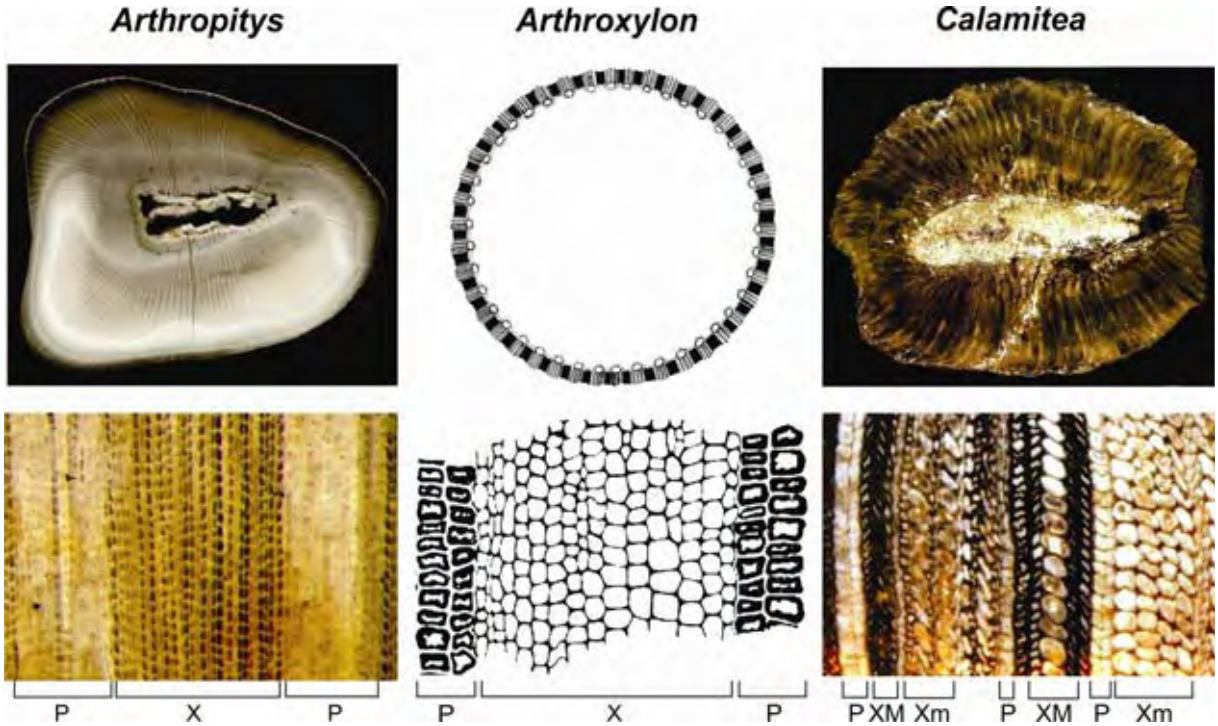

Figura I.39. Diferenças em corte transversal entre os três gêneros de esfenófitas permineralizadas. P = parênquima; X = xilema; XM = xilema com células maiores; Xm = xilemas com células menores. **Imagens da fileira superior**: detalhe do corpo secundário. Ilustração do meio: Reed (1952); Foto da direita: Röβler & Noll (2007a). **Imagens da fileira inferior**: detalhe do arranjo celular dos feixes fasciculares e interfasciculares. Ilustração do meio: Reed (1952); Foto da direita: Röβler & Noll (2007b).

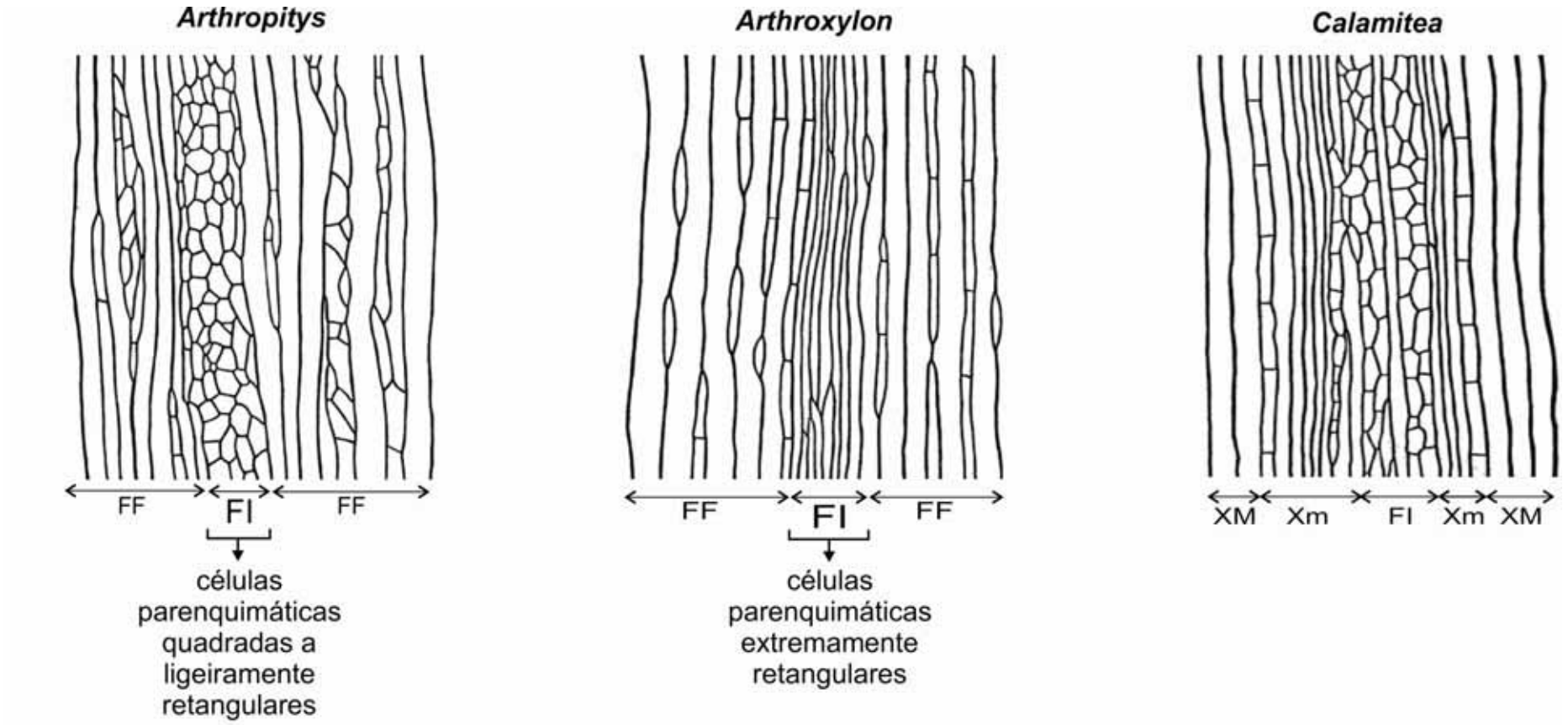

Fig. I.40: cortes tangenciais mostrando a diferença entre os três gêneros de esfenófitas permineralizadas. FF: feixe fascicular; FI: feixe interfascicular; XM: células xilemáticas grandes; Xm: células xilemáticas pequenas. Figuras: Andrews (1952).

II.4.3. Estróbilos conhecidos como impressões (Figura I.41)

Os gêneros *Palaeostachya*, *Calamostachys*, *Mazostachys, Calamocarpon*, *Huttonia*, *Macrostachya*, *Paracalamostachys* e *Kallostachys* representam estróbilos conhecidos como impressões, cuja diferença se dá pelo posicionamento dos esporangióforos no eixo dos estróbilos, número de esporângio por esporangióforo e pela homosporia/heterosporia.

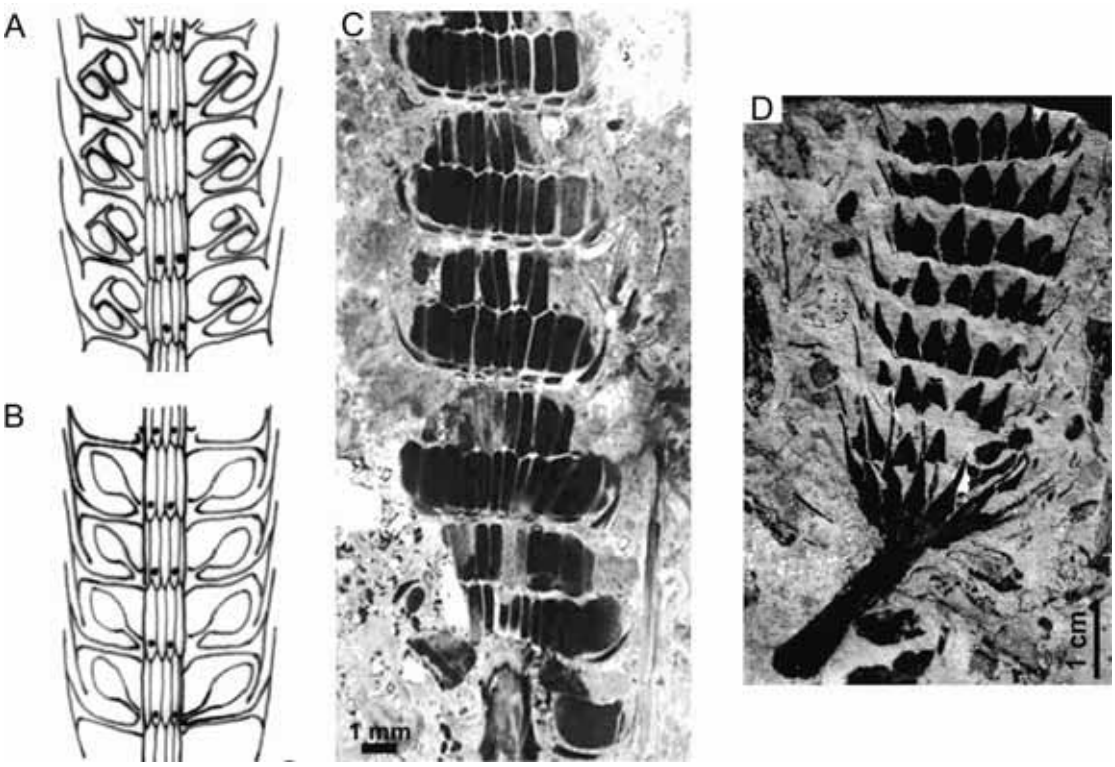

Figura I.41. A e **B**: Ilustrações de *Palaeostachya* e *Huttonia*, respectivamente. **C:** Impressão de *Calamostachys zeilleri.* **D**: Impressão de *Huttonia spicata*. A, B e D: Libertín & Bek (2004). C: Galtier (2008).

II.5. Família Sorocaulaceae Radczenko, 1956 (Figura I.42)

Família representada por impressões de caules e folhas. O gênero *Koretrophyllites* é bastante representativo da família. São plantas herbáceas, irregularmente ramificadas, em geral com terminações. O caule possui estrias e sulcos bem marcados e que não se desviam na passagem dos nós. As folhas dispõem-se em verticilos e são livres ou soldadas na base. São longas, mais compridas que os entrenós e com veia mediana fina. Os ramos férteis se situam entre os verticilos de folhas estéreis. Outros gêneros da família: *Sorocaulus* (caules com ramos e folhas) e *Corynophyllites* (folhas).

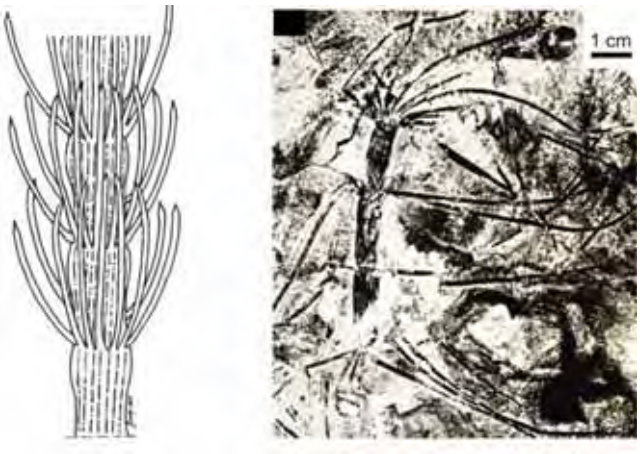

Figura I.42. Ilustração da esquerda: *Koretrophyllites* sp. (Roesler, 2008). Imagem da direita: impressão de *Koretrophyllites lineares* (Boureau, 1964).

II.6. Família Neurophyllaceae Kon´no, 1941

Família com apenas um gênero, *Neurophyllum.* São caules monopodiais, articulados irregularmente com estrias e sulcos que não se desviam na passagem dos nós.

4) Ordem Equisetales: plantas extintas e atuais (*Equisetum*), herbáceas, sem crescimento secundário. Compreende as famílias Phyllotecaceae, Schizoneuraceae e Equisetaceae.

Família Phyllothecaceae Surange e Prakash, 1962 (Figura I.43)

Impressões de caules e folhas. Família caracterizada por folhas longas dispostas em verticilo bastante soldadas na base. O gênero *Phyllotheca* é o mais característico da família. Outros gêneros: *Stellotheca, Annulina, Gamophyllites, Raniganjia* e *Equisetinostachys.*

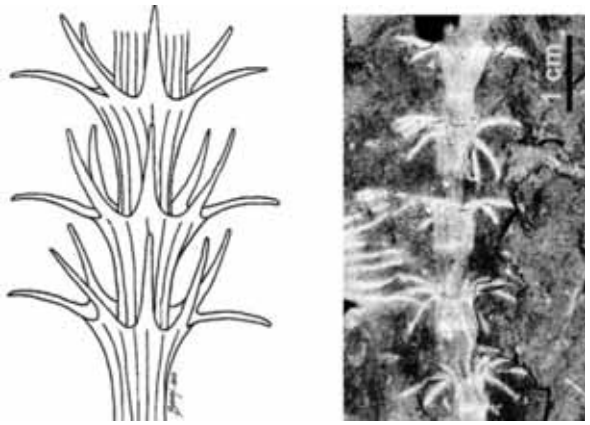

Figura I.43. Ilustração de esquerda: *Phyllotheca* sp. Impressão da direita: *Phyllotheca brevifolia* (Roesler et al., 2008).

Família Schizoneuraceae Schimper e Mougeot, 1844 (Figura I.44)

Família caracterizada por caules com folhas lateralmente soldadas entre si formando lobos foliares. O gênero *Schizoneura* é o mais característico da família. Outros gêneros: *Manchurostachys, Aethophyllum* e *Paraschizoneura.*

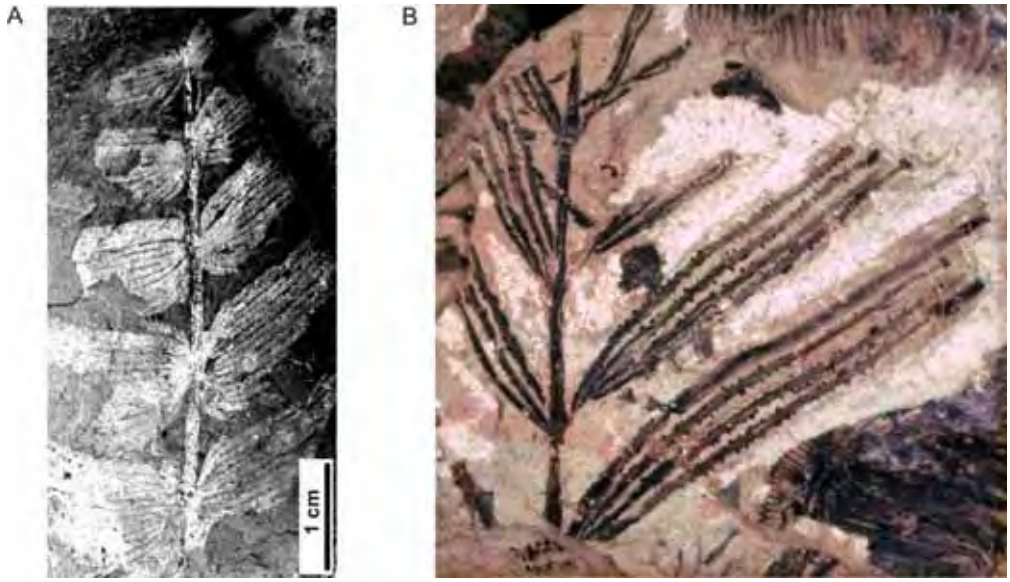

Figura I.44. A: Impressão de *Schizoneura manchuriensis* (Yang et al., 2011). **B**: Impressão de *Schizoneura paradoxa* (http://steurh.home.xs4all.nl/engplant/ekelber2.html) em 01/02/2012).

Família Equisetaceae (Figura I.45)

Família que contem o gênero *Equisetites* e o único gênero existente do grupo das esfenófitas, *Equisetum*. *Equisetites* distribuiu-se do Carbonífero ao Quaternário, com seu apogeu no Triássico, e pode representar as folhas de *Equisetum;* às vezes é encontrado associado a folhas férteis portando estróbilos.

Figura I.45. Ilustração de esquerda: estróbilo de *Equisetites arenaceous* (Boureau, 1964). Impressão da direita: folhas isoladas de *Equisetites* (DiMichele et al., 2005).

II. Annotated catalog of *Arthropitys* Goeppert 1864-5: considerations about nomenclature, classification criteria and validity of species

1. Introduction

Arthropitys Goeppert 1864-5, *Arthroxylon* Reed, 1952 and *Calamitea* (Cotta) emend. Rößler & Noll, 2007 represent the three sphenophyta genus found as permineralizations. *Arthropitys* is the genus that presents the largest number of species and the highest stratigraphic amplitude, distributed from the Serpukovian, Late Mississippian (326-318 Ma), represented by a species in open nomenclature which might belong to *A. communis* (Gerrienne, 1999) to the Lopingian, Late Permian (251 Ma) with the species *A. yunannensis* (Wang et al., 2006).

The first specimens of sphenophyta with preserved cellular structures was described by Cotta (1832) and named *Calamitea bistriata*. Later on, when Goeppert (1864-65) noticed great anatomic and morphologic differences among Cotta's "*bistriata*" species, he created the *Arthropitys* genus and determined *A. bistriata* as the type species.

2. Research Objectives

Although the literature about this genus, describing 24 species and six varieties, is from over 180 years, each author has virtually used their own terminology for the same character, thus generating uncertainties when it is necessary to compare one species to another. Thereby, the first purpose of this paper is to draw a parallel among the various terms used for anatomical descriptions.

The other issue, of more complex nature, concerns the anatomical characters that must be valued to limit the species; each author attributes relevance degrees to the same anatomical character. Furthermore, some authors created species based on a small fragment only. This way, the second purpose of this paper is to formalize a diagnosis character hierarchy for the species and, from that point and as final purpose, critically review the species described so far. These species described herein were sorted out into six groups according to their thacheid thickening.

3. Material and methods

In this work were analyzed the original papers of Renault (1896), Knoell (1935), Andrews (1952), Anderson (1954), Boureau (1964), Cichan & Taylor (1983), Wang et al. (2003, 2006), Rößler & Noll (2006, 2010) and Rößler et al. (2012) to search for diagnoses, descriptions, locality and age of all species of the genus. In each paper, we looked for anatomical structures in cross, tangential and radial sections to understand the body of the plants.

In the cross section, width of the fascicular and interfascicular wedges, the number of rows in these wedges throughout the secondary body and parenchymatous cells in the fascicular rays were analized. In the radial section, mostly thickening types in the tracheid secondary walls were analized. In the tangential section, the contribution of tracheids and parenchymatous cells in fascicular and interfascicular wedges was analyzed, respectively. For the composition of the plates, we searched for at least one figure of each of the above cuts.

4. Nomenclature issue

The secondary body of a sphenophyte with cellular preservation is formed by wedges containing protoxylem and metaxylem cells, rows of tracheids and parenchymatous cells, as well as wedges containing rows of parenchymatous cells only (Figure II.1). However, a number of terms were used to describe the anatomy of this group.

Renault (1986) referred to the xylem wedges as “lignified wedges” (*coins ligneux*) and to the rows of parenchymatous cells inside these wedges as “lignified cell rays” (*rayon cellulares ligneaux*). However, what are lignified in these wedges are only the tracheids. Already the wedges composed of parenchymatous cells were called “cellular rays” (*rayon cellulares*) or “secondary fundamental tissue” (*tissu fondamental secondaire*).

Andrews (1952) called the secondary body of the plant “wood sector” to designate the wedges composed of tracheids; and the rows of parenchymatous cells in the wood sector were called “secondary ray” one moment and “small ray” the next. The wedges containing parenchymatous cells were called “primary rays”.

Anderson (1954) called the tracheid wedges “fascicular segment”; and their rows of parenchymatous cells, “secondary rays”. The wedges with

parenchymatous cells were either named “interfascicular segment” or “primary ray”; and their rows, “cell rays”.

Boureau (1964) might have been the author who used the largest number of terms to describe these sphenophytes. The protoxylem cells were referred to as “the latest wood” (*bois centripéde plus recent*); and the carinal canals, “reabsorption gaps of first centripede lignified elements” (*lacune de résorption des premiers element lignified centripètes*). The tracheid wedges were named “centrifuge wood” (*bois centrifuge*); the rows of parenchymatous cells, “secondary lignified rays” [*rayon ligneous secondaires* (*fasciculariresi*)]. The wedges of parenchymatous cells were referred to as “primary medullary rays” [*rayon médullaires primaries* (*interfascicullaires*)].

Cichan & Taylor (1983) referred to the tracheid wedges as “fascicular wedges” and their rows of parenchymatous cells were called “secondary rays”. The wedges of parenchymatous cells were called “parenchymatous interfascicular zones”.

Wang et al. (2003, 2006) named the tracheid wedges “fascicular wedge of wood” or “fascicular ray” and their rows of parenchymatous cells were called “fascicular secondary rays”. The wedges containing parenchymatous cells were called “interfascicular rays” one moment and “interfascicular parenchymatous rays” the next.

Rößler & Noll (2006, 2010) and Rößler et al. (2012) referred to the tracheid wedges as “fascicular wedges”; and their rows of parenchymatous cells, “fascicular rays”. The wedges presenting parenchymatous cells were called “interfascicular rays or primay rays” and the rows that make them up were named “ray cells”.

In this work the terms proposed by Rößler & Noll (2006, 2010) and Rößler et al. (2012) will be used, and Table II.1 comparatively shows the terms above used by different authors.

5. Hierarchy of important anatomical and morphological characters when limiting species

Renault (1886) deemed cross-section highly important for limiting species: the number of rows in both the fascicular and interfascicular wedges, cells shapes, and number of cells in the row heights.

Anderson (1954) regarded as important for species classification characters such as: i) diameter of secondary body; ii) node length; iii) branching system; iv) medullary characteristics: diameter, cell shape, cell wall thickness, dark content inside the cells; v) primary body characteristics: carinal canals and rows of cells that surround them, size of tracheid and their wall thickening; and vii) characteristics of interfascicular rays: persistence in secondary body, width, characteristics of their cells. Nevertheless, the branching system and tracheid thickening might change from one individual to another in the same species; they are regarded herein as stable within the species. To illustrate that: *A. ezonata* (Goeppert, 1864-5) was originally described as presenting a 14-cm diameter; a specimen of the same species found by Rößler & Noll (2006) presented a diameter between 47 and 60, depending on the part of the stem analyzed – a diameter virtually four times as large as the first specimen found.

Since the specimens found by Rößler & Noll (2006, 2010) and Rößler et al. (2012) in Chemitz, Germany, the branching system has become a morphological character used to supplement the description of *A. ezonata* and *A. bistriata* and the introduction of *A. sterzelli*. Therefore, this work is a sequel to the one proposed above, which formalizes a hierarchy that add both anatomical and morphological criteria, tracheid thickenings and branching system, respectivally (Table II.2), understood as genetically conditioned, thus allowing the creation of species that look as much as possible like natural ones.

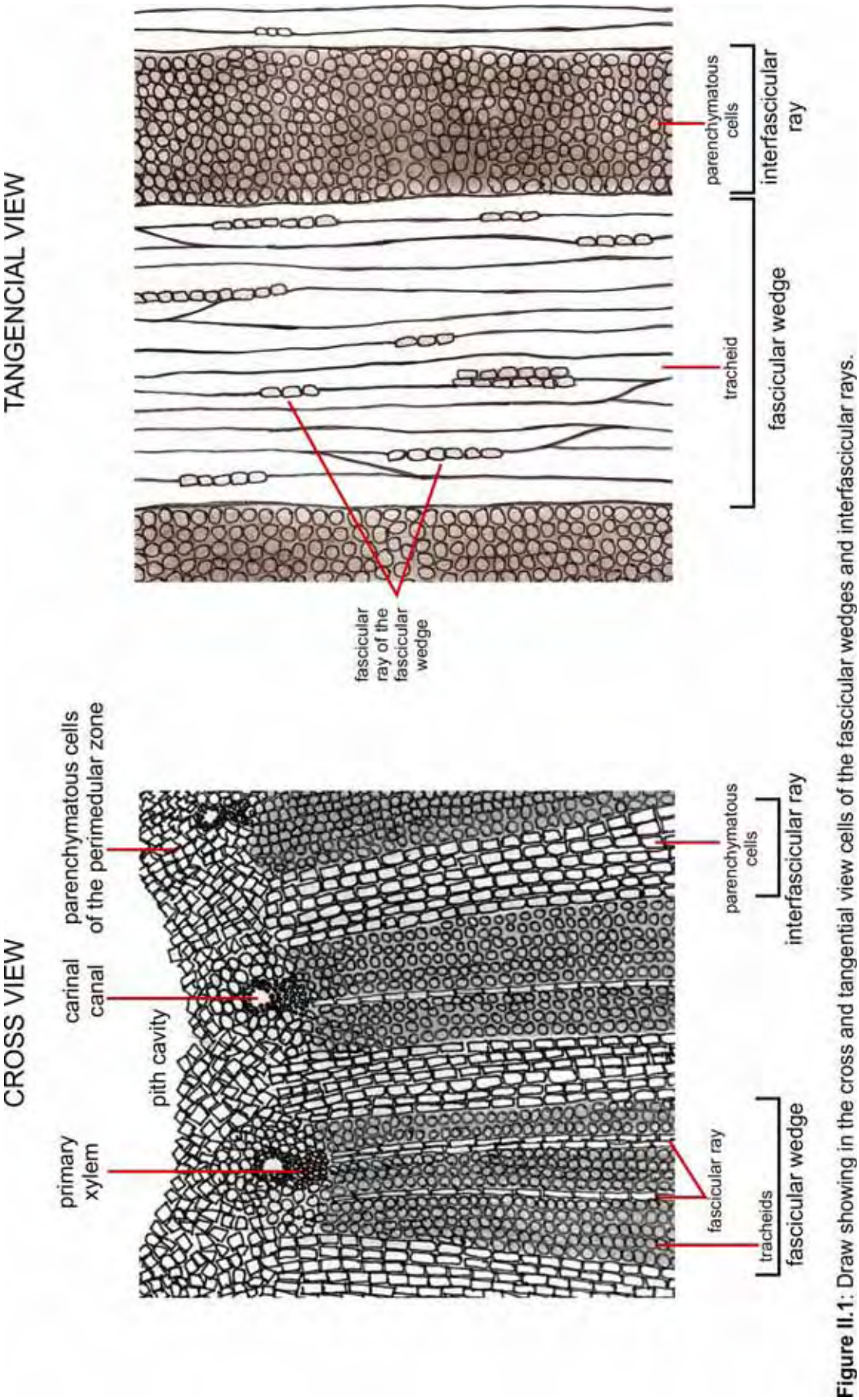

Figure II.1: Draw showing in the cross and tangential view cells of the fascicular wedges and interfascicular rays.

Anatomical characters	Renault (1896)	Andrews (1952)	Anderson (1954)	Boureau (1964)	Cichan & Taylor (1983)	Wang et al. (2003, 2006)	Roßler & Noll (2006, 2006) and Roßler et al. (2012)
Wedges composed by tracheids and parenchymatous cells	coins ligneux	wood sector	fascicular segment	bois centrifuge	fascicular wedge	fascicular wedge of wood or fascicular ray	fascicular wedge
Tracheid rows in the wedges composed by tracheids and parenchymatous cells					secondary ray	fascicular secondary ray	tracheid row
Parenchymatous cell rows in the wedges composed by tracheids and parenchymatous cells	rayon cellulare ligneux	secondary ray or small ray	secondary ray	rayon ligneux secondaire			fascicular ray
Wedges composed by parenchymatous cells	rayon cellulare or tissu fondamental secondaire	primary ray	interfascicular segment or primary ray	rayon meddulaire primaire	parenchymatous interfascicular zone	interfascicular ray or interfascicular parenchymatous ray	interfascicular ray
Parenchymatous cell rows in the wedges composed by parenchymatous cells			cell ray				cell ray

Table II.1: Anatomical characters used by different authors in the *Arthropitys* descriptions.

A - ANATOMY
1. Thickenings of secondary wall tracheids
1.1. Scalariform
1.2. Circular reticulated
1.3. Elongate reticulated
2. Number of vascular segments (min/max)
3. Segmenttion of secondary body into fascicular wedges and interfascicular rays
in cross view
3.1. Interfascicular rays visible throughout secondary body
3.2. Interfascicular rays visible only in the pith region
3.3. Interfascicular rays not clearly visible with homogeneous secondary body
4. Pith cavity and stem diameter ratio
B - MORPHOLOGICAL CHARACTERS
1. Branch growing
1.1. Branches with secondary growth in the same plant
1.2. Branches withou secondary growth in the same plant
1.3. Branches with and without secondary growth in the same plant
2. Branch disposition
2.1. Branches at every node
2.1.2. Disposed in alternate positions between nodes
2.1.2. Disposed in line between nodes
2.1.3. Disposed randonly between nodes
2.2. Branches not at every node
2.2.1. Disposed in alternate positions between nodes
2.2.2. Disposed in line between nodes
2.2.3. Disposed randonly between nodes
3. Number of branches per node
4. Diameter of branches with secondary growth
5. Diameter of branches without secondary growth

Table II.2: The data above show the proposed classification for *Arthropitys* genus based on antomical and morphological characters. Bold characters are important when delimiting the species, whereas normal charcaters present limited taxonomic use, reflecting principally growth stages and/or environmental conditions.

6. Annotated catalog

Not all the original descriptions of *Arthropitys* mentioned the branching system or the kind of tracheid thickening. Therefore, the species were sorted out into groups: from I to III according to tracheid secondary wall thickening, IV for the species described by Hirmer and Knoell (in Knoell, 1935), V for the species presenting lack of anatomical data and VI for the varieties. Presented below is the genus diagnosis, the description of the type species and the suprageneric taxonomic classification according to Frey (2009).

Division Tracheophyta

Superclass Moniliformopses

Class Equisetopsida

Order Calamitales

Family Calamitaceae Suckow, 1784

Genus *Arthropitys* Goeppert, 1864-5

Type-species: *Arthropitys bistriata* (Cotta) Goeppert *emend*. Röβler, Feng & Noll, 2012 (Plate 1)

Generic diagnosis (Goeppert, 1864-5, p.183)**:** Arboreal plants with whorled branches. Stem branched and furrowed. Secondary body presents large pith cavity. In radial section tracheids present scalariform secondary wall thickenings, composing a zone with small and large medular rays.

Type-species diagnosis (Goeppert, 1864, p.185): Secondary body divided into interfascicular rays composed of 6-7 cell rows, wider than fascicular wedges whose height is equal to one internode. Fascicular wedges composed of some rows and thracheids present scalarifom thickenings tending to circular reticulated.

Type-species emended diagnosis (Röβler, Feng & Noll, 2012, p. 65-6): Arborescent articulate woody plant characterized by at least three orders of woody axes, and whorls of leafy twigs regularly occurring at every 5th to 9th (rarely to 18th) node. Stems possess a circular central pith/cavity, primary and secondary vascular tissues. Parenchymatous pith is composed of circular to polygonal cells in perimedullary zone and diaphragms in nodal region. Internode length varies from 9.5 to 30 mm. Primary xylem strands consist of circular carinal canals surrounded by metaxylem. Metaxylem elements are variable in diameter from 20 to 90 μm that centrifugally arranged in 2 to 5 layers, the smallest cells are directly connecting with the central carinal canals. Secondary body is composed of fascicular wedges and interfascicular rays and gradually diminishes distally. Interfascicular rays are continuous between successive nodes, taper distally and are visible through the whole secondary tissue. Fascicular wedges gradually enlarge in width centrifugally, consist of radial files of thick-walled tracheids and narrow thin-walled fascicular rays. In transverse view, interfascicular rays are less than 1 mm wide and are made of 3–7 variable parenchymatous cells having a square to rectangular outline in transverse and radial views, irregular to polygonal outline in

tangential view, and usually less high than wide in radial view. Secondary xylem has commonly scalariformsecondary wall thickenings and horizontally elongated pits on radialwalls. Thickenings are 2–4 μm apart (excluding the pit's width) and are sometimes forked, or very rarely reticulated. Tracheids are up to several millimeters in length. In transverse view, tracheid diameters average 20–100 μm radially and 35–70 μm tangentially. The outer surface is striate reflecting segmentation of the secondary body. Nodes are slightly incised with small, acute, millimeter–diameter, vertically enlarged leaf traces at every second or third fascicle. Leafy twigs depart from whorls of usually 9–16 branches. Nodes between these whorls usually lack leafy twigs. Leafy twigs are 2–6 mm in diameter, lack secondary growth, are slightly enlarged centrifugally, and circular or elliptical in outline with an acute tip. Several orders of woody branches form a complex branching system, either by successive unequal bifurcations of the main stem or occasionally from inside the wood as adventitious shoots. Secondary roots of several millimeters to centimeters in diameter depart from the trunk base, show considerable secondary growth and lack carinal canals.
Locality: Zeisigwald Tuff Horizon, Leukesdorf Formation, Chemnitz (Germany).
Age: Sakmarian, Early Permian.

Group I: In this group tracheids present scalariform secondary wall thickenings.

Arthropitys communis (Binney) Renault, 1896 (Plate 2)
Locality: England, Autun and Champ des Borgis (France).
Age: Carboniferous (England) and Permian (Autun and Champ des Borgis).
Description: Interfascicular rays are wide in the pith region, but they decrease abruptly towards cortex, virtually disappearing and becoming almost indistinguishable by the intrusion of tracheid neighbors. This species presents cells with dark contents in the pith region, which may have been reservatory cells. There is no information in the original description of the branching system.
Comments: The abrupt narrowing of the radially-oriented interfascicular rays is the greatest differential of this species.

Arthropitys lineata Renault, 1896 (Plate 3)
Locality: Champ des Borgis and Autun (France).

Age: Permian.

Description: Fascicular wedges present practically parallel sides throughout the secondary body in cross section. Interfascicular rays are very narrow; they are generally trisseriates and often invaded by tracheids of neighboring fascicular wedges. There is no information in the original description of the branching system.

Comments: The fascicular wedges with parallel sides and radially-oriented, quite narrow interfascicular wedges are the greatest differential of the species. However, there is no description concerning the width of interfascicular rays throughout the secondary body; just the fact that they are narrow. Thus, the presence of parallel sides of the fascicular wedges and very narrow interfascicular rays can associate *Arthropitys lineata* with *A. bistriata*.

Arthropitys gallica Renault, 1896 [apud Andrews (1952); Boureau (1964); Wang et al. (2003)]

Locality: Montrambert (France).

Age: Late Carboniferous (Andrews, 1952).

Description: Fascicular wedges are composed of 10 cell rows in cross section. Interfascicular rays in cross section are initially wide, composed of 7 cell rows and become narrow in the cortex region, besides consisting of 2 cell rows. This species presents dark cell in medullary area, which were possibly resinous cells. There is no information in the original description of the branching system.

Comments: This species is quite similar to *Arthropitys communis* because both species have the same interfascicular ray configuration, tracheids with secondary wall thickenings and dark cells in the medullary zone. However, in *A. gallica* the fascicular wedges are composed of 10 cell rows, whereas in *A. communis* these wedges are composed of 25-30 cell rows.

Arthropitys medullata Renault, 1896 (Plate 4)

Locality: Autun, Saint-Étiene and Champ des Borgis (France).

Age: Permian.

Description: Fascicular wedges and interfascicular rays are very wide in cross section. The interfascicular rays are composed of 4-5 cell rows in width. There is no information in the original description of the branching system.

Comments: There is nothing in the diagnosis that justifies *Arthropitys medullata* as a new species.

Arthropitys deltoides Cichan & Taylor, 1983 (Plate 5)

Locality: Copland Coal, Breathitt Formation, Kentucky (USA).

Age: Early or Early-Middle Pennsylvanian.

Description: Stem diameter ranges between 6.5 and 10 mm. Interfascicular rays widen radially in cross section; in tangential section, they present rectangular cells that are higher than wide, showing an average height of 86 µm and an average width of 16 µm in the pith region, and an average height of 55 µm and an average width of 35 µm in the cortex region. Tracheids of the fascicular wedges are arranged in concentric bands with relatively square cells in cross section, averaging 78 µm in radial dimension and 72 µm in tangential dimension. There is no information in the original description of the branching system.

Comments: The great differential of *Arthropitys deltoides* is the concentric organization of the fascicular wedges and their small size, leading the authors to interpret it as a climbing habit unlike other species of the genus.

Arthropitys junlianensis Wang, Hilton, Li & Galtier, 2003 (Plate 6)

Locality: Junlian Formation, South Sichuan Province (southwest China).

Age: Capitanian-Longtanian, Late-Midlle Permian to Late Permian.

Description: The perimedullary region presents cells with dark contents. Fascicular wedges increase in width radially and present 15 cell rows in cross section; fascicular rays are uni- or bisseriate. They rarely have 3 or 4 rows. Interfascicular rays in cross section have 4-6 cell rows in the pith region and narrow abruptly. There is no information in the original description of the branching system.

Comments: *Arthropitys junlianensis* is very similar to *A. communis* and *A. gallica*: the three species have interfascicular rays abruptly narrowing radially, the same type of thickening in the tracheid secondary walls and the presence of cells with dark contents in medullary and perimedullary zones. In *A. communis,* fascicular wedges in cross-section are formed by 25-30 cell rows, whereas in *A. junlianensis* these wedges are composed of 10 cell rows. *A. gallica* and *A. junlianensis* have

practically the same number of cell rows in the interfascicular rays in the pith region, but in *A. junlianensis* these rays disappear near the cortex. Also, *A. junlianensis* is a small species with reduced diameter in comparison to these species.

Arthropitys yunnanensis (Tian & Gu) *ex* Wang, Hilton, Galtier & Tian, 2006 (Plate 7)

Locality: Housuo Coal Mine, upper part of Xuanwei Formation, eastern Yunnan Province (China).

Age: Wuchiapingian-Changhsingian, Late Permian.

Description: Perimedullary zone presents cells with dark contents. Fascicular wedges in cross section increase in width radially and are composed of 14-16 cell rows in the pith region and 30-40 rows in the cortex region. Fascicular rays in cross section are uni- or trisseriate; in radial section, they show square to rectangular-shaped cells averaging 50-190 µm in height; in tangential section, these rays are uni- or trisseriate, and they rarely have 4 rows; the height has up to 50 cells, but it commonly has 10-20 cells. Interfascicular rays in cross section are wide in the pith region, tapering gradually from the first innermost 1/3rd of the secondary body, keeping their width toward cortex. The branching system is composed of 4 branches per node.

Comments: This species is characterized by singular configuration of the interfascicular rays in cross section. As in *A. deltoides*, the parenchymatous cells of the fascicular wedges in radial section present different sizes, giving this group of cells a heterogeneous aspect. Also, the fascicular wedges in cross section smoothly increase in width, and it is an important feature to characterize this species.

Arthropitys ezonata (Goeppert) *emend.* Rößler & Noll, 2006 (Plate 8)

Locality: Saint-Etienne and Autun (France), Zeisigwald Tuff Horizon, Leukesdorf Formation, Chemnitz (Germany).

Age: Asselian-Sakmarian, Early Permian (Chemnitz).

Description: Quite homogeneous secundary body, with fascicular wedges and interfascicular rays visible in the pith region only. Fascicular wedges in cross section increase in width radially and are composed of 10-18 cell rows. Fascicular

rays in tangential section present 6 cell rows. Interfascicular rays in cross section are composed of 2-5 cell rows. *Arthropitys ezonata* presents 5 branches per node in young stems and 2-5 in adult stems, disposed alternately from one node to another.

Comments: This species was emended by joining the anatomical and the branching systems, and this additional feature is very important to characterize *Arthropitys ezonata.*

Group II: In this group tracheids present circular and/or elongate reticulated secondary wall thickenings.

Arthropitys major (Weiss) Renault, 1896 [apud Boureau (1964); Wang. et al. (2006)] (Plate 10, Figs. E-F)

Locality: Saint-Étienne, Commentry, Blanzy and Autun (France).

Age: Gzhelian, Late Pennsylvanian (Boureau, 1964).

Description: This species presents tracheids with circular reticulated secondary wall thickenings. Interfascicular rays in cross section are composed of 20-30 cell rows. There is no information in the original description of the branching system.

Comments: *Arthropitys major* is poorly described. There is information neither about the width and number of cell rows in the fascicular wedges nor about the branching system. However, this species presents many cell rows in the interfascicular rays as a great diferential in this group.

Arthropitys kansana Andrews, 1952 (Plate 9, Figs. A-D)

Locality: Fleming coal, upper part of Cherokee shale, Kansas (USA).

Age: Middle Pennsylvanian.

Description: Species with a very developed and uniform secondary body. Fascicular wedges and interfascicular rays in cross section present constant width radially. Fascicular rays in tangential section are unisseriate or have 3-4 cell rows with many cells in height. Tracheids present circular to slightly elongate reticulated secondary wall thickenings. There is no information in the original description of the branching system.

Comments: According to the author, the constant width of fascicular wedges and interfascicular rays throughout secondary body are the diagnostic feature of

Arthropitys kansana. This aspect could relate this species to *A. bistriata* or *A. lineata*; however these species present scalariform thickenings in the tracheids, whereas *A. kansana* presents tracheids with circular to slightly elongate reticulated secondary wall thickenings.

Arthropitys illinoensis Anderson, 1954 (Plate 9, Figs. E-G)

Locality: Calhoun coal, upper part of MacLeansboro Group, Illinois (USA).

Age: Late Pennsylvanian.

Description: This species present 2mm-wide fascicular wedges in cross section, and they do not narrow radially. Interfascicular rays in cross section disappear abruptly towards the cortex region. Tracheids present elongate reticulated secondary wall thickenings. There is no information in the original description of the branching system.

Comments: The interfascicular rays that narrow abruptly radially are the great differential of *Arthropitys illinoensis*, as in *A. communis*; however, this species presents scalariform secondary wall thickenings, whereas A. *illinoensis* presents tracheids with elongate reticulated thickenings. It could represent a specimen of *A. kansana* due to their similarities, but this species presents fascicular and interfascicular wedges of constant width radially, whereas in *A. illinoensis* these wedges narrow towards the cortex region.

Arthropitys cacundensis Mussa, 1984 (in Coimbra & Mussa, 1984) (Plate 10, Figs. A-D)

Locality: Sandstone of Pedra de Fogo Formation, in the Cacunda River margins, between the cities of Araguaína and Carolina (central-northern Brazil).

Age: This information is not available in the original paper.

Description: Species with dark cells in the medullary zone. Fascicular rays in cross section are unisseriate and rarely bi- or trisseriate; in tangential section, they present 21 cells in height. Interfascicular rays in cross section present 5-8 cell rows. Tracheids present circular reticulated secondary wall thickenings. The branching system is composed of 2-3 branches per node, disposed alternately from one node to another.

Comments: Species poorly described, making comparisons difficult. *Arthropitys cacundensis* differs from *A. kansana* because it presents circular reticulated

secondary wall thickenings in the tracheids, whereas *A. kansana* presents tracheids with circular to slightly elongate reticulated thickenings. It differs from *A. illinoensis* because this species presents tracheids with circular reticulated thickenings. Moreover, there is no infomation about the branching system in the North American species.

Arthropitys sterzelii Rößler & Noll, 2010 (Plate 11)

Locality: Zeisigwald Tuff Horizon, Leukesdorf Formation, Chemnitz (Germany).

Age: Asselian-Sakmarian, Early Permian.

Description: Fascicular wedges in cross section increase in width radially and are composed of 12 cell rows internally and 78 rows externally. Tracheids present circular reticulated secondary wall thickenings. Interfascicular rays in cross section slightly narrowing towards the cortex and are composed of 2-6 cell rows. The branching system is irregular, and it commonly presents branches in each node -5 in young stems and 2-5 in adult stems- without secondary growth and it is disposed alternately from one node to another.

Comments: Fascicular wedges in *Arthropitys sterzelli* increase significantly in width towards the cortex, whereas *A. kansana* presents these wedges with constant width. Unlikely *A. illinoensis*, *A. sterzelli* presents interfascicular rays in cross section slightly narrowing radially. Tracheids with circular reticulated secondary wall thickenings make *A. sterzelli* different from *A. kansana*, containing circular to slightly reticulate thickenings. However, *A. sterzelii* is very similar to *A. cacundensis*: the same type of thickenings in the tracheids; interfascicular rays with practically the same number of cell rows; and branches disposed alternately from one node to another. The difference is in the number of branches: *A. sterzelii* presents 5 branches in young stems and 2-5 in adult stems, whereas *A. cacundensis* presents 2-3 branches per node, but was described based on two small fragments.

Group III: In this group tracheids present scalariform and reticulated secondary wall thickenings.

Arthropitys gigas (Brongniart) Renault, 1896 (Plate 12, Figs. A-E)

Locality: Saint-Étiene, Commentry, Autun and Saarbürck (France), Piskork (Russia).

Age: Late Carboniferous to Middle Permian.

Description: Stem diameter ranging between 50 and 70 cm with large pith cavity. Fascicular rays of the fascicular wedges present 3 cell rows in cross section. Interfascicular rays in cross section are wide in the pith region and present intrusion of the neighboring fascicular wedge tracheids. The tracheids present three kinds of secondary wall thickenings: near the pith they are helical; they then become scalariform and lastly they are circular reticulated. There is no information in the original description of the branching system.

Comments: This species was originally described by Brongniart, 1828 (apud Renault, 1896) and called *Calamites gigas*. Renault (1896) described it in detail and classified it into the *Arthropitys* genus created by Goeppert (1864-5), naming it *Arthropitys gigas.* The three kinds of thickenings in the tracheid secondary walls are the great differential of *A. gigas*.

Arthropitys versifoveata Anderson, 1954 (Plate 12, Figs. F-H)

Locality: Fleming Coal, upper part of Cherokee shale, Kansas (USA).

Age: Midlle Pennsylvanian.

Description: Fascicular wedges are not narrow shaped in the pith region. Fascicular rays in cross section are unisseriate in the pith region and become bisseriate in the cortex region. Tracheids present scalariform and elongate reticulated secondary wall thickenings randomly distributed throughout the secondary body. Interfascicular rays in cross section present 4-6 cell rows. *Arthropitys versifoveata* presents 4 branches of 4 mm in diameter per node, inserted in a 90^{o} angle in relation to the stem, and disposed alternately from one node to another.

Comments: As *Arthropitys illinoensis, A. versifoveata* do not present narrow fascicular wedges in the pith region, but differ from *A. illinoensis* because this species presents tracheids with circular reticulate secondary wall thickenings, whereas in *A. versifoveata* these cells present scalariform and elongate reticulate thickenings. It differs from *A. gigas* because this species presents three kinds of

thickenings, whereas *A. versifoveata* presents two kinds of thickenings. The number of branches is an important differentiation feature of this species.

Arthropitys porosa Renault, 1896 (Plate 13, Figs. A-D)
Locality: Autun France (France).
Age: Permian (Boureau, 1964).
Description: Fascicular wedges in cross section are composed of 15-18 cell rows. Fascicular rays in cross section are composed of 1-3 cell rows; in radial section, they present cells 4 to 5 times higher than wide. Tracheids present three kinds of secondary wall thickenings: they are circular reticulate in the pith region; then they are elongate reticulate and lastly scalariform. There is no information in the original description of the branching system.
Comments: While in *Arthropitys gigas* tracheids present a sequence of helical, scalariform and reticulate secondary wall thickenings, from the pith to the cortex region, in *A. porosa* this sequence is composed of circular reticulate, elongate reticulate and scalariform thickenings.

Arthropitys rochei Renault, 1896 (Plate 13, Figs. E-F)
Locality: Champ des Borgis and Autun (France).
Age: Late Carboniferous to Permian (Andrews, 1952).
Description: Interfascicular rays in cross section are composed of rectangular cells slightly higher than wide. Tracheids present three kinds of secondary wall thickenings: scalariform, alongate reticulate, and circular reticulate, from the pith to the cortex region. There is no information in the original description of the branching system.
Comments: *Arthropitys rochei* also presents a very peculiar sequence of thickenings, the greatest differential of this species.

Group IV: Species without information about secondary wall thickenings in the tracheids.

Arthropitys renaultii Boureau, 1964 (Plate 14, Figs. A-C)
Locality: Autun (France).
Age: Permian.

Description: Species lacking secondary formations and showing very large pith. This species presents stem of 2.5 cm in diameter and cortex of 3-mm thickenings. There is no information in the original description of the branching system.
Comments: This species is poorly described and there is no information about the radial and tangential sections, making comparisons difficult. Boureau (1964) arguded that *Arthropitys renaultii* differs from *A. herbacea* because it presents preserved pith, but these structures represent primary structures in the plant body and they are not used to limit species. Thus, *A. renaultii* and *A. herbacea* could represent young specimens. Although *A. renaultii* represented a young stem with very degradable cells because of the absence of lignified structures, Galtier et al. (2011) found a specimen in Sardinia Island which is very similar to it.

Arthropitys approximata (Schlotheim) Renault, 1896 [apud Andrews (1952); Boureau (1964)] (Plate 14, Fig. D)
Locality: Saint-Étienne, Commentry and Autun (France).
Age: Late Carboniferous (Andrews, 1952).
Description: Stem is 10 cm in diameter and internode distances are between 5-20 mm. Fascicular wedges present 1.5-mm width separated by interfascicular rays of tenths of a millimeter. There is no information in the original description of either the branching system or the secondary wall thickenings in the tracheids.
Comments: The description is very generic and there is no information available to consider *Arthropitys approximata* a new species. The lack of tracheid thickenings in makes it rather difficult to compare it with the other species.

Group V: The species described by Hirmer and Knoell.

Hirmer and Knoell (in Knoell, 1935) described five species based principally on cross section; only *Arthropitys felixi* has radial section showing secondary wall thickenings in the tracheids. The absence of radial and tangential sections makes it impossible to affiliate these species with other described species. Even when cross-sectioned, fascicular wedges and interfascicular rays are totally different from the other species and can not be neglected when it is necessary to compare them with a newly-discovered species. In these species, there is no information about the branching system.

Arthropitys bistriatoides Hirmer & Knoell (in Knoell, 1935) (Plate 15, Figs. A-C)
Locality: England and Ruhr (Germany).
Age: Late Bashkirian, Early Pennsylvanian (England) and Bashkirian-Moscovian, Early Middle Pennsylvanian (Ruhr).
Description: Poorly-developed secondary body with thickness of approximately 3 mm. Fascicular wedges and interfascicular rays present paralell sides throughout the secondary body.
Comments: Poorly-developed secondary body; it could represent an ontogenetic stage because of the large quantity of medullar cells in comparison to the secondary xylem cells. The paralell sides of fascicular wedges and interfascicular rays can associate it with *A. lineata* or *A. bistriata*, but nothing else can be inferred.

Arthropitys herbacea Hirmer & Knoell (in Knoell, 1935) (Plate 15, Figs. D-E)
Locality: Ruhr and Aachen (Germany).
Age: Bashkirian-Moscovian, Early Middle Pennsylvanian.
Description: Secondary body is almost absent, with a thickness of approximately 4 mm, and a large pith cavity with 3.5-cm in diameter. Interfascicular rays in cross section are narrow.
Comments: This species present a poor driscription, but its secondary body in cross section is very different from other species. It could represent a young stem because of the large pith cavity, but nothing else can be inferred.

Arthropitys felixi Hirmer & Knoell (in Knoell, 1935) (Plate 16, Figs. A-D)
Locality: Ruhr (Germany).
Age: Bashkirian-Moscovian, Early Middle Pennsylvanian.
Description: Secondary body is well developed. Interfascicular rays in cross section increase in width radially, and fascicular wedges present constant width throughout secondary body. *Arthropitys felixi* is the only species described by Hirmer & Knoell that presents radial section, showing tracheids with scalariform secondary wall thickenings.
Comments: Unlikely *Arthropitys herbacea* and *A. bistriatoides*, *A. felixi* presents secondary body of considerable thickness. As *Arthropitys lineata, A. felixi* presents fascicular wedges of constant width throughout the secondary body, but in *A. felixi* the interfascicular rays increase in width radially, and in *A. lineata* this information

is not available. It differs from *A. bistriata* because in this species fascicular wedges increase in width and interfascicular rays decrease in width radially; and in *A. felixi* fascicular wedges present constant width and interfascicular rays increase in width radially.

Arthropitys hirmeri Knoell, 1935 (Plate 17, Figs. A-B)
Locality: Ruhr and Aachen (Germany).
Age: Bashkirian-Moscovian, Early Middle Pennsylvanian.
Description: Secondary body with 1.8 mm in thickness. Fascicular wedges are composed of tracheids and narrow rows of parenchymatous cells, and there are no interfascicular rays, giving the secondary body a homogeneous aspect.
Comments: *Arthropitys hirmeri* presents a very singular secondary body among the species of the genus. It could represent a young stem or a species that presents tracheids in the secondary body only.

Arthropitys jongmansi Hirmer, 1927 (in Knoell, 1935) (Plate 19, Fig. C-D)
Locality: Ruhr and Aachen (Germany).
Age: Bashkirian-Moscovian, Early Middle Pennsylvanian.
Description: Poorly-developed secondary body of approximatelly 1.3 mm in thickness and large pith cavity with 3-cm in diameter.
Comments: This species is similar to *Arthropitys herbacea*, but presents a medullary tissue which is more developed between the pith cavity and the fascicular wedges. It differs from *A. renaultii* since it shows no medullary tissue persistence and a large amount of centripetal xylem.

Group VI: *Arthropitys hirmeri*, *A. communis* and *A*. *bistriata* varieties.

The concept of biological variety is applied whem some specimens within a population show differences among them in their distribution area. However, in Palaeontology, when very few specimens are preserved in the record, what is the point in applying this concept?

Arthropitys hirmeri Knoell var. ***intermedia*** Knoell, 1935 (Plate 16, Figs. E)
Locality: England and Aachen and Ruhr (Germany).

Age: Late Bashkirian, Early Pennsylvanian (Ruhr and England) and Bashkirian-Moscovian, Early Middle Pennsylvanian (Ruhr and Aachen).

Description: Species with significant secondary growth. Secondary body is similar to *A. hirmeri*, but interfascicular rays persist between fascicular wedges up to a point and then disappear abruptly, where only tracheids of fascicular wedges persist.

Arthropitys communis (Binney) var. ***interlignea*** Hirmer & Knoell, 1935 (in Knoell, 1935) (Plate 17, Figs. C-F)

Locality: England and Ruhr and Aachen (Germany).

Age: Late Bashkirian, Early Pennsylvanian (England) and Bashkirian-Moscovian, Early Middle Pennsylvanian (Ruhr and Aachen).

Description: Interfascicular wedges are like the ones in *A. communis*, but with smaller width.

Arthropitys communis (Binney) var. ***septata*** Andrews, 1952 (Plate 18)

Locality: Calhoun Coal, upper MacLeansboro Group, Illinois (USA).

Age: Late Pennsylvanian.

Description: This variety presents oblong carinal canals. Pith region cells of different sizes with dark contents; they were probably secretory cells. In radial section, tracheids present scalariform thickenings; in tangential and radial section they are septates. Fascicular wedges in the pith region have the same width as interfascicular rays -approximately 0.5 mm in width. Fascicular rays and their cells radially decrease in width and size, respectively.

Arthropitys bistriata (Cotta) Goeppert var. ***borgiensis*** Renault, 1896 (Plate 19, Fig. A-B)

Locality: Champs des Borgis and Autun (France).

Age: Permian of Autun (França).

Description: Fascicular wedges are thick and present rounded extremities.

Arthropitys bistriata (Cotta) Goeppert var. ***augustodunensis*** Renault, 1896 (Plate 20, Fig. A-C)

Locality: Champs des Borgis and Champs des Espargeolles (France).

Age: Permian of Autun.

Description: Fascicular wedges are thick and rectilinear.

Arthropitys bistriata (Cotta) Goeppert var. ***valdajolensis*** Renault, 1896 (Plate 20, Fig. D-G)

Locality: Autun and Val d'Azol (France).

Age: Permian.

Description: Fascicular wedges are notably separeted by interfascicular rays. Fascicular wedges are thicker than previously.

7. Final considerations

7.1. Nomenclatual questions

- The portions of the secondary body which contain tracheids and parenchymatous cell should be called fascicular wedges; and the parts that contain only parenchymatous cells, interfascicular wedges, once the determination of the sphenophyte groups was based on the geometric shape of such portions (*spheno* = wedge). However, with the aim of no longer creating more terms for the group, the portions containing parenchymatous cells only will be called interfascicular rays, just like the term used by Rößler & Noll (2006, 2010) and Rößler et al. (2012);

- The use of the term "primary" to qualify any parenchymatous structure seems to be a mistake, since the first thing to appear in the vegetal body development must be the tracheids, which may function either as conduction or support (Mosbrugger, 1990).

7.2. The described species

- *Arthropitys bistriata* was emended through anatomical features but especially in relation to branching system; it was composed of 10-15 branches per node, disposed in line along the stem;

- *Arthropitys communis* is a species lacking information about the branching system, but its interfascicular rays present a singular narrowing throughout the secondary body;

- *Arthropitys lineata* do not present information about the width of interfascicular rays throughout the secondary body. It must be known in order to

associate it with *A. felixi* whether the interfascicular rays increase in width radially or it actually respresents another species that presents constant interfascicular ray width;

- *Arthropitys gallica* is very similar to *A. communis*, but it is a valid species because it presents fascicular wedges composed of 10 cell rows, whereas in *A. communis* these wedges are composed of 25-30 cell rows;

- *Arthropitys medullata* presents very generic diagnosis, and there is nothing to justify it as a new species;

- *Arthropitys deltoides* does not present information about the branching system, but its concentric organization of the fascicular wedges makes it a singular species within the genus;

- *Arthropitys junlianensis* is similar *to A. communis* and *A. gallica.* However, the composition of the interfascicular rays is different from these species, making it a valid species;

- *Arthropitys yunnanensis* presents very peculiar interfascicular rays, totally different from other species within the genus;

- *Arthropitys ezonata* is a very well-described species and was emended joining anatomical and morphological features;

- *Arthropitys major* is a poorly-described species, but within the species with reticulate thickenings, it presents a singular constitution of interfascicular rays;

- *Arthropitys cacundensis* is very similar to *A. sterzelii* to. The difference is that *A. sterzelii* presents 5 branches in young stems and 2-5 in adult stems, whereas *A. cacundensis* presents 2-3 branches per node. As *A. cacundensis* was described from only two fragments, we considered it as a fragment of an adult *A. sterzelli* stem*;*

- *Arthropitys gigas*, *A. porosa* and *A. rochei* are especies with no information about branching system available, but they present a sequence of tracheid thickenings totally peculiar within the species of the genus. According to Anderson (1954) and Cutter (1978), because of its developemental stage, the primary xylem usually presents anular and helical thickenings, whereas the secondary xylem presents circular reticulate, elongate reticulate or scalariform thickenings, but it rarely presents the three kinds of thickenings in the same stem. So, it is necessary to revise these structures in *Arthropitys gigas*, *A. porosa* and *A. rochei* to confirm the kinds of thickenings in the tracheid walls;

- *Arthropitys approximata* is a species with very generic description and we did not consider it as a valid species;

- *Arthropitys renaultii* and *A. herbacea*: these species should represent stems in inicial ontogenetic stages, without secondary structures. Therefore, it is impossible to affilliate these species with other species. Thus, we considered that these stems should be classified in open nomenclature;

- *Arthropitys bistriatoides* is a species that presents paralell sides of fascicular wedges and interfascicular rays, and could represent a fragment of *A. lineata* or *A. bistriata*, but the lack of radial section makes this affiliation impossible. It is necessary to realize tangential and principally radial section of this species to validate it completely;

- *Arthropitys felixi* is a species with no information about branching system available; however, because of the scalariform thickenings and the description of fascicular wedges and interfascicular rays, it was considered as a valid species;

- *Arthropitys hirmeri* is a single species among the species of the genus because of the lack of parenchymatous cells of the interfascicular rays in the secondary body; but tangential and radial sections are necessary to validate it completely;

- *Arthropitys herbacea* and *A. jongmansi* are poorly-described species with large pith cavities and may represent young stems, but radial and tangential sections are necessary to validate them;

- The *Arthropitys hirmeri*, *A. communis* and *A*. *bistriata* varieties should be synonymized to their respective species because this concept is not applicable to fossil specimens.

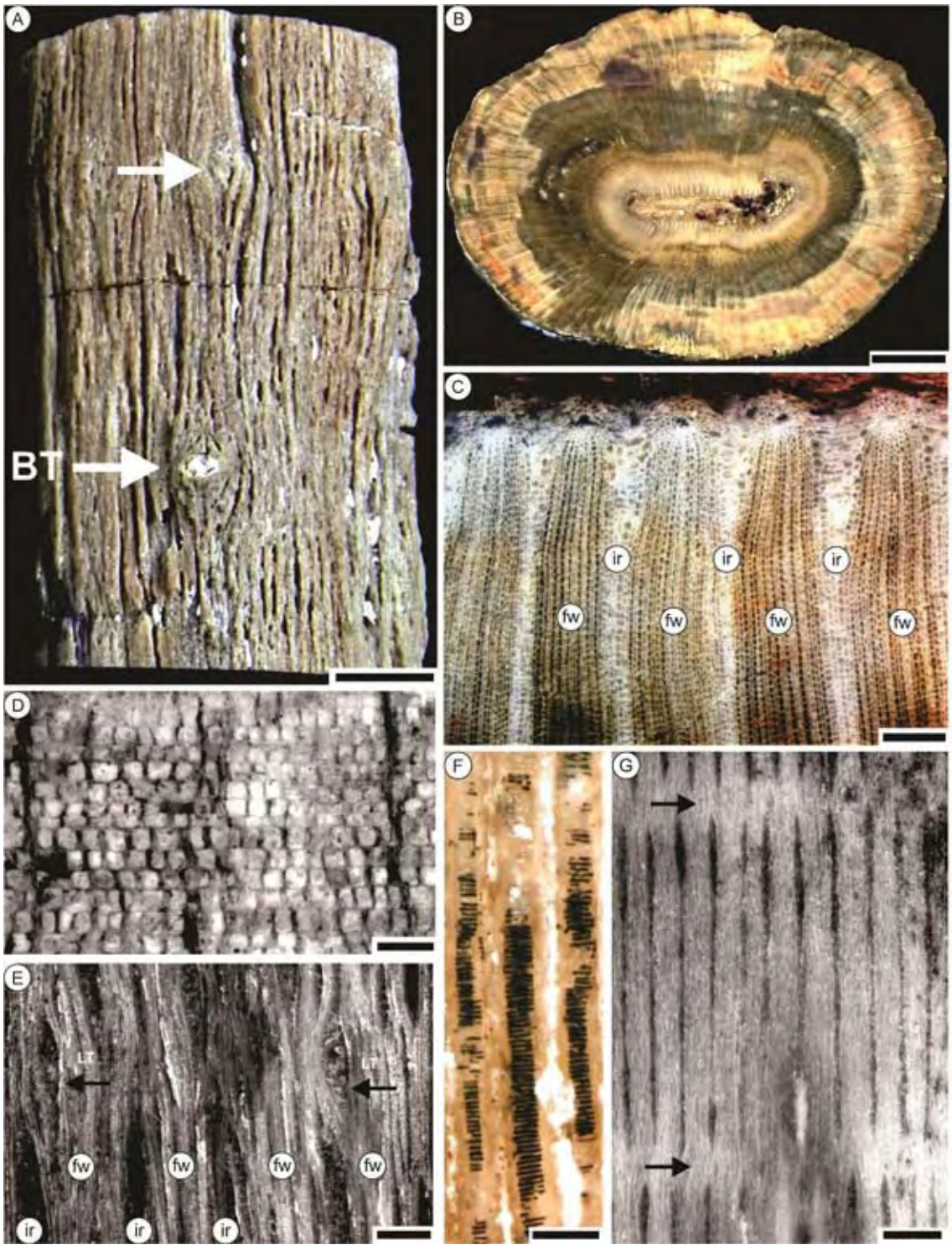

Plate II.1: *Arthopitys bistriata.* A: stem surface showing branch traces (BT). Scale bar = 10 mm; **B**: cross view in the basal part of the stem showing fascicular wedges and interfascicular rays. Scale bar = 10 mm; **C**: cross view showing fascicular wedges, interfascicular rays and carinal canals. Scale bar = 500 µm; **D**: radial view showing parenchymatous cells of interfascicular rays. Scale bar = 200 µm; **E**: tangential view showing leaf traces (LT), fascicular wedges and interfascicular rays. Scale bar = 2 mm; **F**: radial view showing tracheid with scalariform secondary wall thickenings. Scale bar = 100 µm; **G**: tangential view showing fascicular wedges and interfascicular rays in nodal line (arrows). Scale bar = 2 mm. Figs.: Rößler & Noll (2010).

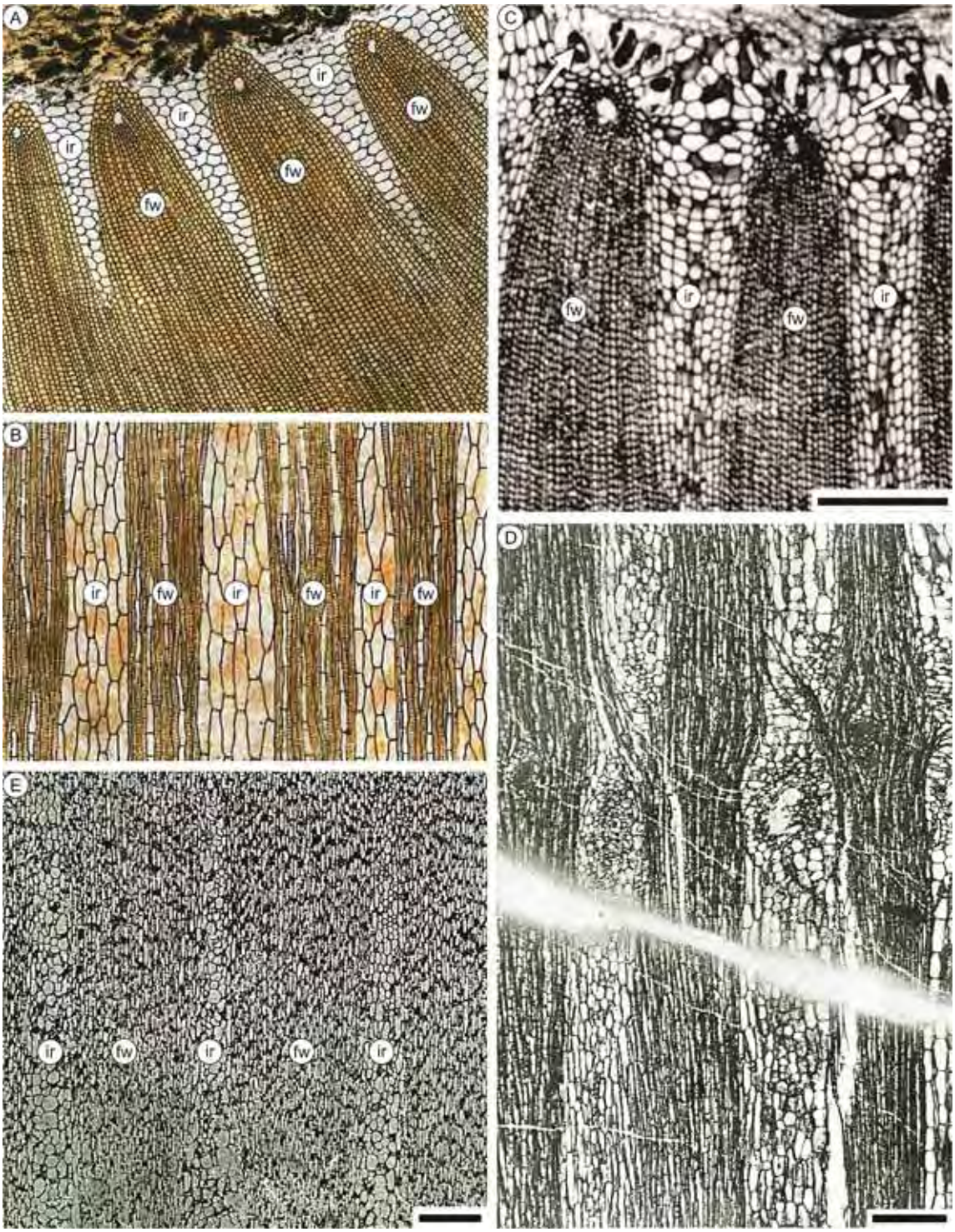

Plate II.2: *Arthopitys communis*. **A**: cross view showing fascicular wedges and interfascicular rays; **B**: tangential view showing cells of fascicular wedges and interfascicular rays; **C**: cross view in the periphery of the pith showing fascicular wedges, interfarcicular rays and secretory cells with dark contents (arrows). Scale bar = 500 µm; **D**: tangential view showing whorled branch scars (arrows) and cells of fascicular wedges and interfascicular rays in nodal line. Scale bar = 500 µm; **E**: tangential view showing parenchymatous cells of interfascicular rays (IR) and tracheids of fascicular wedges (FW). Scale bar = 500 µm. Figs: A-B: Renault (1893); C: Wang et al. (2003); D-E: Knoell (1935).

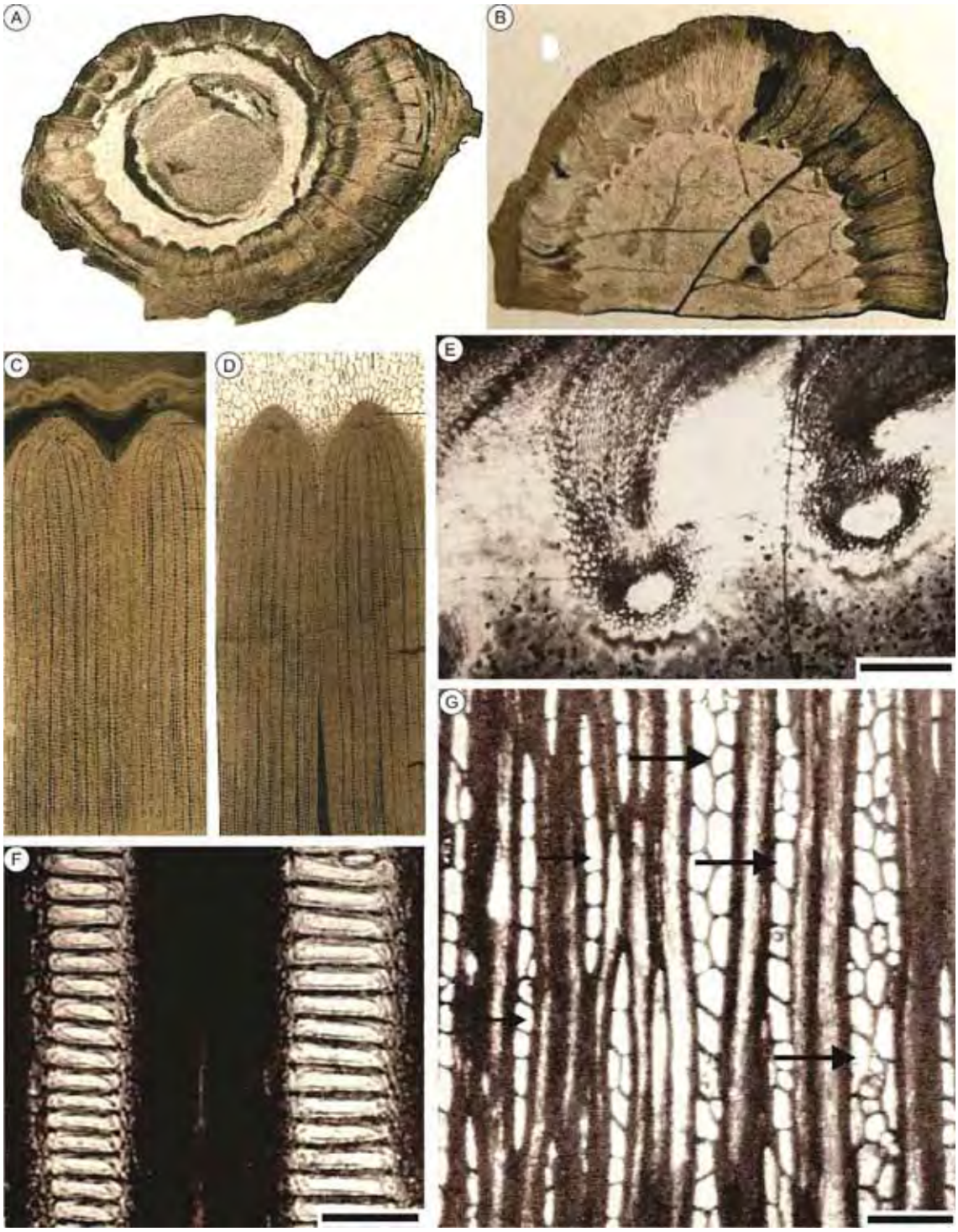

Plate II.3: *Arthopitys lineata.* **A-B**: cross views showing pith, fascicular wedges and interfascicular rays; **C-D:** cross views showing parallel sides of fascicular wedges and interfascicular rays; **E**: cross view showing fascicular wedges and carinal canals. Scale bar = 50 µm; **F**: radial view showing tracheid with scalariform secondary wall thickenings. Scale bar = 25 µm; **G**: tangential view showing tracheids of fascicular wedges and parenchymatous cells of interfascicular rays (large arrows) and cells of fascicular rays (small arrows). Scale bar = 100 µm. Figs: A-D: Renault (1893); E-G: Boureau (1964).

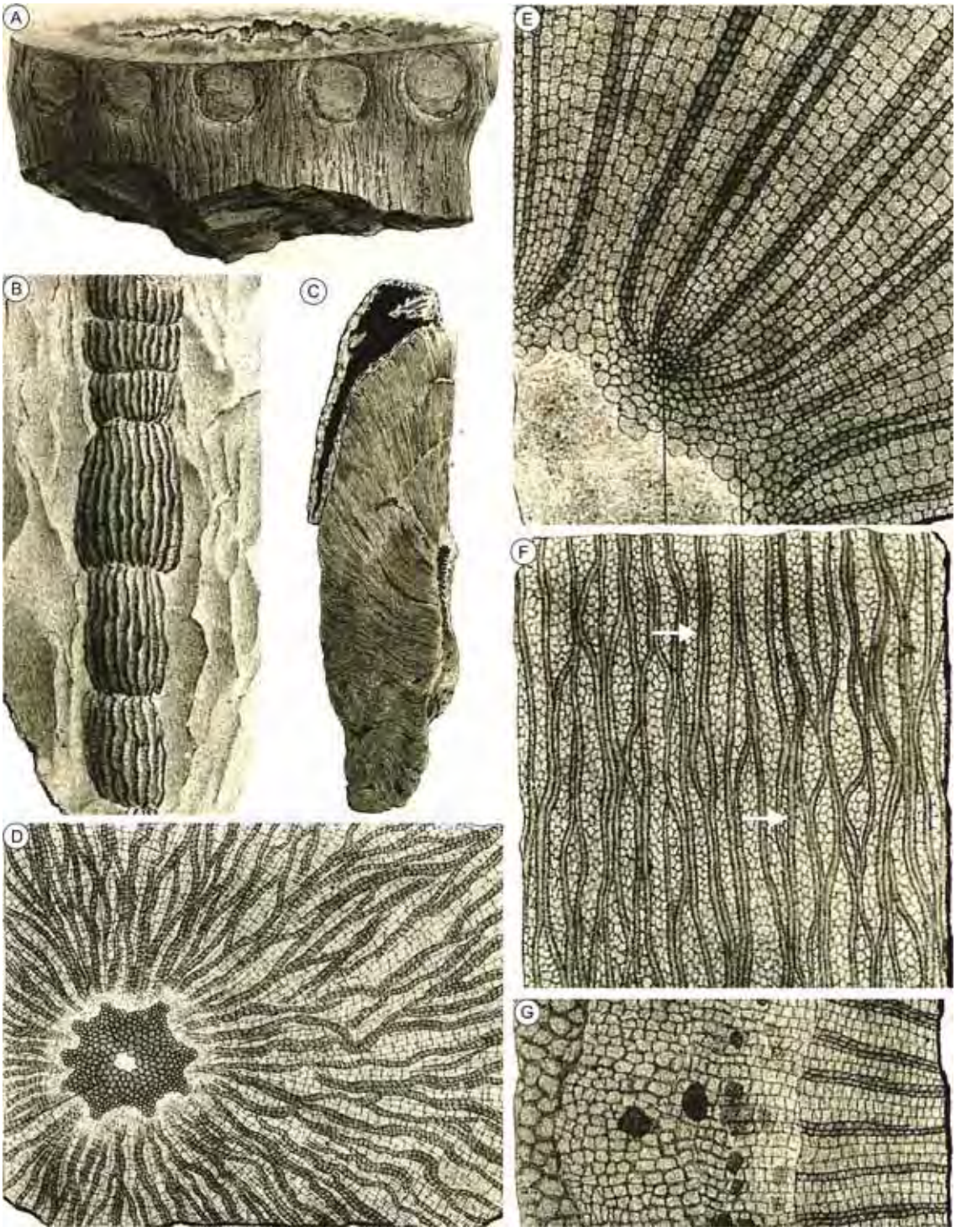

Plate II.4: *Arthopitys medullata*. **A:** stem showing whorls with five branch traces; **B:** cross view showing pith, fascicular wedges and interfascicular rays; **C:** tangential view showing tracheids (arrows) and parenchymatous cells of interfascicular rays; **D:** tangential view of an associated root showing pith cavity and its centripetal cells; **E:** cross view showing pith cavity, fascicular wedges and interfascicular rays; **F:** tangential view showing tracheids (arrows) and parenchymatous cells of interfascicular rays; **G:** cross view in the cortex region. Figs: Renault (1893).

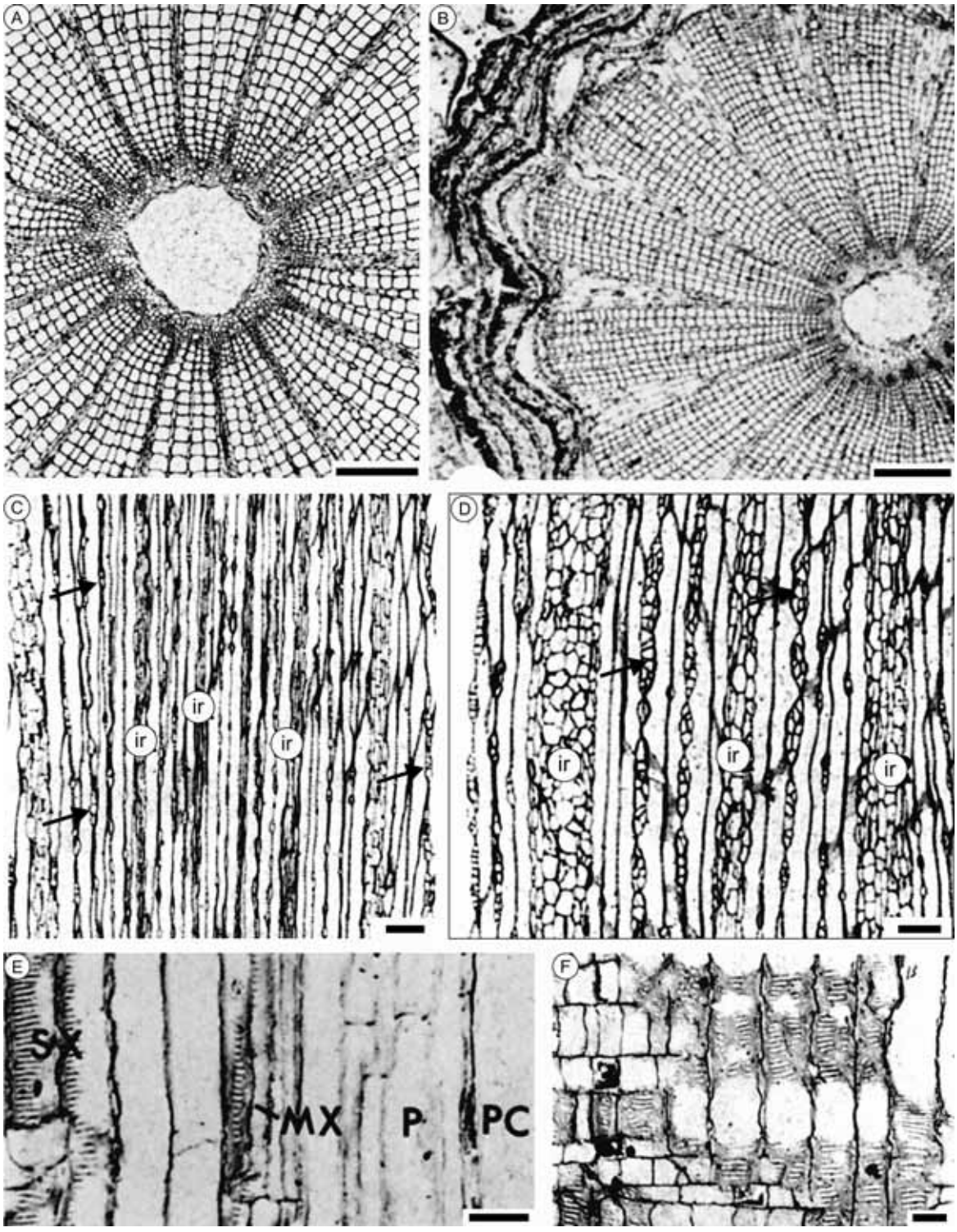

Plate II.5: *Arthopitys deltoides*. **A:** cross view showing pith, carinal canals, fascicular wedges and interfascicular rays. Scale bar = 1 mm; **B:** cross view in the cortex region. Scale bar = 1 mm; **C:** tangential view in the inner part of secondary body showing narrow interfascicular rays (IR) and fascicular rays with few cells in height (arrows). Scale bar = 250 µm; **D:** tangential view in the outer part of secondary body showing the widest interfascicular rays (IR) and the highest fascicular rays (arrows). Scale bar = 250 µm; **E:** radial view showing scalariform thickenings of metaxylem cells (SX) and secondary tracheids (SX). Scale bar = 50 µm; **F:** radial view showing tracheid with scalariform secondary wall thickenings. Scale bar = 50 µm. Figs: Cichan & Taylor (1983).

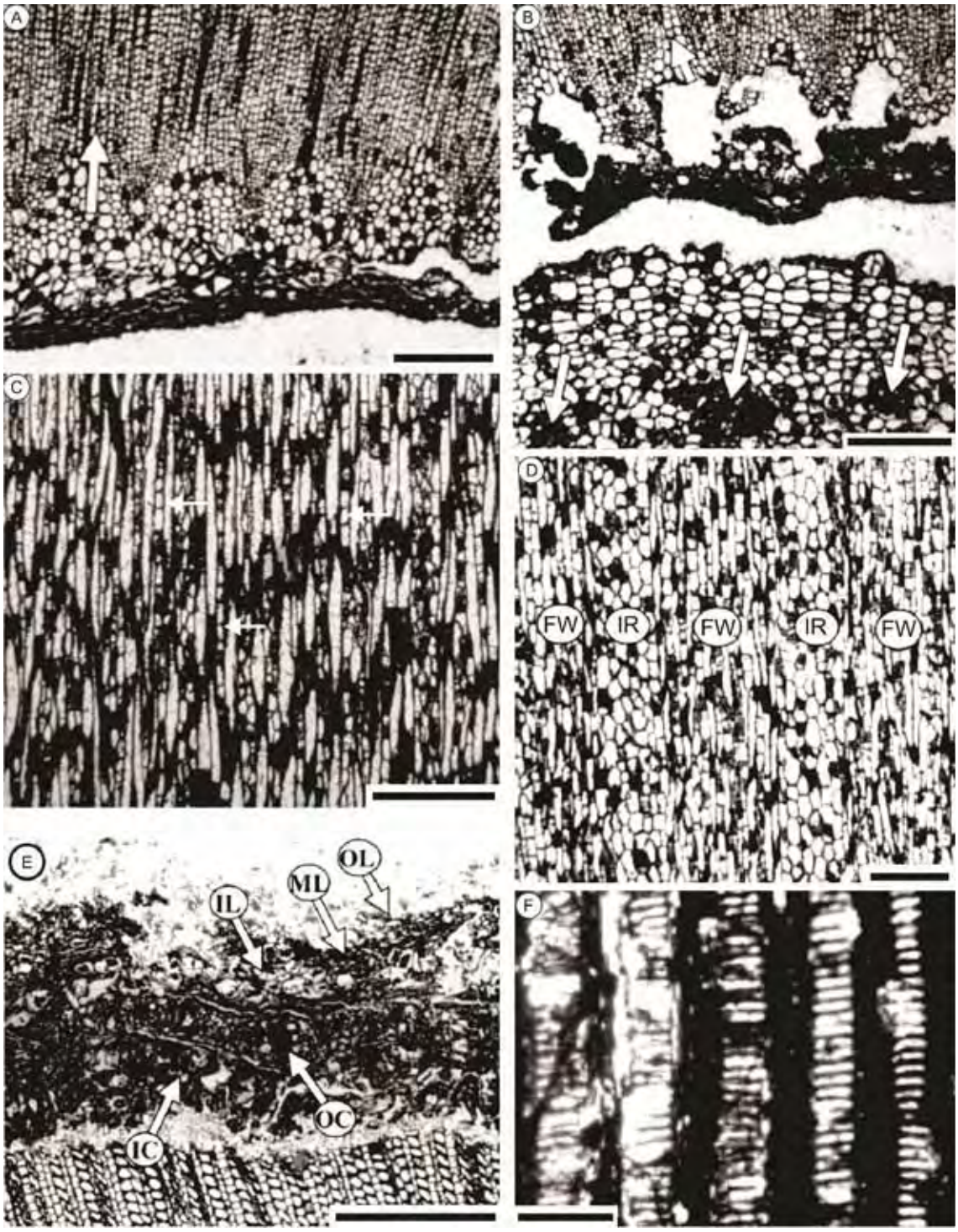

Plate II.6: *Arthopitys junlianensis*. **A:** cross view in the pith region showing abrupt narrowing of the interfascicular rays (arrows). Scale bar = 500 µm; **B:** cross view showing interfascicular rays (small arows) and perimedullary zone containing secretory cells with dark contents (large arrows). Scale bar = 500 µm; **C:** tangential view in the internal part of the stem showing tracheids and fascicular rays (arrows). Scale bar = 500 µm; **D:** tangential view in the internal part of the stem showing fascicular wedges (FW) and interfascicular rays (FI). Scale bar = 250 µm; **E:** cross view showing cortex (IC and OC) and periderm (IL, ML e OL). Scale bar = 1 mm; **F:** radial view showing tracheid with scalariform secondary wall thickenings. Scale bar = 50 µm. Figs: Wang et al. (2003).

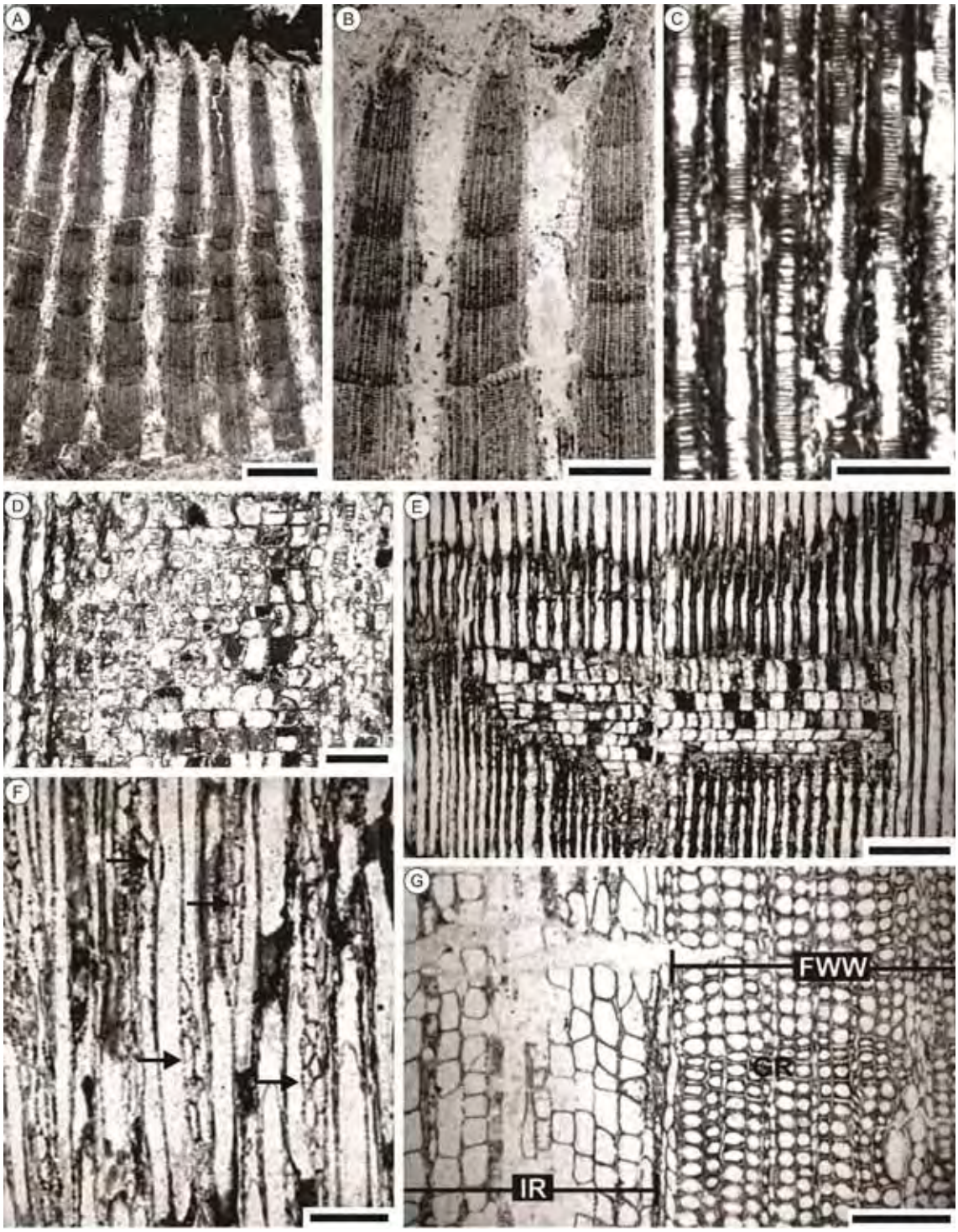

Plate II.7: *Arthopitys yunnanensis*. **A:** cross view showing fascicular wedges and interfascicular rays. Scale bar = 2mm; **B:** cross view showing fascicular wedges and interfascicular rays. Scale bar = 5mm; **C:** radial view showing tracheid with scalariform secondary wall thickenings. Scale bar = 200 µm; **D:** radial view showing fascicular wedges with cells of different sized fascicular rays. Scale bar = 250 µm; **E:** radial view showing fascicular wedges with cells of different sized fascicular rays. Scale bar = 300 µm; **F:** tangential view in the secondary body showing tracheids and cells of fascicular rays (arrows). Scale bar = 250 µm; **G:** cross view showing fascicular wedges (FW), interfascicular rays (IR) and growth rings (GR). Scale bar = 300 µm Figs: Wang et al. (2006).

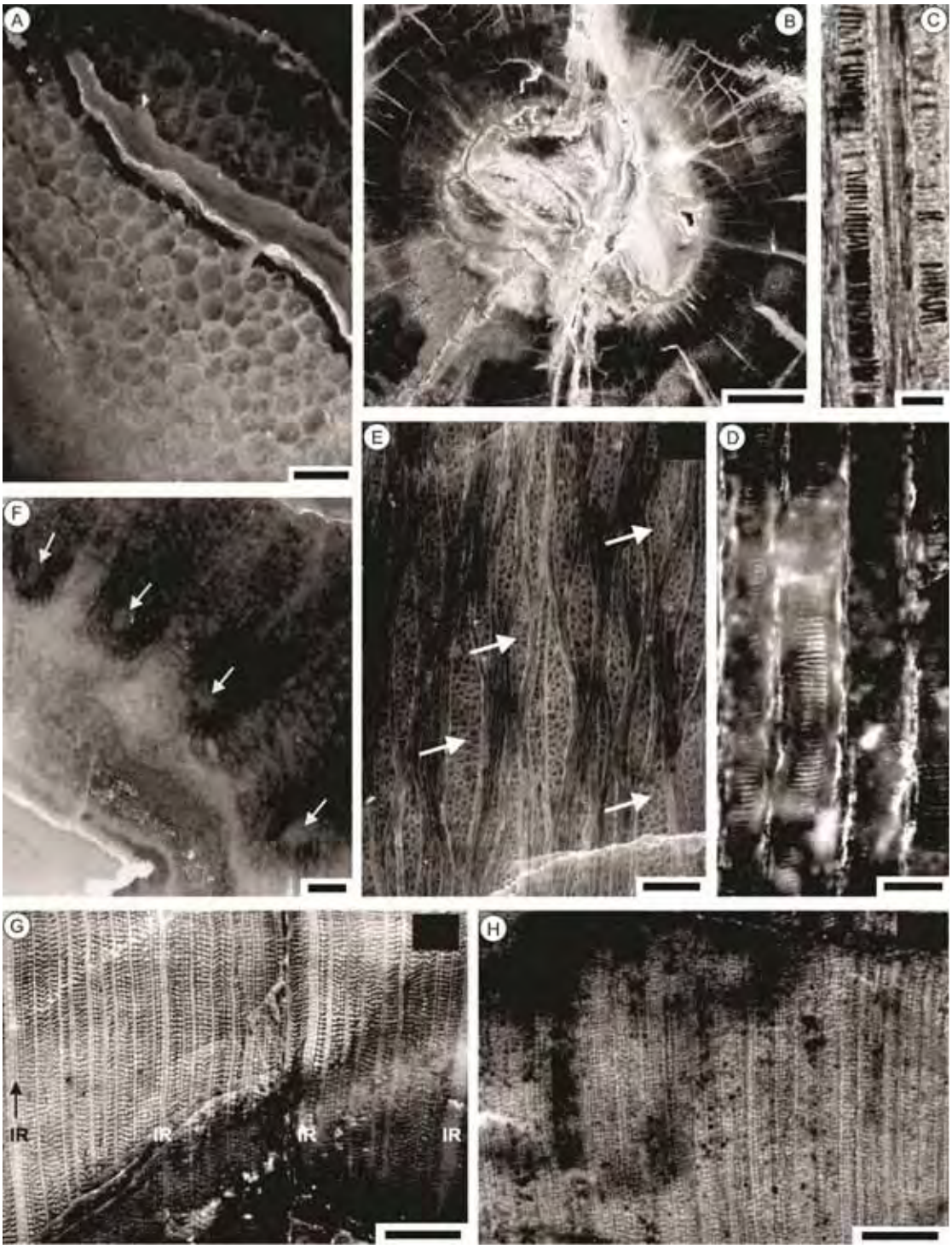

Plate II.8: *Arthopitys ezonata*. **A:** cross view showing hexagonal parenchymatous cells near the pith. Scale bar = 200 µm; **B:** cross view in the internal part showing the pith cavity. Scale bar = 5 mm; **C:** radial view showing tracheid with scalariform secondary wall thickenings. Scale bar = 100 µm; **D:** radial view showing tracheid with scalariform secondary wall thickenings. Scale bar = 50 µm; **E:** tangential view showing tracheids and a great number of parenchymatous cells in the interfascicular rays (arrows). Scale bar = 500 µm; **F:** cross view showing fascicular wedges, interfascicular rays and carinal canals (arrows). Scale bar = 250 µm; **G:** cross view showing differentiation between fascicular wedges and interfascicular rays (IR) in the inner part of the secondary body. Scale bar = 1mm; **H:** cross view showing the homogeneity between fascicular wedges and interfascicular rays (IR) in the outer part of the secondary body. Scale bar = 1mm. Figs: Rößler & Noll (2006).

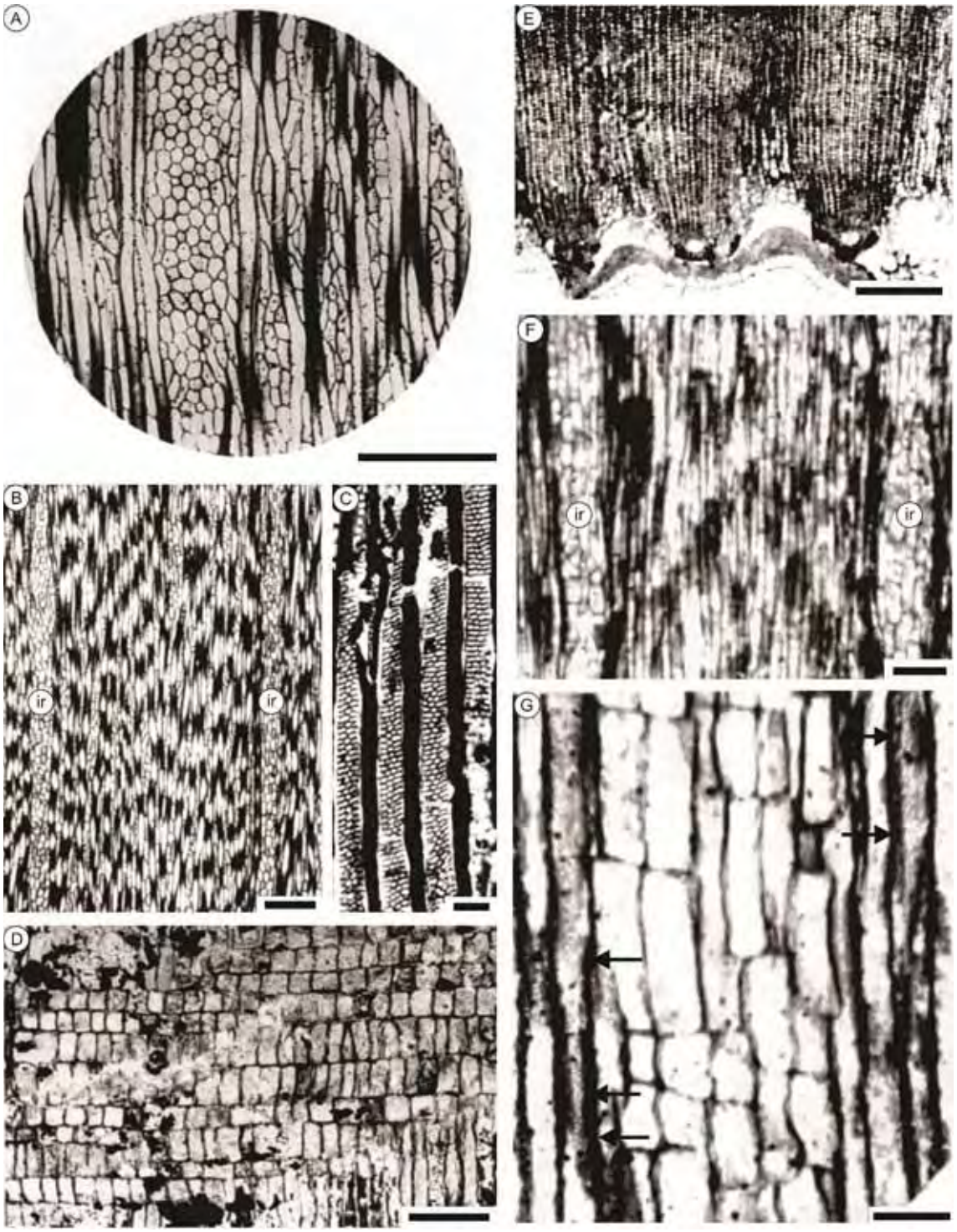

Plate II.9: *Arthopitys kansana* (A-D) and *Arthopitys illinoensis* (E-G). **A**: tangential view showing cells of fascicular wedges and interfascicular rays. Scale bar = 5 mm; **B**: tangential view showing cells of fascicular wedges and interfascicular rays. Scale bar = 250 µm; **C**: radial view showing tracheids with circular to elongate reticulate secondary wall thickenings of the. Scale bar = 50 µm; **D**: radial view showing parenchymatous cells of the fascicular wedges. Scale bar = 250 µm; **E**: cross view showing fascicular wedges and interfascicular rays in the pith region. Scale bar = 1 mm; **F**: tangential view showing fascicular wedges and interfascicular rays. Scale bar = 25 µm; **G**: radial view showing tracheids with circular reticulate secondary wall thickenings (arrows) and rectangular cells of interfascicular rays. Scale bar = 20 µm. Figs: Andrews (1952).

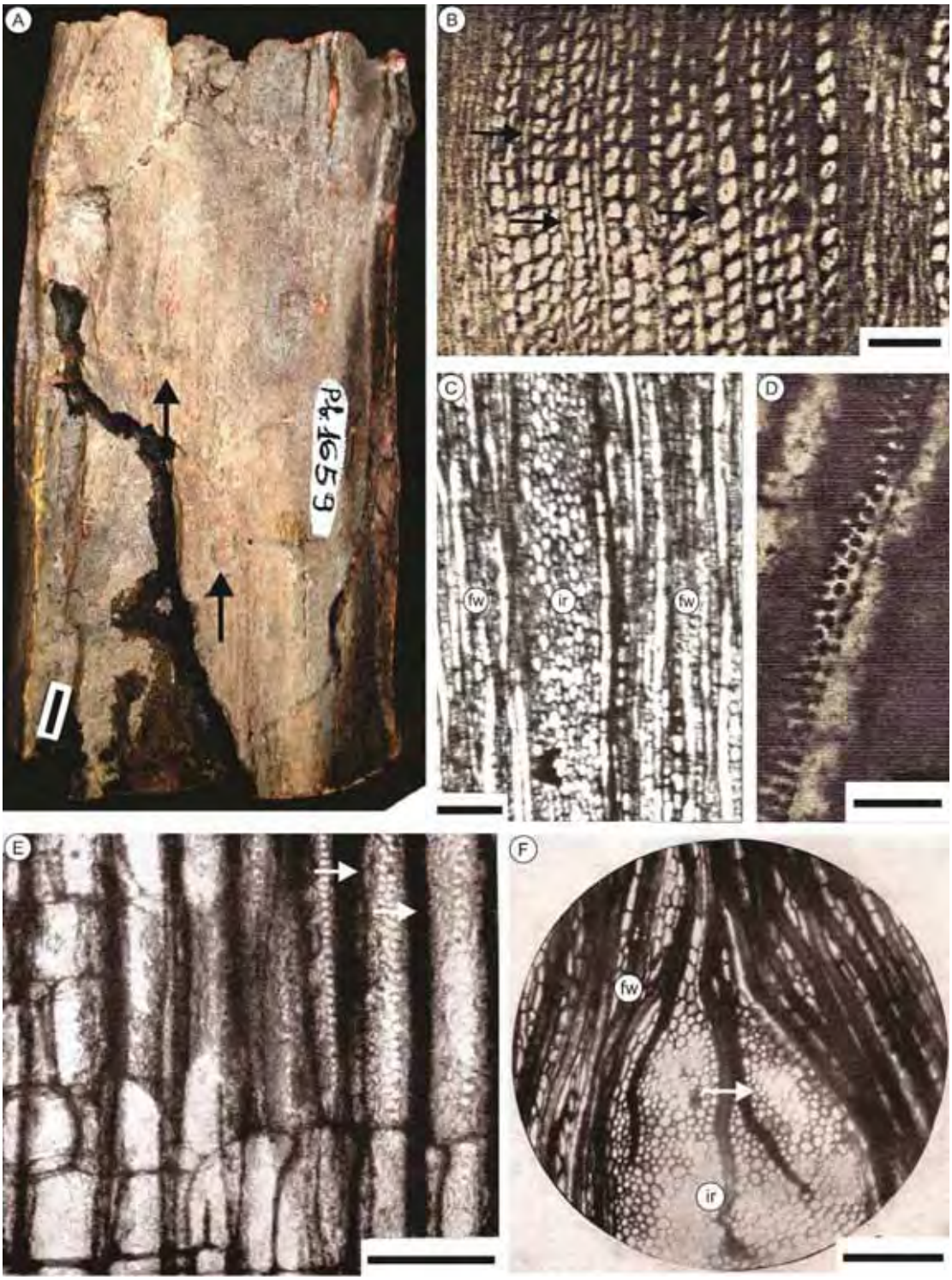

Plate II.10: *Arthopitys cacundensis* (A-D) and *Arthopitys major* (E-F). **A**: stem surface showing branch traces (arrows). Scale bar = 1 cm; **B**: cross view showing fascicular wedges with tracheids and fascicular rays (arrows). Scale bar = 125 µm; **C:** tangential view showing tracheids of the fascicular wedges and parenchymatous cells of interfascicular rays. Scale bar = 250 µm; **D**: radial view showing tracheid with circular reticulate secondary wall thickenings. Scale bar = 40 µm; **E:** tangential view showing tracheid with reticulate secondary wall thickenings (arrows) and parenchymatous cells of the interfascicular rays. Scale bar = 125 µm; **F**: radial view showing fascicular wedges (fw), interfascicular ray (ir) and the intrusion of one tracheid in the interfascicular ray (arrow). Scale bar = 5 mm. Figs: 1: Rosemarie Rohn; 2-4: Coimbra & Mussa (1984); 5-6: Boureau (1964).

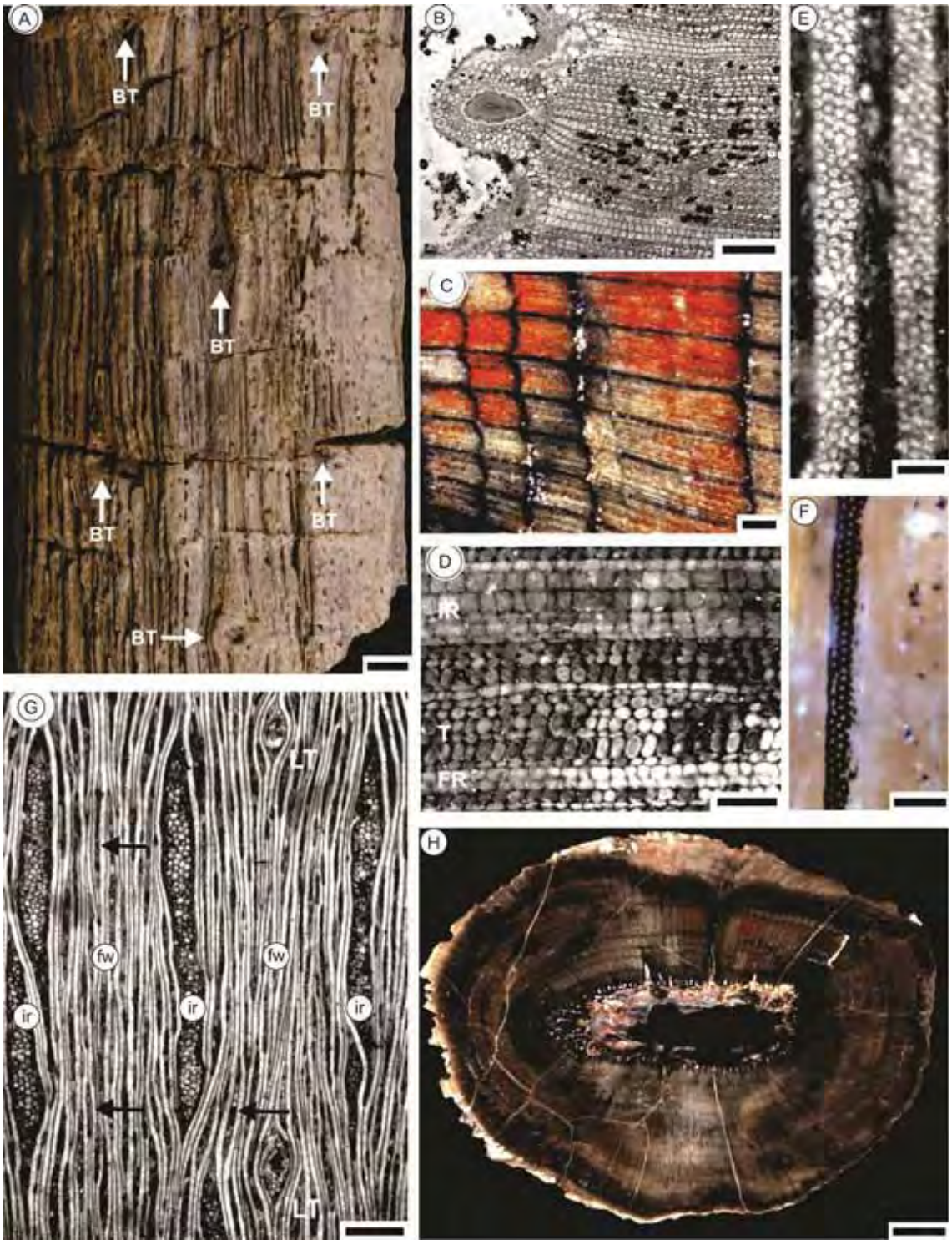

Plate II.11. *Arthopitys sterzelli*. **A**: stem surface showing branch traces (BT). Scale bar = 1 cm; **B**: cross view showing carinal canals. Scale bar = 400 µm; **C:** cross view showing growth rings. Scale bar = 1 mm; **D:** cross view showing fascicular ray (FR), tracheids and interfascicular ray (IR). Scale bar = 200 µm; **E**: radial view showing tracheid with circular reticulate secondary wall thickenings. Scale bar = 25 µm; **F:** radial view showing tracheid with circular reticulate secondary wall thickenings. Scale bar = 50 µm; **G**: tangential view showing tracheids of the fascicular wedges (FF) with fascicular ray cells (arrows), interfascicular ray cells (FI) and leaf traces (LT). Scale bar = 500 µm; **H**: cross view of the stem. Scale bar = 1 cm. Figs: Rößler & Noll (2010).

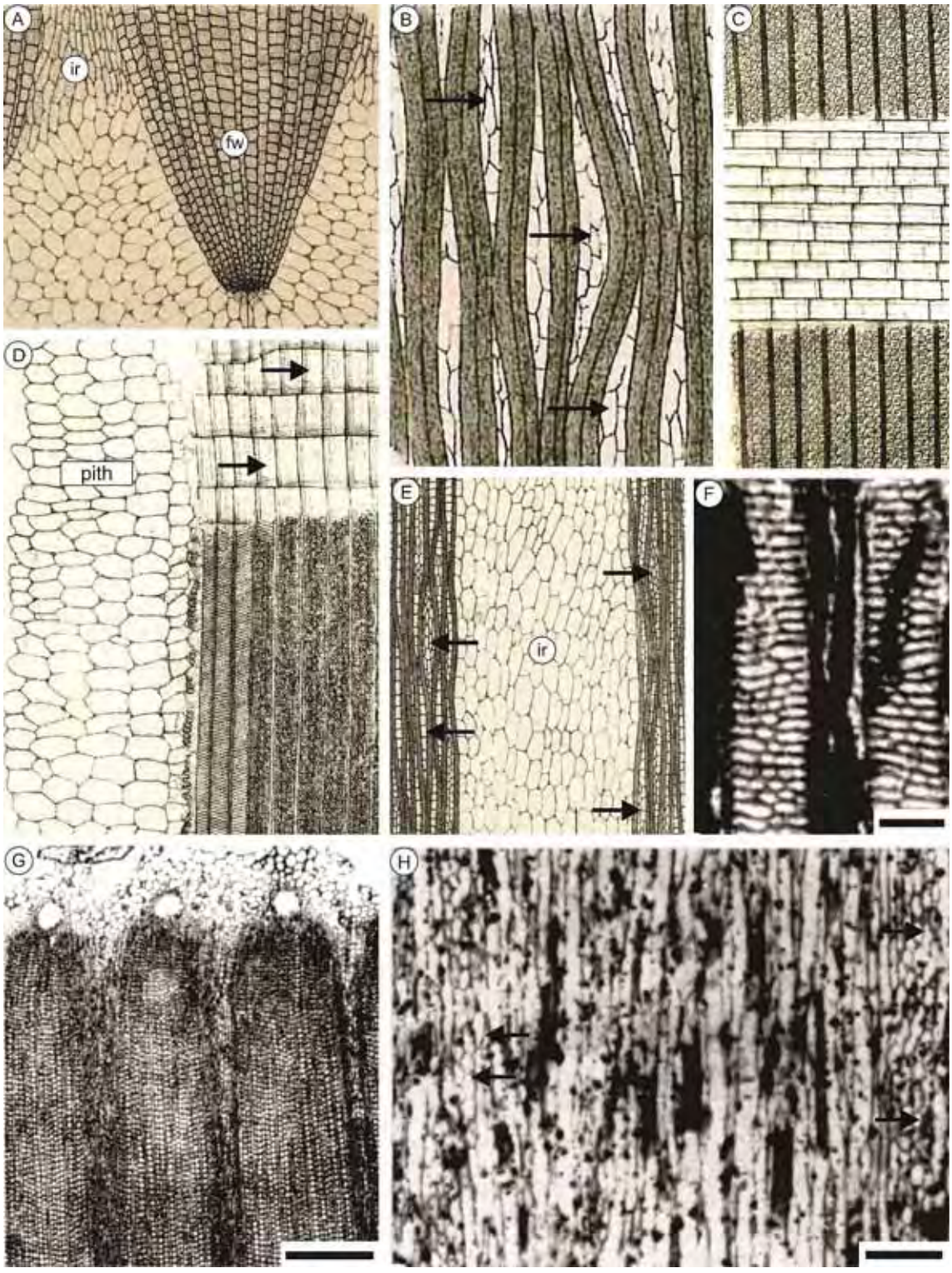

Plate II.12: *Arthopitys gigas* (A-E) and *Arthopitys versifoveata* (Figs. F-H). **A**: stem surface showing furrows and ridges in nodal line; **B**: cross view showing fascicular wedges and interfascicular rays in pith region; **C**: radial view showing tracheid with circular reticulate secondary wall thickenings; **D**: tangential view showing tracheids and fascicular rays (arrows); **E**: radial view showing the three kinds of tracheid thickenings and cells of higher than wide fascicular rays (arrows); **F**: radial view showing tracheid thickenings. Scale bar = 50 µm; **G**: cross view showing fascicular wedges, interfascicular rays and carinal canals. Scale bar = 100 µm; **H**: tangential view showing tracheids of fascicular wedges and parenchymatous cells of interfascicular rays. Scale bar = 250 µm. Figs: A-E: Renault (1893); F-H: Anderson (1954).

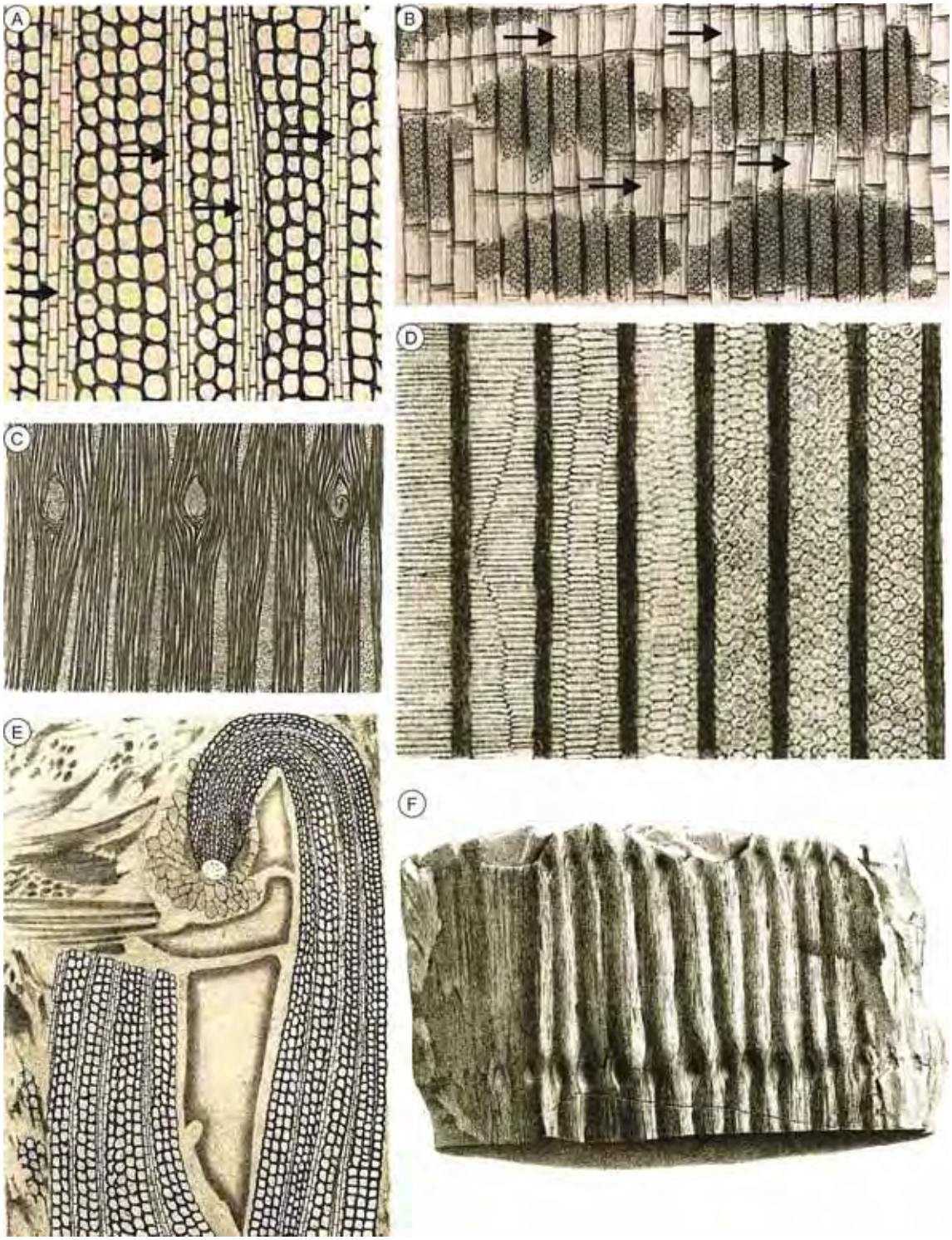

Plate II.13. *Arthopitys porosa* (A-D) and *Arthopitys rochei* (E-F). **A**: fascicular wedges in cross view showing tracheids and rectangular parenchymatous cells of the fascicular rays (arrows); **B**: radial view showing tracheid with circular reticulate secondary wall thickenings and higher than wide fascicular ray cells (arrows); **C**: tangential view showing fascicular wedges and interfascicular rays in nodal line; **D**: radial view showing the three kinds of tracheid thickenings; **E**: cross view showing curved fascicular wedges; **F**: stem surface showing furrows and ridges. Figs.: Renault (1893).

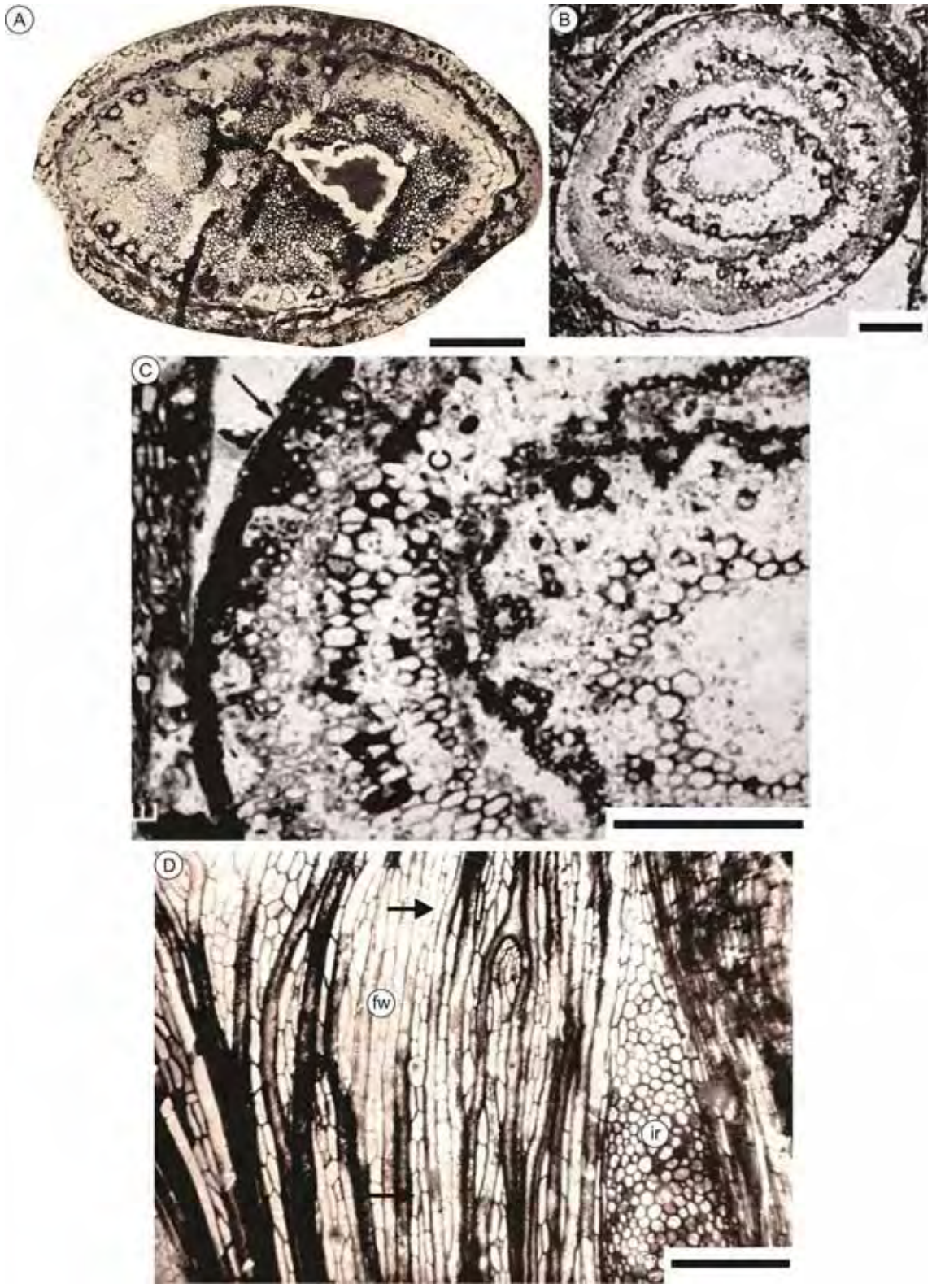

Plate II.14. *Arthopitys renaultii* (A-C) and *Arthopitys approximata* (D). **A-C**: cross views showing pith, fascicular wedges and interfascicular rays. Scale bar = 0.5 mm; **D**: cross view showing fascicular wedges, interfascicular rays and fascicular rays. Scale bar = 500 µm. Figs.: A and D: Boureau (1964), B-C: Galtier et al. (2011).

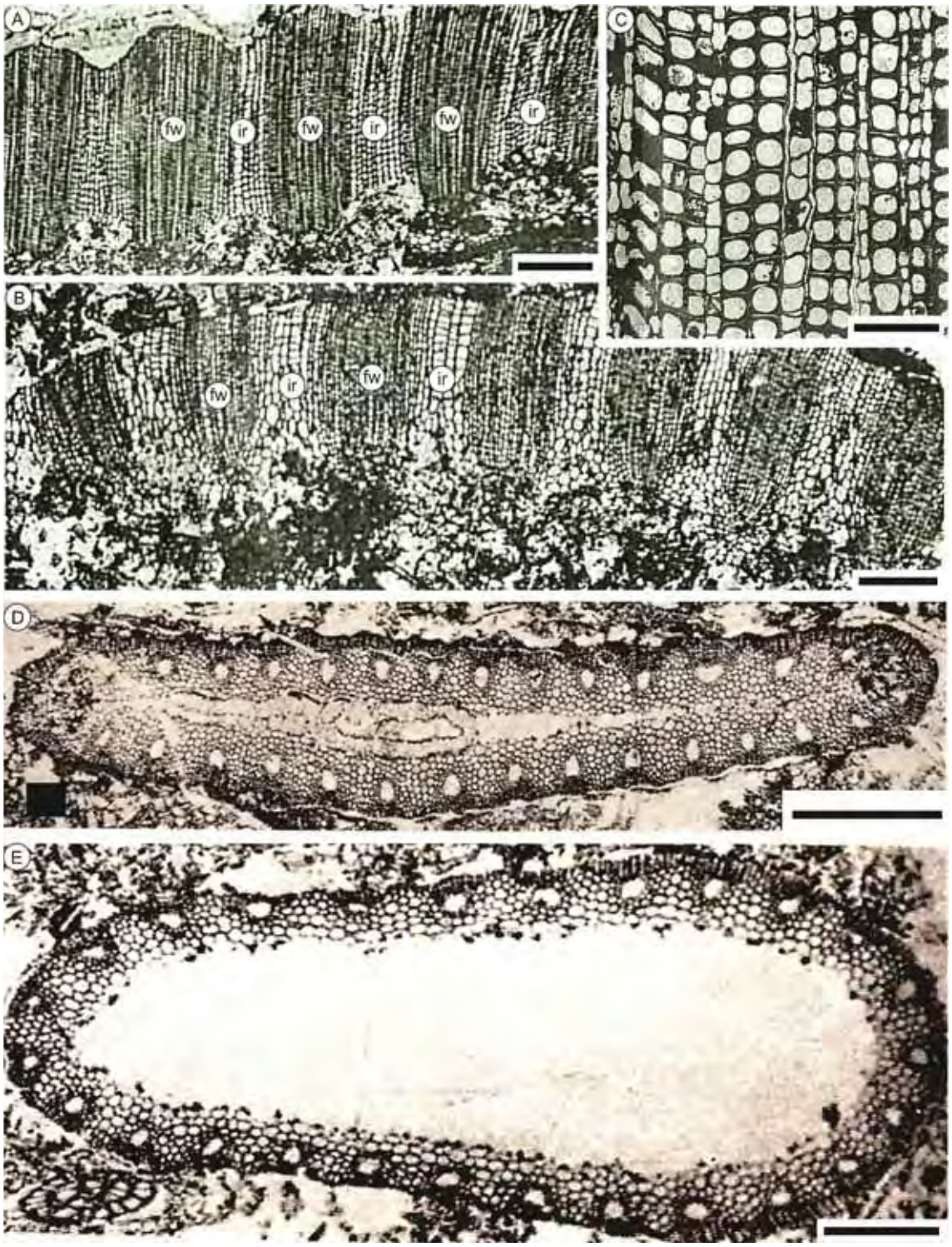

Plate II.15. *Arthopitys bistriatoides* (A-C) and *Arthopitys herbacea* (D-E). **A-B**: cross views showing fascicular wedges, interfascicular rays and the reduced secondary body. Scale bar = 1 mm; **C**: cross view showing tracheids (square cells) and rectangular parenchymatous cells. Scale bar = 500 µm; **D**: cross view showing large pith cavity and the reduced secondary body. Scale bar = 1 mm; **E**: cross view showing large pith cavity and the reduced secondary body. Scale bar = 0.5 mm. Figs: A-C: Knoell (1935); D-E: Boureau (1964).

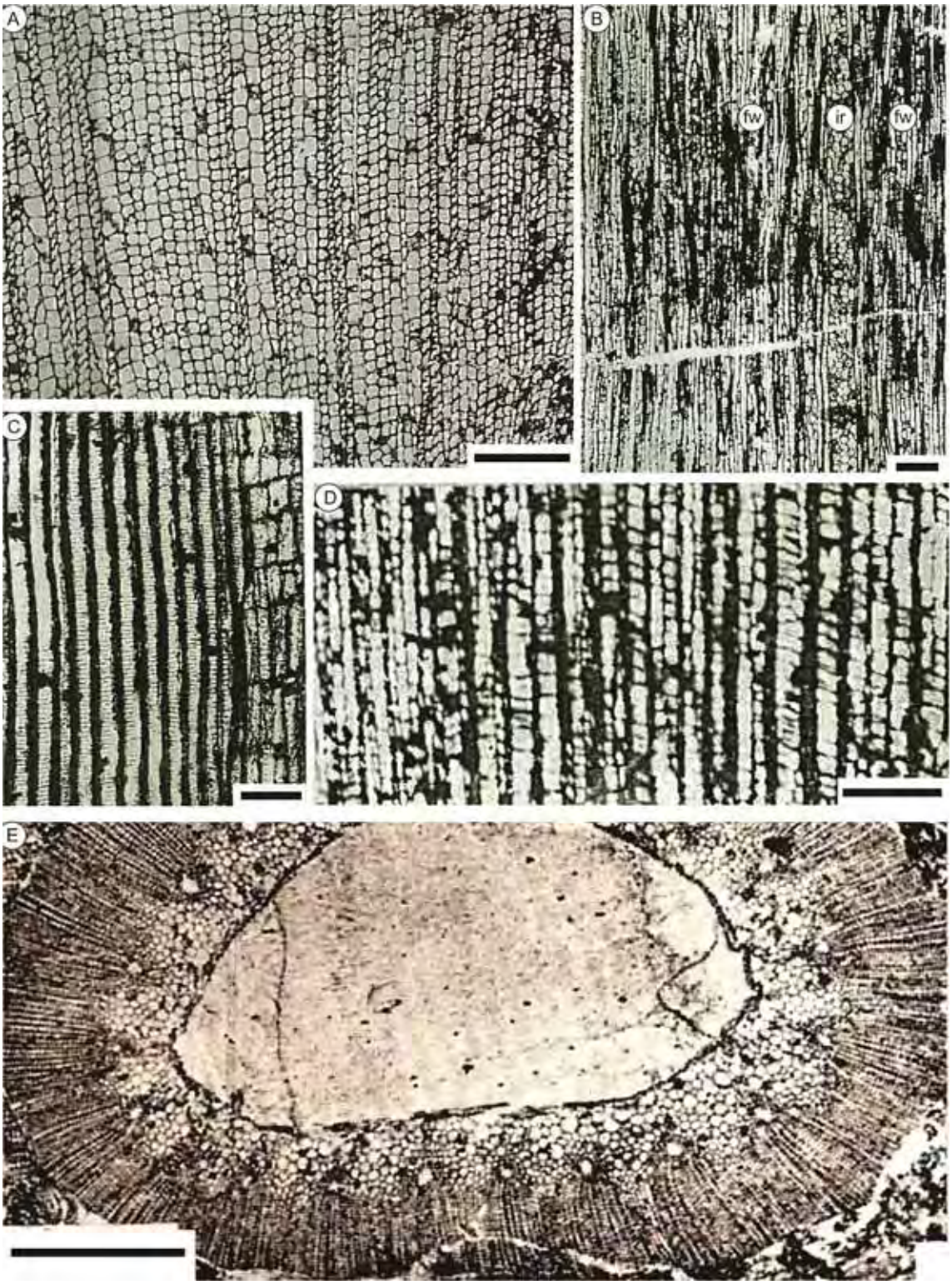

Plate II.16. *Arthopitys felixi* (A-D) and *Arthopitys hirmeri*. var. *intermedia* (E). **A**: cross view in the internal part showing tracheids and parenchymatous cells. Scale bar = 250 µm; **B**: tangential view showing tracheids of the fascicular wedges (fw) and parenchymatous cells of the interfascicular rays (ir). Scale bar = 250 µm; **C**: radial view showing tracheid thickenings. Scale bar = 100 µm; **D**: magnification of Fig. A. Scale bar = 250 µm; **E**: cross view showing pith cavity and well-developed secondary body. Scale bar = 1 mm. Figs: A-D: Knoell (1935); E: Boureau (1964).

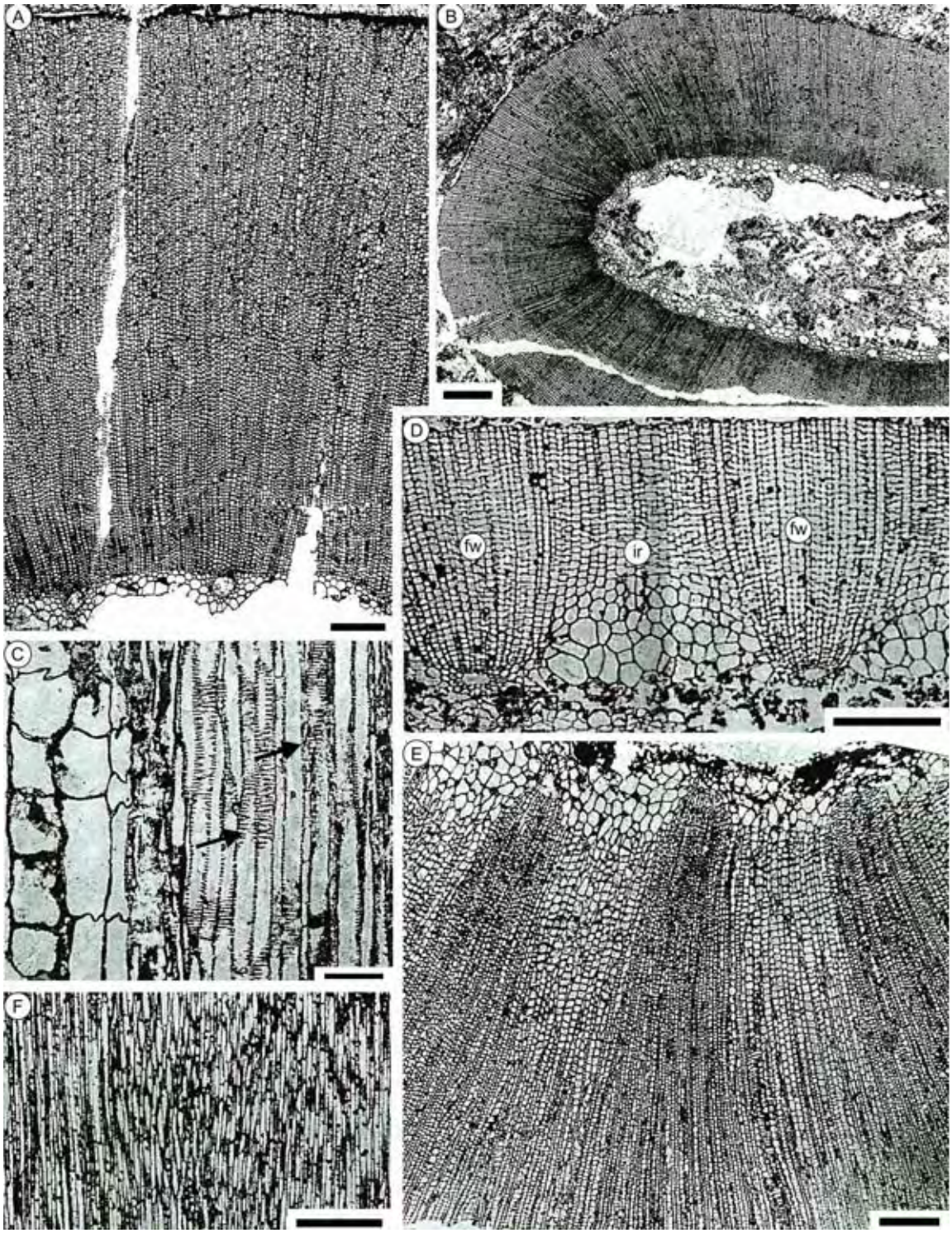

Plate II.17. *Arthopitys hirmeri* (A-B) and *Arthopitys communis* var. *interlignea* (C-F). **A**: cross view showing well-developed secondary body composed of fascicular wedges only. Scale bar = 500 µm; **B**: cross view showing well-developed secondary body composed of fascicular wedges only. Scale bar = 1 mm; **C**: tangential view showing parenchymatous cells of the interfascicular rays and tracheid thickenings (arrows). Scale bar = 100 µm; **D**: cross view showing fascicular wedges and interfascicular rays in the pith region. Scale bar = 1mm; **E**: cross view showing secondary body with fascicular wedges and interfascicular rays. Scale bar = 250 µm; **F**: tangential view showing parenchymatous cells and tracheids. Scale bar = 250 µm. Figs: Knoell (1935).

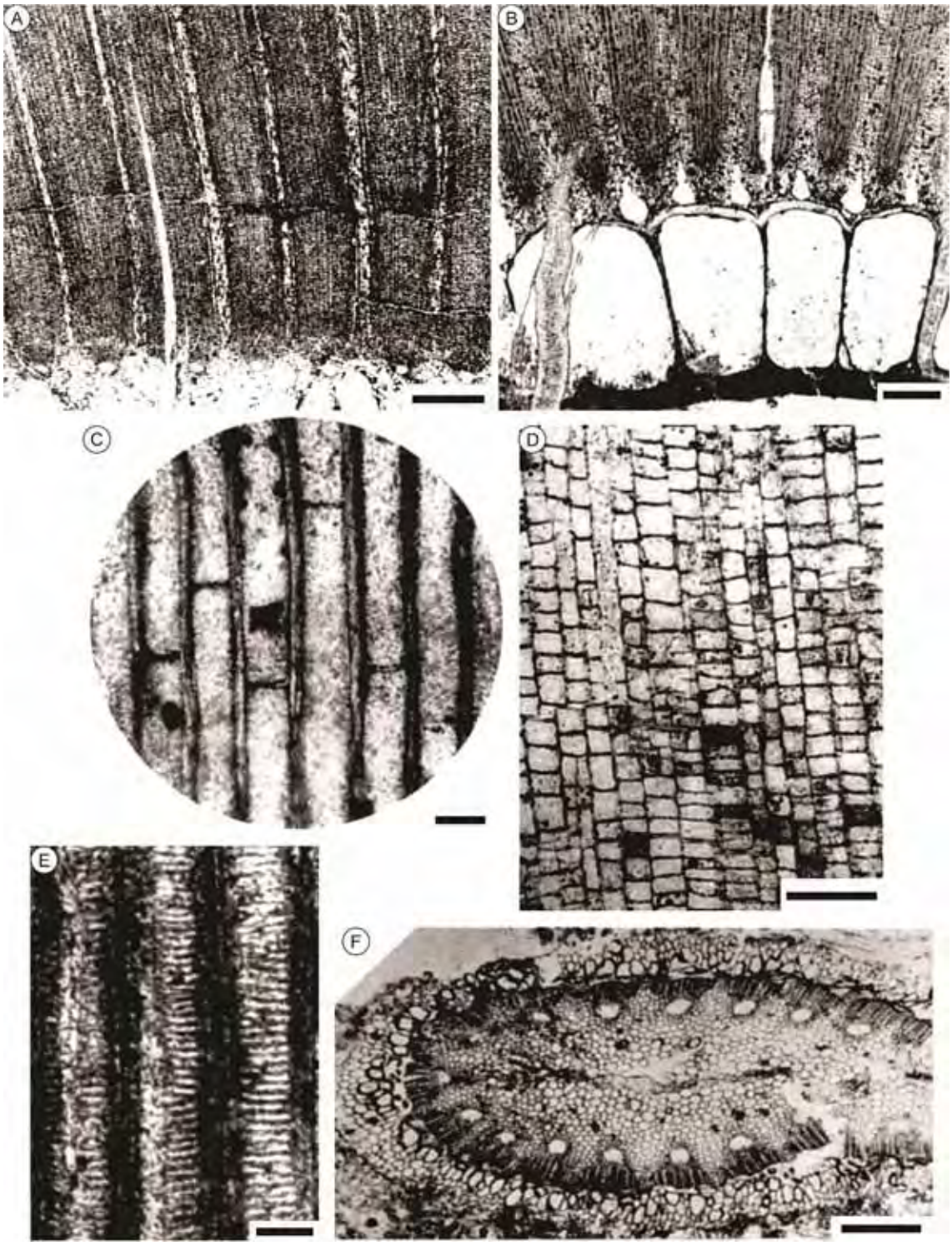

Plate II.18. *Arthopitys communis* var. *septata*. **A**: cross view showing secondary body. Scale bar = 250 µm; **B**: cross view in the pith region showing carinal canals. Scale bar = 1 mm; **C**: tangential view showing tracheid septation. Scale bar = 50 µm; **D**: radial view of the interfascicular ray showing square and rectangular-shaped parenchymatous cells. Scale bar = 250 µm; **E**: radial view showing tracheid with scalariform secondary wall thickenings. Scale bar = 25 µm; **F**: cross view showing pith cavity, fascicular wedges and interfascicular rays. Scale bar = 250 µm; Figs.: Andrews (1952).

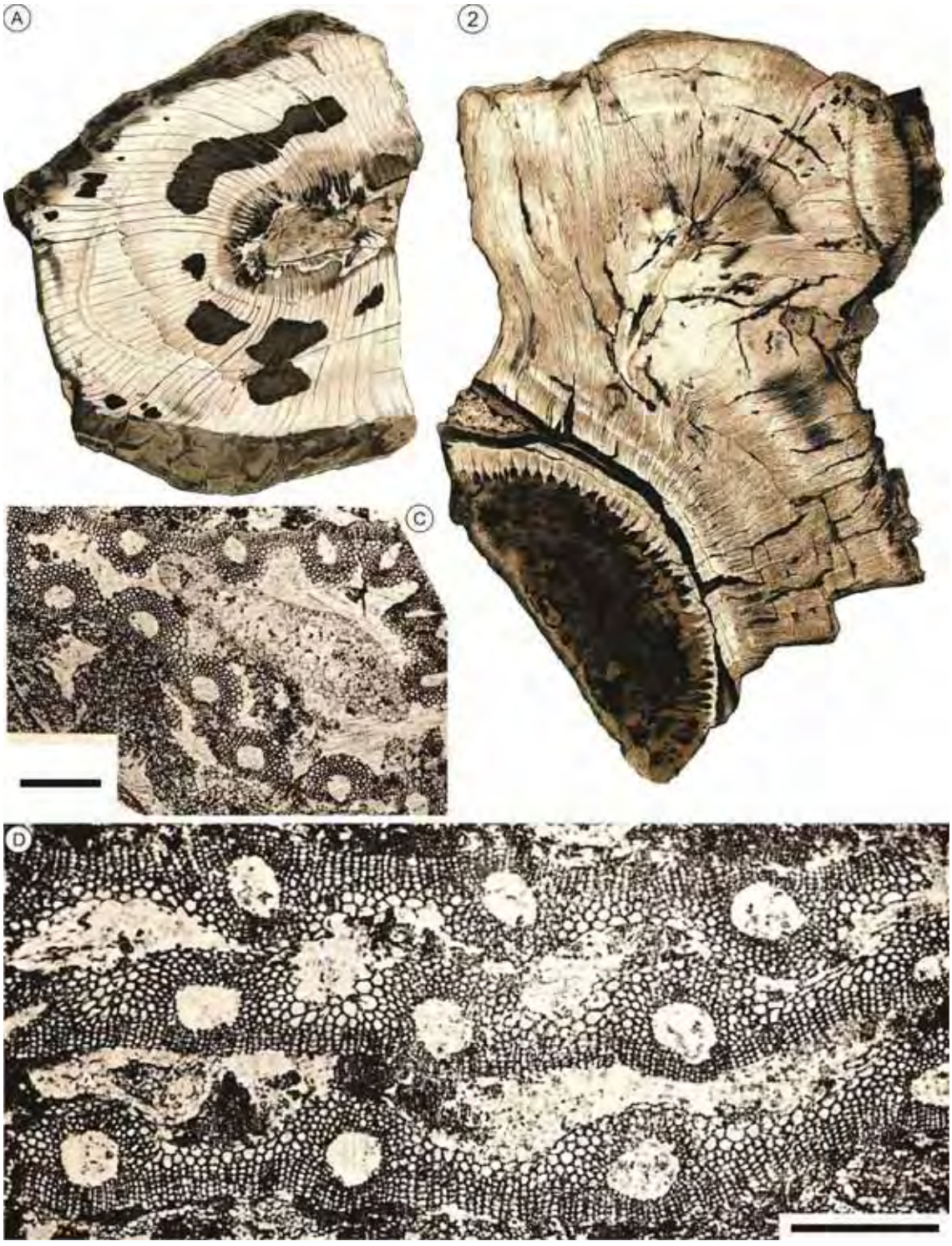

Plate II.19. *Arthopitys bistriata* var. *borgiensis* (A-B) and *Arthopitys jongmansi* (C-D). **A**: cross view showing pith, fascicular wedges and interfascicular rays of the secondary body; **B**: cross view showing secondary body and a root fragment; **C-D**: cross views showing pith cavity, large carinal canals and the reduced secondary body. Scale bar = 1mm. Figs.: A-B: Renault (1893); C-D: Boureau (1964).

Plate II.20. *Arthopitys bistriata* var. *augustodunensis* (A-C) and *Arthopitys bistriata* var. *valdajolensis* (D-G). **A-C**: cross views showing pith cavity, fascicular wedges and interfascicular rays; **D**: cross view showing pith cavity, fascicular wedges and interfascicular rays; **E**: tangential view showing depart of a branch, tracheids and parenchymatous cells of the interfascicular rays (arrows); **F**: tangential view in the depart of a branch; **G**: cross view showing fascicular wedges (fw) with carinal canals and cells of the interfascicular rays (ir). Figs.: Renault (1893).

III. The sphenophyte stems in the studied area

1. Introduction

Huge quantities of petrified stems are exposed in the Permian of the Parnaíba Basin in the northern State of Tocantins, central-north Brazil (Figure III.1), which led to the establishment of the Tocantins Fossil Trees Natural Monument (TFTNM). These plants were preserved by the process of silica permineralization. They are not in life position, neither necessarily were fossilized near to the original living place, but this occurrence was included in the ranking of the 32 most important petrified forests of the world (Dernbach, 1996) and is considered as one of the most significant geological and palaeontological sites of Brazil (Dias-Brito et al., 2007). Additionally, the plants of the Parnaíba Basin represent a rare Permian record of relatively low latitude paleofloras of Gondwana.

The fossil plants of the TFTNM are preserved in the lower part of Motuca Formation (Barbosa & Gomes, 1957; Pinto & Sad, 1986). According to Rößler (2006), the paleoenvironments in the studied area, located in the southern Parnaíba Basin, belonged to a meandering fluvial system, where a riparian vegetation was composed predominantly by tree ferns and sphenophytes; the areas a little more distant from the channels had gymnosperms. However, in the major part of the basin, the Motuca Formation evidences relatively dry conditions according to the presence of eolian dune deposits and evaporites (Góes & Feijó, 1994; Lima Filho, 1998). The rivers in the TFTNM region probably were active only during the rainy seasons, particularly in consequence of heavy storms, when extensive areas were flooded and plants were toppled or uprooted, transported and buried (Capretz & Rohn, in press).

Until this moment, the sphenophytes of the Parnaíba Basin, especially stems of *Arthropitys,* were studied only preliminarily by Coimbra & Mussa (1984) and Röβler & Noll (2002). Thus, the present work contributes with more detailed stem descriptions and comparisons, including some paleophytogeographical and paleoecological discussions, with emphasis on the first record of a three-dimensionally preserved subterraneous root still attached to a long stem. This exceptional specimen allows change radically the traditional reconstruction of the root-stem system of *Arthropitys* (Hirmer, 1927; Eggert, 1962; Boureau, 1964).

The described species were found at Andradina, Buritirana and Peba farms

inside the area of the TFTNM (Figure III.2).

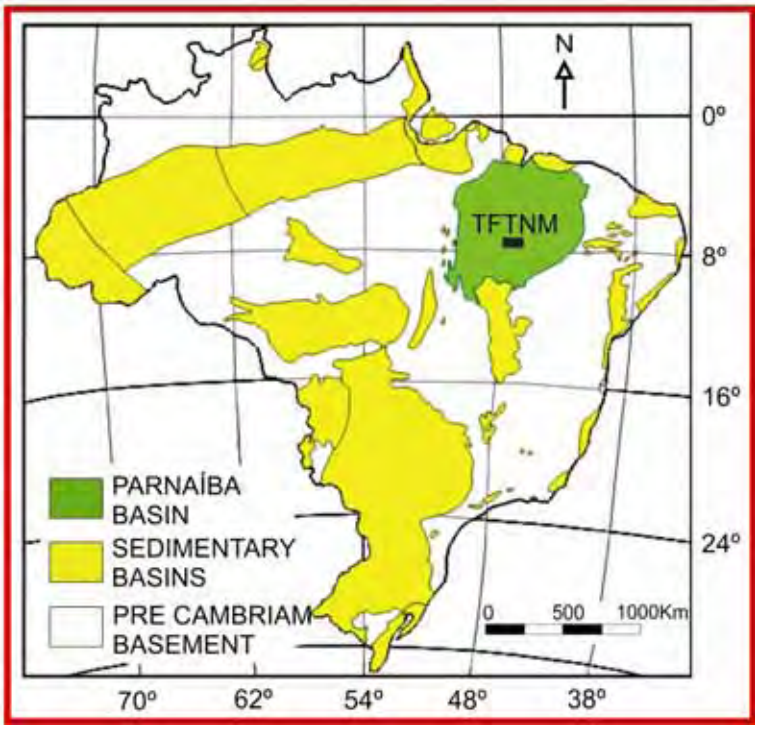

Figure III.1. Map with the major sedimentary Brazilian basins, Parnaíba Basin in green and the TFTNM area (modified from Schobbenhaus et al., 1984).

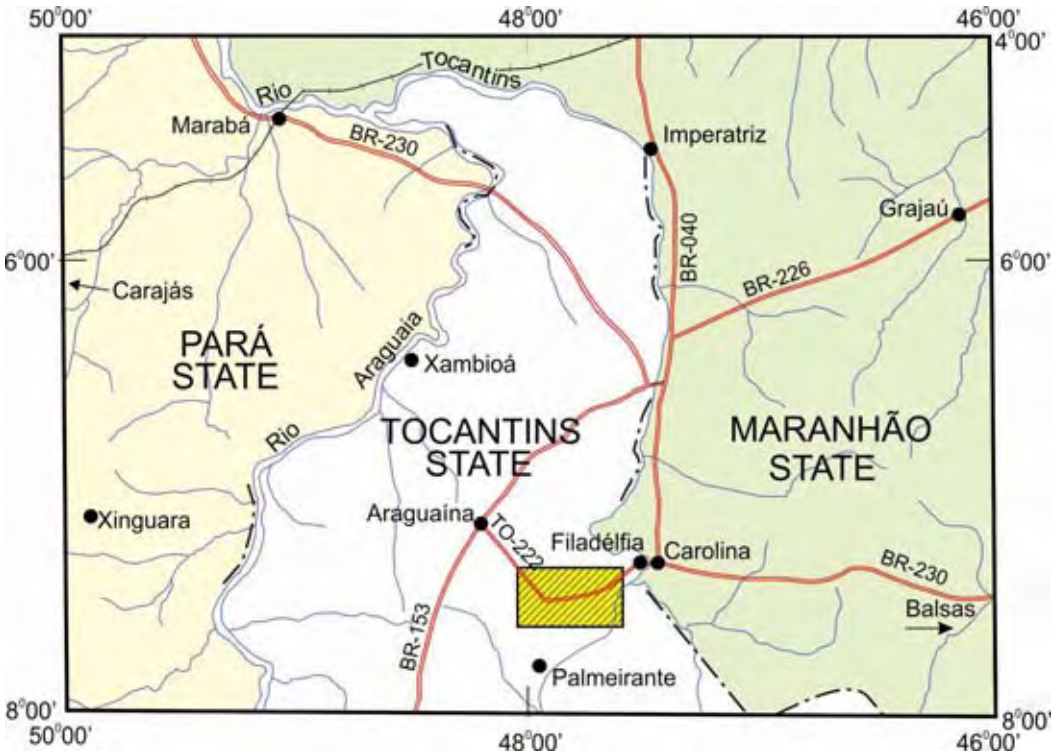

Figure III.2. Map of the northern State of Tocantins with the area of the TFTNM (yellow rectangle). Peba Farm is located in the West side, Andradina Farm in the center and Buritirana Farm in the East side of this area.

2. Research objectives

- To describe in detail the anatomical and morphological characters of the permineralized sphenophytes found in the Tocantins Fossil Trees Natural Monument (TFTNM), Permian of the Parnaíba Basin;

- To reconstruct the sphenophytes from the TFTNM and carry out paleoecological and paleoenvironmental analysis;

- To discuss the paleogeographic characteristics of the paleoflora by comparing sphenophytes from different regions of the earth;

- To discuss the age of the fossils and the deposits where they were found.

3. Materials and methods

The specimens studied herein were found between Filadélfia and Araguaína in the Andradina Farm (7°27'53"S, 47°50'37"W, near to the Bielândia District), Buritirana Farm (7°27'58"S, 47°42'00"W) and Peba Farm (7°25'15"S, 47°57'18"W), which belong to the Tocantins Fossil Trees Natural Monument (TFTNM). The stems were mostly lying on the ground and they rarely were still embedded in sediments. In general, they were very fragmented, but several small pieces were reconnected with glue.

The fossils are stored in the collection of Museum of Paleontology and Stratigraphy "Prof. Paulo Milton Barbosa Landim" of the Geosciences and Exact Sciences Institute of the University of the State of São Paulo - UNESP - Rio Claro *Campus*, identified with label **TOF** and in the Museum für Naturkunde, Chemnitz, Germany, identified with label **MfNC K**.

Incrusted sediments to the fossil stem surfaces were removed with a sand blaster. The internal structures were exposed on highly polished cross, radial and tangential sections. Reflected light microscopes were used for morphological and anatomical analyses in detail. At UNESP, the photographs were made with a Canon Powershot S70 digital camera attached to a Leica MZ8 steromicroscope and, for lower magnification images, a Sony DSC-HX1 digital camera. At the Museum für Naturkunde, the used equipments were Nikon Eclipse ME 600 and Nikon SMZ 1500 microscopes with Nikon DS-5M-L1 digital camera. General overview were made using Epson Perfection V330 scanner. Images treatments for contrast and colour were done with Microsoft Office Picture Mannager and Corel Draw version X6.

4. Paleobotanical systematics

The Permo-Carboniferous silica-permineralized sphenophyte stems of the literature are classified as *Arthropitys* Goeppert, 1864-5, *Arthroxylon* Reed, 1952 or *Calamitae* (Cotta) *emend.* Röβler & Noll, 2007b. In cross sections, the studied specimens present fascicular wedges alternating with parenchymatous cells of interfascicular rays, differently from *Calamitae* (Röβler & Noll, 2007b). In tangential section, they show square to slightly rectangular parenchymatous cells of interfascicular rays, what indicates that they may be included in *Arthropitys;* in *Arthroxylon*, otherwise, these parenchymatous cells are extremely elongated with tapering end walls (Andrews, 1952; Röβler & Noll, 2006, 2010). In addition to the traditional anatomical characteristics of the sphenophyte stems, considered that their external morphology (as arrangement of branches) is essential for the classification at the species level.

Considering that all studied specimens were included in *Arthropitys*, they were initially separated in three groups.

The first group is represented by specimens with large pith cavity, secondary body clearly divided into fascicular wedges and interfascicular rays visible throughout secondary body, scalariform and rare circular reticulate secondary wall thickenings in the tracheids and branches at all nodes. It includes two new species. One of the species in this group is represented by 11 specimens and another by six specimens.

The second *Arthropitys* group of Tocantins encompasses specimens with narrow pith cavity, almost completely undifferentiated secondary body (i.e. without clear fascicular wedges and interfascicular rays except close to the pith), scalariform and very rare reticulate secondary wall thickenings in the tracheids and branches at all nodes. Two new species belong to this group with six specimens in one species and three specimens in the another.

Finally, the third group of the studied sphenophyte stems corresponds to one new species characterized by an intermediate size of the pith cavity in comparison to the other two groups, with clear light fascicular wedges and even lighter interfascicular rays until the middle of the secondary body, tracheids with scalariform secondary wall thickenings and branches at every node and one specimen in this species.

Class Sphenopsida

Order Calamitales

Family Calamitaceae

Genus: *Arthropitys* Goeppert, 1864-5

Type-species: *Arthropitys bistriata* (Cotta) Goeppert *emend.* Rößler, Feng & Noll, 2012

***Arthropitys isoramis* n. sp.**

(Plates III.1 to III.5)

Holotype: TOF 187.

Paratype: K 4552.

Additional material: K 4486, K 4804, K 5407, K 5446, K 5448, K 5449, K 5451, K 5788, K 5872.

Type locality: Andradina Farm, Tocantins State, Parnaiba Basin, central-north Brazil.

Type stratum: Motuca Formation, Lower Permian.

Etymology: the specific name refers to the very regular branch system, generally four, and more rarely three branches per node.

Diagnosis according to the rules of the International Code of Botanical Nomenclature: Species similar to *Arthropitys versifoveata* Anderson, 1954, except for the preserved attached root system, the circular reticulate and scalariform secondary wall thickenings in the tracheids in radial view, four branch scars at every node, rarely three, disposed in alternate positions from one node to another, without secondary growth.

Description

Macroscopic stem characteristics- The holotype **TOF 187** is 2.35 m long (Plate III.4, 1), considering the stem and the attached root system. It was completely fragmented in the field, collected as separate pieces, which were rejoined and glued together in the laboratory. This stem has an elliptical outline in cross section because of compression. Approximately 65 cm above the lowest/most extreme preserved point of the root system, the stem reaches 5.3 x 11.8 cm in cross section, girth of 29 cm, pith cavity completely collapsed and equals 5.1 cm in

width, and the pith/stem diameter ratio equals 1:2.9 (Plate III.4, 6). In the most distal preserved part of the stem, the outline dimensions of the cross section are 3 x 10.6 cm, girth of 25 cm, the pith cavity is completely collapsed and 6.5 cm wide, the pith/stem ratio approximately equals 1:2.5 (Plate III.4, 2). The external surface shows longitudinal ridges of 1 mm in width alternated with 0.3 mm wide furrows. The internodes length (36 measurements in total) ranges between 1.5 and 6.0 cm (mean: 3.4 cm). The longest internode (6.0 cm) was observed approximately 1.9 m from the lowest/most extreme point of the root.

The paratype **K 4552** is a permineralized stem, 3.3 m long, with elliptical outline and pith cavity because of compression. At the base, the stem diameter measures 6 x 7.6 cm (Plate III.1, 3); distant 60 cm from the base, 6 x 7.5 cm; 1.2 m from the base, 6.2 x 8.3 cm; 1.8 m from the base, 6.3 x 8.3 cm; 2.4 m from the base, 5.6 x 7.7 cm; 3 m from the base, 5.2 x 6 cm; and at the top, 3.6 x 5.5 cm (Plate III.1, 4). The internodes length (66 measurements in total) range between 1.4 and 5.3 cm (mean: 3.38 cm). Approximately 1.2 m above the preserved base, the internodes reach their longest length: 5.3 cm. At the basal part of the paratype **K 4552**, the girth is 21.5 cm and the pith/stem diameter ratio equals 1:4.3 (Plate III.1, 3). At the upper preserved part, girth is 14.3 and pith/stem ratio equals 1:1.8 (Plate III.1, 4).

In the specimens **K 5407,** 15 measurements in total (Plate III.1, 1) and **K 5872,** 19 measurements in total (Plate III.2, 1), the average internodes length is 2.3 cm and in **K 5788** (12 measurements in total), is 3.4 cm (Plate III.3.1). Some specimens present diaphragms preserved at nodes in the pith cavity, like in the paratype **K 4552** (Plate III.1, 2) and in the specimens **K 5407** (Plate III.1, 1) and **K 5449** (Plate III.3, 2 and 3).

Branching system- This species presents four branch scars at every node, rarely three, disposed in alternate positions from one node to another. In the specimen **K 5449** they are circular-shaped, 5-8 mm in diameter (Plate III.3, 4), without secondary growth (Plate III.3, 5). The specimens **K 5872** (Plate III.2, 1), **K 5788** (Plate III.3, 1), and **K 5449** (Plate III.3, 4) present the best preserved branch scars. In the specimen **K 5872**, they are circular with diameters of 5-8 mm (Plate III.2, 1), and in the **K 5449,** diameters of 5-9 mm (Plate III.3, 4).

Orders of branching- in the last upper fragment of the stem, was recognized a bifurcation in the secondary body, indicating at least two orders of wood axes

(Plate III.5, 4).

Primary body- In the holotype **TOF 187**, the carinal canals and metaxylem cells are not well preserved. The carinal canals in cross section are elliptical-shaped, on average 75 (60-90) µm long radially and 105 (90-120) µm tangentially and the metaxylem cells are polygonal-shaped, on average 52 (20-90) µm in diameter (Plate III.4, 5).

In the paratype **K 4552**, which has a better preserved primary body, the carinal canals are elliptical-shaped in cross section, on average 186 (141-218) µm long radially and 148 (142-183) µm tangentially, surrounded by circular to slightly circular metaxylen cells, on average 30 (19-40) µm in diameter (Plate III.1, 5).

The specimen **K 4486** has two very well preserved carinal canals, slightly circular-shaped with 156 and 215 µm in diameter (Plate III.2, 3).

Secondary body- In these Permian calamites, in cross section, the secondary body is clearly divided into fascicular wedges and interfascicular rays visible throughout secondary body, both increasing in width radially (Plate III.4, 4; Plate III.2, 2; Plate III.3, 6; Plate III.3, 8; Plate III.3, 9). In the holotype **TOF 187** secondary body is between 2 and 3 cm thick, presenting 142 fascicular strands at the base of the stem (Plate III.4, 6) and 160 fascicular strands at the top (Plate III.4, 2).

At the basal part of the paratype **K 4552**, the number of fascicular strands is 108 (Plate III.1, 3) and at the upper part, the number of fascicular wedges increases to 145 strands (Plate III.1, 4). On a cross section of the upper portion of this stem, the fascicular wedges in the proximal region of the secondary body average 845 (659-1056) µm in width and are composed of approximately 25 cell files. Tracheids are square to rectangular-shaped, on average 78 (65-92) µm long radially and 39 (33-46) µm tangentially. The fascicular rays consist of 1 to 2 files of rectangular-shaped parenchymatous cells, which average 110 (80-120) µm in length radially and 26 (20-30) µm tangentially. The interfascicular rays average 362 (200-552) µm in width and are composed of 6 to 12 cell files on average 122 (91-157) µm long radially and 35 (25-49) µm tangentially (Plate III.1, 5).

In the middle of the secondary body on a cross section of the holotype **TOF 187** (approximately 1 cm from the pith cavity), the fascicular wedges average 905 (710-1140) µm in width and are composed of approximately 25 cell files. Tracheids average 67 (39-103) µm in length radially and 43 (28-49) µm tangentially. The

fascicular rays present one or two files of parenchymatous cells on average 86 (79-106) µm long radially and 18 (14-22) µm tangentially. Interfascicular rays average 345 (200-451) µm in width and consist of 9-11 files of parenchymatous cells with mean length of 120 (85-168) µm radially and 39 (27-54) µm tangentially. Some of them show circular pits on the walls (Plate III.2, 4 and 5).

At the distal secondary body on a cross section of the holotype **TOF 187** (about 2.5 cm from the pith cavity), the fascicular wedges average 1245 (1020-1395) µm in width and are composed of 25 to 30 cell files with square to rectangular-shaped tracheids with mean length of 62 (37-87) µm radially and 47 (31-75) µm tangentially. The fascicular rays become multisseriate with very rectangular parenchymatous cells, on average 119 (85-157) µm long radially and 19 (12-26) µm tangentially. The interfascicular rays present mean width of 442 (318-590) µm and are composed of 9-12 rectangular-shaped cell files, that on average are 178 (101-258) µm long radially and 50 (27-80) µm tangentially.

In radial section, the tracheids of the fascicular wedges in this species show circular reticulate (Plate III.1, 8 and 9; Plate III.2, 6) and scalariform secondary wall thickenings (Plate III.1, 6 and 7; Plate III.3, 7).

In the holotype **TOF 187** these cells are very long axially and average 25 (22-33) µm in width radially, the vertical distance between thickenings varies from 5.5 to 7.5 µm and the horizontal distance from 28 to 33 µm, with some bifurcations in the scalariform thickenings. The circular reticulate thickenings show pits with an average diameter of 7.6 (5.7-9.8) µm.

In the paratype **K 4552**, the tracheids are rectangular-shaped, very long axially, with average width of 46 (28-65) µm radially, vertical distance between thickenings varies from 5.5 to 7.5 µm and the horizontal distance, from 21 to 48 µm, with some bifurcations (Plate III.1, 6 and 7). The circular reticulate thickenings show pits with an average diameter of 13 (12-16) µm (Plate III.1, 8). The specimen **K 5451** shows the best preserved circular reticulate thickenings: the tracheids are very long axially, with average width of 88 (65-106) µm radially, and the pits are slightly circular with mean diameter of 7.4 (5-9.5) µm (Plate III.1, 9).

In tangential sections, in the holotype **TOF 187**, tracheids reach 50% and parenchymatous cells 50% of the secondary body (Plate III.4, 3). The tracheids are very long axially and average 44 (37-54) µm in width tangentially. The fascicular rays show more than 30 consecutive rectangular-shaped cells in height

direction, on average 98 (73-123) µm long axially and 42 (34-53) µm tangentially. Interfascicular rays are composed by parenchymatous polygonal-shaped cells on average 95 (47-144) µm in diameter

Root system- In the holotype **TOF 187**, the stem is connected to a ‘’root system’’ (Plate III.5, 1-3), here described considering the original growth position of the plant, from the stem towards the deepest positions in the soil. This system is composed of branched root axes with two main directions of growth.

The transitional region from the stem to the root system is very discrete, without significant change of diameter, characterized by the disappearance of the nodes and by the presence of small stumps of broken root axes in a whorl disposition. These stumps have circular sections with diameters of 0.5-1.5 cm or elliptical sections 1.0-1.5 cm wide and 0.7-1.0 cm high. It is not possible to recognize the departure angle of these root axes (Plate III.5, 1, smaller arrows). Some centimeters further down, other axe stumps are observed, disposed irregularly, but at a departure angle of approximately 30 to 35^0 in relation to the main axis of the stem. They are larger, also with circular-shaped sections of 1.0-1.5 cm in diameter or elliptical-shaped sections of 2.0-4.0 x 1.3-2.5 cm [Plate III.5, 1 (larger arrows) and 3 (arrows)].

Below these short root stumps, there are three main central axes basically parallel to the stem. The largest one is 28 cm long, with a diameter at the emergence region of 4.5 cm, narrowing down slightly (Plate III.5, 2, arrow a). At the end, it is coiled, but incomplete because not all fossil fragments were recovered in the field work. The second relatively large almost vertical axe is 16.5 cm long, but is also incomplete, with a diameter at the base of 4.0 cm (Plate III.5, 2, arrow b). The smallest one, also only partially preserved, is 12 cm long, with a diameter of 2.5 cm (Plate III.5, 2, arrow c). These ramified axes present many small scars, probably root hairs.

Leaf traces and cortical elements- Leaf traces, phloem, periderm and cortical tissues are not preserved.

Comparisons

The studied specimens differ from *Arthropitys bistriata* (Cotta) Goeppert *emend*. Rößler, Feng & Noll, 2012, *A. communis* (Binney) Renault, 1896, *A. lineata* Renault, 1896, *A. gallica* Renault, 1896 [apud Andrews (1952); Boureau

(1964); Wang et al. (2003)], *A. felixi* Hirmer & Knoell (in Knoell, 1935), *A. deltoides* Cichan & Taylor, 1983, *A. junlianensis* Wang, Hilton, Li & Galtier, 2003, *A. yunnanensis* (Tian & Gu) *ex* Wang, Hilton, Galtier & Tian, 2006, and *A. ezonata* (Goeppert) *emend.* Rößler & Noll, 2006, because they present scalariform and circular reticulate secondary wall thickenings in the tracheids, not only scalariform thickenings as in the mentioned species;

The two types of tracheid wall thickenings of the studied specimens also represent an important difference in comparison to *Arthropitys major* (Weiss) Renault, 1896 [apud Boureau (1964); Wang. et al. (2006)], *A. kansana* Andrews, 1952, *A. illinoensis* Anderson, 1954, *A. cacundensis* Mussa, 1984 (in Coimbra & Mussa, 1984), *and A. sterzelii* Rößler & Noll, 2010, which only bear circular and/or elongated reticulate secondary wall thickenings in the tracheids. Finally, the two types of thickenings in the studied stems are also distinct from the three types recognized in *Arthropitys gigas* (Brongniart) Renault, 1896, *A. rochei* Renault, 1896, and *A. porosa* Renault, 1896;

The diagnoses of *Arthropitys renaultii* Boureau, 1964 and *A. approximata* (Schlotheim) Renault, 1896 [apud Andrews (1952); Boureau (1964)], do not inform the type(s) of tracheid thickenings, what prevents the use of this criterion to compare these species;

Arthropitys herbacea Hirmer & Knoell (in Knoell, 1935), *A. bistriatoides* Hirmer & Knoell (in Knoell, 1935) and *A. jongmansi* Hirmer, 1927 (in Knoell, 1935) present a secondary body poorly developed and without information about secondary wall thickenings in the trackeids. Therefore, the analyzed specimens from Tocantins were not properly compared to these species;

The studied specimens here differ from *Arthropitys hirmeri* Knoell, 1935 because they present conspicuous fascicular wedges and interfascicular rays in the secondary body, whereas the mentioned species has only fascicular wedges.

The analyzed specimens are very similar to *Arthropitys versifoveata* Anderson, 1954 of the Middle Pennsylvanian of the Fleming Coal, upper part of Cherokee shale, Kansas (USA): their fascicular wedges increase in width radially; the fascicular rays are uni or bisseriate; in tangential sections, the two species have interfascicular rays with isodiametrically-shaped cells. The studied specimens present four branches or rarely three branches per node, disposed in alternate positions from one node to another, without secondary growth, and in *A.*

versifoveata the branch system is very similar, composed of four branches per node, but without information about a possible secondary growth. The main difference is the number of files of parenchymatous cells of the interfascicular rays in cross section: 9 to 11 files in the studied specimens and 5 files in *A. versifoveata*, other differences are the tracheids with circular reticulate and scalariform thickenings in the specimens of Tocantins instead of scalariform and elongate reticulate thickenings as in *A. versifoveata*.

Considering these comparisons, the studied specimens are distinct from all sphenophyte species of the literature, what supports the proposal of the new species designated as ***Arthropitys isoramis*** and Table III.1 presents the main anatomical and morphological data of *Arthropitys isoramis* and Figure III.3 the proposed reconstruction of this species.

Plate III.1: *Arthropitys isoramis*

1: longitudinal section of the stem **K 5407** showing secondary body, internodes and diaphragm at nodes in the pith cavity.

2: longitudinal section of the paratype **K 4552** showing secondary body, internodes and diaphragms.

3: cross section of the paratype **K 4552** at the basal part showing fascicular wedges and interfascicular rays.

4: cross section of the paratype **K 4552** at the upper part showing pith, fascicular wedges and interfascicular rays.

5: cross section of the paratype **K 4552** at the pith periphery showing carinal canals, metaxylem and the beginning of fascicular wedges.

6-7: radial sections of the paratype **K 4552** showing scalariform secondary wall thickenings of the tracheids.

8: radial section of the paratype **K 4552** showing tracheids with circular reticulate secondary wall thickenings (long arrows) and parenchymatous cells of the interfascicular rays with circular pits on their radial walls (short arrows).

9: radial section of the stem **K 5451** showing scalariform and circular reticulate secondary wall thickenings of the tracheids.

PLATE III.1

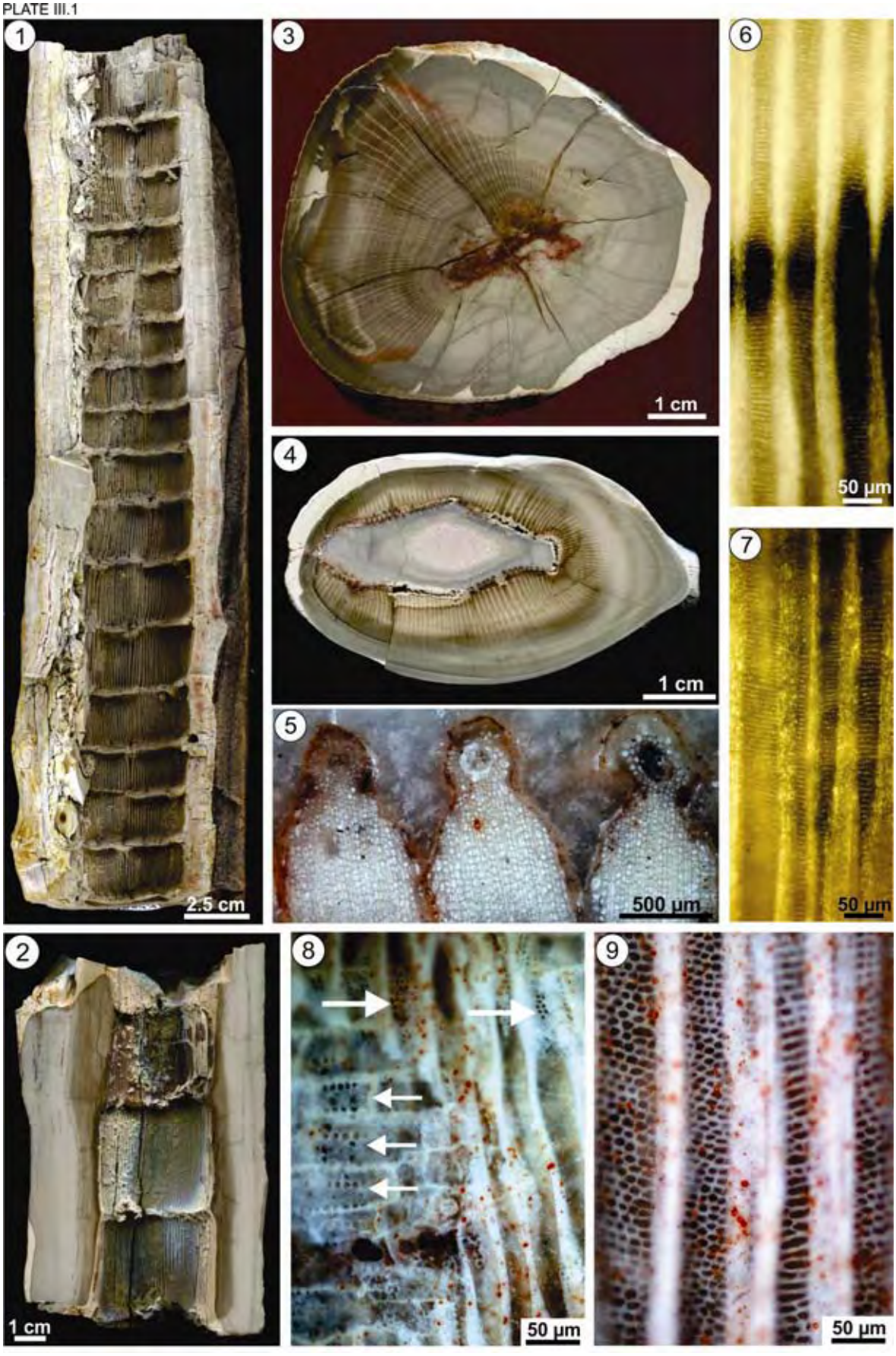

Plate III.2: *Arthropitys isoramis*

1: surface of the stem **K 5872** showing branch scars (arrows) in alternating position from one node to another.

2: cross section of the stem **K 4486** showing pith cavity, fascicular wedges and interfascicular rays.

3: cross section of the stem **K 4486** at the pith cavity periphery showing carinal canals, metaxylem, proximal fascicular wedges and the interfascicular rays.

4: cross section of the stem **K 4486** showing tracheids of fascicular wedges (fw) and parenchymatous cells of the interfascicular rays (ir) with circular pits on the walls.

5: magnification of 4 showing the pits on parenchymatous cell walls (arrows).

6: radial sections of the stem **K 4486** showing circular reticulate secondary wall thickenings of the tracheids.

PLATE III.2

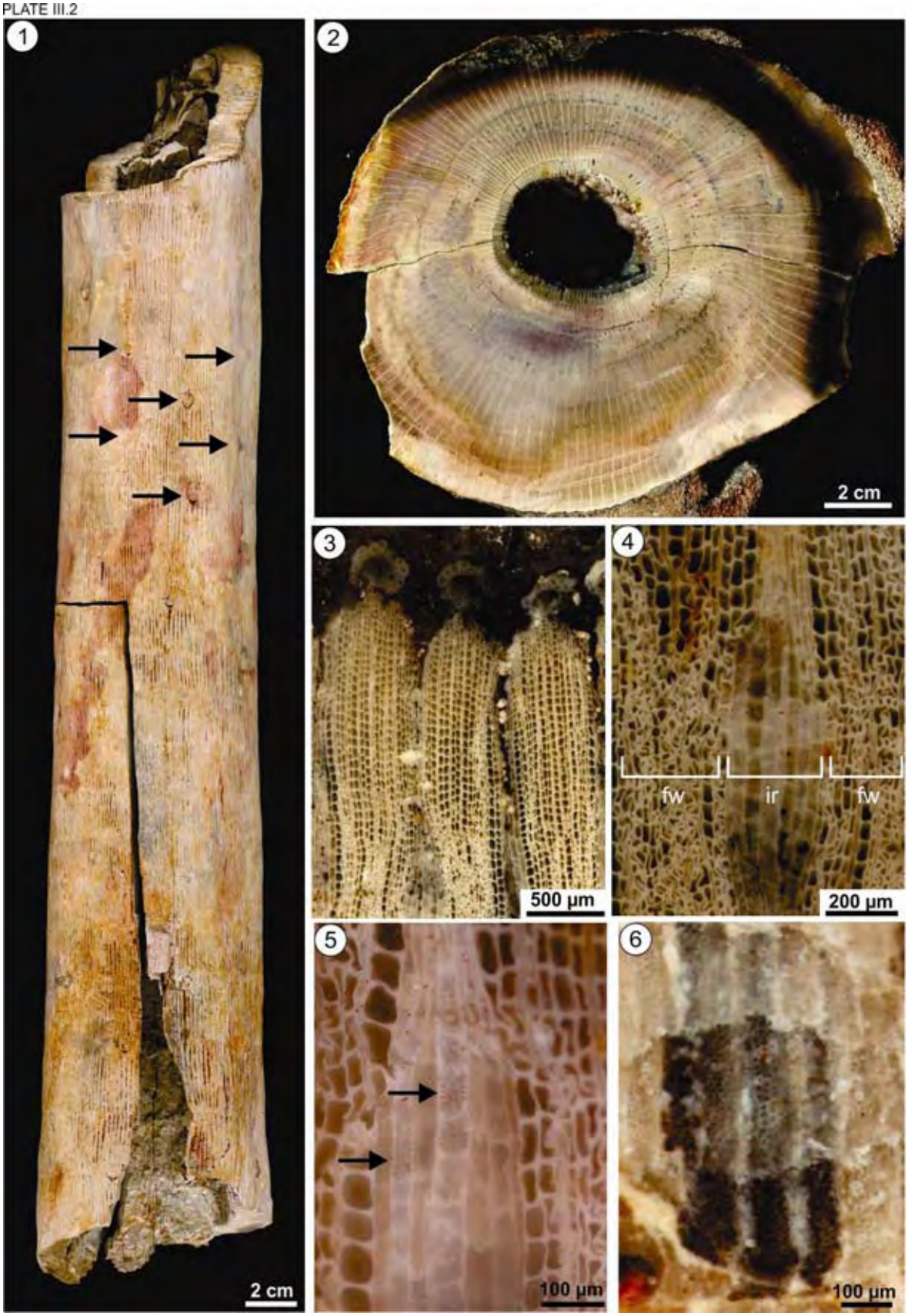

Plate III.3: *Arthropitys isoramis*

1: surface of the stem **K 5788** showing alternating positions of branch scars (arrows) from one node to another.

2-3: longitudinal sections of the stem **K 5449** showing secondary body, internodes and diaphragms in the pith cavity.

4: surface of the stem **K 5449** showing branch scars (arrows) in alternating positions from one node to another.

5: tangential section of the stem **K 5449** showing a branch trace without secondary growth.

6: cross section of the stem **K 5446**, a relatively flattened stem, showing pith cavity, fascicular wedges and interfascicular rays.

7: radial sections of the stem **K 5778** showing scalariform secondary wall thickenings of the tracheids.

8: cross section of the stem **K 4804** showing pith cavity, fascicular wedges and interfascicular rays.

9: cross section of the stem **K 5448** showing pith cavity, fascicular wedges and interfascicular rays.

PLATE III.3

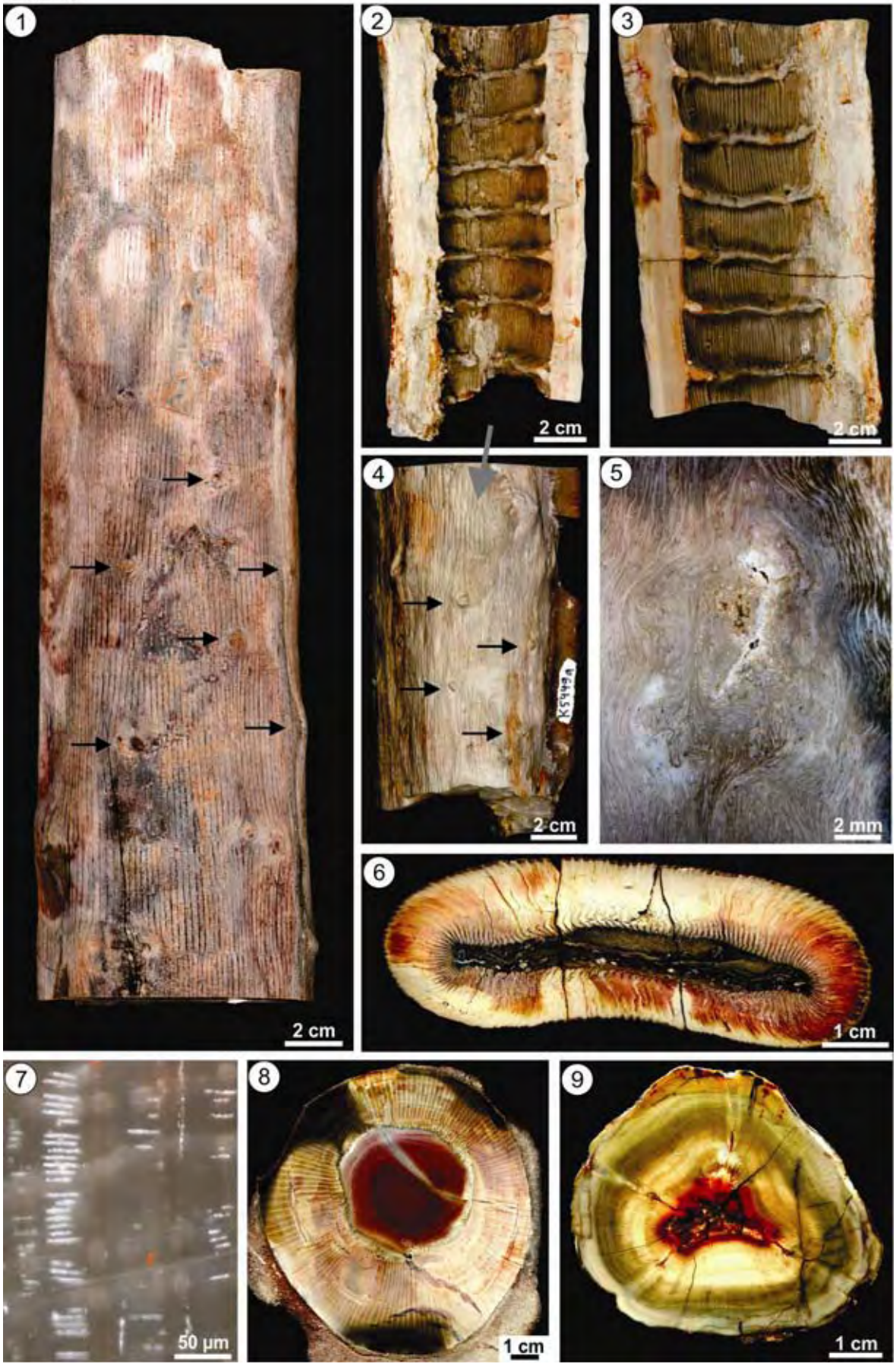

Plate III.4: *Arthropitys isoramis*

1: general view of the holotype **TOF 187** with attached root.

2: cross section of the upper part of the holotype **TOF 187** showing completely collapsed pith cavity, fascicular wedges and interfascicular rays.

3: tangential section of the holotype **TOF 187** showing tracheids of fascicular wedges (fw) and parenchymatous cells of the interfascicular rays (ir).

4: cross section of the holotype **TOF 187** showing fascicular wedges and interfascicular rays in the periphery of a collapsed pith cavity.

5: cross section of the holotype **TOF 187** showing the badly preserved carinal canals (arrows) and the proximal fascicular wedges (fw) and the interfascicular rays (ir).

6: cross section at the basal part of the holotype **TOF 187** showing flattening of the stem, a completely collapsed pith cavity, fascicular wedges and interfascicular rays.

PLATE III.4

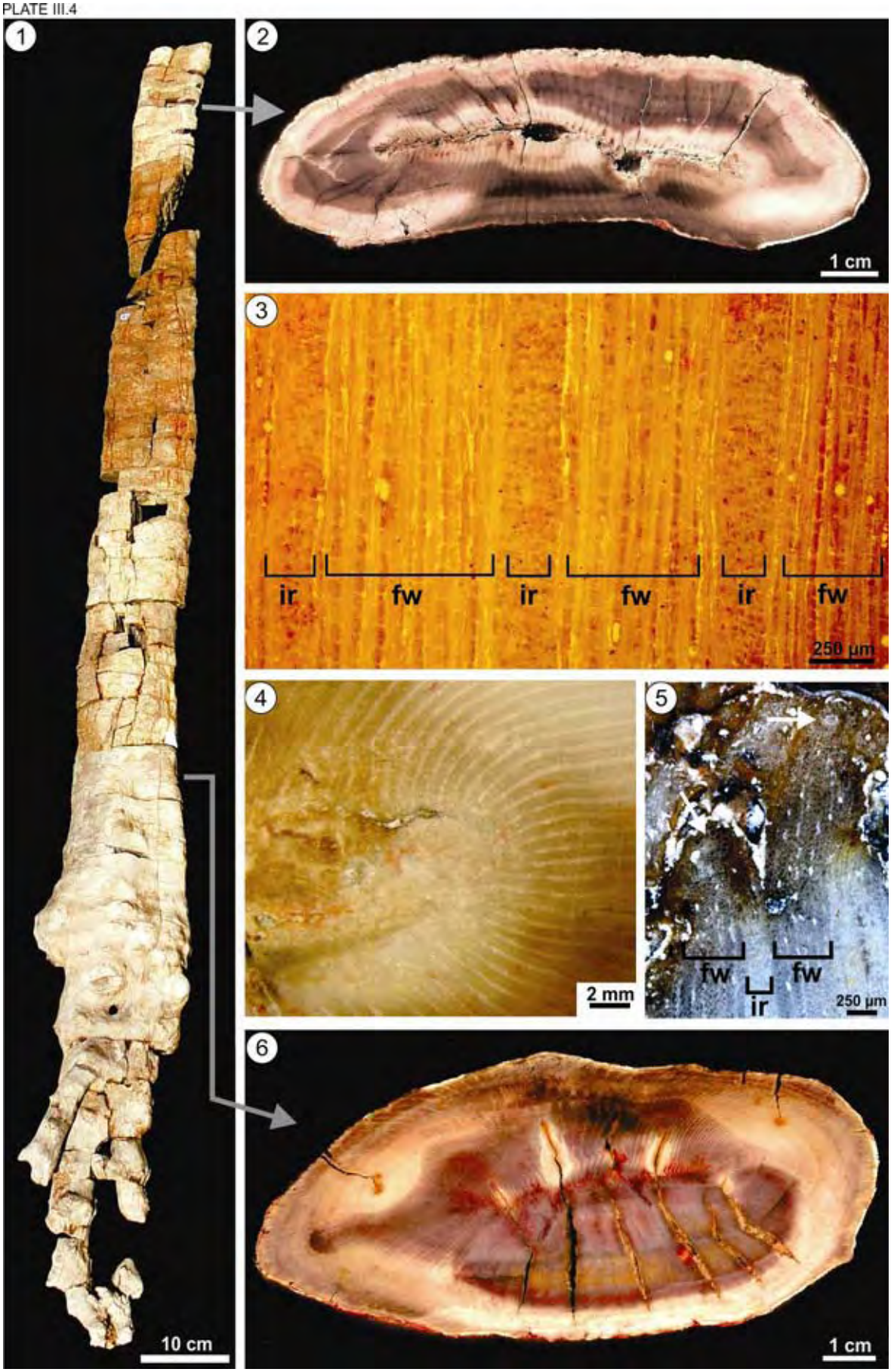

Plate III.5: *Arthropitys isoramis*

1: general view of the holotype **TOF 187** showing small stumps of root axes, without angle to the stem (smaller arrows) and large axe stumps with an angle of approximately 30 to 35^0 in relation to the stem (larger arrows).

2: general view of the holotype **TOF 187** showing three main central axes practically parallel to the stem (arrows a, b and c).

3: draw showing the root-stem system with details of the trace roots, disposed irregularly, but probably representing adventitious roots at a possible departure angle of the approximately 30 to 35^0 in relation to the stem (arrows).

4: cross section at the upper part of the holotype **TOF 187** showing bifurcation of the secondary body (red curves), indicating at least a two orders of wood axes. Arrows indicate the collapsed pity cavities.

PLATE III.5

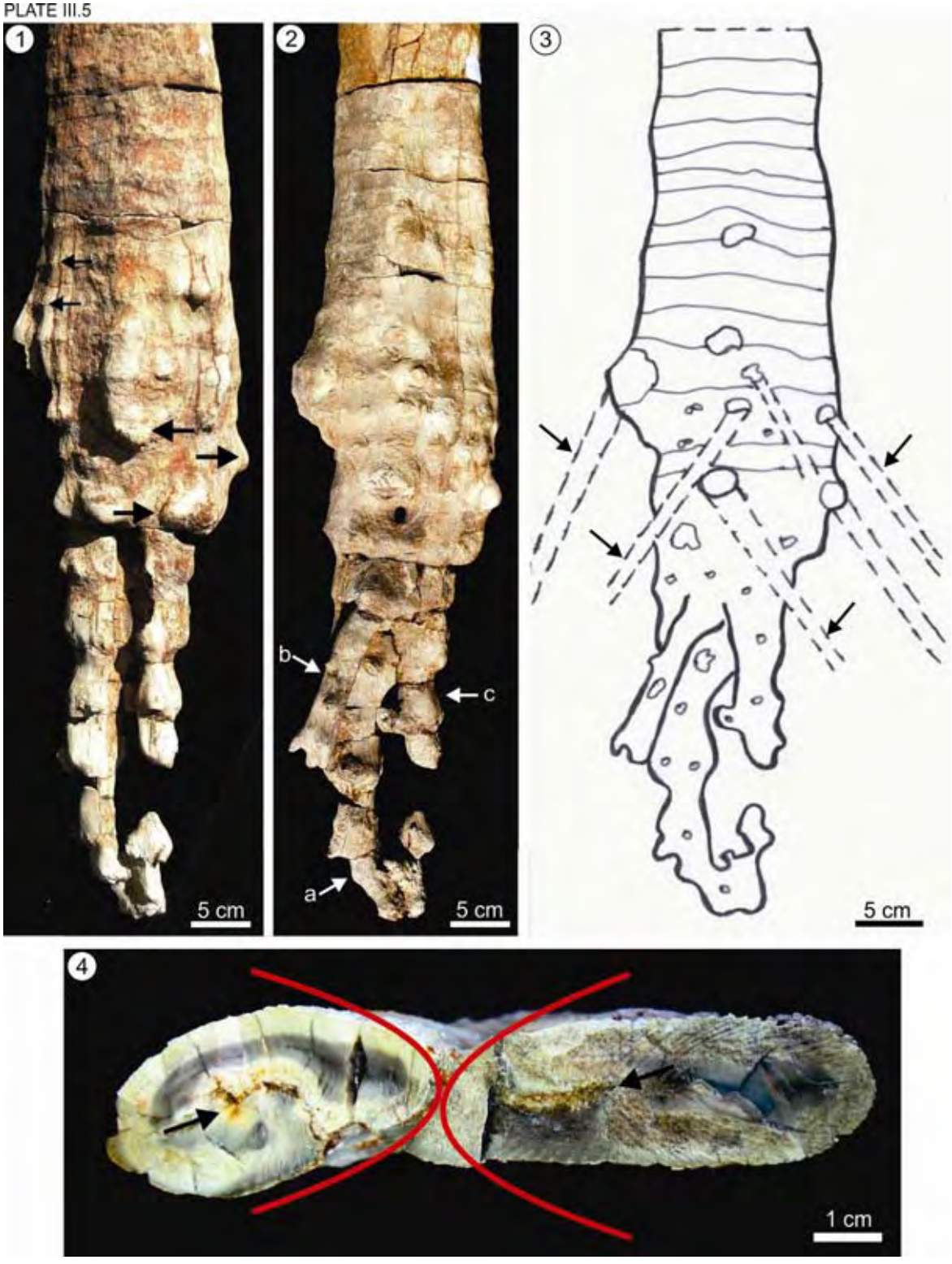

Taxon	Locality / Stratigraphy	Collection
Arthropitys isoramis	central-north Brazil, Parnaiba Basin / Early Permian	UNESP - TOF 187 (holotype)

Part of the plant	Length	Girth	Diameter stem (S)	Diameter pith (P)	P/S ratio	Wood
basal stem with attached rhyzome	2.35 m	29 cm at base 25 cm at top	5.3 x 11.8 cm at base 3.0 x 10.6 cm at top	collapsed = 5.1 cm collapsed = 6.5 cm	1:2.9 at the base 1:2.5 at the top	14-22 mm divided in distinct wedges usually visible to the margin fasc. width: initially: 845 µm (659-1056), distally: 1245 µm (1020-1395)

Morphology/Branching	Type	Branch traces	Leaf traces	Rhyzome traces
primary/secondary growth	without secondary growth	4, rarely 3 per node departing at the pith's margin at node not visible at pith mould, disposed alternaly circular in shape, diameter: 5 to 8 mm	not preserved	two main directions: smallest at 30-35° with stem; largest parallel with the stem

Internode length	34 mm (15-60), 36 measurements

Primary tissues	Vascular strands number	Carinal canal radially / tangentially (µm)	Px tracheids/tyloses	Mx tracheids
	142 at the base 160 at the top	75 (60-90) / 105 (90-120) elliptical-shaped	not preserved	52 µm (20-90) polygonal-shaped

Secondary tissues	Tracheids (cross view) radially / tangentially (µm), files per fascicle	Thickening (radial view)	Outline
	initially: 78 (65-92) / 39 (33-46), 7-25 files per fascicle medially: 67 (39-103) / 43 (28-49), 25 files per fascicle distally: 62 (37-87) / 47 (31-75), 25-30 files per fascicle	scalariform (close to pith): distance 5.5-7.7 µm vertically and 28-33 µm horizontally; circular reticulated: pits 5.7-9.8 µm	rectangular to square

	Interfascicular rays (cross view) number of files / width (µm)	Cells (radial view) axially (µm)	Cells (tangential view) diameter (µm)	Cells (cross view) radially / tangentially (µm)
	made of 6-12 parenchym. files initially: 362 (200-552) medially: 345 (200-451) distally: 442 (318-590) running from node to node	93 (20-150) brick-shaped, wider than high	95 (47-144) polygonal-shaped	initially: 122 (91-157) / 35 (25-49) medially: 120 (85-168) / 39 (27-54) distally: 178 (101-258) / 50 (27-80) rectangular-shaped, frequently circular pits of 12 µm in diameter

	Fascicular rays (cross view) number files / width	Cells (radial view) axially / radially (µm)	Cells (tangential view) axially / tangentially (µm)	Cells (cross view) radially / tangentially (µm)
	made of 1-3 files 62 µm (30-120)	Not visible	98 (73-123) / 42 (34-53) rectangular-shaped more than 30 cells in heigh, higher than wide	initially: 110 (80-120) / 26 (20-30) medially: 86 (79-106)/ 18 (14-22) distally: 119 (85-157) / 19 (12-26) rectangular-shaped

Cortex / Periderm / special characters	not preserved

Table III.1: main anatomical and morphological data of *Arthropitys isoramis*.

Figure III.3: proposed reconstruction of *Arthropitys isoramis* by Frederic Spindler (Freiberg, Germany).

***Arthropitys tabebuiensis* n. sp.**

(Plates III.7 to III.9)

Holotype: K 5867.

Paratype: K 5447.

Additional material: K 5394, K 5453, K 5450, K 5540.

Type locality: Tocantins State, Parnaíba Basin, central-north Brazil.

Type stratum: Motuca Formation, Lower Permian.

Etymology: The name refers to genus *Tabebuia* as the most common representative tree of the modern Cerrado landscape, where our *Arthropitys* finds have been made.

Diagnosis according to the rules of the International Code of Botanical Nomenclature: Stems distinct from all other *Arthropitys* species because of the presence of longitudinally aligned 8 to 15 branches at every node, with and without secondary growth, and the circular reticulate secondary wall thickenings of the tracheids in radial view.

Description

Macroscopic stem characteristics- The holotype **K 586**7 is a 36.5 cm long stem (Plate III.6, 1), elliptically-shaped in transversal sections due to compression. The mean internodes length, according to 10 measurements, is 32 mm (min. 16 mm, max. 55 mm). At the base of the stem fragment the size of the cross section is 81 x 102 mm, girth is 29 cm, the pith cavity 29 x 41 mm, pith/stem diameter ratio equal to 1:2.6 (Plate III.6, 3). At the upper part the size of the stem section is 68 x 80 mm, girth is17.5 cm, the pith cavity is 19 x 30 mm, and the pith/stem diameter ratio is approximately 1:2.2 (Plate III.6, 2).

Branching system- The branching system is composed of 8-15 branches at every node, with and without secondary growth. In the holotype **K 5867**, the branching system is evidenced by branch stumps (mainly in the upper part) and branch scars (mainly in the lower part), with diameters between 2 and 14 mm, disposed in line along the stem (Plate III.6, 1). Eleven whorls are preserved along the holotype.

A cross section of the paratype **K 5447** shows branch traces extended from the periphery of the pith cavity towards the stem margin (Plate III.6, 5).The specimen **K 5394** shows slightly elliptical-shaped branch scars, oriented

longitudinally, with very uniform dimensions, 8 mm long, and 0.45-0.67 cm wide (Plate III.6, 4). In a cross section of the holotype **K 5867**, the branch traces are exposed from the middle part of the secondary body until the stem margin (Plate III.7, 5) and in **K 5453,** a branch trace can be followed in longitudinal section (Plate III.8, 1).

Primary body- In the primary body of the holotype **K 5867**, the metaxylen cells and the carinal canals are badly preserved. The carinal canals show diameters between 150-160 µm and metaxylen cells are circular-shaped, 25-40 µm in diameter.

In the specimen **K 5540,** despite the bad preservation, it is possible to see the shape of the carinal canals (Plate III.8, 7 and 8).

Secondary body- In this species**,** the secondary body is clearly divided into fascicular wedges and interfascicular ray (Plate III.6, 2 and 3; Plate III.8, 5, 6 and 9). The fascicular wedges are composed of tracheids and parenchymatous cells, and the interfascicular rays, only parenchymatous cells.

The holotype **K 5867** presents secondary body between 12-40 mm thick (Plate III.6, 2 and 3). At the base, the stem fragment shows 88 fascicular wedges and at the upper part 88 fascicular wedges also. In the most internal part of the secondary body, in cross section, fascicular wedges average 1.07 (0.77-1.84) mm in width and are composed of 16-33 cell files. Tracheids are square to rectangular-shaped, with average width of 63 (40-90) µm radially and 41 (20-60) µm tangentially. The fascicular rays show 1-3 files of parenchymatous rectangular-shaped cells, on average 118 (60-220) µm wide radially and 25 (10-50) µm tangentially. Interfascicular rays average 551 (330-750) µm in width and are composed of 4-9 files of parenchymatous rectangular-shaped cells, on average 125 (60-220) µm wide radially and 67 (20-110) µm tangentially, practically two times longer than wide.

In cross section of the middle part of the secondary body, approximately 1.6 cm from the pith cavity, fascicular wedges average 2022 (1710-2390) µm in width with approximately 35 cell files. Tracheids show square to rectangular-shaped cells on average 70 (67-73) µm long radially and 34 (25-46) µm tangentially (Plate III.7, 1 and 2). The fascicular rays show 1-2 parenchymatous rectangular-shaped cell files, on average 87 (73-96) µm long radially and 27 (18-37) µm tangentially (Plate III.7, 1). The interfascicular rays average 436 (365-511) µm in width with 5-8

files of parechymatous cells. These rectangular-shaped cells are on average 116 (111-123) µm long radially and 58 (32-90) µm tangentially and present many pits on their radial walls (Plate III.7, 2). In this part, the secondary body shows very evident growth rings and the tracheids become smaller (Plate III.7, 3). The parenchymatous cells of the interfascicular rays do not change as the tracheids (Plate III.7, 4).

In the distal part of the secondary body, in cross section, the fascicular rays average 2870 (2550-3450) µm in width. The tracheids show square to rectangular-shaped cells on average 78 (40-150) µm long radially and 50 (30-80) µm tangentially. The fascicular rays show 1-2 parenchymatous rectangular-shaped cells on average 105 (70-230) µm long radially and 36 (20-60) µm tangentially. The interfascicular rays in this part are indistinct and interwoven with tracheids of rectangular-shaped cells on average 204 (90-340) µm long radially and 48 (30-60) µm tangentially.

In radial section, tracheids of this species presents circular reticulate secondary wall thickenings. In the holotype **K 5867**, the fascicular wedges are organized in axial files with axially very long cells, on average 70 (40-55) µm radially and show circular reticulate thickenings of pits on average 8.3 (6.5-9.5) µm in diameter (Plate III.8, 3 and 4). In this section the interfascicular rays are composed of files of parenchymatous brick- shaped cells, wider than high, on average 68 (40-120) µm long axially and 128 (90-180) µm radially. Fascicular rays are composed of files of parenchymatous brick-shaped cells on average 73 (52-90) µm long axially and 87 (73-96) µm radially.

In tangential section, in the holotype **K 5867**, tracheids represent 50% and parenchymatous cells 50% in the composition of the secondary body (Plate III.7, 6 and 7). The fascicular wedges are composed of approximately 35 cell files in width and the tracheids are very long axially, on average 48 (40-55) µm long tangentially. The fascicular rays are composed of 1-3 files between 20 and 30 µm wide, 4-5 and commonly 30-40 cells in height. The cells are square to rectangular-shaped, on average 79 (63-94) µm long axially and 43 (30-51) µm tangentially (Plate III.7, 7). Parenchymatous cells of interfascicular rays are organized in 5-9 files, running along the successive nodes with polygonal-shaped cells, on average 67 (40-103) µm long axially and 62 (40-98) µm tangentially (Plate III.7, 7; Plate III.8, 2). There are tracheids files dispersed in these rays (Plate III.8, 2).

Leaf traces, root system and cortical elements - Leaf traces, root system, phloem, periderm and cortical tissues are not preserved in the holotype and in the other specimens.

Comparisons

The described specimens differ from *Arthropitys bistriata* (Cotta) Goeppert *emend*. Röβler, Feng & Noll, 2012, *A. communis* (Binney) Renault, 1896, *A. lineata* Renault, 1896, *A. gallica* Renault, 1896 [apud Andrews (1952); Boureau (1964); Wang et al. (2003)], *A. felixi* Hirmer & Knoell (in Knoell, 1935), *A. deltoides* Cichan & Taylor, 1983, *A. junlianensis* Wang, Hilton, Li & Galtier, 2003, *A. yunnanensis* (Tian & Gu) *ex* Wang, Hilton, Galtier & Tian, 2006, and *A. ezonata* (Goeppert) *emend.* Rößler & Noll, 2006, because of the circular reticulate secondary wall thickenings in the tracheids, not scalariform thickenings as in the mentioned species;

In this character, the studied specimens also differ from *Arthropitys gigas* (Brongniart) Renault, 1896, *A. porosa* Renault, 1896, *A. rochei,* Renault, 1896, which present three kinds of secondary wall thickenings in the tracheids;

They also are distinct from *Arthropitys kansana* Andrews, 1952, which has circular to slightly elongate secondary wall thickenings in the tracheids, in addition to differences concerning the fascicular wedges and interfascicular rays in cross sections: they become wider radially in the studied specimens, but keep constant in the compared species;

Finally, the secondary wall thickenings in the tracheids of the studied specimens represent an important difference in relation to the scalariform and elongate reticulate thickenings in *Arthropitys versifoveata* Anderson, 1954 and also in comparison to the elongate reticulate thickenings in *Arthropitys Illinoensis* Anderson, 1954. In addition, cross sections of the studied specimens show that the interfascicular rays increase slightly in width, whereas these rays narrow abruptly in *A. Illinoensis*;

Information about the thickenings in the tracheids are missing in *Arthropitys renaultii* Boureau, 1964 and *A. approximata* (Schlotheim) Renault, 1896 [apud Andrews (1952); Boureau (1964)], what discourages comparisons.

The tracheid thickenings are also unknown in *Arthropitys bistriatoides* Hirmer & Knoell (in Knoell, 1935), *A. herbacea* Hirmer & Knoell (in Knoell, 1935)

and *A. jongmansi* Hirmer, 1927 (in Knoell, 1935) and the studied specimens additionally differ from these species because of the well developed secondary body, with clear fascicular wedges and interfascicular rays. In this aspect, the studied specimens also differ from *Arthropitys hirmeri* Knoell, 1935, which presents only fascicular wedges;

Concerning the circular reticulate secondary wall thickenings of the tracheids, the described specimens are similar to *Arthropitys major* (Weiss) Renault, 1896 [apud Boureau (1964); Wang. et al. (2006)], *A. cacundensis* Mussa, 1984 (in Coimbra & Mussa, 1984) and *A. sterzelli* Rößler & Noll, 2010. However, they differ from the first species by the much lower number of cell files in the fascicular wedges (4 to 9 files instead of 20 to 30 in *A. major*). The main difference in relation to the other two species is the much higher number of branches per node (8 to 15 in the studied specimens instead of 2 to 5). A possible additional divergence is that the branches present secondary growth, not only primary growth as in *A. sterzelli*.

Considering the presented comparisons, the studied specimens are distinct from all species of the literature. Therefore, ***Arthropitys tabebuiensis*** is proposed and the Table III.2 presents main anatomical and morphological data of this species.

Plate III.6: *Arthropitys tabebuiensis*

1: lateral surface of the holotype **K 5867** showing stumps of branches (mainly in the upper part) and branch scars (mainly in the lower part).

2: cross section of the paratype **K 5447** with branch traces (arrows) extending from the pith cavity to the stem surface.

3: cross section of the holotype **K 5867** at the basal part of the stem showing pith cavity, fascicular wedges and interfascicular rays.

4: lateral surface of the stem **K 5394** showing branch scars (arrows) at a nodal line.

5: detail of the branch traces at pith cavity periphery (arrows) in the stem of the paratype **K 5447**.

PLATE III.6

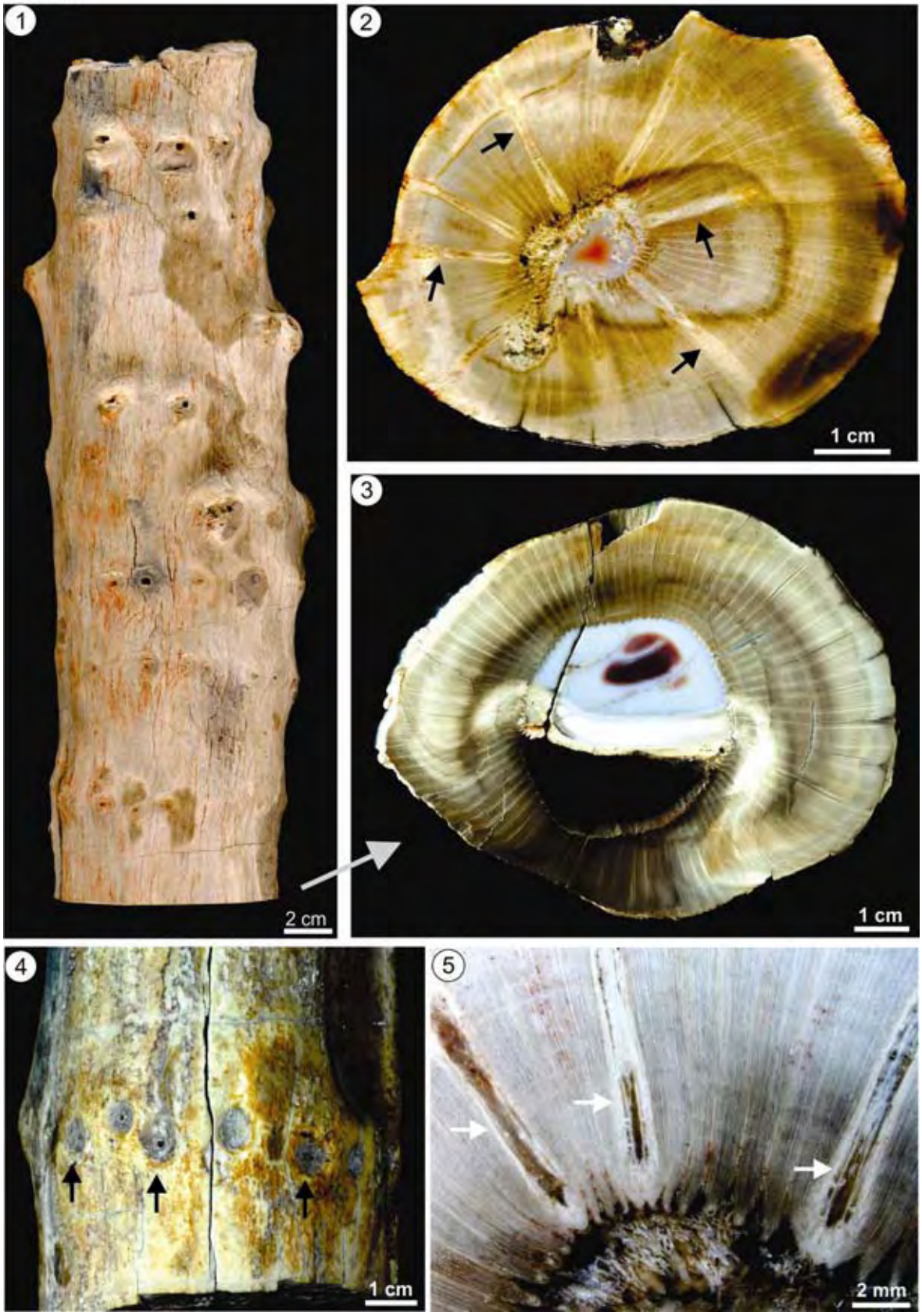

Plate III.7: *Arthropitys tabebuiensis*

1: cross section of the holotype **K 5867** showing tracheids of fascicular wedges and parenchymatous cells of the interfascicular rays.

2: magnification of 1. Arrows indicating pits on radial walls of the parenchymatous cells.

3: cross section of the holotype **K 5867** showing growth rings (arrows) throughout the secondary body.

4: magnification of 4. Cross section of the holotype **K 5867** in the middle part of the secondary body showing details of the cells in the growth rings (arrows), the fascicular wedges (fw) and the interfascicular rays (ir).

5: cross section of the holotype **K 5867** showing departure of branch traces (arrows).

6: tangential sections of the holotype **K 5867** showing secondary body divided by fascicular wedges (fw) and interfascicular rays (ir).

7: magnification of 6 showing tracheids of fascicular wedges (fw), fascicular rays (arrows) and parenchymatous cells of the interfascicular rays (ir).

PLATE III.7

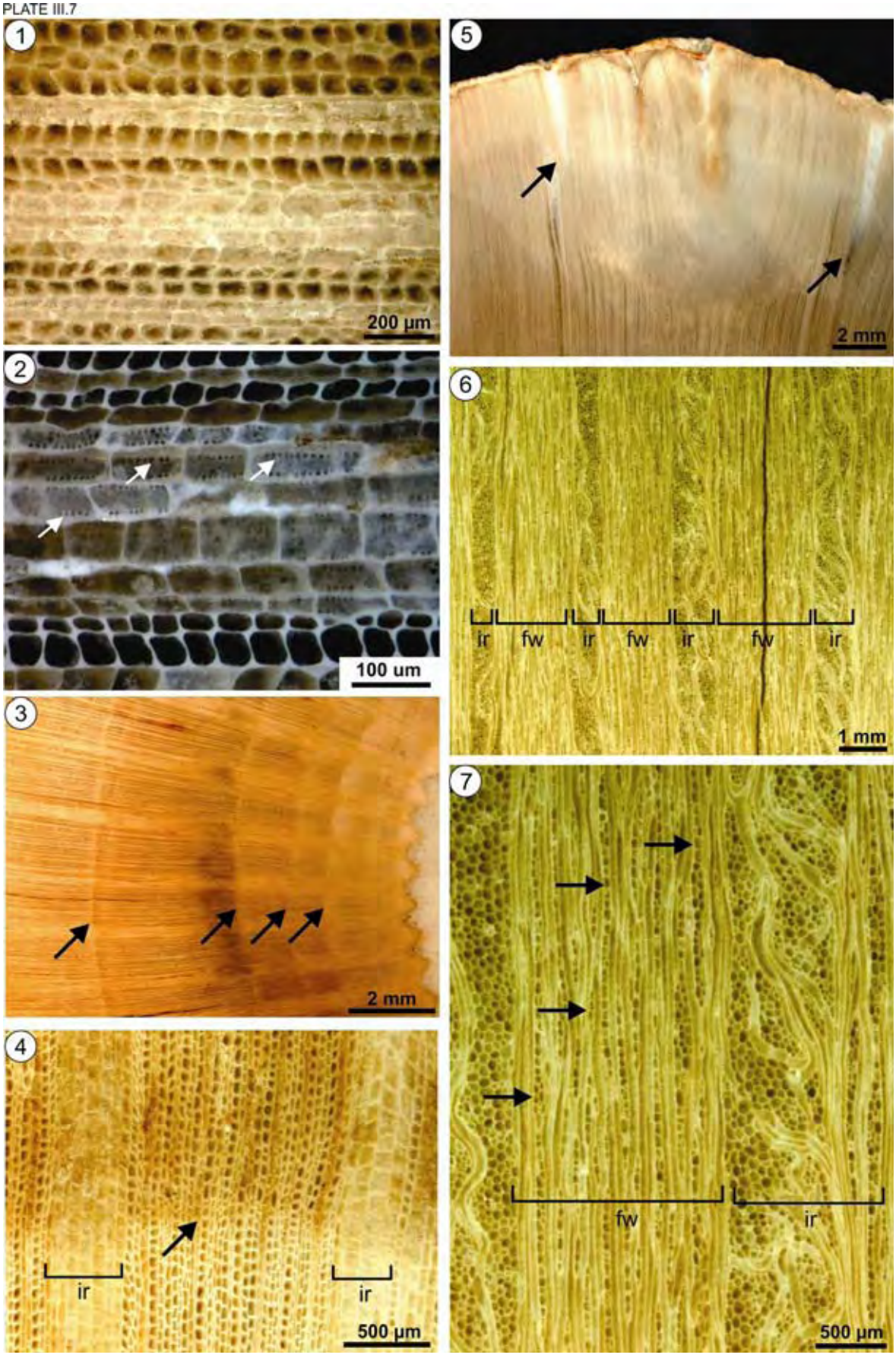
1
200 µm
2
100 um
3
2 mm
4
ir
ir
500 µm
5
2 mm
6
ir
fw
ir
fw
ir
fw
ir
1 mm
7
fw
ir
500 µm

Plate III.8: *Arthropitys tabebuiensis*

1: longitudinal section of the stem **K 5453** showing secondary body, pith cavity and one branch trace (arrow) in the middle of the secondary body.

2: tangential section of the holotype **K 5867** showing tracheids (long arrows) dispersed in the interfascicular rays (short arrows).

3-4: radial sections of the holotype **K 5867** showing circular reticulate secondary wall thickenings of the tracheids.

5: cross section in the specimen **K 5453** showing slightly flattening of the stem, pith cavity, fascicular wedges and interfascicular rays.

6: cross section of the stem **K 5445** showing pith cavity, fascicular wedges and interfascicular rays.

7: weathered cross section of the specimen **K 5540** showing pith cavity, fascicular wedges and interfascicular rays.

8: magnification of 7 showing details of carinal canals.

9: cross section of the stem **K 5394** showing pith cavity, fascicular wedges and interfascicular rays.

PLATE III.8

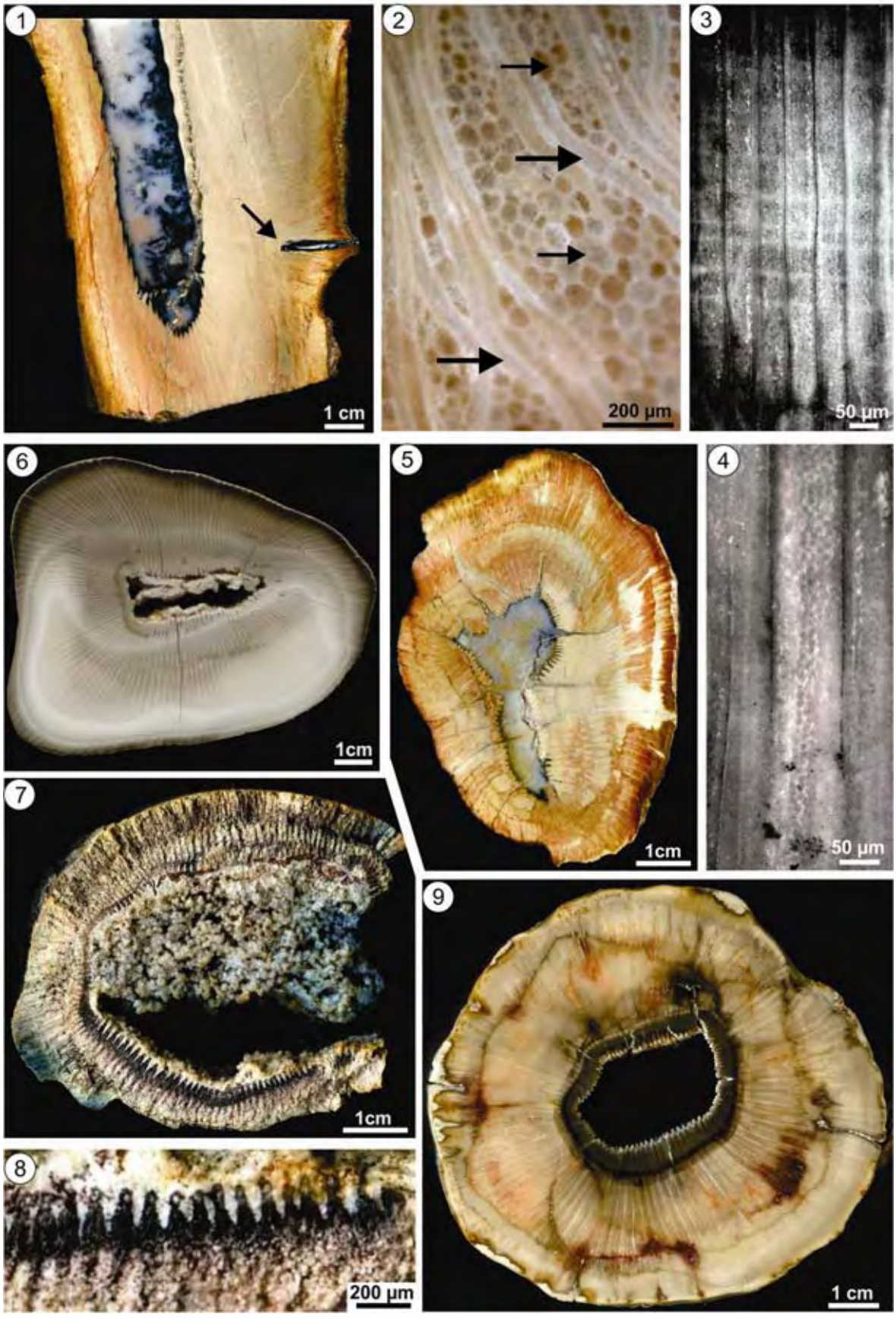

Taxon	Locality / Stratigraphy	Collection
Arthropitys tabebuiensis	central-north Brazil, Parnaiba Basin / Early Permian	MfNC / K 5867 (holotype)

Part of the plant	Length	Girth	Diameter stem (S)	Diameter pith (P)	P/S ratio	Wood
Stem	36.5 cm	29 cm at base 17.5 cm at top	8.1 x 10.2 cm at base 6.8 x 8.0 cm at top	2.9 x 4.1 cm at base 1.9 x 3.0 cm at top	1:2.6 at base 1:2.2 at top	12-40 mm divided in distinct wedges usually visible to the margin fascicle width: initially 1.07 mm (0.77-1.84), distally: 2.87 mm (2.55-3.45)

Morphology/Branching	Type	Branch traces	Leaf traces	Root traces
primary/secondary growth	with and without secondary growth	8-15 at every node, departing at the pith's margin rarely visible at pith mould, disposed in line along the stem circular in shape, 2-14 mm in diameter	not preserved	not preserved

Internode length	32 mm (16-55), 10 measurements

Primary tissues	Vascular strands number	Carinal canal diameter	Px tracheids/tyloses	Mx tracheids
	88 strands	150-160 µm badly preserved	not preserved	25-40 µm, circular-shaped badly preserved

Secondary tissues	Tracheids (cross view) radially / tangentially (µm), files per fascicle	Thickenings (radial view)	Outline
	initially: 63 (40-90) / 41 (20-60), 16-33 files per fascicle medially: 70 (67-73) / 34 (25-46), 35 files per fascicle distally: 78 (40-150) / 50 (30-80)	circular reticulated pits: 6.5-9.5 µm	rectangular to square

	Interfascicular rays (cross view) number of files / width (µm)	Cells (radial view) axially / radially (µm)	Cells (tangential view) axially / tangentially (µm)	Cells (cross view) radially / tangentially (µm)
	made of 4-9 parenchym. files initially 551 (330-750) medially: 436 (365-511) distally indistinct and interwoven with tracheids running from node to node	68 (40-120) / 128 (90-180) brick-shaped, rather wider than high	67 (40-103) / 62 (40-98) polygonal outine	initially: 125 (60-220) / 67 (20-110) medially: 116 (111-123) 58 (32-90) distally: 204 (90-340) / 48 (30-60) narrow marginal, widest medially

	Fascicular rays (cross view) number of files / width	Cells (radial view) axially / radially (µm)	Cells (tangential view) axially / tangentially (µm)	Cells (cross view) radially / tangentially (µm)
	made of 1-3 files 62 µm (30-120)	73 (52-90) / 87 (73-96) brick-shaped, wider than wide	79 (63-94) / 43 (30-51) square to rectangular-shaped 4-5 and common 30-40 files in height, higher than wide	initially: 118 (60-220) / 25 (10-50) medially: 87 (73-96) / 27 (18-37) distally: 105 (70-230) / 36 (20-60)

Cortex / Periderm / special characters	not preserved / growth rings weak

Table III.2: main anatomical and morphological data of *Arthropitys tabebuiensis.*

***Arthropitys tocantinensis* n. sp.**

(Plates III.9 to III.12)

Holotype: specimen K 4965.

Paratype: specimen K 5266.

Additional material: K 5107, K 5399, K 5455, K 5456.

Type locality: Parnaíba Basin, central-north Brazil.

Type stratum: Motuca Formation, Lower Permian.

Etymology: the specific name refers to the locality where this species was found, Tocantins State, Northeastern Brazil.

Diagnosis according to the rules of the International Code of Botanical Nomenclature: Stems distinct from all other *Arthropitys* species because of narrow pith cavity, pith/stem diameter ratio equal to 1:4.5-1:8.0, three to seven branches at every node, disposed in line along the stem, with and without secondary growth, and the scalariform and rare circular reticulate secondary wall thickenings of the tracheids in radial view.

Description

Macroscopic stem characteristics- The holotype **K 4965** is a 110 cm long stem (Plate III.9, 1-3), circular in section with diameter of 9.4 x 10.4 cm, girth is 31 cm, pith cavity diameter of 24 x 27 mm and pith/stem diameter ratio equal to 1:6.3 (Plate III.9, 8). In the paratype **K 5266**, this ratio is equal to 1:5 (Plate III.10, 5), in the specimem **K 5455** is 1:4.5 (Plate III.12, 1), in **K 5456** is 1:2.7(Plate III.11, 7) and in the specimen **K 5399** is 1:8 (Plate III.12, 3).

In the paratype **K 5266 i**nternodes average length of 32 mm (min. 16 mm, max. 55 mm) (Plate III.9, 4). The surface shows furrows, which are continuous at the nodes, not alternated. In the specimen **K 5455** it is possible to see a little part of the structure of the pith cavity (Plate III.12, 2). In these permineralized specimens, the secondary body is divided into fascicular wedges and interfascicular rays only visible at the pith cavity periphery (Plate III.9, 8; Plate III.10, 5; Plate III.11, 7 and 9; late III.12, 1, 3 and 4). The fascicular rays are composed of tracheids and parenchymatous cells and the interfascicular rays, of parenchymatous cells.

Branching system – The branching system in this species is composed of 3-7 branches at every node, without secondary growth (Plate III.10, 1 to 4) and with secondary growth (Plate III.11, 4 and 5).

The holotype **K 4965** has 11 whorls, which presents circular branch scars, with diameters between 4-40 mm, and stumps of branches, disposed in line along the stem. The larger stump of branch presents diameter of 3.5 cm and a departure angle of 60^{o} and the smaller stump diameter of 2 cm and angle of 80^{o}. These stumps are not in the same whorl, but present one with other an angle of approximately 90^{o} (Plate III.9, 1-3).

In the specimen **K 5456** the branch scars are very evident (Plate III.11, 6).

Leaf scars – Some leaf scars were recognized in the specimen **K 5266**. They are disposed in a verticilar arrangement, beneath the branch scars, slightly elliptical with diamenters of 0.5 mm (Plate III.10, 9).

Primary body - The carinal canals and metaxylen cells are not well preserved in the holotype, but they can be better characterized in the paratype **K 5266** (Plate III.9, 6) and in the specimen **K 5107** (Plate III.11, 3), specially in the last one. These carinal canals are surrounded by 2 or 3 files of circular to elliptical metaxylem cells on average 39 µm (20-54) in diameter. Furthermore, there are important tyloses in these carinal canals: 4 parenchymatous cells of 246 and 285 µm in diameter (Plate III.11, 3 - arrows).

Secondary body – The secondary body is clearly divided into fascicular wedges and interfascicular rays in the pith cavity periphery (Plate III.9, 8; Plate III.10, 5; Plate III.11, 7 and 9; Plate III.12, 1, 3 and 4). In more external regions, these rays are almost indistinct, resulting in an undifferentiated secondary body in longitudinal sections of some specimens (Plate III.9, 9; Plate III.11, 8 and 10).

In the holotype **K 4965**, the secondary body is between 12-40 mm thick (Plate III.9, 8) and composed by 77 vascular strands. In the internal part of the stem, in cross section, the fascicular wedges are composed of 25-30 cell files on average 138 µm (118-166) in width. Tracheids show square to rectangular-shaped cells on average 65 µm (51-87) radially and 48 µm (40-54) tangentially. The fascicular rays show uni to trisseriate cell files, rarely four, and are composed by parenchymatous rectangular-shaped cells on average 94 µm (56-135) radially and 21 µm (16-26) tangentially. The interfascicular rays are in average 189 µm wide, made of 3 parenchymatous rectangular-shaped cell files on average 138 µm (110-

174) radially and 46 µm (31-75) tangentially, practically 2,5 times longer than wide (Plate III.9, 5). In the paratype **K 5266**, the secondary body shows 13-23 mm thick (Plate III.10, 5), 65 fascicular strands, fascicular wedges average 594 µm (498-722) wide and interfascicular rays average 178 µm (119-252) in width composed by 7 cells files.

In the middle part of the secondary body, the holotype **K 4965** does not show cells in good condition. In the other hand, the paratype **K 5266** presents a good preservation of the cells. Tracheids show square to rectangular-shaped cells average 55 µm (41-75) radially and 36 µm (22-60) tangentially, and the fascicular rays show uni to trisseriate cell files, rarely four, composed by parenchymatous rectangular-shaped cells on average 55 µm (39-60) radially and 18 µm (15-22) tangentially (Plate III.10, 7).

In the middle part of the secondary body, in cross section, the paratype **K 5266** (Plate III.11, 1; Plate III.12, 4) and the specimens **K 5455** (Plate III.12, 1) and **K 5399** (Plate III.12, 3) present very evident growth rings, which correspond to alternating larger and smaller tracheids. In the specimen **K 5399**, parenchymatous cells of the interfascicular rays do not suffer modifications of the size on the growth rings (Plate III.11, 2).

In the more external region of the secondary body in the holotype **K 4965**, in cross section, fascicular wedges and interfascicular rays continue indistinct and the latter show an invasion of the tracheids of the former. Tracheids average 33 µm (28-40) tangentially. Parenchymatous cells of interfascicular rays are rectangular-shaped, on average 61 µm (47-78) radially and 24 µm (16-33) tangentially.

In radial section, tracheids of this species present scalariform (Plate III.9, 10; Plate III.10, 6) and rare circular reticulate secondary wall thichenings Plate III.12, 7). In the holotype **K 4965**, tracheids of the fascicular wedges are organized in axial files, are very long axially and average 54 µm (37-67) radially. These cells show scalariform thickenings in secondary walls with a vertical distance of 6-10 µm and 12-28 µm horizontally (Plate III.9, 10). The interfascicular rays are composed of brick-shaped parenchymatous cell files, wider than high, on average 61 µm (42-96) axially and 135 µm (110-164) radially with some pits on the radial walls (Plate III.9, 7).

In the specimen **K 5107**, the metaxylem cells present poorly developed scalariform thickenings (Plate III.12, 6) and tracheids present rare circular reticulate thickenings with pits of 6.5-12 µm in diameter (Plate II.12, 7).

In tangential section, in the holotype **K 4965**, tracheids make up 65% and parenchymatous cells 35% of the secondary body. The tracheids are very long axially averaging 33 µm (28-40) tangentially. Parenchymatous cells of the interfascicular average 61 µm (47-78) axially and 24 µm (16-33) tangentially. The fascicular rays present uni to bisseriate files, the cells are higher than wide averaging 86 µm (58-127) axially and 30 µm (25-35) tangentially and composed by 10 to more than 40 cells in height. In the paratype **K 5266**, the fascicular rays are very preserved and is possible to see the height of them (Plate II.10, 8 and 10).

In the specimen **K 5107**, the composition of the fascicular rays is very clear: the rays present 1-3 and more rarely 4 files of rectangular cells in width, on average 87 µm (54-134) axially and 56 µm (39-71) tangentially and 5 to more than 40 cells in height. Interfascicular rays present rectangular-shaped cells on average 61 µm (47-78) axially and 24 µm (16-33) tangentially, higher than wide (Plate III.12, 5).

Root system and cortical elements – The root system, phloem, periderm and cortical tissues are not preserved in the holotype and in the other specimens.

Comparisons

The studied specimens differ from *Arthropitys major* (Weiss) Renault, 1896 [apud Boureau (1964); Wang. et al. (2006)], *A. kansana* Andrews, 1952, *A. illinoensis* Anderson, 1954, and *A. sterzelii* Rößler & Noll, 2010, *A. cacundensis* Mussa, 1984 (in Coimbra & Mussa, 1984), because the species from Tocantins present scalariform and rare circular reticulate secondary wall thickenings whereas the species above present reticulate thickenings only;

The studied specimens are different from *Arthropitys gigas* (Brongniart) Renault, 1896, *A. rochei* Renault, 1896, and *A. porosa* Renault, 1896, because the species studied here present scalariform and rare circular reticulate secondary wall thickenings whereas the species above present three kinds of thickenings in the tracheids;

Arthropitys renaultii Boureau, 1964, and *A. approximata* (Schlotheim) Renault, 1896 [apud Andrews (1952); Boureau (1964)], do not present the kind of thickenings, dificulting comparisons with the species described in this study and these two species mentioned;

Differ from *Arthropitys bistriatoides* Hirmer & Knoell (in Knoell, 1935), *A. herbacea* Hirmer & Knoell (in Knoell, 1935), and *A. jongmansi* Hirmer, 1927 (in Knoell, 1935), because the species from Tocantins has a secondary body well developed and the species above present a poorly developed secondary body. Also, the mentioned species do not present the kind of thickenings in the tracheids, difficulting the accurate comparison with the species studied here. Also differ from *A. hirmeri* Knoell, 1935, because the calamites from Tocantins bear secondary body composed by fascicular wedges and interfascicular whereas the species mentioned above presents only fascicular wedges in the secondary body;

The species studied here differ from *Arthropitys bistriata* (Cotta) Goeppert *emend*. Rößler, Feng & Noll, 2012, *A. communis* (Binney) Renault, 1896, *A. lineata* Renault, 1896, *A. gallica* Renault 1896 [apud Andrews (1952); Boureau (1964)], *A. versifoveata* Anderson, 1954, *A. deltoides* Cichan & Taylor, 1983, *A. felixi* Hirmer & Knoell (in Knoell, 1935), *A. junlianensis* Wang, Hilton, Li & Galtier, 2003, *A. yunnanensis* (Tian & Gu) Wang, Hilton, Galtier & Tian, 2006, and *A. ezonata* Goeppert *emend*. Rößler & Noll, 2006, because the stems described here present scalariform and rare circular reticulate secondary wall thickenings and the species above presents only scalariform thickenings in the tracheids. Also, present a branching system completely different from all mentioned species.

In conclusion, the analyzed specimens are distinct from all previously known species of *Arthropytis* and, therefore, they are classified as a new species, ***Arthropitys tocantinensis*** and the Table III.3 presents main anatomical and morphological data of this species.

Plate III.9: *Arthropitys tocantinensis*

1-3: general views of the paratype **K 5266**. In the Fig. 2, the arrows indicate branch traces.

4: detail of a small longitudinal section of the stem in Fig. 3 showing secondary body, internodes and diaphragm in the pith cavity.

5: cross section of the holotype **K 4965** showing tracheids of interfascicular wedges and rectangular parenchymatous cells of the interfascicular rays.

6: cross section of the paratype **K 5266** at the internal part of the secondary body showing carinal canals, metaxylem cells, fascicular wedges and interfascicular rays.

7: tangential section of the paratype **K 5266** showing parenchymatous cells with pits in the radial walls (arrows).

8: cross section of the holotype **K 4965** showing pith cavity and secondary body.

9: longitudinal section of the holotype **K 4965** showing pith cavity, secondary body at internodes.

10: radial section of the holotype **K 4965** showing scalariform secondary wall thickenings of the tracheids.

PLATE III.9

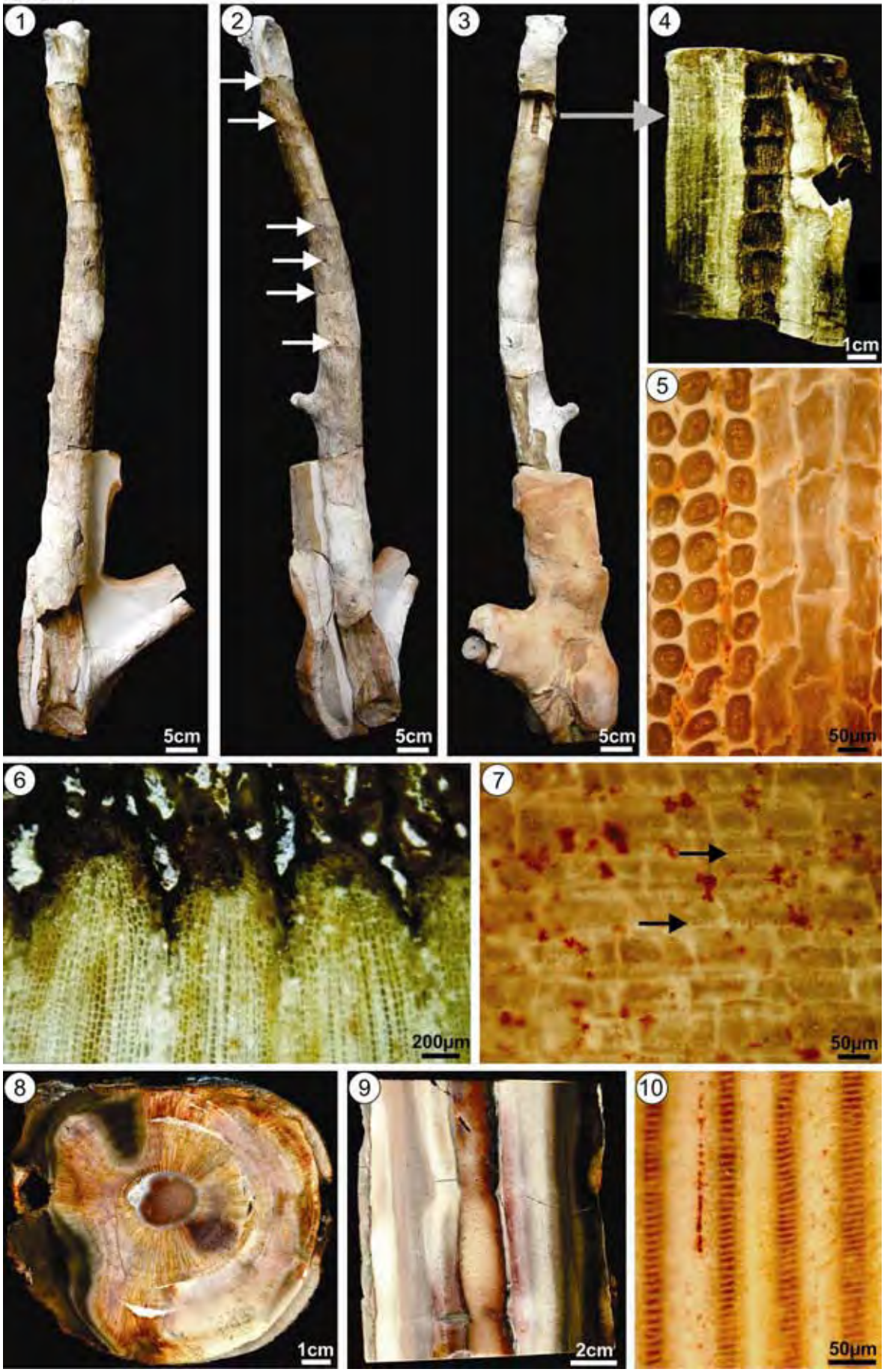

Plate III.10: *Arthropitys tocantinensis*

1-2: tangential sections of the paratype **K 5266** showing a conspicuous branch (at right in figure 2) and branch scars on the lateral surface, with a tangential section in the lower part, showing fascicular wedges, interfascicular rays and transversal branch traces.

3-4: tangential sections of the paratype **K 5266** showing details of cells in branch traces.

5: cross section of the paratype **K 5266** showing pith cavity and secondary body.

6: radial section of the paratype **K 5266** showing scalariform secondary wall thickenings of the tracheids.

7: cross section of the paratype **K 5266** showing cells of the interfascicular wedges (fw) and cells of interfascicular rays (ir).

8: tangential section of the paratype **K 5266** showing fascicular wedges (fw), interfascicular rays (ir) and fascicular rays (arrows).

9: tangential section of the paratype **K 5266** showing two branch traces and two leaf traces (arrows).

10: magnification of 8 showing tracheids of fascicular wedges (fw), cells of interfascicular rays (ir) and fascicular rays (arrows).

PLATE III.10

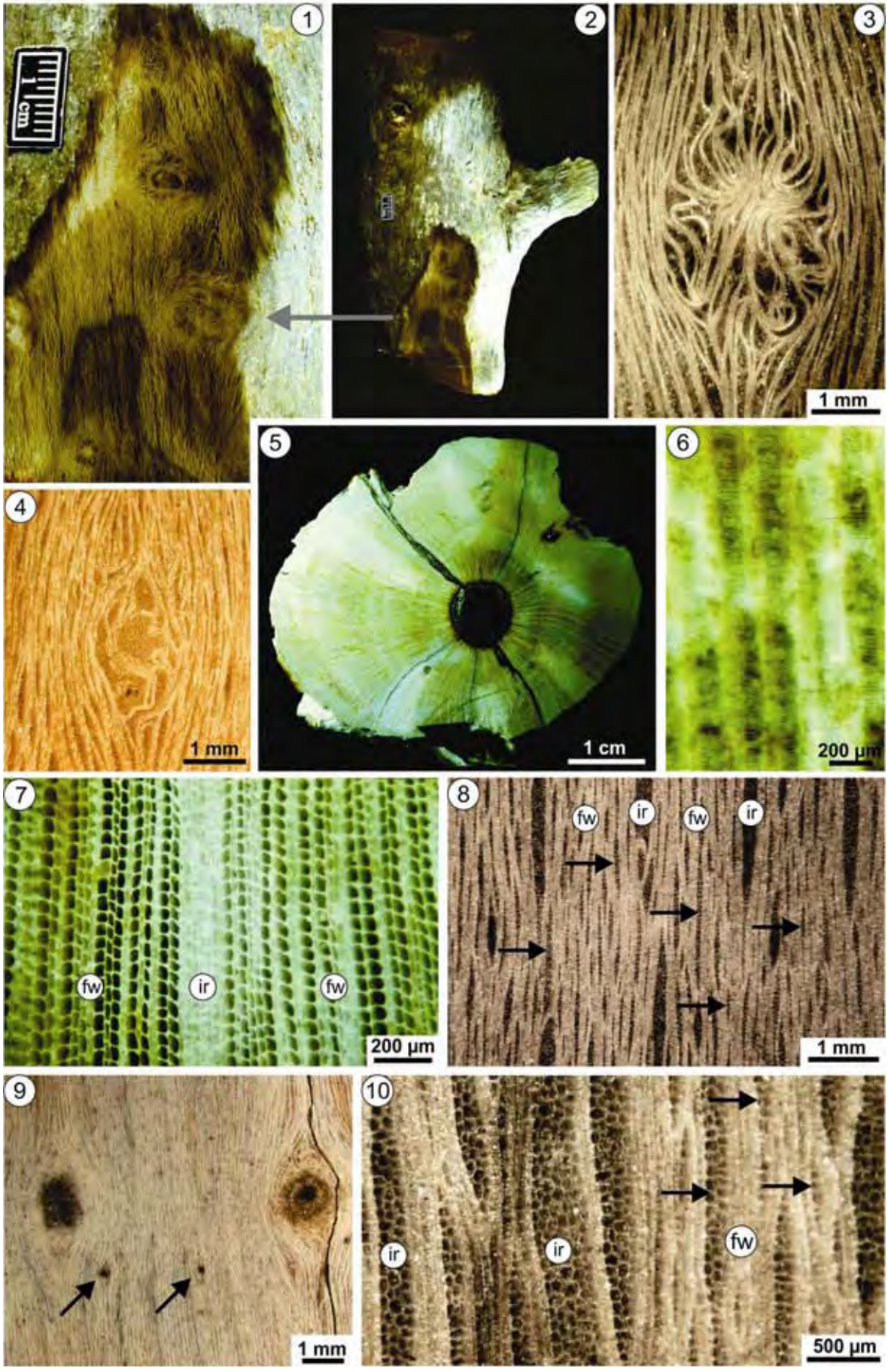
1
1 cm
2
3
1 mm
4
1 mm
5
1 cm
6
200 µm
7
fw
ir
fw
200 µm
8
fw
ir
fw
ir
1 mm
9
1 mm
10
ir
ir
fw
500 µm

Plate III.11: *Arthropitys tocantinensis*

1: cross section of the paratype **K 5266** showing growth rings (arrows at boundaries of growth rings) in the secondary body.

2: magnification of 1 showing cells at the boundary of two growth rings (small arrows), particularly no size decrease of the interfascicular ray cells (large arrow).

3: cross section of the stem **K 5107** at the internal part of secondary body showing carinal canals with tyloses (arrows) and fascicular wedges.

4: tangential section of the stem **K 5107** showing a branch trace.

5: magnification of 4 showing secondary growth in the branch.

6: general view of **K 5456** showing branch scars (arrows) and a stump of branch inserted in an inflated region of the stem (at right).

7: cross section of the stem **K 5456** showing pith cavity and secondary body with slightly marked growth rings.

8: tangential section of the stem **K 5456** showing pith cavity, secondary body and diaphragm.

9: cross section of the stem **K 5107** showing pith cavity, fascicular wedges and interfascicular rays.

10: tangential section of the stem **K 5107** showing secondary body and a branch trace (arrow).

PLATE III.11

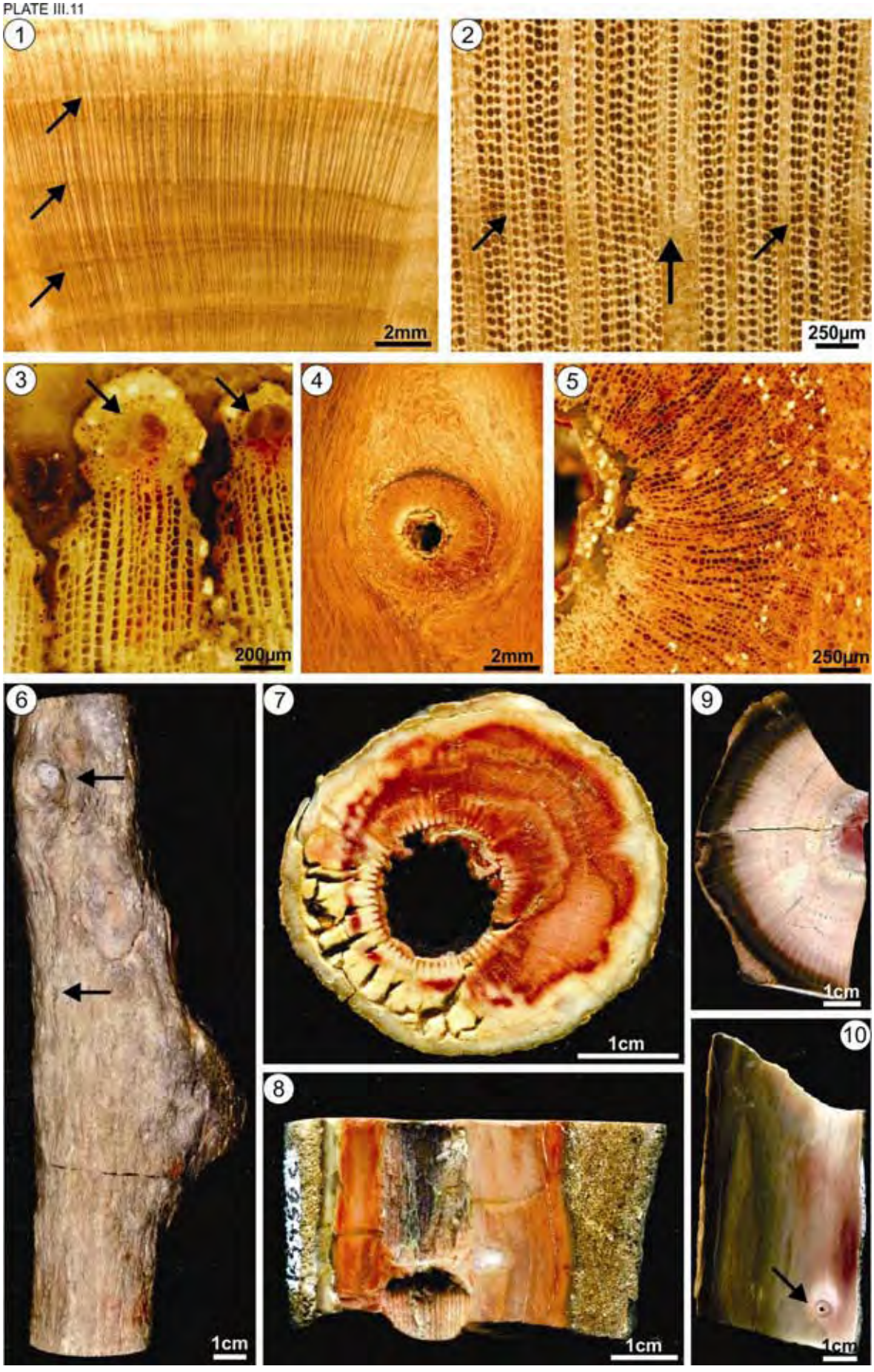

Plate III.12: *Arthropitys tocantinensis*

1: cross section of the stem **K 5455** showing pith cavity, fascicular wedges, interfascicular rays and growth rings (arrows at the boundaries between growth rings) in the secondary body.

2: general view of **K 5455** with a stump of a branch in the left and rounded lower extremity of the stem probably caused by abrasion during transport. Arrow indicates the structure of the pith cavity.

3: cross section of the stem **K 5399** showing pith cavity, fascicular wedges, interfascicular rays and growth rings (arrows at boundaries growth rings) in the secondary body.

4: cross section of the paratype **K 5266** showing growth rings and one adventitious branch trace (arrow) in the secondary body.

5: tangential section of the stem **K 5107** showing cells of fascicular wedges (fw), interfascicular rays (ir) and fascicular rays (arrows).

6: radial section of the stem **K 5107** showing scalariform thickenings in the metaxylem cells.

7: radial section of the stem **K 5107** showing rare circular reticulate secondary wall thickenings of the tracheids.

PLATE III.12

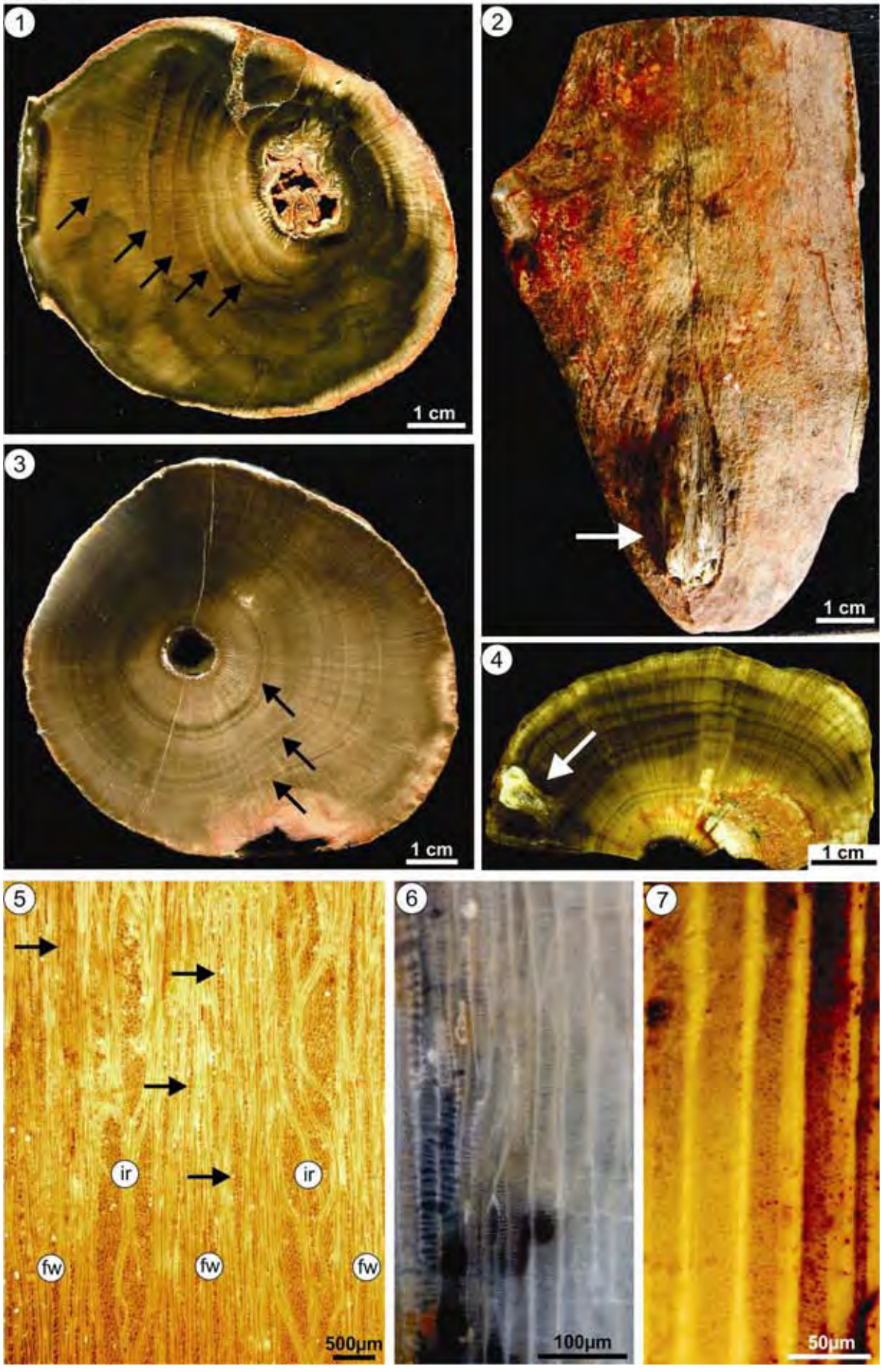

Taxon	Locality / Stratigraphy	Collection
Arthropitys tocantinensis	central-north Brazil, Parnaiba Basin / Early Permian	MfNC / K 4965 (holotype)

Part of the plant	Length	Girth	Diameter stem (S)	Diameter pith (P)	P/S ratio	Wood
Stem	110 cm	31 cm	9.4 x 10.4 cm	24 x 27 mm	1:6.3	12-40 mm divided in distinct wedges only visible at the pith periphery fascicle width: initially: 138 µm (118-166)

Morphology/Branching	Type	Branch traces	Leaf scars	Root traces
primary/secondary growth	with and without secondary growth	3-7 at every node, departing at the pith's margin not visible at pith mould circular in shape, 4-40 mm in diameter	beneath branch scars, verticilar, sligtly elliptical, diameter 0.5 mm	not preserved

Internode length	32 mm (min. 16, max. 55)

Primary tissues	Vascular strands number	Carinal canal	Px tracheids/tyloses	Mx tracheids
	77 strands	badly preserved	not preserved	badly preserved

Secondary tissues				
	Tracheids (cross view) radially / tangentially (µm), files per fascicle initially: 65 (51-87) / 48 (40-54), 25-30 files	**Thickening (radial view)** scalariform: distance 6-10 µm vertically and 12-28 µm horizontally; **K 5107**: rare circular reticulate thickenings: pits: 6.5-12 µm	**Outline** rectangular to square	
	Interfasc. rays (cross view) number of files / width (µm) made of 3-7 parenchym. files initially: 189 µm distally: indistinct running from node to node	**Cells (radial view) axially / radially (µm)** 61 (42-96) / 135 (110-164) rectangular-shaped, wider than high	**Cells (tangential view) axially / tangentially (µm)** 61 (47-78) / 24 (16-33) rectangular-shaped, wider/higher than wide/high	**Cells (cross view) radially / tangentially (µm)** initially: 138 (110-174) / 46 (31-75) distally: 61 (47-78) / 24 (16-33) rectangular-shaped
	Fascicular rays (cross view) number files / width µm made of 1-3, rarely 4 files	**Cells (radial view) axially / radially (µm)** not visible	**Cells (tangential view) axially / tangentially (µm)** 86 (58-127) / 30 (25-35) rectangular-shaped, higher than wide, 10 to more than 40 cells in height	**Cells (cross view) radially / tangentially (µm)** initially: 94 (56-135) / 21 (16-26) rectangular-shaped

Cortex / Periderm / special characters	no extraxylary tissues preserved / growth rings

Table III.3: main anatomical and morphological data of *Arthropitys tocantinensis*

***Arthropitys barthelii* n. sp.**

(Plates III.13 and III.14)

Holotype: specimen K 5787.

Paratype: specimen K 5500.

Additional material: K 4874.

Type locality: Tocantins Fossil Trees Natural Monument (TFTNM), Parnaiba Basin, central-north Brazil.

Type stratum: Motuca Formation, Lower Permian.

Etymology: the specific name is in honor to Manfred Barthel, imprescidible paleobotanist in the Ronny Röβler and Robert Noll's careers.

Diagnosis according to the rules of the International Code of Botanical Nomenclature: This species is distinct from all other *Arthropitys* species because of the very narrow pith cavity, with pith/stem diameter ratio equal to 1:5-1:54, the presence of longitudinal randomly 1 to 15 branches at every node without secondary growth, and the scalariform secondary wall thickenings of the tracheids in radial view.

Description

Macroscopic stem characteristics- The three stems are silica-permineralized. The holotype **K 5787** is 1.4 m long and the original circular shape in cross section is preserved, presenting diameters of 16.5 x 17.5 cm at the base of the specimen, 17 cm at 35 cm from the base, 15 cm at 75 cm from the base, 15 cm at 110 cm from the base and 12 cm at the top of the specimen (Plate III.13, 1-5). The secondary body range between is very undifferentiaded with fascicular and interfascicular rays only visible at the pith periphery (Plate III.14, 1, 4 and 7). In the holotype, at the base, the girth is 53.4 cm and pith/stem diameter ratio is equal to 1:5 (Plate III.14, 1), in the paratype **K 5500** is 1:36 (Plate III.14, 7), and in the specimen **K 4874**, this ratio reaches 1:54 (Plate III.14, 4).

In the holotype **K 5787**, the internodes lengths average 71 mm (min. 44, max. 94) in total of 19 measurements and approximately at the top of the stem, the internodes reach their longest dimension: 9.4 cm (Plate III.13, 1- 5).

Branching system- In this species the branching system is very variable, composed of 1-15 branches per node, without secondary growth and disposed in

randomly way from one node to another (Plate III.13, 1-5). In general, the branch characteristics are only evidenced by circular branch scars.

Primary body- In the holotype **K 5787**, the primary body metaxylen cells and carinal canals are very badly preserved. One of the better preserved carinal canals is elliptical-shaped with 220 µm in radial dimension and 153 µm in tangential dimension surrounded by slightly elliptical metaxylen cells with average diameter of 36 µm (29-50) (Plate III.13, 6).

Secondary body- In this species, the secondary body is clearly divided into fascicular wedges and interfascicular rays only in the pith cavity periphery.

In the holotype **K 5787**, the secondary body range between 75-82 mm in thickness (Plate III.14, 1). In the internal part of the secondary body, in cross section, fascicular wedges present approximately 25-28 cell files. Tracheids have rectangular-shaped cells on average 45 µm (32-71) radially and 23 µm (17-28) tangentially. The fascicular rays show uni to bisseriate parenchymatous rectangular-shaped cell files on average 54 µm (45-65) radially and 16 µm (14-20) tangentially. Interfascicular rays present 3-5 parenchymatous rectangular-shaped cell files, on average 80 µm (45-116) radially and 52 µm (39-63) tangentially.

The middle part of the secondary body becomes undifferentiated, without differentiation between fascicular and interfascicular rays (Plate III.14, 1 and 7). Tracheids present rectangular-shaped cells, on average 59 µm (41-78) radially and 44 µm (25-62) tangentially (Plate III.14, 2). The fascicular rays present 50 µm in width and are composed by bisseriate parenchymatous rectangular-shaped cell files, on average 69 µm (49-89) radially and 21 µm (19-23) tangentially. Interfascicular rays have rectangular-shaped cells with average dimensions of 115 µm (88-156) radially and 32 µm (26-41) tangentially (Plate III.14, 2).

The holotype **K 5787**, in the external part of the secondary body presents the same composition as the middle part, but xylem cells present thicker secondary walls in comparison to middle part.

The differentiations of the fascicular wedges and the interfascicular rays only in pith periphery result in a very undifferentiated secondary body in longitudinal sections, like in the paratype K 5550 (Plate III.14, 6).

In radial section, tracheids of this species present scalariform secondary wall thickenings. In the holotype **K 5787**, fascicular wedges are very long axially, on average 58 µm (45-68) radially, the vertical spacing between thickenings of 6.5-

9.5 µm and a horizontal distance of 22-40 µm (Plate III.13, 7). The specimen **K 4874** presents very well preserved tracheids. These cells are very long axially on average 53 µm (40-73) radially, vertical distance between 5.5-8.0 µm and horizontal distance between 18-34 µm (Plate III.14, 5).

In this section, the holotype **K 5787** presents interfascicular rays composed by files of brick-shaped parenchymatous cells, which are wider than high, on average 103 µm (77-122) axially and 174 µm (162-200) radially.

In tangential section, in the holotype **K 5787**, the secondary body is very undifferentiated (Plate III.14, 6), where approximately 40% correspond to tracheid cells and 60% to the parenchymatous cells.

In the paratype **K 5550**, the fascicular wedges are composed of axially very long tracheids, on average 72 µm (49-91) tangentially, and parenchymatous cells of interfascicular rays are organized in tangentially files with polygonal cells on average 88 µm (70-120) in diameter (Plate III.14, 3).

Leaf traces, root system and cortical elements - Leaf traces, root system, phloem, periderm and cortical tissues are not preserved.

Comparisons

The studied specimens differ from *Arthropitys gigas* (Brongniart) Renault, 1896, *A. rochei* Renault, 1896, and *A. porosa* Renault, 1896, because these specimens from Tocantins present scalariform secondary wall thickenings in the tracheids and the species mentioned present three kinds of thickenings in the tracheids;

The studied specimens are different from *Arthropitys major* (Weiss) Renault, 1896 [apud Boureau (1964); Wang. et al. (2006)], *A. kansana* Andrews, 1952, *A. illinoensis* Anderson, 1954, *A. cacundensis* Mussa, 1984 (in Coimbra & Mussa, 1984), and *A.sterzelii* Rößler & Noll, 2010, because the species described here present scalariform secondary wall thickenings in the tracheids, whereas the species mentioned present tracheids with circular reticulate thickenings;

Arthropitys renaultii Boureau, 1964, because does not present secondary structures, only large pith cavity and primary structures, difficulting comparisons with the species here;

The species described by Hirmer and Knoell do not show radial and tangential sections, complicating any more accurate comparison. Differ from

Arthropitys bistriatoides Hirmer & Knoell (in Knoell, 1935), *A. jongmansi* Himer, 1927 (in Knoell, 1935), and *A. herbacea* Hirmer & Knoell (in Knoell, 1935), because the species studied here present secondary body well developed and these species present secondary body poorly developed;

Arthropitys felixi is the only species described by Hirmer & Knoell (in Knoell, 1935) that present radial section, showing the scalariform thickenings in the tracheids, but there is not information in diagnosis of *A. felixi* about branch system, difficulting the association with the species described here. Differ from *Arthropitys felixi* Hirmer & Knoell (in Knoell, 1935), because the species studied here present fascicular wedges and inerfascicular rays and this species presents only fascicular wedges in the secondary body;

The studied specimens are similar to *Arthropitys bistriata* (Cotta) Goeppert *emend*. Rößler, Feng & Noll, 2012, *A. communis* (Binney) Renault, 1896, *A. lineata* Renault, 1896, *A. lineata* Renault, 1896, *A. gallica* Renault, 1896 [apud Andrews (1952); Boureau (1964)], *A. versifoveata* Anderson, 1954, *A. deltoides* Cichan & Taylor, 1983, *A. junlianensis* Wang, Hilton, Li & Galtier, 2003, *A. yunnanensis* (Tian & Gu) *ex* Wang, Hilton, Galtier & Tian, 2006, *A. ezonata* (Goeppert) *emend.* Rößler & Noll, 2006, because present scalariform secondary wall thickenings of the tracheids, but differ from all in the branching system, 1 to 15 in the species described here;

Thus, the described specimens are distinct from all previously known species of *Arthropytis* and, therefore, they are classified as a new species, ***Arthropitys barthelii*** and Table III.4 presents main anatomical and morphological data and Figure III.4 the proposed reconstruction of this species.

Plate III.13 *Arthropitys barthelii* n. sp.

1-5: general views of the stem **K 5787**, holotype of *Arthropitys barthelli.* Red points indicate branch traces.

6: cross section of the holotype **K 5787** showing carinal canal badly preserved (arrow).

7: radial section of the holotype **K 5787** showing scalariform secondary wall thickenings in the tracheids.

PLATE III.13

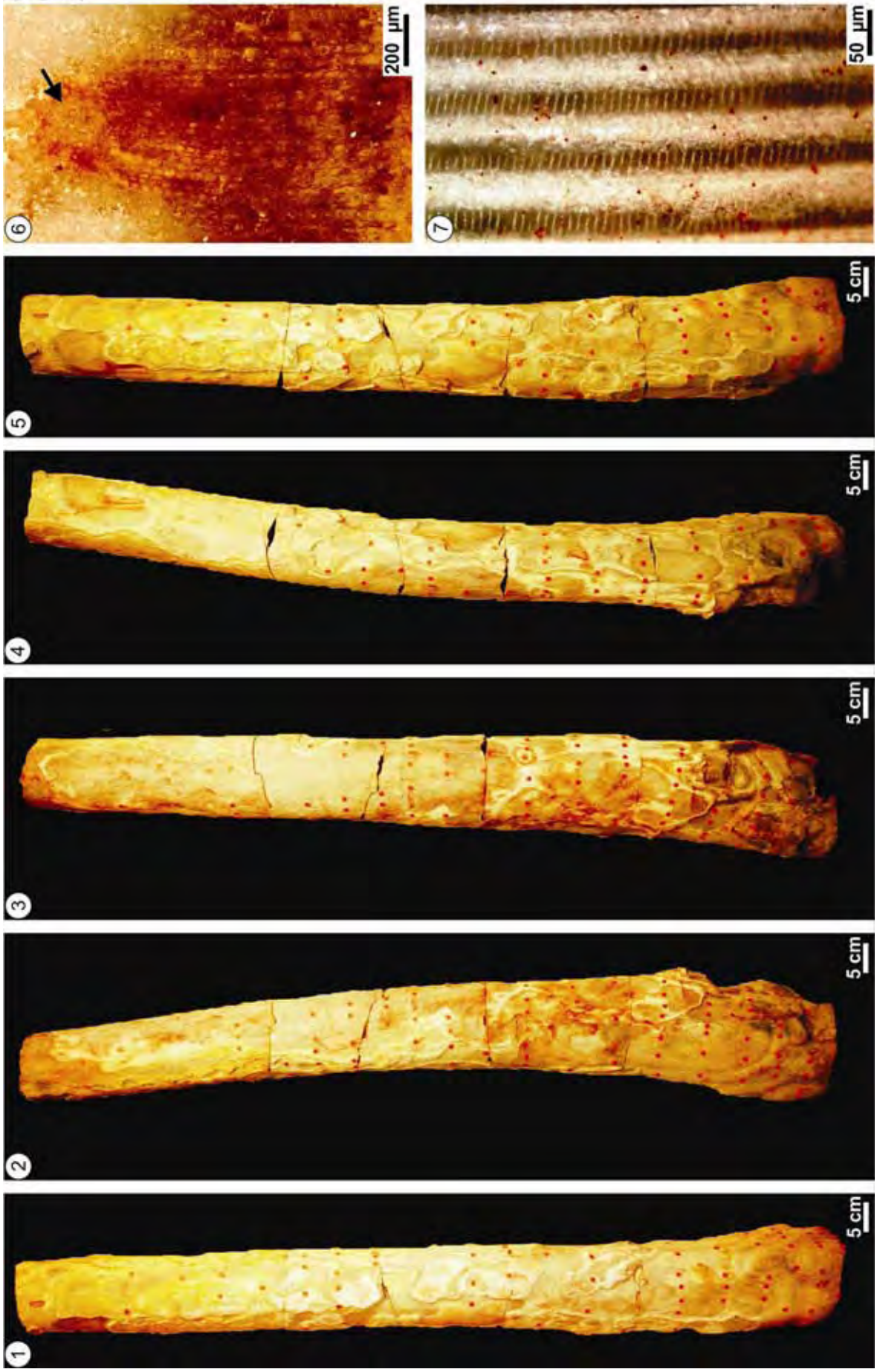

Plate III.14: *Arthropitys barthelii*

1: cross section of the holotype **K 5787** showing the small pith cavity and almost undifferentiated secondary body. The division into fascicular wedges and interfascicular rays only visible at pity periphery.

2: cross section of the holotype **K 5787** in the middle part of the secondary body showing tracheids of fascicular wedges (square cells) and parenchymatous cells of the interfascicular rays (rectangular cells).

3: tangential section of the paratype **K 5550** showing tracheids of the fascicular wedges and parenchymatous cells of the interfascicular rays.

4: cross section of the stem **K 4874** showing very small pith cavity and almost undifferentiated secondary body.

5: radial section of the stem **K 4874** showing scalariform thickenings of the tracheids.

6: longitudinal section of the paratype **K 5500** showing almost undifferentiated secondary body.

7: cross section of the stem **K 5500** showing the very small pith cavity and the almost undifferentiated secondary body.

PLATE III.14

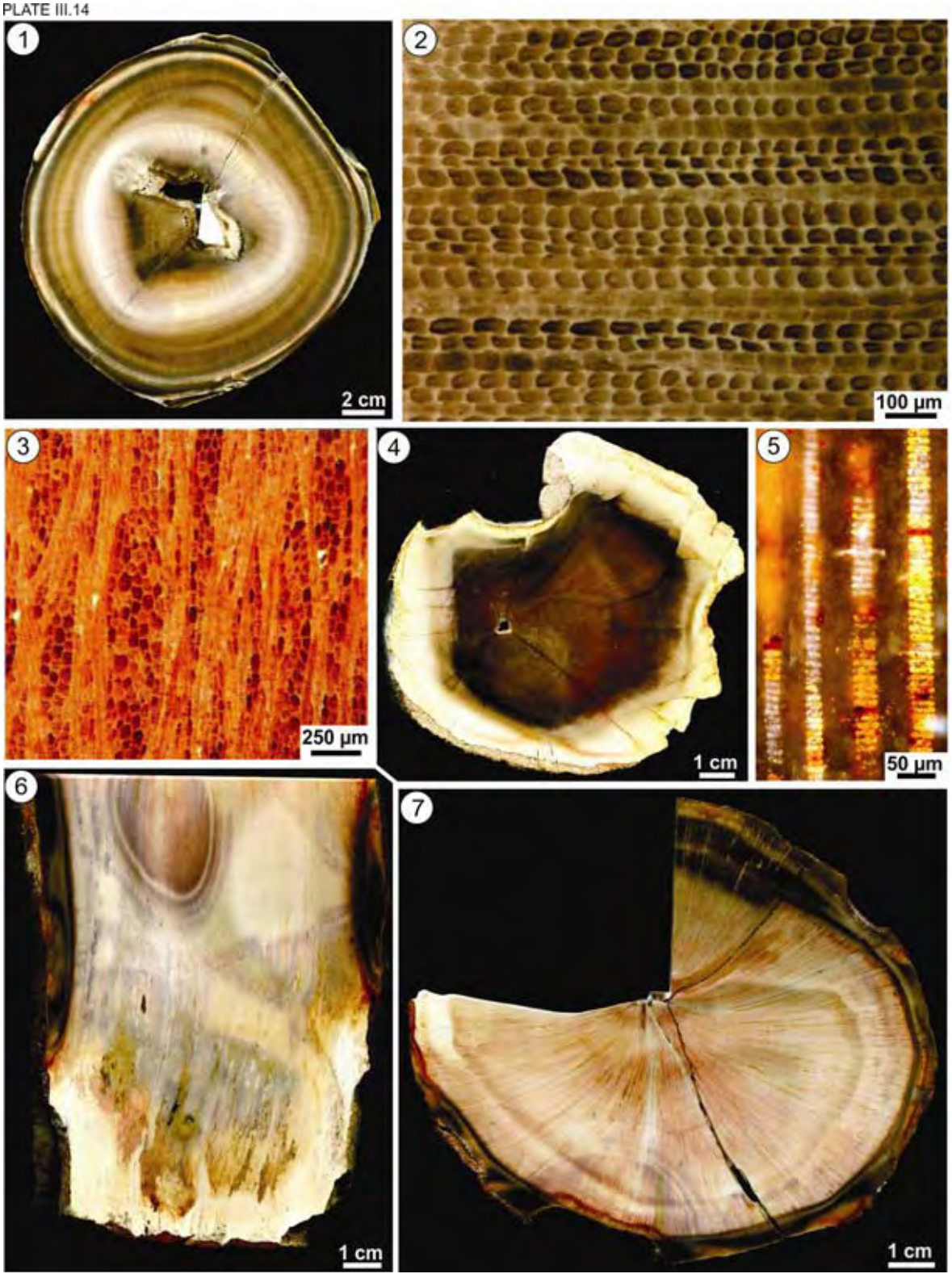

Taxon	Locality / Stratigraphy	Collection
Arthropitys barthelii	central-north Brazil, Parnaiba Basin / Early Permian	MfNC / K 5787 (holotype)

Part of the plant	Length	Girth	Diameter stem (S)	Diameter pith (P)	P/S ratio	Wood
Stem	1.4 m	54 cm at base	17 x 17.5 cm at base 12 cm at the top	1.3 x 4.9 cm at the base	1:4.7 at the base	75-82 mm very homogeneous with fascicular wedges and interfascicular rays only visible in the pith periphery

Morphology/Branching	Type	Branch traces	Leaf traces	Root traces
primary/secondary growth	without secondary growth	1-15 at every node, disposed in aleatory way not visible at pith mould circular in shape	not preserved	not preserved

Internode length	71 mm (44-94), 19 measurements			
Primary tissues	**Vascular strands number** xx strands at the base	**Carinal canal radially / tangentially (µm)** 220 / 153 badly preserved	**Px tracheids/tyloses** not preserved	**Mx tracheids** 36 µm (29-50) elliptical-shaped
Secondary tissues	**Tracheids (cross view) radially / tangentially (µm), files per fascicle** initially: 45 µm (32-71) / 23 µm (17-28), 25-28 files medially: 59 µm (41-78) / 44 µm (25-62)	**Thickening** scalariform: distance 6.5-9.5 µm vertically and 22-40 µm horizontally	**Outline** rectangular	
	Interfasc. rays (cross view) number of files / width (µm) made of 3-5 parenchym. files running from node to node	**Cells (radial view) axially / radially (µm)** 103 (77-122) / 174 (162-200) brick-shaped, wider than high	**Cells (tangential view) diameter (µm)** 88 (70-120) poligonal-shaped	**Cells (cross view) radially / tangentially (µm)** initially: 80 (45-116) / 52 (39-63) medially: 115 (88-156) / 32 (26-41) rectangular-shaped
	Fascicular rays (cross view) number files / width made of 1-2 files 50 µm in width in middle part	**Cells (radial view) axially / radially (µm)** not visible	**Cells (tangential view) axially / tangentially (µm)** not visible	**Cells (transverse view) radially / tangentially (µm)** xxxxtially: 54 (45-65) / 16 (14-20) rectangular-shaped
Cortex / Periderm / special characters	no extraxylary tissues preserved / growth rings very well preserved			

Table III.4: main anatomical and morphological data of *Arthropitys barthelii*.

Figure III.4: proposed reconstruction of *Arthropitys barthelii* by Frederic Spindler (Freiberg, Germany).

***Arthropitys buritiranensis* n. sp.**

(Plate III.15 and III.16)

Holotype: specimen K 5457.

Type locality: Buritirana Farm, Tocantins State, Parnaiba Basin, central-north Brazil.

Type stratum: Motuca Formation, Lower Permian.

Etymology: the specific name refers to the locality where this species was found, the Buritirana Farm.

Diagnosis according to the rules of the International Code of Botanical Nomenclature: These permineralized stems are different from other *Arthropitys* species because the branching system, composed of 8 to 11 branches at every node, disposed in line along the stem without secondary growth, and the presence of the scalariform secondary wall thickenings in the tracheids.

Description

Macroscopic stem characteristics – The holotype **K 5457** is represented by a principal stem (Plate III.15, 1) with an attached large branch and a stem fragment of a slightly lower region of the original plant (here designated as “lower stem fragment” (Plate III.16, 1). The principal stem is 50 cm long, girth at the base of 17.2 cm, slightly elliptical section of 35 x 42 mm, elliptical pith cavity section of 6 x 10 mm, pith/stem diameter ratio equal to 1:6.4, and secondary body divided into fascicular wedges and interfascicular rays (Plate III.15, 9). The internodes lengths range between 12-24 mm, average equal to 17 mm in a total of 16 measurements (Plate III.15, 1).

The lower stem fragment is 22 cm long, girth is 11.5 cm, 23 x 40 mm in diameter, elliptical pith cavity section of 8 x 12 mm and pith/stem diameter ratio equal to 1:3.7 (Plate III.16, 5). Internodes lengths range between 12-26 mm in a total of 10 measurements and in mean equal to 17 mm (Plate 7.16, 1).

The large branch attached to the main stem is 37 cm long, diameter of 20 mm, internodes lengths ranging between 6-18 mm, average equal to 10 mm in a total of 19 measurements (Plate 7.15, 1).

Branching system - This species presents 8 to 11 branches at every node, disposed in line from one node to the next (Plate 7.15, 1; Plate 7.16, 1, 2 and 3),

without secondary growth (Plate III. 15, 7; Plate III.16, 6). The branch stumps in the main stem are circular, with diameters between 3-6 mm. In the large branch, these scars present diameters between 2-4 mm. Well preserved slightly circular leaf scars (Plate III.16, 2 and 3).

Primary body - In the main stem, elliptical carinal canals present average sizes of 190 µm (170-200) radially and 122 µm (110-140) tangentially. The metaxylem cells are elliptical-shaped with average sizes of 103 µm (73-143) radially and 70 µm (52-86) tangentially (Plate III.15, 5 and 8).

Secondary body – In this species, the stem in cross section is divided into fascicular wedges and interfascicular rays visible throughout secondary body. In the holotype **K 5457**, the secondary body present 11-15 mm thick and at the margin of the pith cavity, 24 fascicular strands are recognized (Plate III.15, 9; Plate III.16, 5).

In the internal part of the secondary body, in cross section, fascicular wedges average 490 µm (420-600) in width with 15-20 cell files. Tracheids show square to rectangular cells of average 56 µm (30-80) radially and 40 µm (30-50) tangentially. The fascicular rays are composed of 1-3 parenchymatous cell files of 20-90 µm in width with rectangular cells on average 75 µm (70-90) radially and 40 µm (20-60) tangentially. Interfascicular rays average 176 µm (148-232) in width and are composed by 3-7 parenchymatous cell files with rectangular cells on average 124 µm (70-195) radially and 31 µm (10-50) tangentially (Plate III.15, 8).

In the middle part of the secondary body, in cross section, tracheids of the fascicular wedges are square to rectangular on average 57 µm (55-61) radially and 39 µm (33-45) tangentially. The fascicular rays are composed of 1-2 parenchymatous rectangular cells on average 76 µm (66-100) radially and 36 µm (27-50) tangentially. Interfascicular rays average 137 µm (115-160) in width and are composed by 5-8 parenchymatous cell files, with many pits on the walls (Plate III.15, 6).

In this part, the secondary body shows very evident growth rings and the tracheids become smaller. Curiously, the parenchymatous cells of the interfascicular rays do not change (Plate III.15, 6).

In the external part of the secondary body, in cross section, fascicular wedges average 1.91 mm (1.51-2.40) in width and interfascicular rays 163 µm (120-250) in width. Cells in this part are not preserved.

In radial section, tracheids in this permineralized stems present scalariform secondary wall thickenings (Plate III.15, 3). The fascicular wedges are organized in axial files, several millimeters long, on average 44 µm (33-58) radially, with simple scalariform thickenings, vertical distance between them of 6.5-7.5 µm, horizontal distance of 21-32 µm, some bifurcations and upright link bars (Plate III.15, 3). Fascicular rays present rectangular cells on average 71 µm (50-110) axially and 59 µm (30-120) radially and are higher than wide.

In tangential section, tracheids reach approximately 60% and parenchymatous cells 40% of the secondary body body (Plate III.15, 7). Tracheids are very long axially and average 41 µm (36-47) tangentially. The fascicular rays show width of 1-3 files, 3-90 cells in height and are composed of rectangular parenchymatous cells, higher than wide, on average 62 µm (40-110) axially and 45 µm (30-70) tangentially. Interfascicular rays are composed of rectangular cells on average 69 µm (30-110) axially and 57 µm (40-90) tangentially, running from node to node (Plate III.15, 4 and 7; Plate III.16, 4).

Other elements - Phloem, periderm and cortical tissues are not preserved.

Comparisons

The studied specimens are different from *Arthropitys gigas* (Brongniart) Renault, 1896, *A. rochei* Renault, 1896, and *A. porosa* Renault, 1896, because the permineralized species studied here present scalariform secondary wall thickenings and these mentioned species present three kinds of thickenings in the tracheids;

The studied specimens differ from *Arthropitys major* (Weiss) Renault, 1896 [apud Boureau (1964); Wang. et al. (2006)], *A. kansana* Andrews, 1952, *A. illinoensis* Anderson, 1954, *A. cacundensis* Mussa, 1984 (in Coimbra & Mussa, 1984), and *A. sterzelii* Rößler & Noll, 2010, because the sphenophytes here present scalariform secondary wall thickenings and the species above present circular reticulate thickenings in the tacheid walls;

Differ from Hirmer and Knoell´species. The calamitaleans from Tocantins present a secondary body well developed whereas *Arthropitys bistriatoides* Hirmer

& Knoell (in Knoell, 1935), *A. herbacea* Hirmer & Knoell (in Knoell, 1935), and *A. jongmansi* Himer, 1927 (apud Knoell, 1935), present a secondary body poorly developed. Also, these mentioned species do no present the kind of secondary wall thickenings in the tracheids, difficulting the accurate comparisons. Is different from *A. hirmeri* Knoell, 1935, because the species studied here present fascicular wedges and interfascicular rays whereas the Hirmer & Knoell's species only fascicular wedges in the secondary body;

Arthropitys renaultii Boureau, 1964, and *A. approximat**a*** (Schlotheim) Renault, 1896 [apud Andrews (1952); Boureau (1964)] do not present the kind of thickenings, difficulting the comparison with the species here;

This species from Tocantins is similar to *Arthropitys bistriata* (Cotta) Goeppert *emend*. Rößler, Feng & Noll, 2012, *A. felixi* Hirmer & Knoell (in Knoell, 1935), *A. communis* (Binney) Renault, 1896, *A. lineata* Renault, 1896, *A. gallica* Renault, 1896 [apud Andrews (1952); Boureau (1964); Wang et al. (2003)], *A. versifoveata* Anderson, 1954, *A. deltoides* Cichan & Taylor, 1983, *A. junlianensis* Wang, Hilton, Li & Galtier, 2003, *A. yunnanensis* (Tian & Gu) *ex* Wang, Hilton, Galtier & Tian, 2006, and *A. ezonata* (Goeppert) *emend.* Rößler & Noll, 2006, in relation to scalariform secondary wall thickenings of the tracheids, but present 8-11 branches per node, without secondary growth, differently from all species above mentioned.

Considering the presented comparisons, the studied specimens must be classified in a new species, here designated as ***Arthropitys buritiranensis*** and Table III.5 presents the main anatomical and morphological data of this species.

Plate III.15: *Arthropitys buritiranensis*

1: general view of the holotype **K 5457** showing a large branch attached to the main stem.

2: general view of a stem fragment of the same specimen as that of figure 1, but in a slightly lower position of the original plant, showing branch scars (arrows).

3: radial section of the holotype **K 5457** showing scalariform secondary wall thickenings in the tracheids.

4: tangential section of the holotype **K 5457** showing a branch trace (arrow), sections of nodal lines (red lines) and secondary body.

5: magnification of 8 showing carinal canal, metaxylem cells (arrow) and fascicular wedges in the pith cavity periphery.

6: cross section of the holotype **K 5457** showing fascicular wedges (fw), interfascicular rays (ir) and boundaries between growth rings (arrows).

7: tangential section of the holotype **K 5457** showing fascicular wedges (fw), interfascicular rays (ir) and a branch trace without secondary growth in the section of a nodal line (arrow).

8: cross section of the holotype **K 5457** showing carinal canal, metaxylem cells (arrow) and proximal fascicular wedge (fw) and interfascicular rays (ir).

9: cross section of the main stem of the holotype **K 5457** showing pith cavity and secondary body.

PLATE III.15

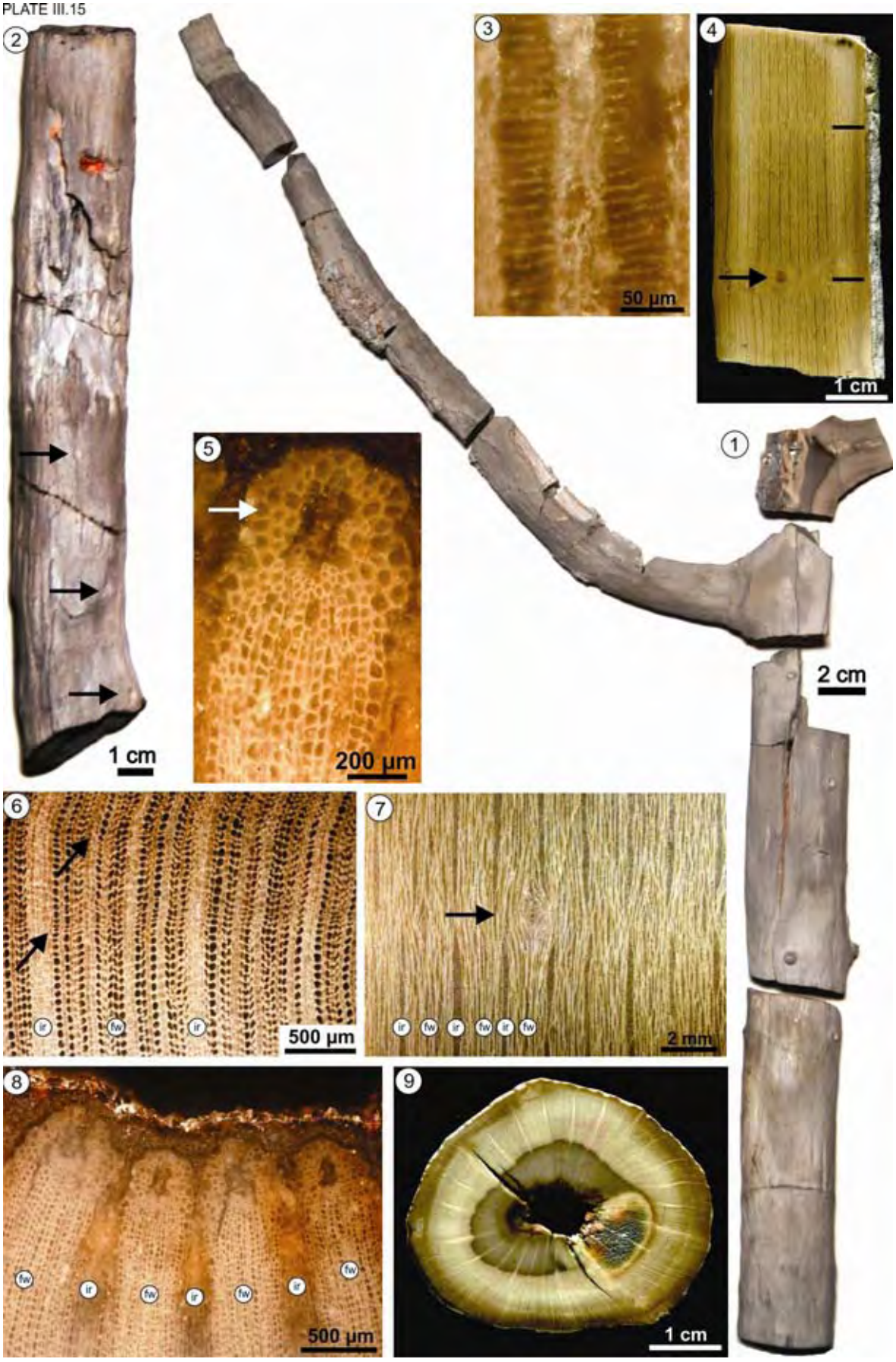
2
3
50 µm
4
1 cm
1
2 cm
5
200 µm
1 cm
6
ir
fw
ir
500 µm
7
ir
fw
ir
fw
ir
fw
2 mm
8
fw
ir
fw
ir
fw
ir
fw
500 µm
9
1 cm

Plate III.16: *Arthropitys buritiranensis*

1: detail of main stem of *A. buritiranensis* showing the branch scars (arrows).

2: general view of the branch of *A. buritiranensis* showing branch traces (long arrows) and leaf traces (short arrows).

3: general view of the branch of *A. buritiranensis* showing the branch scars (larger arrows) and leaf traces (smaller arrows).

4: tangential section of the holotype **K 5457** showing nodal line (red lines) and leave scars (arrows).

5: cross section of the lower part of the holotype **K 5457** showing branch traces extended from the pith cavity until the stem surface (arrows).

6: tangential section of the holotype **K 5457** showing details of fascicular wedges, interfascicular rays and a branch trace without secondary growth (in the center).

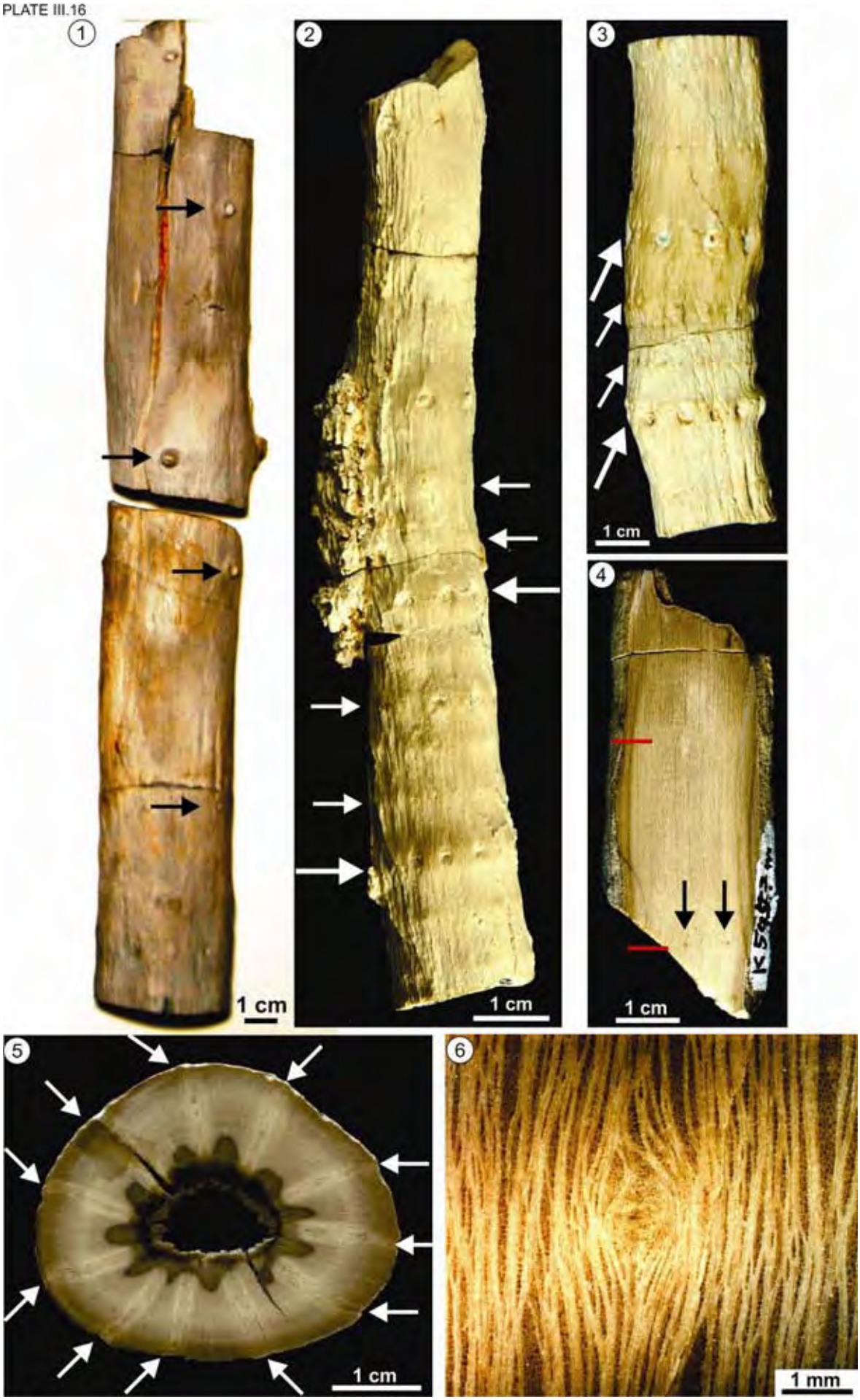
PLATE III.16
1
1 cm
2
1 cm
3
1 cm
4
1 cm
5
1 cm
6
1 mm

Taxon	Locality / Stratigraphy	Collection
Arthropitys buritiranensis	Buritirana Farm, Tocantins State, central-north Brazil / Early Permian	MfNC / K 5457 (holotype)

Part of the plant	Length	Girth	Diameter stem (S)	Diameter pith (P)	P/S ratio	Wood
Main stem Lower stem Branch	50 cm 22 cm 37 cm	17.2 cm at base 11.5 cm 6.3 cm	35 x 42 mm at base 23 x 40 mm 20 mm	6 x 10 mm at base 8 x 12 mm	1:6.4 at base 1:3.7	13-15 mm 11-15 mm secondary body divided in distinct wedges fascicle width: initially: 490 µm (420-600), distally: 1.91 mm (1.51-2.40)

Morphology/Branching	Type	Branch traces	Leaf traces	Root traces
primary/secondary growth	without secondary growth	8-11 per whorl, departing from leaf traces which do not have whorls underneath (branch traces at the leaf traces level) disposed in line along the stem, diameter 3 to 6 mm	under branch traces	not preserved

Internode length	main stem: 17 mm (min. 12, max. 24) of 16 measurements; secondary stem: 17 mm (min., max. 26) of 10 measurements; shoot: 10 mm (min. 6, max. 18) of 19 measurements

Primary tissues	Vascular strands number	Carinal canal radially / tangentially (µm)	Px tracheids/tyloses	Mx tracheids radially / tangentially (µm)
	24 strands	190 (170-200) / 122 (110-140) elliptical-shaped	not preserved	103 (73-143) / 70 (52-86) elliptical-shaped

Secondary tissues				
Tracheids (cross view) radially / tangentially (µm), files per fascicle initially: 56 (30-80) / 40 (30-50), 15-20 files medially: 57 (55-61) / 39 (33-45), 26 files distally: not preserved	Thickening (radial view) scalariform: distance 6.5-7.5 µm vertically and 21-32 µm horizontally; some bifurcations and upright link bars	Outline rectangular to square		
Interfasc. rays (cross view) number of files / width made of 3-8 parenchym. files initially: 176 µm (148-232) distally: 163 µm (120-250) running from node to node	Cells (radial view) axially / radially (µm) not visible	Cells (tangential view) axially / tangentially (µm) 69 (30-110) / 57 (40-90) rectangular-shaped higher than wide	Cells (cross view) radially / tangentially (µm) initially: 124 (70-195) / 31 (10-50) distally: not preserved rectangular-shaped	
Fascicular rays (cross view) number files / width µm made of 1-3 files 20-90 µm	Cells (radial view) axially / radially (µm) 71 (50-110) / 59 (30-120) rectangular-shaped, higher than wide	Cells (tangential view) axially / tangentially (µm) 62 (40-110) / 45 (30-70) rectangular-shaped 3-90 files in height, higher than wide	Cells (cross view) radially / tangentially (µm) initially: 75 (70-90) / 40 (20-60) medially: 76 (66-100) / 36 (27-50) distally: not preserved rectangular-shaped	

Cortex / Periderm / special characters	no extraxylary tissues preserved / growth rings weak

Table III.5: main anatomical and morphological data of *Arthropitys buritiranensis*.

To evaluate the new five species of the permineralized calamitaleans from Tocantins, the Table III.6 shows a comparison between them and the type-species of the genus, *Arthropitys bistriata.*

Arthropitys isoramis is quite similar to *A. versifoveata* Anderson, 1954, and *A. tabebuiensis* to *A. bistriata* Röβler, Feng & Noll, 2012. All the other species studied are relatively different from the other described species, mainly because of the branching system and the small pith cavity.

	Arthropitys bistriata	*Arthropitys isoramis*	*Arthropitys tabebuiensis*	*Arthropitys tocantinensis*	*Arthropitys barthelii*	*Arthropitys buritiranensis*
Fascicular wedges (cross view)						
Width	increase radially	increase radially	increase substantially radially	increase in the inner part and after become indistinct	increase in the inner part and after become indistinct	increase substantially radially
Number of cell rows	10-25 rows	25-30 rows	16-33 rows	25-30 rows	25-30 rows	15-26 rows
Secondary wall thickenings of the tracheids	scalariform and very rare reticulated	scalariform and circular reticulated	circular reticulated	scalariform and rare circular reticulated (K 5107)	scalariform	scalariform
Fascicular rays						
Number rows in cross view	1-2, rarely 3 rows	1-3 rows	1-3 rows	1-3 rows	1-2 rows	1-3 rows
Heigth in tangential view		more than 30 cells	4-5 and common 30-40 cells	10 to more than 40 cells		3-90 cells
Interfascicular rays (cross view)						
Width	decrease radially	increase sligthly radially	constant radially	constant in the inner part an after they become indistinct	increase slightly in the inner part an after they become indistinct	constant radially
Number of cell rows	3-8 rows	9-12 rows	4-9 rows	3-7 rows	3-5 rows	3-8 rows
Throughout secondary body	visible throughout secondary body	visible throughout secondary body	visible throughout secondary body	visible only at the pith periphery of secondary body	visible only at the pith periphery of secondary body	Visible throughout secondary body
Tangential view						
% tracheids	70 %	50 %	50 %	65 %	40 %	60 %
% parenchymatous cells	30%	50%	50%	35%	60%	40%
Branching system						
Number of branches	9-16 per node	4 in every node, rarely 3	8-15 per node	3-7 per node	1-15 per node	8-11 per node
Disposition on the stem	in line	alternate	in line	in line	randomly	in line
Growth type	without secondary growth	without secondary growth	with and without secondary growth	with and without secondary growth	without secondary growth	without secondary growth

Table III.6: comparison between studied sphenophytes from Tocantins, central-north Brazil and type-species *Arthropitys bistriata* Rößler, Feng & Noll, 2012.

5. Implications of Brazilian sphenophytes

Up until now, the only *Arthropitys* species described in Brazil had been the *A. cacundensis* Mussa, 1984 (in Coimbra & Mussa, 1984). With the present study, new elements are added for improvement of the chronostratigraphy, paleoecology and paleobiogeography.

5.1. Chronostratigraphic considerations

The plant bearing beds in Tocantins, southern Parnaíba Basin, belong to the Motuca Formation of the Balsas Group, which is divided into the Piauí, Pedra de Fogo, Motuca and Sambaíba formations (Góes & Feijó (1994). Palynologic analyses carried out by Souza et al. (2010) suggested a very late Moscovian age (~306 Ma) for the Piauí Formation, that is, the end of the Late Carboniferous. Vertebrates and palynomorphs in the Pedra de Fogo Formation cannot be younger than Middle Permian (see Dias-Brito et al., 2007, 2009). The genus *Grammatopteris* identified in the study area (Röβler & Galtier, 2002a), was previously recorded in very Early Permian deposits in Germany and France. The eolian deposits of the Sambaíba Formations are sterile in fossils.

The analyzed fossils, although assigned to new species and obviously considered distinct from other species in the literature, possibly had a relative phylogenetic proximity to some North-American and German species.

Arthropitys isomaris is quite similar to *Arthropitys versifoveata* Anderson, 1954, from the upper part of the Cherokee Shale in the Breathitt Formation, Kansas State, and interpreted as lower Middle Pennsylvanian (Eble & Greb, 1997; Milliken, 2001). They have the same secondary wall thickening of the tracheids, an equivalent number of branches per node and the same alternate arrange of braches per node. *A. isoramis* presents branches with primary growth only, whereas this information is not available for *A. versifoveata*.

Arthropitys tabebuiensis is quite similar to *Arthropitys bistriata* (Cotta) Goeppert *emend*. Röβler, Feng & Noll, 2012 of the Leukesdorf Formation, in Chemnitz, Germany, of Asselian-Sakmarian age, Early Permian (Rößler & Noll, 2006, 2010; Matysová et al., 2010). They share similarities in the secondary body and in the number and attachment organization of the branches. However, they differ in the tracheid thickenings and in the secondary growth only observed in branches of the studied species.

In addition to the species studied herein, *Arthropitys cacundensis* Mussa (in Coimbra & Mussa, 1984) probably collected in the same area or in great proximity, originally assigned to the Pedra de Fogo Formation, shows great similarities to *Arthropitys sterzelii* Rößler & Noll, 2010 of the Asselian-Sakmarian Leukesdorf Formation, Chemnitz: both have circular reticulate tracheid thickenings, a low number of branches per node (2 to 3 in the Brazilian species and 2 to 5 in the German species, but depending on the ontogenetic stage of the stem), an alternate disposition of the branches in the consecutive nodes, only lacking information in respect to the presence of secondary growth in the branches of the Brazilian species. According to the similarities, these species might belong to a single natural species, so that *A. cacundensis* would represent a more basal part of a stem than *A. sterzelli.*

In conclusion, the sphenophytes of the southern Parnaíba Basin apparently corroborate the possible Early Permian age of the deposits suggested by the record of *Grammatopteris*. A possible diachronism between the compared elements of the northern Gondwana and Euramerican paleofloras cannot be completely ruled out, considering the high control of the climate, but up to now other chronostratigraphic data are almost absent.

5.2. Paleophytogeography considerations

So far, the Parnaíba Basin has presented 35 species distributed into 22 genera and 10 endemic genera, representing an endemic genera degree of 45.5%.

Fernia Tavares, 2011, *Tocantinorachis* Tavares, 2011, *Dernbachia,* Rößler & Galtier, 2002b, and *Araguainorachis* Mussa (in Mussa & Coimbra, 1987) are endemic genera in the fern group; *Carolinapitys* Mussa (in Coimbra & Mussa, 1987), *Cyclomedulloxylon* Mussa (in Mussa & Coimbra, 1987), *Teresinoxylon* Mussa (in Caldas et al., 1989), *Parnaiboxylon* Kurzawe et al., 2013a, *Ductoabietoxylon* Kurzawe et al., 2013a, and *Scleroabietoxylon* Kurzawe et al., 2013a, represent the endemic genera within gymnosperms. No sphenophytes genus is endemic in the Parnaíba Basin.

Although they have a high level of generic endemism, 8 genera are not endemic, and some comparisons could be made to help in the floristic affiliation of the Parnaíba Basin during the Late Paleozoic [*Psaronius* Brongniart, 1972,

Pelourde, 1914, Herbst, 1985, Rößler & Noll, 2002, Tavares, 2011, *Pecopteris* Tavares, 2011, *Arthropitys* Mussa (in Coimbra & Mussa, 1984), and *Sphenophyllum* Rößler & Noll, 2002, are cosmopolitan, found in the Gondwana, Euroamerican and Cathaysia Provinces].

Bothriopteris Rößler & Galtier, 2003, and *Amyelon* Mussa (in Coimbra & Mussa, 1984), are found in the Euramerican and Cathaysia Provinces.

Grammatopteris Rößler & Galtier, 2002, and *Cydadoxylon* Mussa (in Mussa & Coimbra, 1987) are found in the Euramerican Province only.

Tietea Herbst, 1986, 1992, Rößler & Noll, 2002, Tavares, 2011, *Damudoxylon* Kurzawe et al., 2013b, *Taeniopteris* Kurzawe et al., 2013b, and *Kaokoxylon* Kurzawe et al., 2013a, are found in the Gondwana Province only.

Thus, according to the genera below, notice that four of them are exclusively from the Gondwana Province (*Tietea*, *Damudoxylon*, *Taeniopteris* and *Kaokoxylon*), representing 50% of the total genera found in the Parnaíba Basin; two genera are exclusively from the Euramerican Province (*Grammatopteris* and *Cydadoxylon*), representing 25% of the total genera; *Bothriopteris* and *Amyelon* are both found in the Euramerican and Cathaysia Provinces, representing 25% of the total.

However, comparing the genera from the Northern Hemisphere (Euramerican and Cathaysia Provinces) versus the genera from the Southern Hemisphere (the Gondwana Province), the following is noticed: 50% of the genera are from the former (*Grammatopteris*, *Cydadoxylon Bothriopteris* and *Amyelon*), whereas 50% are from the latter (*Tietea*, *Damudoxylon*, *Taeniopteris* and *Kaokoxylon*).

Coimbra & Mussa (1984) and Mussa & Coimbra (1987) advocated a greater contribution of the Northern Hemisphere in the flora of the Parnaíba Basin to the disadvantage of the Southern Hemisphere. However, with these new data, 50% of the genera are from the former hemisphere whereas the other 50% are from the latter, contradicting the old argument of the authors cited above.

5.3. Morphological considerations about the attached root in the holotype of *Arthropitys isoramis*

The holotype of *Arthropitys isoramis* (**TOF 187**) from the Parnaiba Basin is the first record of a permineralized sphenophyte that presents root organically

jointed to stem and shows aspect totally different from the classical reconstructions of *Arthropitys* in the literature (Hirmer, 1927; Eggert, 1962) (Figure III.5, 1).

It was previously assumed that all fossil horsetails were similar to *Equisetum*, the only living genus of Sphenopsida, which has a horizontal rhizome fixed to the soil a few centimeters below the surface. Therefore, these reconstructions considered that the stems emerged from a horizontal rhizome and that the very proximal part of the stems was conical. Some fossil rhizomes and stems bear, in fact, a similar structure (DiMichele & Falcon-Lang, 2012). However, Rößler & Noll (2006) and Rößler et al. (2012) already commented that the Palaeozoic sphenophytes probably were much more diversified than in the traditional interpretation.

In the studied root, the vertical axes possibly provided water supply and the more oblique axes (30-35^{o}) possibly had an anchoring function to unstable substrate. Moreover, a horizontal root system is applied to the tree with a horizontal canopy, biomechanically necessary to keep the stem straight, and the sphenophytes don't have a canopy as in gymnosperms and angiosperms. Unfortunately, this specimen doesn't present cell preservation, impossibling the affiliation of this unprecedent structure with the root genera even described in the literature.

This root presents morphology much more consistent with the large height and weight of many Palaeozoic stems than the classical reconstructions with horizontal root, which only may support small stems. The aspects of this root system resemble those plants that live in mangroves, but there are not elements to close this opinion.

This new consideration does not discard totally the interpretation of horizontal rhizomes in the case of small stems with relatively large pith cavity and thin woody cylinders, usually preserved as molds/casts, like the species *Calamites* (*Stylocalamites*) *suckowii* ilustrated by DiMichele & Falcon-Lang (2012).

5.4. Morphological considerations about the root system in the specimens K 5258 and TOF 79

In contrast to specimen **TOF 187**, which belongs to *Arthropitys isoramis,* and presents organically-conected stem root*,* two other roots were found in the

TFTNM area, although they have no connection to their respective stems. Again, these structures do not present silmilarities with classical reconstructions to *Arthopitys* genus (Figure III.5, 1).

The specimen **K 5258** (Figure III.5, 2 to 5) presents cell preservation and probably represents the basal part of a stem from which some adventitious roots emerge (Figure III.5, 2). A cross sectional analysis shows this specimen has an epliptical shape of 47 x 27 cm, a small pith 16 mm mm in diameter and elliptically-shaped adventitious roots between 7.4 and 10 cm of diameter.

When cross-sectioned, the pith region shows primary sligtly circular-shaped xylem cells of 68 µm in diameter (37-105) (Figure III.5, 3). It is a little difficult to recognize parenchymatous cells and the tracheids due to the weak segmentation of this body. Parenchymatous cells are rectangular-shaped reaching 70 µm (61-93) radially and 51 µm (48-59) tangentially (Figure III.5, 4). The tracheids reach 54 µm (32-68) radially and 39 µm (24-51) tangentially. A radial section anlaysis shows scalariform secondary wall thickenings, with a vertical 5-9 µm distance between thickenings (Figure III.5, 5).

The petrified calamitaleans with cell preservation are represented by four genera: *Astromyelon*, Williamson, 1878, *Myriophylloides*, Hick & Cash, 1881, *Asthenomyelon*, Leistikow, 1962, and Zimmermannioxylon, Leistikow, 1962. Because of its anatomical features, this specimen can be related to *Astromyelon* type Williamson, 1878, and the kind of thickenings can associate this specimen with *Arthropitys tocantinensis* or *A. barthelii*.

The other specimen found in the TFTNM area is **TOF 79** (Figure III.6), and it probably represents a fragment of the stem-root connection. The superior view presents an elliptical outline with a collapsed pith cavity (Figure III.6, 3). In a polished surface, it presents a pith cavity sourronded by adventitious roots (Figure III.6, 4, arrows).

Four root stumps are observed in this specimen and they are totally abraded by the fluvial system of the studied area (Figure III.6, 1, arrows; Figure III.6, 2, large arrows). In the external surface, it is possible to recognize weak nodal lines (Figure III.6, 2).

TOF 79 shows no cell preservation, but it represents an important fragment to visualize the root system in Permian calamitaleans.

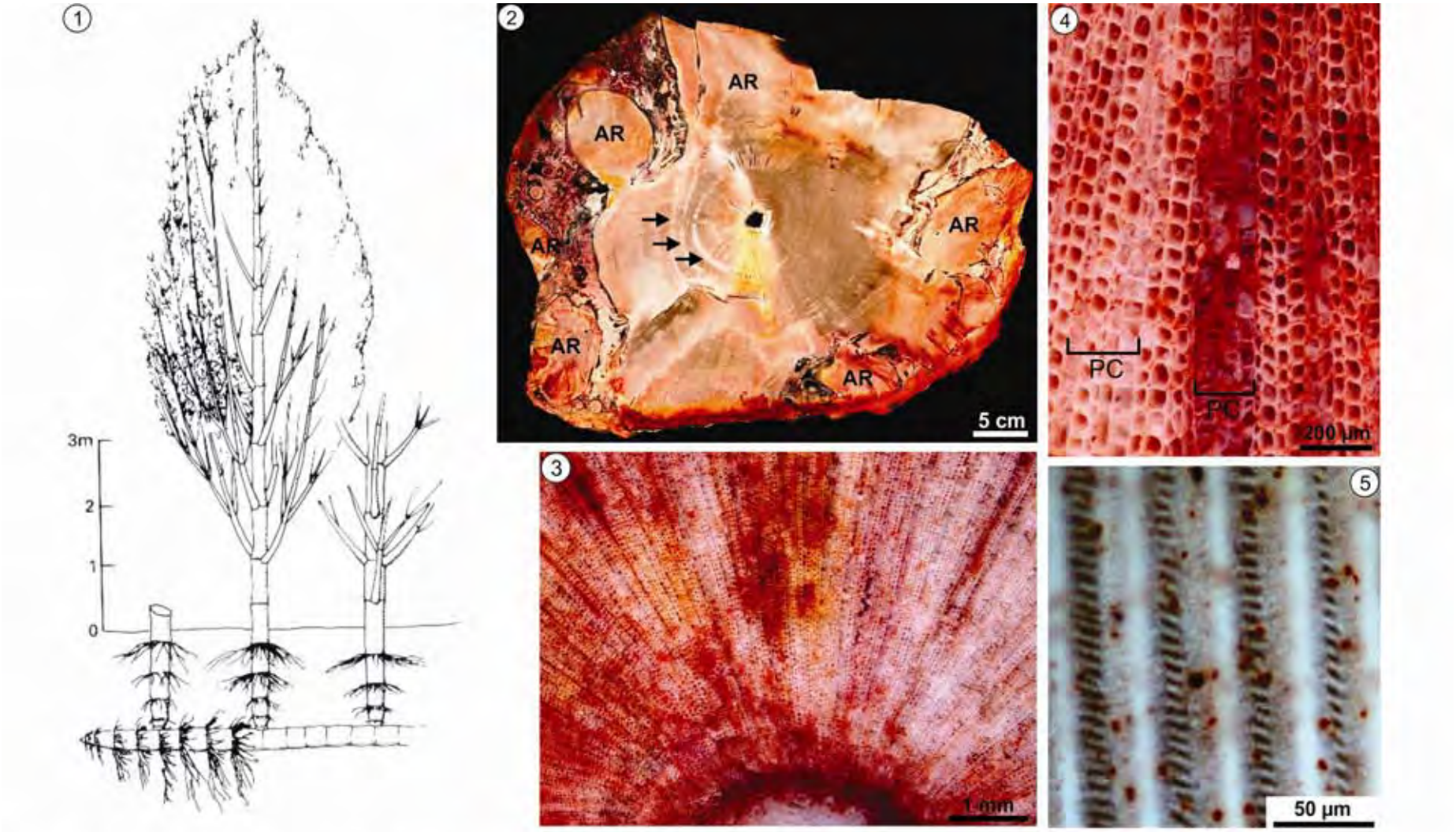

Figure III.5. 1: classical reconstruction of the root-stem system in permineralized sphenophytes (Boureau, 1964); **2**: distal portion of the specimen **K 5258** showing the adventitious roots (AR) and the growth rings (arrows); **3**: cell details in the pith cavity of the specimen **K 5258**; **4**: magnification of 3, showing parenchymatous cells (PC) and the square-shaped tracheids; **5**: scalariform thickenings in specimen **K 5258**, that could associate it to *Arthropitys tocantinensis* or *A. barthelii*.

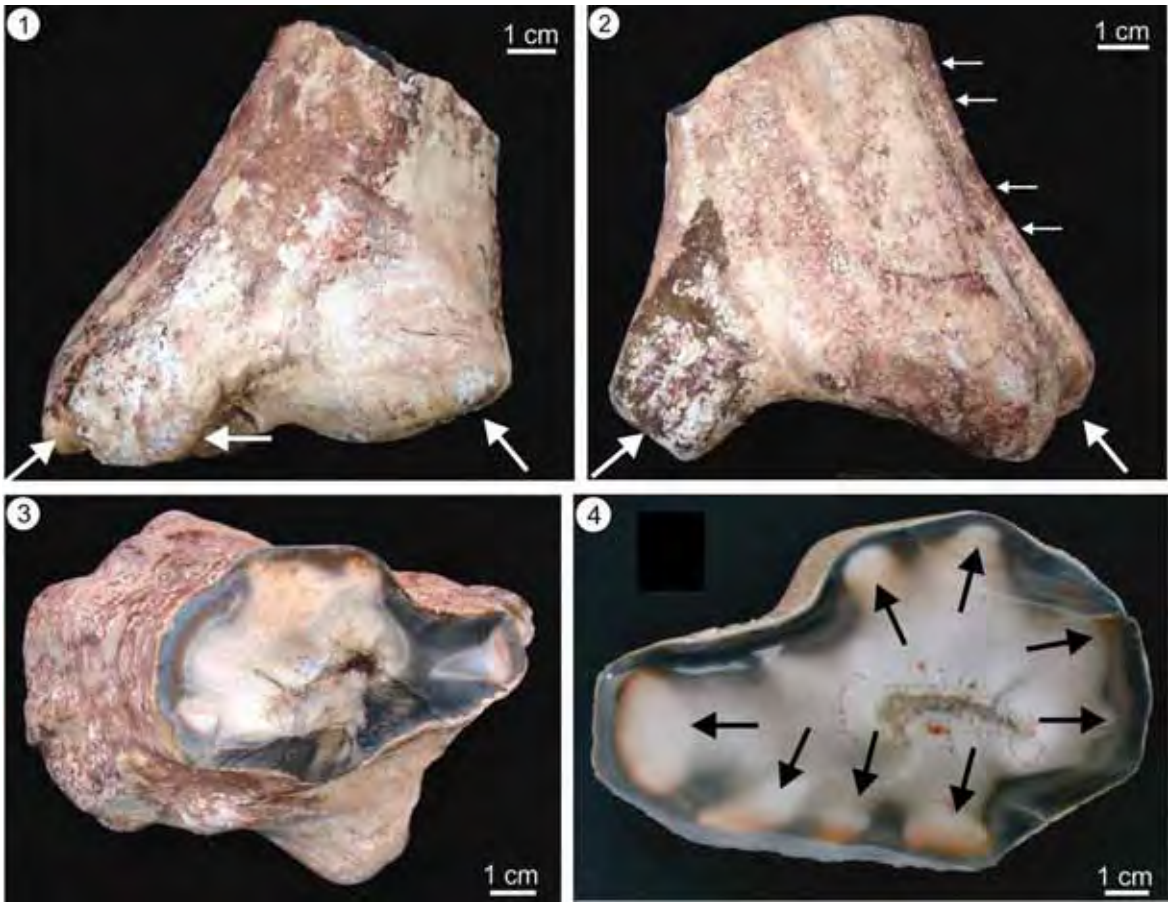

Figure III.6: TOF 79. 1: lateral view with arrows indicating root stumps; **2**: lateral view with small arrows indicating the nodal lines and large arrows the root stumps; **3**: superior view before cut showing the collapsed pith cavity; **4**: polished transversal section showing the collapsed pith cavity and the departure of root stumps (arrows).

5.5. Environmental inferences

During the Eopermian, the Parnaíba Basin was positioned close to the 30°S latitude, the Pangea arid belt, and it was seasonally marked by the monsoon climate (Crowley, 1994; Parrish, 1995; Rees et al., 1999; Gibbs et al., 2002; DiMichele et al., 2006; Roescher & Schneider, 2006; Schneider et al., 2006; Poulsen et al., 2007), with surface temperatures between 15 and 20°C and average rainfall between 0 and 4 mm/day (Gibbs et al., 2002), presenting desert to humid temperate bioma (Rees et al., 1999).

The sphenohytes studied here present few xeromorphic structures. *Arthropitys tocantinensis* have tylosis in one of their carinal canals (Plate III.11, 3). These parenchimatous structures develop internally to the tracheal vessels to avoid either pathogen attacks or collpase at water scarcity moments during arid times.

Plants that inhabit arid climates have reduced fronds, deep stomas, thorn and/or hair at an attempt to retain water in the leaves (Kerp, 1990; Algeo & Scheckler, 1998). Pinnules associated with the genera *Pecopteris* and *Fernia* found by Tavares el al. (2008) and Tavares (2012) in the TFTNM area are quite curved to the abaxial side in order to protect the synangia, representing evident xeromorphic adaptation. *Annularia* and *Asterophyllites* are the two kinds on foliar most commonly associated with *Arthropitys*. *Arthropitys buritiraensis* shows evident foliar traces (Plate III. 16, 2-4), although no stem-related leaf has been found yet.

On the other hand, growth rings are closely related to environmental seasonal changes (Creber & Francis, 1999). In temperate regions, they can mark seasons of the year; in the tropics, they indicate environmental changes, such as prolonged rainfall periods, among other climate factors. Growth rings are formed by thin-walled cells and big lumens, constituting spring log, followed by thick-walled cells and smaller lumens, contituting winter log, the moment at which cambial activity is lower (Salgado-Labouriau, 1994; Costa et al., 2006).

Arthropitys barthelii and *A. tocantinensis* show highly evident growth rings (Plate III.11, 1- 2; Plate III.12, 1, 3 and 4). If on the one hand they do show proeminent xeromorphic structes, through the gorwth rings, these two species corroborate the possible seasonality in the basin during the Eopermian. The permineralization fossilization process itself suggests wet and dry season alternation, in order to obtain silicate minerals and precipitation on vegetal tissues, respectively.

5.6. Inferences about Brazilian calamitaleans habits

As for paleoenvironment, a fluvial environment with braided canals where the preterite flora inhabited (Rößler, 2006; Dias-Brito et al., 2007). However, the esphenophytes studied here have stem constitutions quite different among one another. *Arthropitys isoramis* have adventitious roots at a 30 to 35° angle to the stem as well as parallel adventitious roots to it, which could anchor the plant in this habitat.

Moreover, it has relatively large pith cavity compared to the stem diameter. Therefore, the stem constitution and its adventitious roots at an angle to the stem could enable this species to inhabit river banks, where sediment is uncosolidated.

For *Arthropitys tabebuiensis* and *A. buritiranensis*, even lacking its roots, the same habitat can be thought, since they have stem constitution similar to *A. isoramis*, that is, less succulent stem.

Arthropitys tocantinensis and A. barthelii, species with quite reduced pith cavity, and consequently more solid stems, might have inhabited areas a little farther from bodies of water, since their more succulent and heavier stems enabled them to inhabit unconsolidated subtstrates such as the river banks. So far, only the roots shown in Figures III.5 and III.6 have been found. A fact that confirms the fluvial environment in the Motuca Formation is the abraded aspect in the extreme basis of specimen **K 5455** which belongs to *A. tocantinensis*, an already observed aspect in many samples of *Tietea* and *Psaronius* (Caprets, 2010), although it has not been observed for the sphenophyte group.

5.7. Comparisons with the *Calamites* genus

Arthropitys and *Calamites* are generated by the same plant, the former as a permineralized stem; the latter, according to the traditional viewpoint, as a medullary cast, allowing for some occasional comparison. The genus *Calamites* has some subgenera depending on way the ribs and the furrows are displayed between nodes, the branching system and their aspect (Boureau, 1964; Stewart & Rothwell, 1993; Taylor et al., 2009).

The subgenus *Diplocalamites* has two or three branches per node, whereas the *Crucicalamites* presents from three to six branches per node, both with an alternate pattern between nodes. The *Arthropitys isoramis* n. sp. has four, and rarely, three branches per node, an intermediate number between the above-mentioned subgenus. *Arthropitys tocantinensis* n. sp. has from three to seven branches per node, making it more closely related to the *Crucicalamites*. *Arthropitys tabebuiensis* n. sp., *A. barthelii* n. sp. and *A. buritiranensis* n. sp. have a number of branches per node which do not relate them to any of the *Calamites* subgenera. Nevertheless, DiMichele & Falcon-Lang's recent work (2012) brings a very important discussion about this subject.

According to these authors, a great part of the *Calamites* does not represent medullary casts, represent the external casts: later on, with the plant tissue degradation, a new load of sediments would fill the space previously taken by the plant, thus forming an external cast, not a medullary cast. The authors state

that there are true medullary casts, although they would be quite rare. Therefore, if this hypothesis is accepted, a review of the genus *Calamites* is needed, which might increase the chances of comparing the sphenophytes in the Paraná Basin, an area in which the sphenophytes are preserved as “medullary casts’’.

IV. Conclusões

- Pela primeira vez são descritos caules de esfenófitas permineralizados por sílica do Monumento Natural das Árvores Fossilizadas do Tocantins (MNAFTO), entre Araguaína e Filadélfia (TO), provenientes da Formação Motuca, Bacia do Parnaíba, Eopermiano. Estes caules são secundários em relação à enorme quantidade de caules de samambaias arborescentes, porém estão muito bem preservados tridimensional e anatomicamente, ultrapassando, às vezes, 2 m de comprimento. Todos os caules pertencem ao órgão-gênero *Arthropitys*, muito abundante na Província Euramericana e também encontrados na Província Cataísia;

- As espécies de *Arthropitys* foram por décadas descritas apenas por suas características anatômicas. A partir dos trabalhos de RöβLer & Noll (2006, 2010), características dos ramos, como sua disposição ao longo do caule e a presença/ausência de corpo secundário, começou a figurar como um caráter importante na delimitação das espécies. Dando continuidade a essa idéia, este trabalho formaliza um *ranking* de critérios anatômicos e morfológicos para classificar as espécies e apresenta um catálogo crítico sob este ponto de vista para todas as espécies descritas do gênero. Esse sinaliza que a diversidade de espécies pode ter sido superestimada;

- *Arthropitys cacundensis* descrita por Mussa (in Coimbra & Mussa, 1984) foi uma espécie analisada cuidadosamente no catálogo crítico: era a única espécie registrada não só na Bacia do Parnaíba como no Gondwana Ocidental. Há poucas informações anatômicas e morfológicas no trabalho original, mas a espécie apresenta grandes semelhanças a *Arthropitys sterzelli,* proveniente da cidade de Chemnitz, Alemanha: mesmo tipo de espessamento dos traqueídes e mesma composição do corpo secundário. Assim, de acordo com o padrão de saída dos ramos, admite-se que *Arthropitys cacundensis* coaduna perfeitamente com a porção basal de *Arthropitys sterzelli*. Portanto, faz-se necessário sua revisão;

- *Arthropitys isoramis* n. sp. apresenta feixes fasciculares e interfasciculares que aumentam de largura radialmente, sistema de ramos composto por quatro e mais raramente três ramos por nó, dispostos de modo alterno entre os sucessivos nós e sem crescimento secundário; os traqueídes apresentam espessamento

escalariforme e raramente reticulado circular em suas paredes radiais. Seu holótipo (**TOF 187**) possui raiz preservada, o que possibilitou, também pela primeira vez, descrever a morfologia do sistema radicular no gênero *Arthopitys.* Esse espécimen apresenta três raízes praticamente paralelas ao caule e outros em porções mais superiores dispostos de modo oblíquo, cuja morfologia é muito mais condizente com a altura e diâmetro alcançado por estes vegetais, em detrimento da reconstrução tradicionalmente aceita para o gênero, fortemente baseada em *Equisetum*, o único gênero vivente dentro do grupo das esfenófitas;

- *Arthropitys tabebuiensis* n. sp. apresenta feixes interfasciculares bastante estreitos em relação aos feixes fasciculares e ambos são visíveis por todo corpo secundário. O sistema de ramos é caracterizado por oito a 15 ramos por nó, dispostos em linha ao longo do caule e não possuem crescimento secundário. Os traqueídes apresentam espessamento reticulado circular em suas paredes radiais;

- *Arthropitys tocantinensis* n. sp.*,* apresenta feixes fasciculares mais largos na região da medula, feixes interfasciculares com largura constante pelo corpo secundário, três a sete ramos por nó, dispostos alinhadamente pelo caule, com e sem crescimento secundário. Os traqueídes apresentam espessamento escalariforme e raramente reticulado circular em suas paredes radiais;

- *Arthropitys barthelii* n. sp. apresenta feixes fasciculares que aumentam de largura radialmente e os feixes interfasciculares apresentam pequena largura na região medular e tornam-se indistintos em direção ao córtex. O sistema de ramos é caracterizado por um a 15 ramos por nó, dispostos aleatoriamente pelo caule e sem crescimento secundário. Os traqueídes apresentam espessamento escalariforme em suas paredes radiais;

- *Arthropitys buritiranensis* n. sp. é caracterizado por medula de tamanho intermediário em relação às outras espécies. Os feixes fasciculares aumentam de largura e os feixes interfasciculares diminuem de largura radialmente, visíveis até a metade do corpo secundário e indistintos a partir deste ponto até o cortex. O sistema de ramos é caracterizado por oito a 11 ramos por nó, dispostos em linha ao longo do caule e não apresentam crescimento secundário. Os traqueídes possum espessamento escalariforme em suas paredes radiais;

- Embora as espécies descritas neste trabalho sejam espécies novas, guardam semelhanças com espécies da Província Euramericana. *Arthropitys*

isoramis n. sp é bastante semelhante a *Arthropitys versifoveata* de Illinois, EUA; *Arthropitys tabebuiensis* n. sp. assemelha-se a *Arthropitys bistriata* de Chemnitz, Alemanha; *Arthropitys tocantinenses* n. sp. e *Arthropitys barthelli* n. sp. assemelham-se a *Arthropitys ezonata,* também proveniente da cidade de Chemnitz. Assim, por semelhanças anatômicas e morfológicas, a parte basal da Formação Motuca foi posicionada no intervalo Asseliano-Sakmariano, Eopermiano;

- Muitas espécies de *Arthropitys* da Euramérica estão associadas a depósitos de carvão, tendo ocupado áreas provavelmente úmidas às margens de pântanos. No caso das espécies de Tocantins, as condições ambientais e climáticas eram bastante diferentes, dominados por um sistema fluvial com estações secas bem marcadas e clima monçônico. A presença de tiloses nos canais carinais em alguns exemplares de *Arthropitys tocantinensis* e a existência de anéis de crescimento em *Arthropitys tocantinensis* e *Arthropitys tabebuiensis* corroboram a interpretação ambiental e climática acima mencionada;

- *Arthropitys isoramis, Arthropitys tabebuiensis* e *Arthropitys buritiranensis*, em vista das dimensões relativamente grandes das cavidades das medulas, eram vegetais relativamente leves que poderiam ter vivido às margens dos rios. *Arthropitys tocantinensis* e *Arthropitys barthelli,* com cavidades das medulas muito menores e corpo secundário mais maciço, portanto com pesos relativos muito maiores, devem ter vivido em áreas mais afastadas das drenagens, em substratos mais firmes;

- A semelhança de *Arthropitys isoramis* n. sp com *Arthropitys versifoveata* de Illinois, EUA, *Arthropitys tabebuiensis* n. sp. com *Arthropitys bistriata* de Chemnitz, Alemanha, e *Arthropitys tocantinenses* n. sp. e *Arthropitys barthelli* n. sp. com *Arthropitys ezonata,* também proveniente de Chemnitz, aproximam muito mais a Bacia do Parnaíba à Província Euramericana e menos à Província Gondwana, como pensado por Coimbra & Mussa (1984) e Mussa & Coimbra (1987).

V. Referências bibliográficas

ABBOTT, M.L. 1958. The American species of *Asterophyllite*s, *Annularia*, and *Sphenonphyllum*. **Bulletins of American Paleontology**, v.38, p.289-390.

AGUIAR, G.A. 1971. Revisão geológica da Bacia Paleozoica do Maranhão. In: CONGRESSO BRASILEIRO DE GEOLOGIA, 25., São Paulo. **Anais**..., São Paulo, SBG, v.3, p.113-122.

ALGEO, T.J.; SCHECKLER, S.E. 1998. Terrestrial-marine teleconnections in the Devonian: links between the evolution of land plants, weathering processes, and marine anoxic events. **Philosophycal *Transactions of Royal Society of London,*** *ser. B, v.*353, p.113-130.

ANDERSON, B.R. 1954. A study of American petrified calamites. **Annals of the Missouri Botanical Garden**, v.41(4), p.395-418.

ANDREWS, H.N. 1952. Some American petrified calamitean stems. **Annals of the Missouri Botanical Garden**, v.39(4), p.189-206.

ANTUNES, T.; PINTO, I.S. 2006. **Botânica**: a passagem à vida terrestre – atlas e texto. Lisboa: Lidel, 133p.

BALME, B.E. 1995. Fossil in situ spores and pollen grains: an annotated catalogue. **Review of Palaeobotany and Palynology**, v.87, p.81-323.

BAMFORD, M.K; PHILIPPE, M. 2001. Jurassic-Early Cretaceous Gondwanan homoxylous woods: a nomenclatural revision of the genera with taxonomic notes. **Review of Palaeobotany and Palynology**, v.133, p.287-297.

BANERJEE, M.; MITRA, S.; DUTTA, S. 2009. On the occurrence of three species of *Annularia* Sterberg in the Early Permian *Glossopteris* Flora of peninsular India. **Review of Paleobotany and Palynology**, v.153, p.394-407.

BARBOSA, O.; GOMES, F.A. 1957. Ministério da Agricultura - Departamento de Produção Mineral - Divisão de Geologia e Mineralogia. **Boletim n. 174**: Carvão mineral na Bacia Tocantins - Araguaia. Rio de Janeiro: Serviço Gráfico do Instituto Brasileiro de Geografia e Estatística, 38p.

BARRON, E.J.; FAWCETT, P.J. 1995. The climate of Pangaea: A review of climate simulations of the Permian. In: SCHOLLE, P.A.; PERYT, T.M.; ULMER-SCHOLLE, D.S. (Eds.) **The Permian of the Northern Pangea***.* Berlin: Springer Verlag, p.37-52.

BATEMBURG, L.H. 1977. The *Sphenophyllum* species in the carboniferous flora of Hols (Westphalian D, Saar Basin, Germany). **Review of Paleobotany and Palynology**, v.24, p.69-99.

BERRY E.W. 1912. American Triassic Neocalamites. **Botanical Gazette**, v.53(2), p.174-180.

BLAKEY, R.C. 2008. Gondwana paleogeography from assembly to breakup - a 500 m.y. odyssey. **The Geological Society of America**, Special Paper, n. 441, p.1-28.

BOUREAU, E. 1964. **Traité de Paléobotanique**, Tome III – Sphenopsida, Noeggerathiophyta. Paris: Masson et Cie Éditeurs, 544p.

BRASIL, Ministério do Meio Ambiente, 2000. **Sistema Nacional de Unidades de Conservação**. Lei 9985, de 18 de julho de 2000.

BRONGNIART, A. 1872. Notice sur le *Psaronius brasiliensis*. **Bulletin de la Societé Botanique de France**, Ser. 5, v.19, p.3-10.

CALDAS, E.B.; MUSSA, D.; LIMA-FILHO, F.P.; RÖSLER, O. 1989. Nota sobre a ocorrência de uma floresta petrificada de idade permiana em Teresina, Piauí. **Boletim IG-USP**, Publ. Esp., v.7, p.69-87.

CAPRETZ, R.L. 2010. Paleoecologia e tafonomia da Floresta Petrificada do Tocantins Setentrional (Bacia do Parnaíba, Permiano). **Tese de Doutoramento**. IGCE-Universidade Estadual Paulista "Júlio de Mesquita Filho", Rio Claro, 172 p.

CAPRETZ, R. L.; ROHN, R. 2013. Lower Permian stems as fluvial paleocurrent indicators of the Parnaíba Basin, northern Brazil. **Journal of South American Earth Sciences**, in press.

CHALONER, W.G.; LACEY, W.S. 1973. The distribution of Late Palaeozoic Flora. In: HUGUES, N.F. (Ed.). **Organisms and continents through time**. Special Papers in Paleontology, v.12, p.271-289.

CHALONER, W.G.; MEYEN, S.V. 1973. Carboniferous and Permian Floras of the Northern Continents. In: HALLAM, A. (Ed.). **Atlas of Palaeobiogeography**. Elsevier, Amsterdam, p.169-186.

CHARBONNIER, S., VANNIER, J., GALTIER, J., PERRIER, V., CHABARD, D., SOTTY, D. 2008. Diversity and paleoenvironment of the flora from the nodules of the Montceau-les-Mines Biota (Late Carboniferous, France). **Palaios**, v.23, p.210-222.

CICHAN, M.A.; TAYLOR, T.N. 1983. A systematic and developmental analysis of *Arthropitys deltoides* sp. nov. **Botanical Gazette**, v.144(2), p.285-294.

CLEAL, C.J.; THOMAS, B.A. 1991. Carboniferous and Permian palaeogeography. In: CLEAL, C.J. (Ed.). **Plant fossils in geological investigation**: the Palaeozoic. England: Ellis Horwood, p.155-181.

COIMBRA, A.M. 1983 Estudo sedimentológico e geoquímico do Permo-Triássico da Bacia do Maranhão. **Tese de Doutoramento,** IG-USP, 150p.

COIMBRA, A.M.; MUSSA, D. 1984. Associação lignitafoflorística na Formação Pedra-de-Fogo, (Arenito Cacunda), Bacia do Maranhão – Piauí, Brasil. In: Congresso Brasileiro de Geologia, 33, Rio do Janeiro. **Anais**..., CBG. p. 591-605.

COSTA, C.G.; CALLADO, C.T.; CORADIN, V.T.R.; CARMELLO-GUERREIRO, S.M. 2006. Xilema. In: APPEZZATO-da-GLÓRIA, B. & CARMELLO-GUERREIRO, S.M. (Eds.). **Anatomia vegetal**. 2.ed. Viçosa, Ed. UFV, 438p.

COTTA, B. 1832. **Die dendrolithen in Bezieihung auf ihren inneren Bau**. Arnoldische buchhandlung. Dresden e Leipizig, 89p.

COX, C.B.; HUTCHINSON, P. 1991. Fishes and amphibians from the Late Permian Pedra de Fogo Formation of Northern Brazil. **Palaeontology**, v.34(3), p.561-573.

CREBER, G.T.; FRANCIS, J.E. 1999. Fossil tree-ring analysis: palaeodendrology. In: JONES, T.P.; ROWE, N.P. (Eds.). **Fossil plants and spores**: modern thechniques. Londres, Geological Society, p.245-250.

CROWELL, J.C. 1995. The ending of the Late Paleozoic Ice Age during the Permian Period. In*:* SCHOLLE, P.A.; PERYT, T.M.; ULMER-SCHOLLE, D.S. (Eds.). **The Permian of the Northern Pangea***.* Vol. I: Paleogeography, Paleoclimates, Stratigraphy. Berlin, Springer Verlag, p.62-74.

CROWLEY, T.J. 1994. Pangean climates. In: KLEIN, G.D. (Ed.). **Pangea**: paleoclimate, tectonics, and sedimentation during accretion, zenith, and breakup of a supercontinent. Boulder, Colorado: Geological Society of America Special Papper 288, p.25-39.

CROWLEY, T.H.; HYDE, W.T.; SHORT, D.A. 1989. Seasonal cycle variations on the supercontinent Pangaea. **Geology**, v.17, p.457-460.

CUTTER, E.G. 1978. **Plant anatomy** – Part I: cells and tissues. 2nd. ed. London, Edward Arnold, 315p.

DELEVORYAS, T. 1962. **Morphology and evolution of fossil plant**s. Nova Iorque: Holt, Rinehart & Winston, 189p.

DERNBACH, U. 1996. **Petrified Forests**. The World's 31 most beautiful petrified forests. Heppenheim: D'Oro-Verlag, 188p.

DIAS-BRITO, D.; CASTRO, J.C. 2005. Caracterização geológica e paleontológica do Monumento Natural das Árvores Fossilizadas do Tocantins. **Relatório final.** Unesp - Rio Claro, 40p. (não publicado).

DIAS-BRITO, D., ROHN, R., CASTRO, J.C., DIAS, R.R.; RÖSSLER, R. 2007. Floresta Petrificada do Tocantins Setentrional – O mais exuberante e importante registro florístico tropical-subtropical permiano no Hemisfério Sul. In: WINGE, M.; SCHOBBENHAUS, C.; BERBERT-BORN, M.; QUEIROZ, E.T.; CAMPOS, D.A.; SOUZA, C.R.G.; FERNANDES, A.C.S. (Eds.). **Sítios Geológicos e Paleontológicos do Brasil**. Acesso em 23/01/2007 no endereço http://www.unb.br/ig/sigep/sitio104/sitio104.pdf.

DIMICHELE, W.A.; ARONSON, R.B. 1992. The Pennsylvanian-Permian vegetation transition: a terrestrial analogue to the onshore-offshore hypothesis. **Evolution**, v.46, p.807-824.

DIMICHELE, W.A.; KERP, H.; CHANEY, D.S. 2004. Tropical floras of the Late Pennsylvanian-Early Permian transition: Carrizo Arroyo context. In: LUCAS, S.G.; ZIEGLER, K.E. (Eds.). **Carboniferous-Permian transition**. New Mexico Museum of Natural History and Science, Bulletin 25, p.105-109.

DIMICHELE, W.A.; VAN CITTERT, J.H.A.V.K.; LOOY, C.V.; CHANEY, D.S. 2005. *Equisetites* from the Early Permian of north-central Texas. In: LUCAS, S.G.; ZEIGLER, K.E. (Eds.). **The Nonmarine Permian.** New Mexico Museum of Natural Histojy and Science Bulletin No. 30, p.56-59.

DIMICHELE, W.A.; TABOR, N.J.; CHANEY, D.S.; NELSON, W.J. 2006. From wetlands to wet spots: environmental tracking and the fate of Carboniferous elements in Early Permian tropical floras. In: GREB, S.F.; DIMICHELE, W.A. (Eds.). **Wetlands through time**. Geological Society of Americam Special Paper, v.399, p.223-248.

DIMICHELE, W.A.; FALCON-LANG, H.J. 2012. Calamitalean ‘’pith casts’’ reconsidered. **Review of Palaeobotany and Palynology**, v.173, p.1-14.

DINO, R., ANTONIOLI, L., BRAZ, S.M. 2002. Palynological data from the Trisidela Member of Upper Pedra de Fogo Formation (‘’Upper Permian’’) of the Parnaíba Basin, Northeastern Brazil. **Revista Brasileira de Paleontologia**, v.3, p.24-35.

DRUM, R.W., 1968. Petrifaction of plant tissue in the laboratory. **Nature,** v.218, p.784– 785.

EBLE, C.F.; GREB, S.F. 1997. Channel-fill coal beds along the western margin of Eastern Kentucky Coal Field. **International Journal of Coal Geology**, v.33, p.183-207.

EGGERT, D.A. 1962. The ontogeny of carboniferous arborescent Sphenopsida. **Palaeontographica Abt. B**, v.110, p.99-127.

EL WARTITI, M.; BROUTIN, J.; FREUTET, P.; LARHRIB, M.; TOUTIN-MORIN, N. 1990. Continental deposits in Permian basins of the Mesetin Marocco, geodynamic history. **Journal of African Earth Sciences**, v.10(1/2), p.261-368.

FARIA Jr., L.E.C.; TRUCKENBRODT, W. 1980. Estratigrafia e petrografia da Formação Pedra de Fogo – Permiano da Bacia do Parnaíba. In: CONGRESSO BRASILEIRO DE GEOLOGIA, 31, Camboriú, **Anais**..., SBP. v.2, p.740-754.

FALCON-LANG H.J. 2003. Late Carboniferous Tropical Dryland Vegetation in an alluvial-plain setting, Joggins, Nova Scotia, Canada**. Palaios**, v.18, p.197–211.

FALCON-LANG, H.J.; DIMICHELE, W.A. 2010. What happened to the coal forests during Pennsylvanian glacial phases? **Palaios**, v.25, p.611–617.

FOSTER, A.S.; GIFFORD Jr., E.M. 1974. **Comparative morphology of vascular plants**. São Francisco: W.H. Freeman & Co., 751p.

FREY, W. 2009. **Syllabus of plant families**: Adolf Engler´s Syllabus der Pflanzenfamilien, Parte 3. 13.ed. Berlin: Gebr. Borntraeger Verlagsbuchhandlung, 419.p.

GALTIER, J. 2008. A new look at the permineralized flora of Grand-Croix (Late Pennsylvanian, Saint-Etienne basin, France). **Review of Palaeobotany and Palynology**, v.152, p.129–140.

GALTIER, J.; RONCHI, A.; BROUTIN, J. 2011. Early Permian silicified floras from the Perdasdefogu Basin (SE Sardinia): comparison and bio-chronostratigraphic correlation with the floras of the Autun Basin (Massif central, France). **Geodiversitas**, v.33(1), p.43-69.

GERRIENNE, P.; FAIRON-DEMARET, M.; GALTIER, J. 1999. A Namurian A (Silesian) permineralized flora from the Carrière du Lion at Engihoul (Belgium). **Review of Paleobotany and Palynology**, v.107, p.1-15.

GIBBS, M.T., REES, P.M., KUTZBACH, J.E., ZIEGLER, A.M., BEHLING, P.J., AND ROWLEY, B. 2002, Simulations of Permian climate and comparisons with climate-sensitive sediments. **Journal of Geology**, v.110, p.33–55.

GÓES, A.M.O.; FEIJÓ, F.J. 1994. Bacia do Parnaíba. **Boletim de Geociências da Petrobrás**, v.8(1), p.57-67.

GOLONKA, J.; FORD, D. 2000. Pangean (Late Carboniferous-Middle Jurassic) paleooenvironment and lithofacies. **Palaeogeography, Palaeoclimatology, Palaeoecology**, v.161, p.1-34.

GOEPPERT, H.R. 1864-65. Die fossile flora der Permischen Formation. **Palaeontographica**, v.12, 64 Est. Cassel, Verlag von Theodor Fisher, 316p.

GOOD, C.W. 1975. Pennsylvanian-age Calamitean cones, elater-bearing spores and associated vegetative remains. **Palaeontographica Abt. B**, v.153, p.28-99.

GOOD, C.W.; TAYLOR, T.N. 1974. Structurally preserved plants from the Pennsylvanian (Monongahela Series) of Southeastern Ohio. **The Ohio Journal of Science**, v.74(5), p.287-290.

HERBST, R. 1985. Nueva descripcion de *Psaronius arrojadoi* (Pelourde) (Marattiales), del Permico de Brasil. **Ameghiniana,** Buenos Aires, v.21, p.243-258.

HERBST, R. 1986. Studies on Psaroniaceae. I. The family Psaroniaceae (Marattiales) and a redescription of *Tietea singularis* Solms-Laubach, from the Permian of Brazil. In: CONGRESO ARGENTINO PALEONTOLOGIA Y BIOESTRATIGRAFIA, 4., 1986, **Actas**… p.163-171.

HERBST, R. 1992. Studies on Psaroniaceae. III. *Tietea derby* n. sp., from the Permian of Brazil. **Cour. Forsch.- Inst. Senckenberg**, v.147, p.155-161.

HERBST, R. 1999. Studies on Psaroniaceae. IV. Two species of *Psaronius* from Araguaina, State of Tocantins, Brazil. **FACENA**, v.15, p.9-18.

HICK, T.; CASH, W. 1881. A contribution to the flora of the Lower Coal-Measures of the parish of Halifax. Part III. **Proceedings of Yorkishire Geological and Polytechnich Society**, New Series, v.7, p.400-405.

HIRMER, M. 1927. **Handbuch der Paläobotanik**. München and Berlin, 708 p.

IANNUZZI, R.; PFEFFERKORN, H.W. 2002. A pre-glacial, warm-temperate floral belt in Gondwana (Late Visean, Early Carboniferous). **Palaios**, v.17, p.571-590.

KERP, J.H.F. 1984a. Aspects of Permian palaeobotany and palynology. III. A new reconstruction of *Lilpopia raciborskii* (Lilpop) Conert et Schaarschmidt (Sphenopsida). **Review of Palaeobotany and Palynology**, v.40, p.237-261.

KERP, J.H.F. 1984b. Aspects of Permian palaeobotany and palynology. V. On the nature os *Asterophyllites dumassi* Zeiller, its correlation with *Calamites gigas* Brongniart and the problem concerning its sterile foliage. **Review of Palaeobotany and Palynology**, v.41, p.301-317.

KERP, J.H.F. 1990. The study of fossil gymnosperms by means of cuticular analysis. **Palaios**, v.5, p.548-596.

KNOELL, H. 1935. Zur Kenntnis der strukturbietenden Pflanzenreste des jüngeren Paläozoikums: 4. Zur Systematik der strukturbietenden Calamiten der Gattung Arthropitys Goeppert aus dem mittleren Oberkarbon Westdeutschlands und Englands. **Palaeontographica Abt. B**, v.80, p.1–51.

KURZAWE, F. 2012. Gimnospermas permineralizadas do Permiano da Bacia do Parnaíba (Formação Motuca), Nordeste do Brasil. **Tese de Doutoramento**, Instituto de Geociências, Universidade Federal do Rio Grande do Sul, 249p.

KURZAWE, F.; MERLOTTI, S. 2009. O complexo *Dadoxylon-Araucarioxylon*, Carbonífero e Permiano do Gondwana: estudo taxonômico do gênero *Dadoxylon*. **Pesquisas em Geociências**, v.36(2), p.223-232.

KURZAWE, F., IANNUZZI, R., MERLOTTI, S., RÖSSLER, R.; NOLL, R. 2013a. New gymnospermous woods from the Permian of the Parnaíba Basin, Northeastern Brazil, Part I: *Ductoabietoxylon*, *Scleroabietoxylon* and *Parnaiboxylon.* **Review of Palaeobotany and Palynology**, In press.

KURZAWE, F., IANNUZZI, R., MERLOTTI, S.; ROHN, R. 2013b. New gymnospermous woods from the Permian of the Parnaíba Basin, Northeastern Brazil, Part II: *Damudoxylon, Kaokoxylon* and *Taeniopitys.* **Review of Palaeobotany and Palynology**, In press.

LEARY, R.L.; PFEFFERKORN, H.W**.** 1977. An Early Pennsylvanian flora with *Megalopteris* and Noeggerathiales from west-central Illinois. **Illinois State Geological Survey Circular**, n.500, 77 p.

LACEY, W.S.; EGGERT, D.A. 1964. A flora from the Chester Series (Upper Mississipian) of Southern Illinois. **American Journal of Botany**, v.51(9), p. 976-985.

LEO, R.F.; BARGHOORN, E.S. 1976. Silicification of wood. **Botanical Museum Leaflets Harvard University**, v.25(1), p.1-47.

LEISTKOW, K.U. 1962. Die Wurzeln der Calamitaceae. **PhD Thesis**. Botanical Institute of University of Tübingen, 99p.

LEJAL-NICOL, A. 1985. Carboniferous megafloras of North Africa. In*:* MATINEZ DIAZ, C. (Ed.) **The Carboniferous of the world**. Madrid, I.G.M.E., Tomo 2, p.386-391.

LIBERTÍN, M.; BEK, J. 2004. *Huttonia spicata* (Sternberg) emend. and its spores, the Radnice Basin (Bolsovian), Carboniferous continental basins of the Czech Republic. **Review of Palaeobotany and Palynology**, v.128, p.247-261.

LIMA FILHO, F.P. 1991. Fácies e ambientes deposicionais da Formação Piauí (Pensilvaniano), Bacia do Parnaíba. **Dissertação de Mestrado.** São Paulo, IG-USP, 137p.

LIMA FILHO, F.P. 1998. A sequência Permo-Pensilvaniana da Bacia do Parnaíba. **Tese de Doutoramento.** São Paulo, IG-USP.

LIMA, E.A.M.; LEITE, J.F. 1978. Projeto estudo global dos recursos minerais da Bacia Sedimentar do Parnaíba: Integração Geológica-Metalogenética. Recife, **Relatório Técnico,** MME/DNPM/CPRM, v.1, 212p.

LUCAS, S.G. 2004. A global hiatus in the Middle Permian tetrapod fossil record. **Stratigraphy**, v.1(1), p.47-64.

LUCAS, S.G.; SCHNEIDER, J.W.; CASSINIS, G. 2006. Non-marine permian biostratigraphy and biochronology: an introduction. In: LUCAS, S.G.; CASSINIS, G.; SCHNEIDER, J.W. (Eds.). **Non-marine Permian biostratigraphy and biochronology**. The Geological Society of London, Special Publication, v.265, p.1-14.

MATYSOVÁ, P.; RÖβLER, R.; GÖTZE, J.; JAROMÍR, L.; FORBES, G.; TAYLOR, E.; SAKALA, J.; GRYGAR, T. 2010. Alluvial and volcanic pathways to silicified plabt stems (Upper Carboniferous-Triassic) and their taphonomic and palaeoenvironmental meaning. **Paleogeography, Palaeoclimatology, Palaeoecology**, v.292, p.127-143.

MEYEN, S.V. 1987. **Fundamentals of Palaeobotany**. London: Chapman and Hall, 432 p.

MILANI E.J., THOMAZ FILHO A. 2000. Sedimentary Basins of South America. In: CORDANI U.G., MILANI E.J., THOMAZ FILHO A., CAMPOS D.A. **Tectonic Evolution of South America.** Rio de Janeiro, p.389-449.

MILLIKEN, K.L. 2001. Diagenetic heterogeneity in sandstone at the outcrop scale, Breathitt Formation (Pennsylvanian), eastern Kentucky. **AAPG Bulletin**, v.85, p.795–815.

MOSBRUGGER, V. 1990. **The tree habit in land plants**: a functional comparison of trunk constructions with a brief introduction into the biomechanics of trees. Springer-Verlag, Berlin, 161p.

MUNE, S.E., BERNARDES-DE-OLIVEIRA, M.E.C. 2007. Revisão da tafoflora interglacial neocarbonífera de Monte Mor, SP (Subgrupo Itararé), nordeste da Bacia do Paraná. **Revista Brasileira de Geociências**, v.37(3), p.427-444.

MUSSA, D.; COIMBRA, A.M. 1987. Novas perspectivas de comparação entre as tafofloras permiannas (de lenhos) das bacias do Parnaíba e do Paraná. In: CONGRESSO BRASILEIRO DE PALEONTOLOGIA, 10, Rio de Janeiro. **Anais**..., SBP, v.2, p. 901-923.

MUSTOE, G.E. 2003. Microscopy of silicified wood. **Microscopy Today**, v.11(6), p.34-37.

NAUGOLNYKH, S.V. 2009. A new fertile Neocalamites from the Upper Permian of Russia and equisetophyte evolution. **Geobios**, v.42, p.513–523.

OGURA, Y. 1972. **Comparative anatomy of vegetative organs of the pteridophytes**. 2. ed. Berlin: Gebrunder Borntraeger, 502p.

ORLOVA, O.A. 2007. Early Carboniferous plants of the Arkhangelsk Region, Russia. **Paleontological Journal**, v.41(11), p.1138–1150.

PARRISH, J.T. 1995. Geologic evidence of Permian climate. In: SCHOLLE, P.A.; PERYT, T.M.;

ULMER-SCHOLLE, D.S. (Eds.). **The Permian of the Northern Pangea**. Vol. I: Paleogeography, Paleoclimates, Stratigraphy Berlin: Springer Verlag, p. 53-61.

PELOURDE, F. 1914. A propos dês Psaroniées du Brésil. Association Française pour l'avancement des Sciences. **Compte-rendu de la 43 session Le Havre.** p.442-445. Disponível em: http://gallica.bnf.fr/ark:/12148/bpt6k201218n/f441.image.

PINTO, C.P.; SAD, J.H.G. 1986. Revisão da estratigrafia da Formação Pedra de Fogo, borda sudoeste da Bacia do Parnaíba. In: CONGRESSO BRASILEIRO DE GEOLOGIA, 34, Goiânia, **Anais**... SBG. v.1, p. 346-358.

POULSEN, C.J.; POLLARD, D.; MONTAÑEZ, I.P.; ROWLEY, D. 2007. Late Paleozoic tropical climate response to Gondwanan deglaciation. **Geology**, v.35(9), p.771–774.

PRICE, L.I. 1948. Um anfíbio labirintodonte da Formação Pedra de Fogo, Estado do Maranhão. **Boletim do DNPM/DGM**, Maranhão, v.124, p. 7-33.

RAVEN, P.T.; EVERT, R.F.; EICHORN, S.E. 2001. **Biologia vegetal**. 6.ed. Rio de Janeiro: Guanabara-Koogan, 906p.

REED, F.D. 1952. *Arthroxylon*, a redefined genus of calamite. **Annals of the Missouri Botanical Garden**, v.39, p.173-187.

REES, P.A. 2002. Land-plant diversity and the end-Permian mass extinction. **Geology**, v.30(9), p.827-830.

REES, P.A.; GIBBS, M.T.; ZIEGLER, A,M. KUTZBACH, J.E.; BEHLING, P.J. 1999. Permian climates: evaluating model predictions using global paleobotanical data. **Geology**, v.27, p.891-894.

REES, P.A; ZIEGLER, A.M.; GIBBS, M.T.; KUTZBACH, J.E; BEHLING, P.J.; ROWLEY, D.B. 2002. Permian phytogeographic patterns and climate data/model comparisons. **The Journal of Geology**, v.110, p.1–31.

RENAULT, B. 1893. **Études des gîtes minéraux de la France**. Bassin houiller et permien d'Autun et d'Epinac. Fascicule IV, Flore Fossile, 2.Partie. **Atlas**. Paris, Imprimerie Nationale. 89 planches.

RENAULT, B. 1896. **Études des gîtes minéraux de la France**. Bassin houiller et permien d'Autun et d'Epinac. Fascicule IV, Flore Fossile, 2.Partie. **Texte**. Paris, Imprimerie Nationale. 578p.

RICARDI, F.; RÖSLER, O.; ODREMAN, O. 1997. *Delnortea* ("Gigantopterid") flora of the Palmarito Formation (Artinskian) in NW Venezuela. In*:* PODEMSKI, M.; DYBOVA-JACHOWICZ, S.; JAWOROWSKI, K.; JURECZKA, J. WAGNER, R. (Eds.). **Proceedings of the XIII international Congress on the Carboniferous and Permian.** Cracow, Poland. Aug. 28-Sept. 2, 1995. Prace Panstwowego Instytutu Geologicznego (1988), 157, Part 3; Pages 123-132.

RICARDI-BRANCO, F. 2008. Venezuelan paleoflora of the Pennsylvanian-Early Permian: paleobiogeographical relationships to Central and Western Equatorial Pangea. **Gondwana Research**, v.14, p.297-305.

RICARDI-BRANCO, F.; ROSLER, O.; ODREMAN, O. 2005. La Flora Euramericana de Carache (Carbonífero Tardío-Pérmico Temprano), Municipio de Carache, Noroeste de Venezuela. **Plântula**, v.3(3), p.153-167.

RIGGS, S.D. ROTHWELL, G.W. 1985. *Sentistrobus goodii* n. gen. and sp., a permineralized Sphenophyllalean cone from the Upper Pennsylvanian of the Appalachian Basin. **Journal of Paleontology**, v.59(5), p.1194-1202.

ROESLER, G.A.; IANNUZZI, R.; ROCKENBACH, D.B.; BARONI, C.L. 2008. Uma nova espécie de *Phyllotheca* Brongniart (Townrow) no Permiano Inferior da Bacia do Paraná, RS. **Gaea**, v.4(1), p.14-23.

ROHN, R.; RÖSLER, O. 1987. Relações entre a Flora Permiana do Gondwana e as floras das províncias setentrionais. In*:* CONGRESSO BRASILEIRO DE PALEONTOLOGIA, 10, Rio de Janeiro. SBP, **Anais**..., V.2, p. 885-899.

ROSCHER, M.; SCHNEIDER, J.W. 2006. Permo-Carboniferous climate: Early Pennsylvanian to Late Permian climate of central Europe in a regional and global context. In: LUCAS, S.G.; CASSINIS, G.; SCHNEIDER, J.W. (Eds.). **Non-marine Permian biostratigraphy and biochronology**. The Geological Society of London, Special Publication, v.265, p.95-136.

RÖβLER, R. 2006. Two remarkable Permian petrified forests: correlation, comparison and significance. In: Lucas, S.G.; Cassinis, G.; Schneider, J.W. (eds.) **Non-marine Permian biostratigraphy and biochronology**. The Geological Society of London, Special Publication, 265: 39-63.

RÖβLER, R.; GALTIER, J. 2002a. First *Grammatopteris* tree ferns from the Southern Hemisphere–new insights in the evolution of the Osmundaceae from the Permian of Brazil. **Review of Paleobotany and Palynology**, v.121, p.205-230.

RÖβLER, R.; GALTIER, J. 2002b. *Dernbachia brasiliensis* gen. nov. et sp. nov. – a new small tree fern from the Permian of NE Brazil. **Review of Paleobotany and Palynology**, v.122, p.239-263.

RÖβLER, R.; GALTIER, J. 2003. The first evidence of the fern *Botryopteris* from the Permian of the Southern Hemisphere reflecting growth form diversity. **Review of Paleobotany and Palynology**, v.127, p.99-124.

RÖβLER, R.; NOLL, R. 2002. Der permische versteinerte Wald von Araguaina/Brasilien - Geologie, Taphonomie und Fossilführung. **Veröffentlichungen des Museums für Naturkunde Chemnitz**, v.25, p.5-44.

RÖβLER, R.; NOLL, R. 2006. Sphenopsids of the Permian (I): the largest known anatomically preserved calamite, an exceptional find from the petrified forest of Chemnitz, Germany. **Review of Paleobotany and Palynology**, v.140, p.145-162.

RÖβLER, R.; NOLL, R. 2007a. Forschungsgeschichte, Paläobiologie und Rekonstruktion eines baumförmigen Schachtelhalmgewächses aus dem Perm: *Calamitea* Cotta 1832. **Veröffentlichungen des Museums für Naturkunde Chemnitz**, v.30, p.61-82.

RÖβLER, R.; NOLL, R. 2007b. *Calamitae* Cotta, the correct name for calamitean sphenopsids currently classified as *Calamodendron* Brongniart. **Review of Paleobotany and Palynology**, v.144, p.157-180

RÖßLER, R.; NOLL, R. 2010. Anatomy and branching of *Arthopitys bistriata* (Cotta) Goeppert – new observations from the Permian Petrified of Chemnitz, Germany. **Int. Journal of Coal Geology**, v.83, p.103-124.

RÖβLER, R.; FENG, Z.; NOLL, R. 2012. The largest calamite and its growth architecture – *Arthropitys bistriata* from the Early Permian Petrified of Chemnitz. **Review of Paleobotany and Palynology**, v.185, p.64-78.

ROWLEY, D.B., RAYMOND, A.; PARRISH, J.T.; LOTTES, A.L.; SCOTESE, C.R.; ZIEGLER, A.M. 1985. Carboniferous paleogeographic, phytogeographic, and paleoclimatic reconstructions. **International Journal of Coal Geology**, v.5, p.7-42.

SALGADO-LABOURIAU, M.L. 1994. **História ecológica da Terra**. 2.ed. São Paulo, Ed. Edgard Blücher Ltda, 307p.

SCHOBBENHAUS, C.; CAMPOS, D.A.; DERZE, G.R.; ASMUS, H.E. (Coords.). 1984. **Geologia do Brasil.** Texto Explicativo do Mapa Geológico do Brasil e da área oceânica adjacente incluindo depósitos minerais. Escala 1:2500.000. Brasília: DNPM, p. 9-53.

SCOTESE, C.S. **Paleomap Project**. Disponível em <http://www.scotese.com/. Acesso em 10/11/2009.

SCOTESE, C.R.; MCKERROW, W.S. 1990. Revised world maps and introduction. In: MCKERROW, W.S.; SCOTESE, C.R. (Eds.). **Palaeozoic, Palaeogeography and Biogeography**. Geological Society Memoir n.12, p.1-21.

SCOTESE, C.R.; LANGFORD, R.P. 1995. Pangea and the paleogeography of the Permian. In*:* SCHOLLE, P.A.; PERYT, T.M.; ULMER-SCHOLLE, D.S. (Eds.). **The Permian of the Northern Pangea***.* Berlin, Springer Verlag, p. 3-19.

SCHOPF, J.M. 1975. Modes of fossil preservation. **Review of Paleobotany and Palynology**, v.20, p.27-53.

SCHNEIDER, J.W.; KÖRNER, F.; ROSCHER, M.; KRONER, U. 2006. Permian climate development in the Northern peri-Tethys area – The Lodève basin, French Massif Central, compared in a European and global contex. **Paleogeography, Palaeoclimatology, Palaeoecology**, v.240, p.161-183.

SCOTT, A.C.; COLLINSON, M.E. 2003. Non-destructive multiple approaches to interpret the preservation of plant fossils: implications for calcium-rich permineralizations. **Journal of the Geological Society**, v.160, p.857-862.

SCURFIELD, G.; SEGNIT, E.R. 1984. Petrification of wood by silica minerals. **Sedimentay Geology,** v.39, p.149-167.

SILVA SANTOS, R. 1946. Duas novas formas de elasmobrânquios do Paleozóico do Meio Norte, Brasil. **Anais da Academia Brasileira de Ciências***,* v.18(4), p.281-285.

SILVA SANTOS, R. 1990. Paleoictiofáunula da Formação Pedra do Fogo, Nordeste do Brasil: Holocephali - Petalodontidae. **Anais da Academia Brasileira de Ciências**, v.62(4), p. 347-355.

SILVA, A.J.P., LOPES, R.C., VASCONCELOS, A.M., BAHIA, R.B. 2003. Bacias sedimentares paleozóicas e meso-cenozóicas interiores. In: BIZZI, L.A., SCHOBBENHAUS, C., VIDOTTI, R.M., GONÇALVES, J.H. (Eds.). **Geologia, Tectônica e Recursos Minerais do Brasil** – texto, mapas e SIG. Brasília- CPRM, 692 p.

SKOG, J.E.; BANKS, H.P. 1973. Ibyka amphikoma, Gen. et sp. n., a new protoarticulate precursor from the Late Middle Devonian of New York State. **American Journal of Botany**, v.60, p.366-380.

SOUZA, P.A.; MATZEMBACHER, L.T.; ABELHA, M.; BORGHI, L. 2010. Palinologia da Formação Piauí, Pensilvaniano da Bacia do Parnaíba: biocronoestratigrafia de intervalo selecionado do Poço 1-UN-09-PI (Caxias, MA, Brasil). **Revista Brasileira de Paleontologia**, v.13, p.57-66.

SPICER, R.A. 1991. Plant taphonomic processes. In: ALLISON, P.A., BRIGGS, D.E.G. (Eds.). **Taphonomy**: releasing the data locked in the fossil record. Plenum Press, Nova Iorque, p.71-113.

STEWART, W.N.; ROTHWELL, G.W. 1993. **Paleobotany and the Evolution of Plants**. 2. ed. Cambridge: Cambridge University Press, 521p.

TAVARES, T.M.V. 2011. Estudo de Marattiales da “Floresta Petrificada do Tocantins Setentrional” (Permiano, Bacia do Parnaíba). **Tese de Doutoramento**. IGCE-Universidade Estadual Paulista “Júlio de Mesquita Filho”, Rio Claro, 184 p.

TAVARES, T.M.V; ROHN, R.; R RÖβLER, R.; NOLL, R; CAPRETZ, R.L. 2008. Permian petrified fern leaves from the Central North Brazil (Parnaíba Basin, Araguaína region, Marattiales). **12th International Palynological Congress (IPC-XII)** & **8th International Organisation of Palaeobotany Conference (IOPC-VIII)**, v.1, p.277-278.

TAYLOR, T.N.; TAYLOR, E.L. 1993. **The biology and evolution of fossil plants**. Nova Jersey: Prentice-Hall Inc., 982p.

TAYLOR, T.N.; TAYLOR, E.L.; KRINGS, M. 2009. **The biology and evolution of fossil plants**. 2. ed. Nova Jersey: Prentice-Hall Inc., 1230p.

THOMAS, B.A.; SPICER, R.A. 1987. **The evolution and palaeobiology of land plants**. London e Sydney: Oregon, Croom Helm, 309p.

TOMESCU, A.M.F. 2008. Megaphylls, microphylls and the evolution of leaf development. **Trends in Plant Science**, v.114(1), p.5-12.

TRAVERSE, A. 2007. **Paleopalynology**. 2.ed. Holanda: Springer Verlag, 813p.

VAZ, P.T.; REZENDE, N.G.A.M.; WANDERLEY FILHO, J.R.; TRAVASSOS, W.A.S. 2007.Bacia do Parnaíba. **Boletim de Geociências da Petrobrás**, v.15(2), p.253-263.

YANG, T., NAULGOLNYKH, S.V., SUN, G. 2011. A new representative of *Neocalamites* Halle from the Upper Permian of Northeastern China (Jiefangcun formation). **Paleontological Journal**, v.45(3), p.335-346.

ZAMPIROLLI, A.P.; BERNARDES-DE-OLIVEIRA, M.E. 2000. O gênero *Paracalamites* Zalessky, 1927, na Tafoflora de Itapeva, Carbonífero Superior do Subgrupo Itararé, Grupo Tubarão, Sudoeste do Estado de São Paulo, Brasil. **Revista do Instituto Geológico**, v.21(1/2), p.7-15.

WANG, S.J.; LI, S.S.; HILTON, J.; GALTIER, J. 2003. A new species of sphenopsid stem *Arthropitys* from Late Permian volcaniclastic sediments of China. **Review of Paleobotany and Palynology**, v.126, p.65-81.

WANG, S.J.; HILTON, J.; GALTIER, J.; TIAN, B. 2006. A large anatomically preserved calamitean stem from the Upper Permiann of southwest China and its implications for calamitean development and functional anatomy. **Plant Systematic and Evolution**, v.261, p.229-244.

WEIBEL, R. 1996. Petrified wood from an unconsolidated sediment, Voervadsbro, Denmark. **Sedimentary Geology**, v.101, p.31-41.

WILLIAMSOAN, W.C. 1878. On the organization of the fossil plantas of the Coal-Measures. Part IX: *Asterophyllites*. **Philosophycal *Transactions of Royal Society of London,*** *ser. B, v.169*, p.319-364.

WNUK, C. 1996. The development of floristic provinciality during the Middle and Late Paleozoic. **Review of Paleobotany and Palynology**, v.90, p.5-40.